

• Report No. FAA-RD-77-94

12  
11.11

AD A 043842

NOISE CHARACTERISTICS OF  
EIGHT HELICOPTERS

H.C. True  
E.J. Rickley

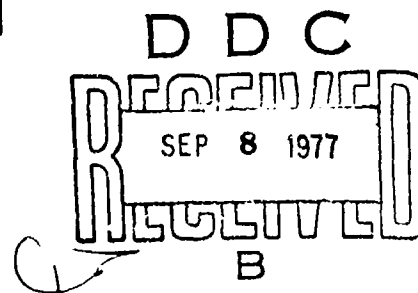


July 1977  
Final Report

Document is available to the U.S. public through  
the National Technical Information Service,  
Springfield, Virginia 22161.

Prepared for

**U.S. DEPARTMENT OF TRANSPORTATION**  
**FEDERAL AVIATION ADMINISTRATION**  
Systems Research & Development Service  
Washington, D.C. 20590



AD No. \_\_\_\_\_  
DDC FILE COPY

#### NOTICE

This document is disseminated under the sponsorship of the Department of Transportation in the interest of information exchange. The United States Government assumes no liability for its contents or use thereof.

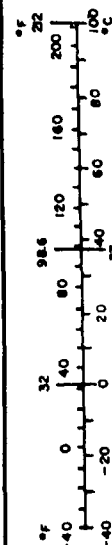
# Technical Report Documentation Page

1. Report No. FAA-RD-77- 94		2. Government Accession No.		3. Recipient's Catalog No.	
4. Title and Subtitle NOISE CHARACTERISTICS OF EIGHT HELICOPTERS				5. Report Date JULY 1977	
				6. Performing Organization Code ARD-550	
7. Author(s) H. C. TRUE, E. J. RICKLEY				8. Performing Organization Report No.	
9. Performing Organization Name and Address Department of Transportation Federal Aviation Administration Systems Research and Development Service Washington, D.C. 20591				10. Work Unit No. (TRAIS)	
				11. Contract or Grant No.	
12. Sponsoring Agency Name and Address Department of Transportation Federal Aviation Administration Systems Research and Development Service Washington, D.C. 20591				13. Type of Report and Period Covered FINAL REPORT	
				14. Sponsoring Agency Code	
15. Supplementary Notes Acoustic data acquired and processed into format by "Noise Measurement and Assessment Laboratory" Transportation Systems Center, Cambridge, Massachusetts					
16. Abstract This report describes the noise characteristics of Eight Helicopters during level flyovers, simulated approaches, and hover. The data was obtained during an FAA/DOT Helicopter Noise Program to acquire a data base for possible helicopter noise regulatory action. The helicopter models tested were the Bell 47G, 206L, and 212 (UHIN), the Hughes 300C and 500C, the Sikorsky S-61 (SH-3B) and S-64 (CH-54B) and the Vertol CH-47C. The acoustic data is presented as Effective Perceived Noise Level, A-weighted sound pressure level and 1/3 octave band sound pressure level with a slow meter characteristic per FAR Part 36. Selected waveforms and narrow band spectra are also shown. Proposed methods to quantify impulsive noise ("blade slap") are evaluated for a level flyover for each of the Helicopters.  The tested helicopters can be grouped into classes depending upon where the maximum noise occurs during a level flyover. Helicopters with the higher main rotor tip speeds propagate highly impulsive noise ahead of the helicopter. The maximum noise for most of the helicopters occurs near the overhead position and appears to originate from the tail rotor. Unmuffled reciprocating engine helicopters appear to have significant engine noise behind the helicopter. Noise levels, when compared as a function of gross weight and flown at airspeeds to minimize "compressibility slap" form a band 7 EPNdB wide with a slope directly proportional to gross weight. The quieter helicopters have multibladed rotors and tip speeds below 700 f.p.s. The duration correction in EPNL is important in evaluating helicopter noise because it penalizes the longer time histories of the helicopters with significant blade slap during a level flyover.					
17. Key Words Helicopter Noise Levels; Effective Perceived Noise Level, Flyover Noise Time History, Main Rotor, Tail Rotor, Impulsive Noise.				18. Distribution Statement This document is available to the public through the National Technical Information Service, Springfield, Virginia 22151	
19. Security Classif. (of this report) UNCLASSIFIED		20. Security Classif. (of this page) UNCLASSIFIED		21. No. of Pages 171	
				22. Price	

ACCESSION for	
NTIS	White Section <input checked="" type="checkbox"/>
DOC	Buff Section <input type="checkbox"/>
UNCLASSIFIED <input type="checkbox"/>	
SECRET/NOV	
BY	
DISTRIBUTION/AVAILABILITY CODES	
Dist	Avail and or SPECIAL
A	

# METRIC CONVERSION FACTORS

Approximate Conversions from Metric Measures			
When You Know	Multiply by	To Find	Symbol
<b>LENGTH</b>			
millimeters	0.04	inches	in
centimeters	0.4	inches	in
meters	3.3	feet	ft
meters	1.1	yards	yd
kilometers	0.6	miles	mi
<b>AREA</b>			
square centimeters	0.16	square inches	in <sup>2</sup>
square meters	1.2	square yards	yd <sup>2</sup>
square kilometers	0.4	square miles	mi <sup>2</sup>
hectares (10,000 m <sup>2</sup> )	2.5	acres	ac
<b>MASS (weight)</b>			
grams	0.035	ounces	oz
kilograms	2.2	pounds	lb
tonnes (1000 kg)	1.1	short tons	ton
<b>VOLUME</b>			
milliliters	0.03	fluid ounces	fl oz
liters	2.1	pints	pt
liters	1.06	quarts	qt
liters	0.26	gallons	gal
cubic meters	35	cubic feet	ft <sup>3</sup>
cubic meters	1.3	cubic yards	yd <sup>3</sup>
<b>TEMPERATURE (exact)</b>			
Celsius temperature	9/5 (then add 32)	Fahrenheit temperature	°F
°C			



Approximate Conversions to Metric Measures			
When You Know	Multiply by	To Find	Symbol
<b>LENGTH</b>			
inches	2.5	centimeters	cm
feet	30	centimeters	cm
yards	0.9	meters	m
miles	1.6	kilometers	km
<b>AREA</b>			
square inches	6.5	square centimeters	cm <sup>2</sup>
square feet	0.09	square meters	m <sup>2</sup>
square yards	0.8	square meters	m <sup>2</sup>
square miles	2.6	square kilometers	km <sup>2</sup>
acres	0.4	hectares	ha
<b>MASS (weight)</b>			
ounces	28	grams	g
pounds	0.45	kilograms	kg
short tons (2000 lb)	0.9	tonnes	t
<b>VOLUME</b>			
teaspoons	5	milliliters	ml
tablespoons	15	milliliters	ml
fluid ounces	30	milliliters	ml
cups	0.24	liters	l
pints	0.47	liters	l
quarts	0.95	liters	l
gallons	3.8	liters	l
cubic feet	0.03	cubic meters	m <sup>3</sup>
cubic yards	0.76	cubic meters	m <sup>3</sup>
<b>TEMPERATURE (exact)</b>			
Fahrenheit temperature	5/9 (after subtracting 32)	Celsius temperature	°C
°F			

\* 1 in = 2.54 exactly. For other exact conversions and more data on factors, see NBS Mon. Publ. 286, Units of Weights and Measures, Price \$2.25, SO Code 95, CI 110 286.

## ACKNOWLEDGEMENTS

This Helicopter Noise Test Program was conducted by the Federal Aviation Administration (FAA), Washington, D.C. The success of this test program was due to the contributions and participation of many individuals from other government agencies, organizations, private industry and the military. We wish to express our gratitude and thanks to the following participants:

FAA/OFFICE OF ENVIRONMENTAL QUALITY - Identification of the program requirement.

FAA/SYSTEMS RESEARCH AND DEVELOPMENT SERVICE, AIRCRAFT SAFETY AND NOISE ABATEMENT DIVISION, ENVIRONMENTAL RESEARCH BRANCH - provided the overall management, test direction and data analysis.

DOT/OFFICE OF THE SECRETARY, OFFICE OF NOISE ABATEMENT - assisted in program organization and data acquisition.

DOT/TRANSPORTATION SYSTEMS CENTER, NOISE MEASUREMENT AND ASSESSMENT LABORATORY - provided the microphone systems and operators, data acquisition and data reduction.

ICAO/INTERNATIONAL CIVIL AVIATION ORGANIZATION - initiated the interest in establishing a possible helicopter noise certification procedure.

HAA/HELICOPTER ASSOCIATION OF AMERICA - supported the FAA effort and encouraged industry participation.

FAA/NATIONAL AVIATION FACILITIES EXPERIMENTAL CENTER (NAFEC) - provided the portable theodolite system and operator.

DULLES INTERNATIONAL AIRPORT/OPERATIONS CHIEF - cooperation in allowing Dulles to be used as a test site.

NASA LANGLEY RESEARCH CENTER/AIRCRAFT NOISE RESEARCH AND ROTORCRAFT RESEARCH DIVISIONS - provided support for the test program, one of the test helicopters (S-61) and crew and also allowed their airfield to be used as a test site.

BELL HELICOPTER - arranged for several of their helicopters to be used in the test program (Bell 47G, 206L, and 212).

HUGHES HELICOPTER - arranged for two of their helicopters to be used in the test program (Hughes 300C and 500C).

SIKORSKY HELICOPTER - arranged for two of their helicopters to be used in the test program (Sikorsky S-61 and S-64 "Skycrane")

BOEING VERTOL - arranged for one of their helicopters to be used in the test program (CH-47C "Chinook").

U.S. AIR FORCE/ANDREWS AIR FORCE BASE, MARYLAND - provided the Bell 212 (UHIN) helicopter and crew.

U.S. ARMY/FT. EUSTIS, VIRGINIA - provided the Sikorsky S-64 "Skycrane" (CH-54B) helicopter and crew.

U.S. ARMY/NEW CUMBERLAND, PENNSYLVANIA - provided the Boeing Vertol CH-47C helicopter and crew.

## TABLE OF CONTENTS

	<u>PAGE</u>
METRIC CONVERSION FACTORS -----	111
ACKNOWLEDGEMENTS -----	v
LIST OF TABLES -----	vi
LIST OF FIGURES -----	ix
SUMMARY -----	1
1.0 INTRODUCTION -----	13
2.0 HELICOPTER DESCRIPTION -----	14
2.1 Physical Characteristics	14
2.2 Power Settings During Test	15
3.0 TEST PROCEDURE -----	27
3.1 Test Plan	27
3.2 Microphone Location	27
3.3 Test Sites	29
4.0 DATA REDUCTION -----	34
5.0 FLYOVER AND APPROACH CHARACTERISTICS -----	35
5.1 Flyover	35
5.1.1 Time Histories	36
5.1.2 One-Third Octave Band Spectra	37
5.2 Approach	39
5.2.1 Time Histories	39
5.2.2 One-Third Octave Band Spectra	40
5.3 Statistical Analysis Of Flyover Noise Data	79
5.4 Effect of Centerline Microphone Reflecting Surface	80
6.0 HOVER NOISE DATA -----	88
6.1 Hover Test Program	88
6.2 Hover Test Results	88
7.0 IMPULSIVE AND NARROW BAND ANALYSIS -----	120
7.1 Waveform Analysis	120
7.2 Narrow Band Spectral	121
7.3 Impulsive Noise Corrections	137
8.0 CONCLUSIONS -----	151
REFERENCES -----	153

LIST OF TABLES

	<u>PAGE NO.</u>
TABLE I. Helicopter Characteristics	16
TABLE II. Helicopter Gross Weight Comparisons	17
TABLE III. Helicopter Power Settings	26
TABLE IV. Comparisons of Centerline and Sideline Microphone Standard Deviations	81
TABLE V. Comparisons of Standard Deviations by Airspeed	82

## LIST OF FIGURES

	<u>PAGE NO.</u>
FIGURE 1. Helicopter Noise Levels	5
FIGURE 2. Helicopter Noise Levels--Technology and Velocity Dependence	6
FIGURE 3. Effect of Airspeed On EPNL Noise Level	7
FIGURE 4. Effect of Airspeed On dBA Noise Level	8
FIGURE 5. A-Weighted Time History Comparisons	9
FIGURE 6. Effect of Glideslope Angle On Noise Level	10
FIGURE 7. Sideline Noise Level Comparisons	11
FIGURE 8. Comparisons Of Acoustic Pressure Waveforms	12
FIGURE 9. Photograph Of Hughes 300C	18
FIGURE 10. Photograph Of Hughes 500C	19
FIGURE 11. Photograph Of Bell 47G	20
FIGURE 12. Photograph Of Bell 206L	21
FIGURE 13. Photograph Of Bell-212 (UHIN)	22
FIGURE 14. Photograph of Sikorsky S-61 (SH-3A)	23
FIGURE 15. Photograph Of Sikorsky S-64 "Skycrane" (CH-59B)	24
<b>FIGURE</b> 16. Photograph Of Boeing Vertol "Chinook" CH-47C	25
FIGURE 17. Approach Procedure	27
FIGURE 18. Helicopter Noise Test Microphone Arrangement	28
FIGURE 19. Helicopter Test Site--Dulles Airport	29
FIGURE 20. Helicopter Test Site--NASA Langley Research Center	30



## LIST OF FIGURES

	<u>PAGE NO.</u>
FIGURE 21. Hughes 300C Flyover Time History Comparisons	41
FIGURE 22. Hughes 500C Flyover Time History Comparisons	42
FIGURE 23. Bell-47G Flyover Time History Comparisons	43
FIGURE 24. Bell-206L Flyover Time History Comparisons	44
FIGURE 25. Bell-212 (UHIN) Flyover Time History Comparisons	45
FIGURE 26. Sikorsky S-61 Flyover Time History Comparisons	46
FIGURE 27. Sikorsky S-64 "Skycrane" (with truck) Flyover Time History Comparisons	47
FIGURE 28. Sikorsky S-64 "Skycrane" (without truck) Flyover Time History Comparisons	48
FIGURE 29. Boeing Vertol "Chinook" CH-47C Flyover Time History Comparisons	49
FIGURE 30. Hughes 300C Flyover 1/3-Octave Band Spectra Comparisons (overhead location)	50
FIGURE 31. Hughes 500C Flyover 1/3-Octave Band Spectra Comparisons (overhead location)	51
FIGURE 32. Bell-47G Flyover 1/3-Octave Band Spectra Comparisons (overhead location)	52
FIGURE 33. Bell-206L Flyover 1/3-Octave Band Spectra Comparisons (overhead location)	53
FIGURE 34. Bell-212 (UHIN) Flyover 1/3-Octave Band Spectra Comparisons (overhead location)	54
FIGURE 35. Sikorsky S-61 Flyover 1/3-Octave Band Spectra Comparisons (overhead location)	55
FIGURE 36. Sikorsky S-64 "Skycrane" Flyover 1/3-Octave Band Spectra Comparisons (overhead location)	56
FIGURE 37. Boeing Vertol "Chinook" CH-47C Flyover 1/3 Octave Band Comparisons (overhead location)	57

## LIST OF FIGURES

	<u>PAGE NO.</u>
FIGURE 38. Sikorsky S-64 "Skycrane" Flyover 1/3-Octave Band Comparisons (before, at and after overhead passage)	58
FIGURE 39. Bell-212 (UHIN) Flyover 1/3-Octave Band Comparisons (before, at and after severe blade slap occurring 12 seconds before reaching overhead location)	59
FIGURE 40. Bell-212 (UHIN) Flyover 1/3-Octave Band Comparisons (before, at and after overhead passage)	60
FIGURE 41. Boeing Vertol CH-47C Flyover 1/3-Octave Band Comparisons (before, at and after severe blade slap occurring 11.5 seconds before reaching overhead location)	61
FIGURE 42. Boeing Vertol CH-47C Flyover 1/3-Octave Band Comparisons (before, at and after overhead passage)	62
FIGURE 43. Hughes 300C Approach Time History Comparisons	63
FIGURE 44. Hughes 500C Approach Time History Comparisons	64
FIGURE 45. Bell 47G Approach Time History Comparisons	65
FIGURE 46. Bell 206L Approach Time History Comparisons	66
FIGURE 47. Bell-212 (UHIN) Approach Time History Comparisons	67
FIGURE 48. Sikorsky S-61 Approach Time History Comparisons	68
FIGURE 49. Sikorsky S-64 "Skycrane" Approach Time History Comparisons	69
FIGURE 50. Boeing Vertol CH-47C Approach Time History Comparisons	70
FIGURE 51. Hughes 300C Approach 1/3-Octave Band Spectra Comparisons (overhead location)	71
FIGURE 52. Hughes 500C Approach 1/3-Octave Band Spectra Comparisons (overhead location)	72

## LIST OF FIGURES

	<u>PAGE NO.</u>
FIGURE 53. Bell 47G Approach 1/3-Octave Band Spectra Comparisons (overhead location)	73
FIGURE 54. Bell-206L Approach 1/3-Octave Band Spectra Comparisons (overhead location)	74
FIGURE 55. Bell-212 (UHIN) Approach 1/3-Octave Band Spectra Comparisons (overhead location)	75
FIGURE 56. Sikorsky S-61 Approach 1/3-Octave Band Spectra Comparisons (overhead location)	76
FIGURE 57. Sikorsky S-64 "Skycrane" Approach 1/3-Octave Band Spectra Comparisons (overhead location)	77
FIGURE 58. Boeing Vertol CH-47C Approach 1/3-Octave Band Spectra Comparisons (overhead location)	78
FIGURE 59. NASA Langley Microphone Reflecting Surface Comparisons (concrete vs. grass)	84
FIGURE 60. NASA Langley Microphone Reflecting Surface Comparisons (concrete vs. grass)	85
FIGURE 61. Dulles Airport Microphone Reflecting Surface Comparisons (dirt vs. plywood)	86
FIGURE 62. Dulles Airport Microphone Reflecting Surface Comparisons (dirt vs. plywood)	87
FIGURE 63. Hover Notation Format	90
FIGURE 64. Comparisons of Typical 5 Foot Hover Time Histories	91
FIGURE 65. Relationship of Helicopter Heading To Microphone Noise Level Assymetry	92
FIGURE 66. Spectral Characteristics of Hover Noise Assymetry	93
FIGURE 67. Correlation of Noise Level Assymetry With Wind Velocity	94

## LIST OF FIGURES

	<u>PAGE NO.</u>
FIGURE 68. Five (5) Foot Hover Noise Levels	95
FIGURE 69. Boeing Vertol CH-47C Hover Directivity	96
FIGURE 70. Boeing Vertol CH-47C Hover Spectra Comparisons (135°)	97
FIGURE 71. Boeing Vertol CH-47C Hover Spectra Comparisons (315°)	98
FIGURE 72. Bell 47G Hover Directivity	99
FIGURE 73. Bell 47G Hover Spectra Comparisons (135°)	100
FIGURE 74. Sikorsky S-61 Hover Directivity	101
FIGURE 75. Sikorsky S-61 Hover Spectra Comparisons (135°)	102
FIGURE 76. Sikorsky S-61 Hover Spectra Comparisons (315°)	103
FIGURE 77. Sikorsky S-64 "Skycrane" (without truck) Hover Directivity	104
FIGURE 78. Sikorsky S-64 "Skycrane" (with truck) Hover Directivity	105
FIGURE 79. Sikorsky S-64 "Skycrane" Hover Spectra Comparisons (180° with and without truck)	106
FIGURE 80. Sikorsky S-64 "Skycrane" Hover Spectra Comparisons (0° with and without truck)	107
FIGURE 81. Hughes 500C Hover Directivity	108
FIGURE 82. Hughes 500C Hover Spectra Comparisons (0°)	109
FIGURE 83. Hughes 500C Hover Spectra Comparisons (225°)	110
FIGURE 84. Bell-212 (UHIN) Hover Directivity	111
FIGURE 85. Bell-212 (UHIN) Hover Spectra Comparisons (135°)	112
FIGURE 86. Bell-212 (UHIN) Hover Spectra Comparisons (225°)	113

## LIST OF FIGURES

	<u>PAGE NO.</u>
FIGURE 87. Hughes 300C Hover Directivity	114
FIGURE 88. Hughes 300C Hover Spectra Comparisons (135°)	115
FIGURE 89. Hughes 300C Hover Spectra Comparisons (270°)	116
FIGURE 90. Bell-206L Hover Directivity	117
FIGURE 91. Bell-206L Hover Spectra Comparisons (315°)	118
FIGURE 92. Bell-206L Hover Spectra Comparisons (180°)	119
FIGURE 93. Bell-212 (UHIN) Acoustic Signature vs. Time (Flyover at 114 Knots)	122
FIGURE 94. Bell-212 (UHIN) Acoustic Signature vs. Time (9° Approach)	123
FIGURE 95. Boeing Vertol CH-47C Acoustic Signature vs. Time (Flyover at 150 knots)	124
FIGURE 96. Hughes 500C Acoustic Signature vs. Time (Flyover at 150 mph)	125
FIGURE 97. Sikorsky S-61 Acoustic Signature vs. Time (Flyover at 100 knots)	126
FIGURE 98. Boeing Vertol CH-74C Narrow Band Spectra (7 seconds before reaching overhead location)	127
FIGURE 99. Boeing Vertol CH-47C Narrow Band Spectra (overhead location)	128
FIGURE 100. Bell-212 (UHIN) Narrow Band Spectra (11 seconds before reaching overhead location)	129
FIGURE 101. Bell-212 (UHIN) Narrow Band Spectra (overhead location)	130
FIGURE 102. Bell-206L Narrow Band Spectra (1 second before reaching overhead location)	131
FIGURE 103. Bell-206L Narrow Band Spectra (overhead location)	132
FIGURE 104. Hughes 500C Narrow Band Spectra (8 seconds before reaching overhead location)	133

## LIST OF FIGURES

	<u>PAGE NO.</u>
FIGURE 105. Hughes 500C Narrow Band Spectra (overhead location)	134
FIGURE 106. Sikorsky S-61 Narrow Band Spectra (6 seconds before reaching overhead location)	135
FIGURE 107. Sikorsky S-61 Narrow Band Spectra (overhead location)	136
FIGURE 108. Impulsive Corrections For Boeing Vertol CH-47C at 141 Knots	143
FIGURE 109. Impulsive Corrections for Sikorsky S-64 "Skycrane" at 95 Knots	144
FIGURE 110. Impulsive Corrections for Sikorsky S-61 at 115 Knots	145
FIGURE 111. Impulsive Corrections for Bell-212 (UHIN) at 110 Knots	146
FIGURE 112. Impulsive Corrections For Bell-206L at 130 mph	147
FIGURE 113. Impulsive Corrections for Bell-37G at 75 mph	148
FIGURE 114. Impulsive Corrections for Hughes 500C at 130 mph	149
FIGURE 115. Impulsive Corrections for Hughes 300C at 75 mph	150

## SUMMARY

The noise characteristics of eight helicopters were measured during October 1976 at Dulles International Airport and Langley Field, Virginia. The helicopter models tested were the Hughes 300C and 500C, the Bell 47G, 206L, and 212 (UHIN, Huey) the Sikorsky S-61 (SH-3B) and S-64 (CH-54B) and the Vertol CH-47C (Chinook). The testing consisted of level flyovers at 500 foot (150m) altitude at several airspeeds, approaches with glide-slopes of 3, 6, and 9 degrees and hover with a wheel clearance of 5 feet. Helicopters were furnished by the manufacturers, U.S. Army, U.S. Air Force, and NASA Langley Research Center (LaRC). The purpose of the testing was to obtain a data base for the development of regulatory standards.

Acoustic data was recorded at the flight path centerline and at 500 feet (150m) sideline on either side of the flight path. Hover data was recorded at distances of 500 and 250 feet (150m and 75m) at eight radial positions around the helicopter. All microphones were 4 feet above the ground. Acoustic data was acquired and reduced by the Noise Measurement and Assessment Laboratory, Transportation Systems Center (TSC), Cambridge, Massachusetts. The data was digitized and reduced in accordance with FAR Part 36 procedures. No weather or distance corrections were applied. All tone corrections in the EPNL calculation procedure below 500 Hz were considered "psuedo tones" caused by ground reflections and were deleted. For the flyovers and approaches the acoustic data was presented as 1/3 octave band spectra, time histories of A-weighted sound level, D-weighted sound level, OASPL, and Perceived Noise Level (PNL) and Effective Perceived Noise Level (EPNL). Hover data was presented as time averaged spectra and weighted overall levels. The data printouts are published in Report No. FAA-RD-77-57, April 1977. The purpose of this report is to present trends of helicopter noise and comparisons between the various models.

Figure 1 shows the EPNL and Maximum A-Weighted Level ( $L_A$ ) as a function of gross weight for the eight helicopters tested. The helicopters were flying at their airspeed for best range which is about 80 or 90 percent of their maximum airspeed. The slope of the average trend line (13 log of the weight) is slightly greater than a linear slope of the weight itself (10 log of weight). The slope of the maximum A-weighted level and the EPNL (which includes a time duration effect) are approximately equal although there is more variation around the EPNL trend line than the peak A-weighted line. Any tone corrections (above 500 Hz) were small

and not readily attributable to turbomachinery noise generation. The EPNL was estimated ( $\pm 1.0$  EPNdB tolerance) for the 300C and 206L because high ambient noise levels made the exact determination of duration difficult for these models. Since measures of maximum noise level during a flyover (A-weighted, D-weighted, PNL) are consistent with each other, the increased variation around the EPNL trend line is attributed to the duration correction in EPNL. The helicopters can be segregated into classes depending upon the magnitude of the duration correction. The duration and shape of the flyover noise time history is influenced by airspeed and the design characteristics of the individual helicopter.

The effect of airspeed upon EPNL is investigated in Figure 2. Here the maximum and minimum EPNL at any airspeed above 60 Kts is plotted as well as the EPNL for the velocity for best range. Only the UHIN (Bell 212) and CH-47C have a consistent trend of higher noise for faster airspeed. This is attributed to "compressibility effects" on the advancing blade. The advancing blade tip Mach number is about 0.94 for the UHIN at 114 Kts and .90 for the CH-47C at 150 Kts. Airspeed, within the range tested, has a negligible effect on the EPNL for the 300C, 47G, S-61 and S-64. The 206L achieves its lowest EPNL at its faster airspeeds because of a shorter time duration. The 500C has a slight increase in peak noise level with faster airspeed and a "bucket" effect when duration is included. The trends of EPNL and peak A-weighted level are shown on Figures 3 and 4.

Some observations as to helicopter configuration and noise level can be drawn from Figure 2. The 300C, S-61 and S-64 obviously creaste the least noise, for their weight, during a flyover. A line drawn through these points has the slope of 10 log of the gross weight which indicates a linear trend of noise level with gross weight. The 300C, S-61 and S-64 have a similar configuration with multibladed rotors with more blades as the weight increases and similar tipspeeds of 660 to 700 fps. The three noisiest helicopters have either tandem rotor blade interaction (CH-47C), a very high main rotor tipspeed (UHIN), or an unmuffled reciprocating engine exhaust (47G). The 206L and 500C are intermediate cases. The 206L is similar in configuration to the UHIN (2 bladed rotors) with lighter weight and lower tipspeeds. The 500C is similar in configuration to the 300C or S-61 but appears to have a noisy tail rotor even though its tipspeed is moderate at 690 fps. If the UHIN and CH-47C are flown at their airspeed for lowest noise, a line with a slope of 10 log of the gross weight can be drawn through the three noisiest helicopters tested. This again indicates that, except for "compressibility bang" on the UHIN and CH-47C, helicopter noise tends to vary logarithmically and directly with weight. That is, as the gross weight of the design point is doubled the noise also doubles resulting in a 3dB increase.



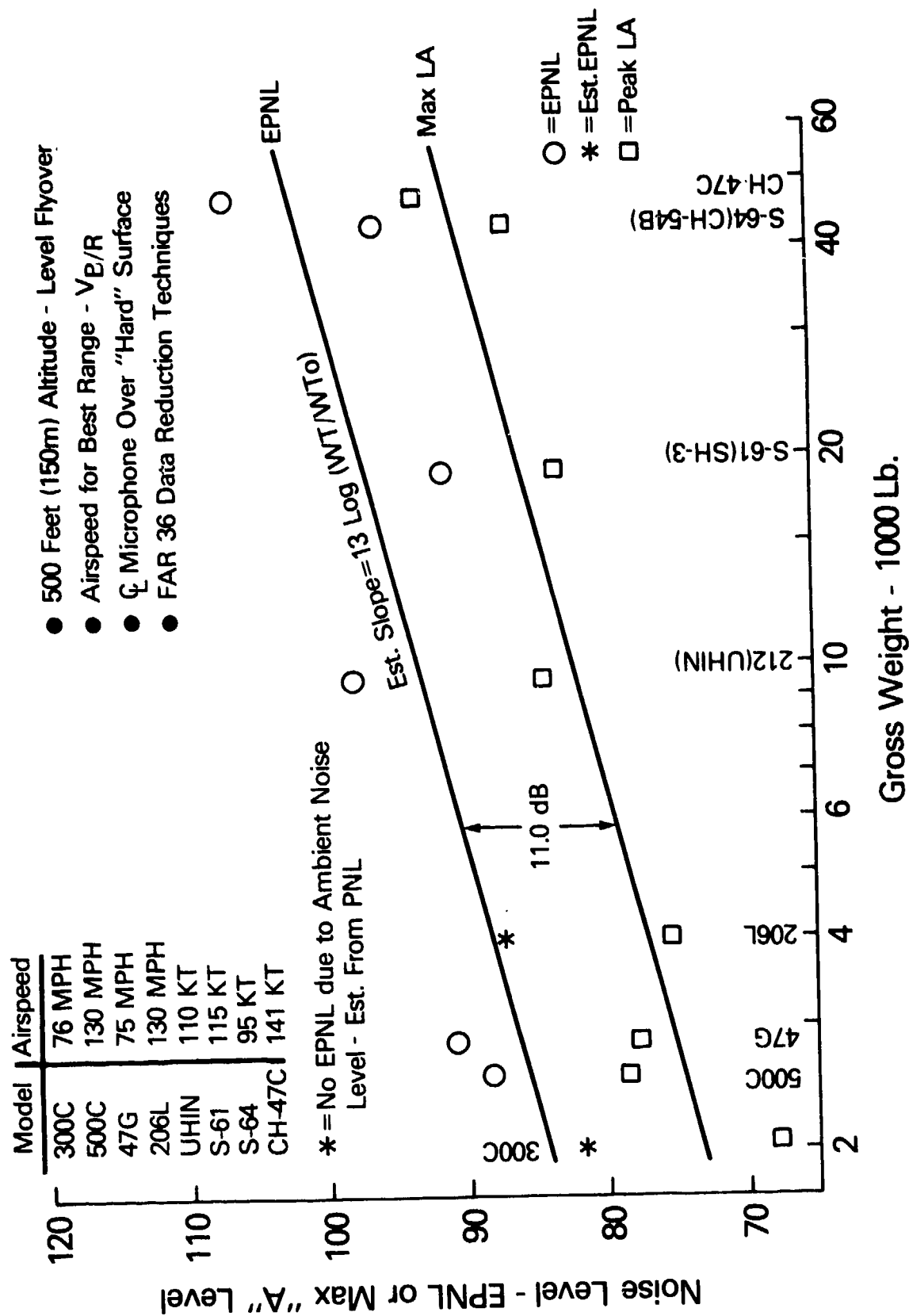
The effect of "compressibility blade slap" on the flyover time history is shown on Figure 5. The S-64 and 500C have a triangular shaped time history with the peak noise occurring just after the helicopter passes over the microphone. The maximum noise is controlled by the tail rotor and sounds somewhat like a propeller driven airplane. The main rotor can only be heard as the helicopter is well ahead of or past the microphones. The CH-47C and UHIN however have peak noise well before overhead passage and a trapezoidal shaped time history caused by the highly directional compressibility blade slap. After overhead passage the noise is controlled by the tail rotor and the shape of the time history is similar to the "non-slapping" 500C and S-64. The location and level of the blade slap on the flyover time history with the resulting long time duration gives "slappers" such as the UHIN and CH-47C and EPNL penalty of 3-5 EPNdB relative to the non-slappers such as the 500C and S-64. Therefore a duration correction is probably needed to assess helicopter noise during a flyover and the duration correction may, by itself, act as a penalty for the annoying nature of blade slap noise.

The effect of glideslope on approach noise level is shown on Figure 6 for both maximum A-weighted level and EPNL. The zero degree glideslope was taken from level flyover data at the approach airspeed of 60 Kts and raised 2dB to account for the 400 foot (120m) altitude of the approaches compared to 500 feet (150m) for the level flyovers. As shown on Figure 6 the noise level does not vary appreciably with glideslope. However, the approach noise for the UHIN and CH-47C is less than during a high speed flyover because of the low airspeed during approach and resulting lower levels of compressibility blade slap. Nearly all of the helicopters had some blade slap during most of the approaches due to the main rotor passing through its downwash. Usually, however, this slap did not occur at the time of peak noise and therefore was not a major factor in determining noise level. Generally the approaches sounded similar to the level flyovers but with more main rotor slap away from the overhead position.

The noise level of the sideline microphones is compared to the centerline microphone on Figure 7 for level flyovers at the velocity for best range. With few exceptions the sideline microphones receive 1 to 3 dB less noise than the centerline microphone. At overhead passage the altitude is equal to the sideline distance and, if the helicopter was a non-directional noise source, the sideline noise level would be about 2dB lower than the centerline due to the longer propagation path for those helicopters with maximum flyover noise at the overhead position. However, the typical helicopter directivity pattern propagates slightly more noise in the direction of the sideline microphone than towards the centerline microphone because the sideline microphones receives more noise relative to the centerline microphone than a non-directional propagation pattern would indicate. This propagation non-uniformity is small and maximum flyover noise generally occurs below the flight path centerline.

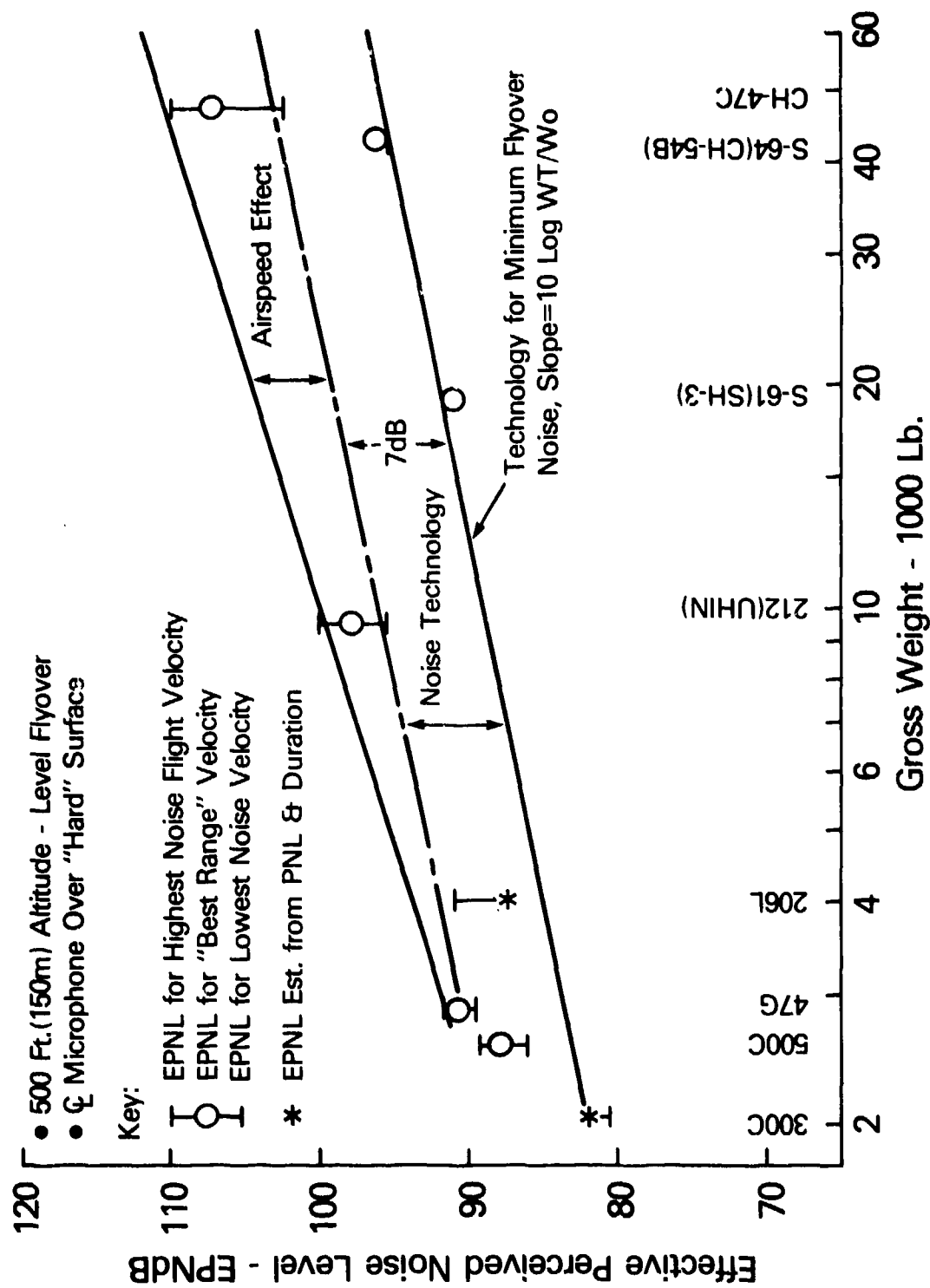
Selected narrow band spectra and sound pressure waveforms during the helicopter flyovers were evaluated. Figure 8 compares the sound pressure waveform of the UHIN and Hughes 500C near the time of maximum noise generation. The UHIN waveform is highly impulsive and characteristic of the noise generated by blade slap with the spikes corresponding to the passage of each main rotor blade. The 500C waveform shows a much more uniform distribution of acoustic energy over time. The taller pulses (25 millisecond spacing) correspond to the main rotor blade passing frequency, adjusted for doppler shift, and the other pulses to the tail rotor at its higher frequency. The higher frequency generated by the tail rotor causes its noise to be more readily heard by the human ear and it appears that the tail rotor controls the subjective noise level of the 500C at the near overhead position shown in Figure 8. The 500C waveform is not appreciably different from that obtained from jet mixing noise generated by jet powered aircraft and is typical of noise generated near the overhead position during a flyover.

The striking difference in the waveforms on Figure 8 has lead to proposed measures, discussed in Section 7.3, to attempt to evaluate the physical penalty which should be placed on impulsive noise. Noise levels in this report are based on a "slow" meter response (about one second averaging time) to be consistent with FAR Part 36. This "slow" response measures the average root mean square sound pressure and the difference between peak sound pressure and average level (crest factor) will be much higher for the UHIN than for the 500C waveform. Since the 500C waveform is fairly similar to the waveform from jet mixing, slow meter response measuring the 500C waveform would give noise levels approximately comparable to those from jet powered aircraft on a peak to average level basis. However, the peak levels on the UHIN waveform would be significantly undermeasured by slow response. The proposed measures (Section 7.3) to penalize impulsive noise generation are an attempt to quantify the peak to average sound pressure level differences between different helicopters and noise generation mechanisms. However, as previously mentioned, the typical directivity pattern of highly impulsive blade slap noise dramatically increases the duration of the noise during a helicopter flyover. Therefore, a duration correction, such as in EPNL, may provide a penalty for highly impulsive blade slap noise sufficient to both adequately raise reported flyover noise levels to account for the presence of blade slap and to discourage design configurations which generate large amounts of blade slap from use in future helicopter designs.



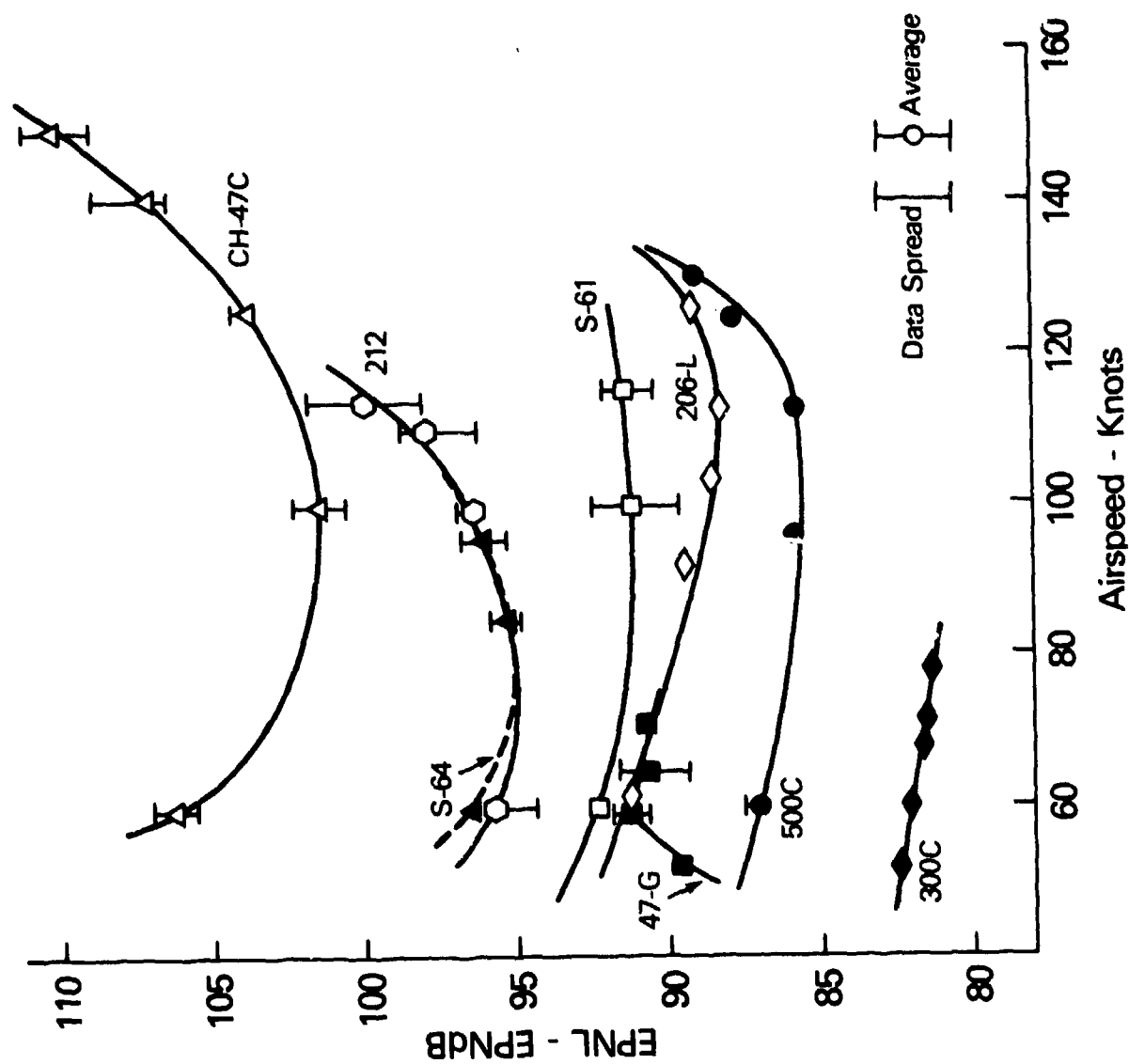
## Helicopter Noise Levels

Figure 1



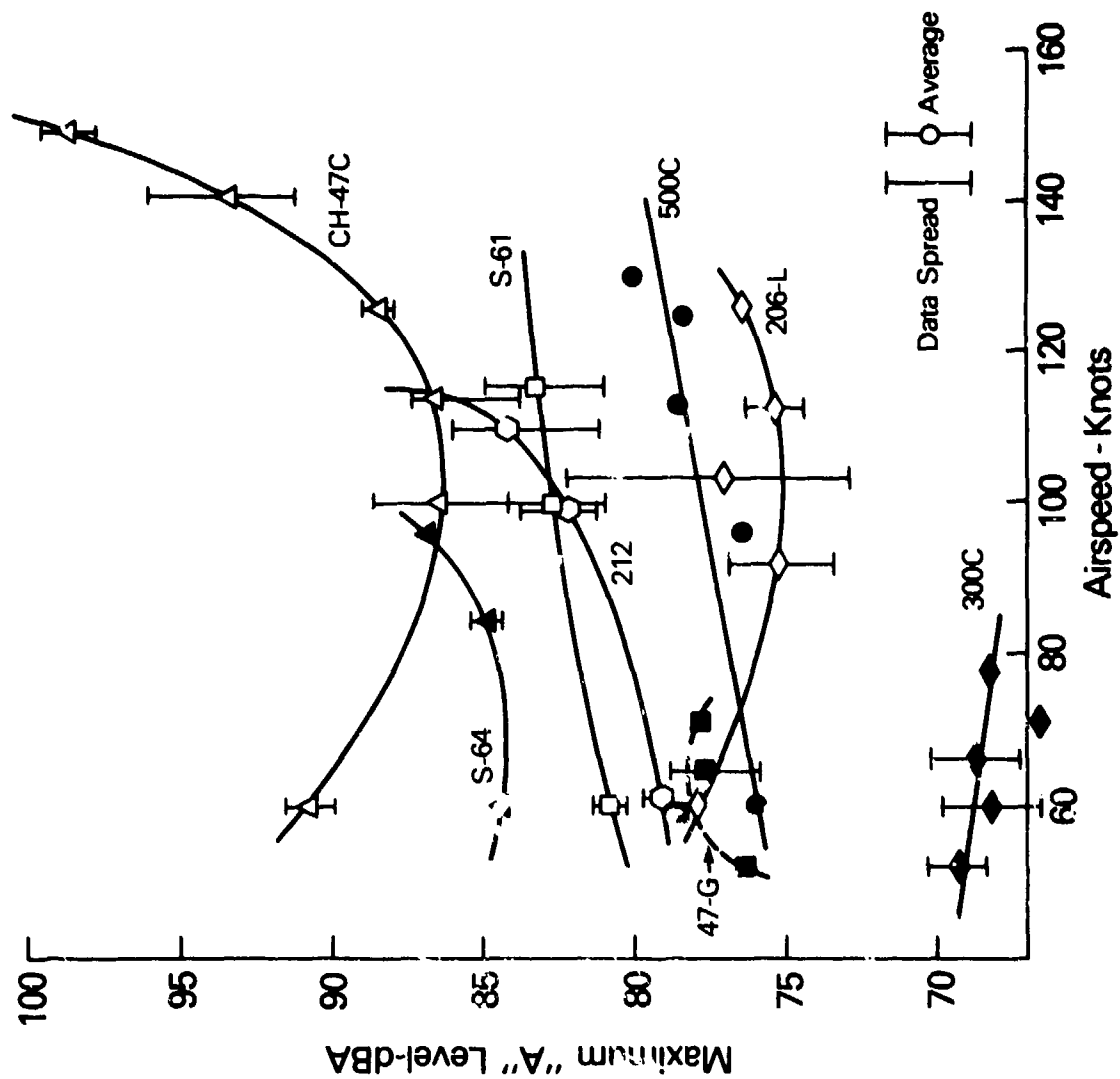
## Helicopter Noise Levels- Technology & Velocity Dependence

Figure 2



**Effect of Airspeed on Noise Level**

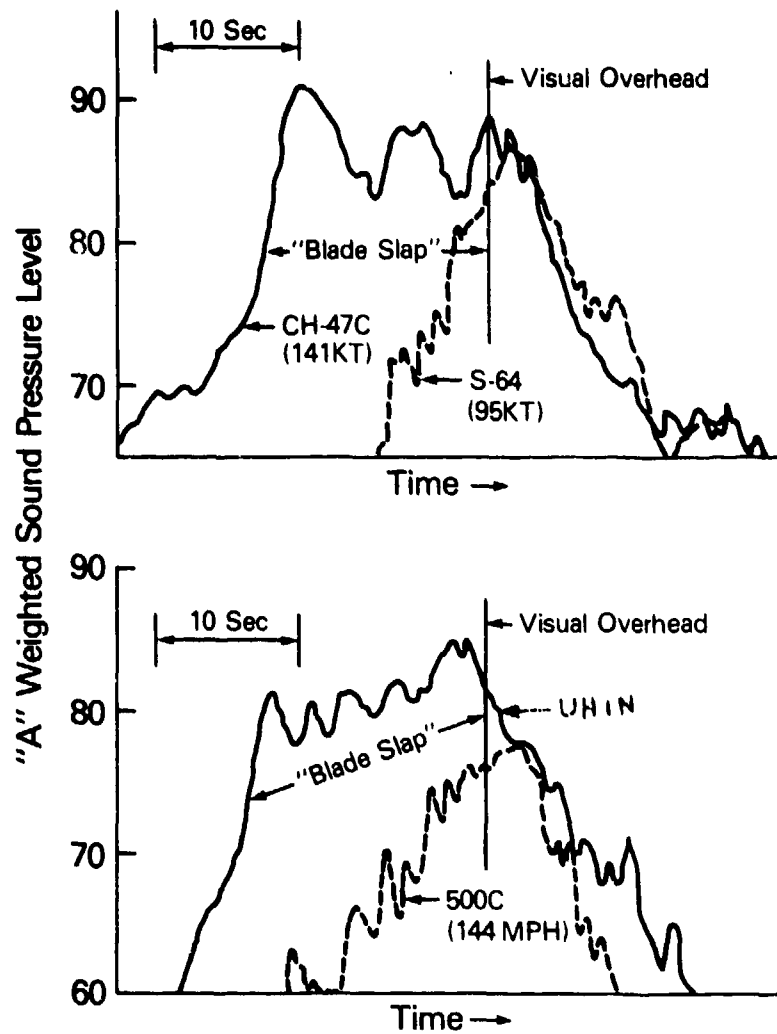
**Figure 3**



**Effect of Airspeed on Noise Level**

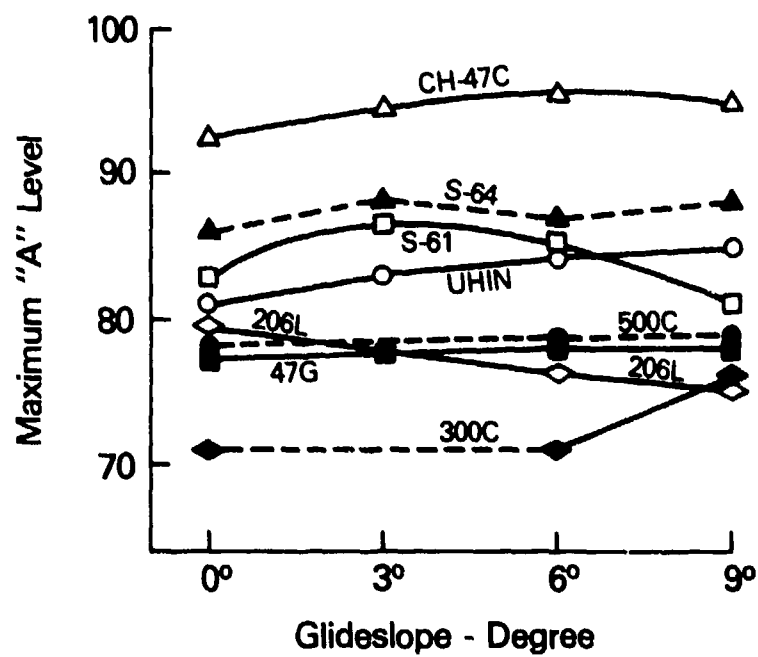
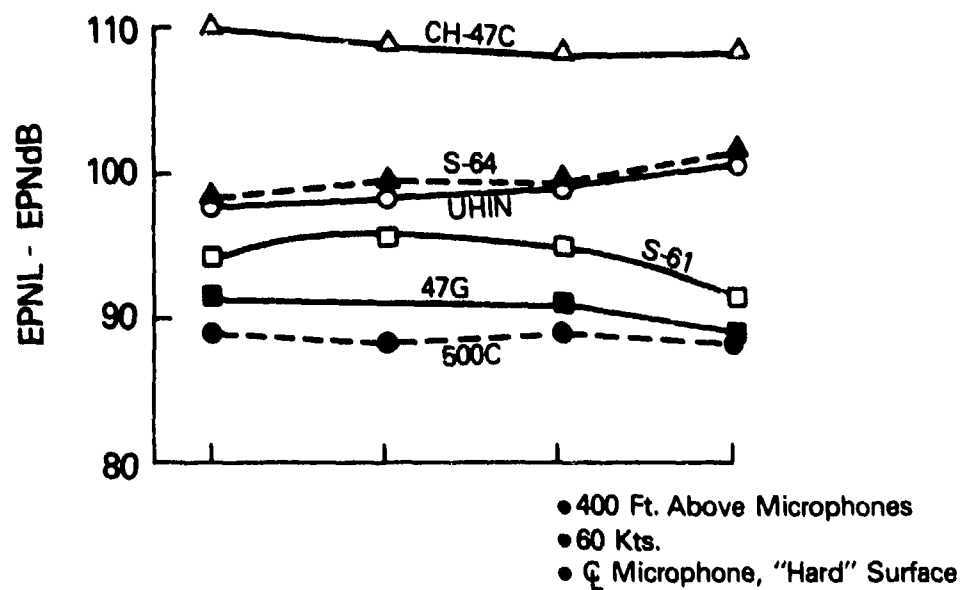
Figure 4

- 500 Ft. (150m) Altitude
- $\phi$  Microphone



## ***"A" Weighted Time Histories***

**Figure 5**



## Effect of Glideslope Angle on Noise Level

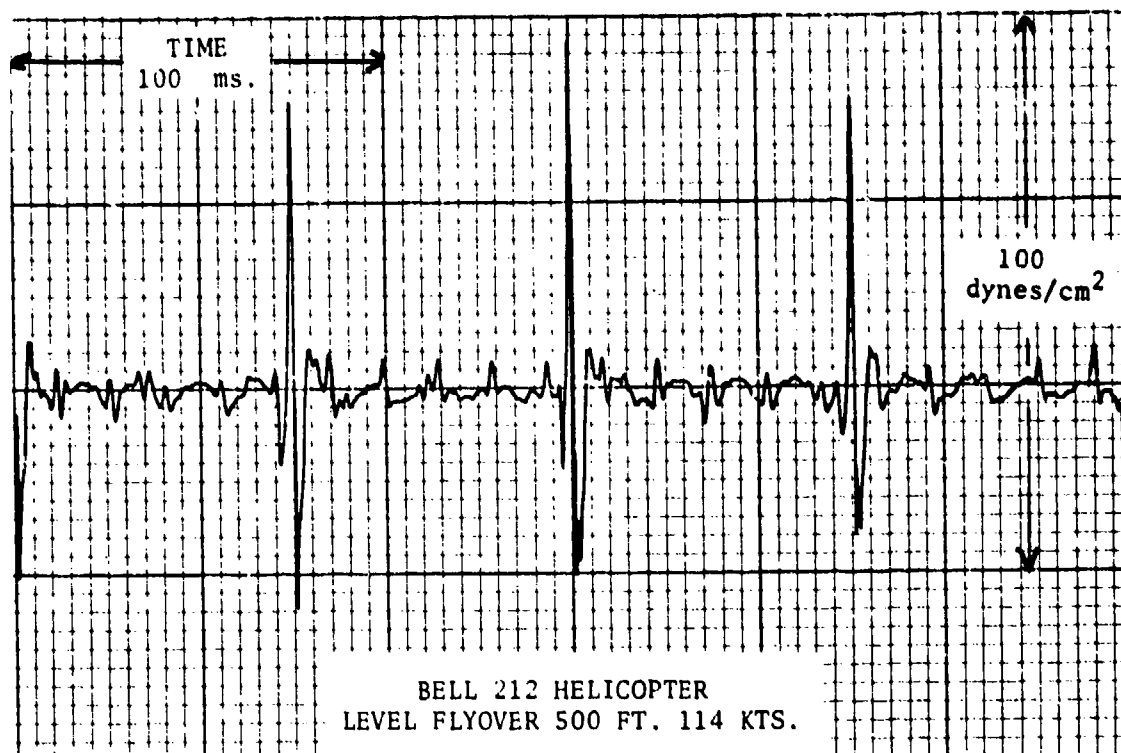
Figure 6





**Figure 7**

PEAK SOUND PRESSURE, DYNES/CM<sup>2</sup>



PEAK SOUND PRESSURE, DYNES/CM<sup>2</sup>

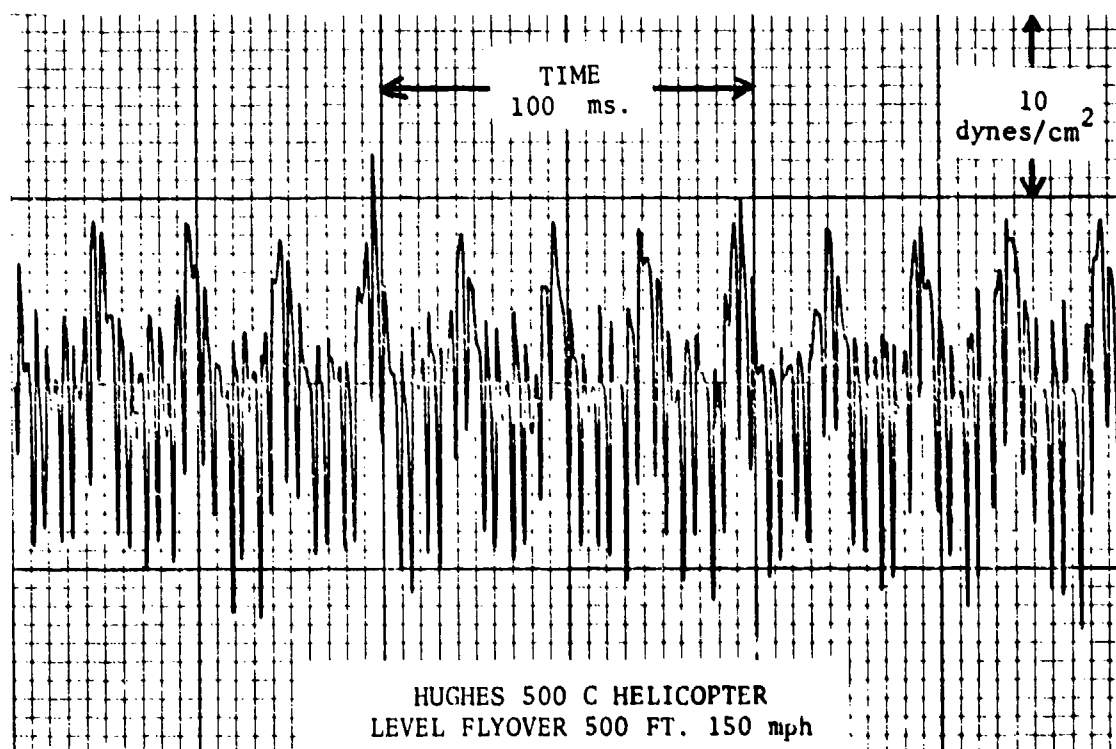


FIGURE 8

COMPARISONS OF ACOUSTIC  
PRESSURE WAVEFORMS

## 1.0 INTRODUCTION

At the request of the Office of Environmental Quality (AEQ), the Environmental Research Branch of the Systems Research and Development Service (SRDS), ARD-550, conducted a helicopter noise test to obtain noise level data as a data base for possible helicopter noise regulatory standards. The test helicopters were provided by the helicopter industry, the U.S. Army, U.S. Air Force and National Aeronautics and Space Administration (NASA) Langley Research Center (LaRC). The noise measurement and assessment laboratory at the Department of Transportation (DOT) Transportation Systems Center (TSC) Cambridge, Massachusetts provided acoustic data acquisition and reduction. The Federal Aviation Administration (FAA) provided test management, analysis and reporting.

This report presents data trends and comparison of the eight helicopters tested. Overall trends of Effective Perceived Noise Level (EPNL) and peak A-weighted noise as a function of flight parameters are described in the report summary along with a brief description of the noise from several classes of helicopters. This is followed by a description of the test helicopters in Section 2.0, the test procedure in Section 3.0 and the data reduction procedures in Section 4.0. A detailed discussion of the flyover and approach noise characteristics is in Section 5.0 including the effect of different noise measures such as A level, D level and PNL. One-third (1/3) octave band spectra are also discussed. Hover noise is discussed in Section 6.0. Narrow-band spectra and corrections for impulsive noise are discussed in Section 7.0. The impulsive noise corrections were performed by Bolt, Beranek and Newman, Incorporated (BBN) under contract to the FAA and tabular printouts of this data are available in BBN Report No. 3425. The TSC 1/3 octave band printouts and time histories are published in FAA Report No. FAA-RD-77-57.

## 2.0 HELICOPTER DESCRIPTIONS

### 2.1 Physical Description

The eight helicopters tested during this Helicopter Noise Test Program constituted a wide range of gross weights and included participation from several helicopter manufacturers. Helicopter availability was initiated by the manufacturers and obtained from user organizations including private business, the military and company demonstration models. The helicopter models used in the test program were:

<u>HELICOPTER MODEL</u>	<u>MILITARY DESIGNATION</u>	<u>TEST DATE</u>	<u>TEST LOCATION</u>
Hughes 300C	--	10/14/76	Dulles Airport
Hughes 500C	--	10/28/76	NASA Langley
Bell 47G	--	10/5/76	Dulles Airport
Bell 206L	--	10/14/76	Dulles Airport
Bell 212	UHIN	10/6/76	Dulles Airport
Sikorsky S-61	SH-3A	10/28/76	NASA Langley
Sikorsky S-64 ("Skycrane")	CH-54B	10/28/76	NASA Langley
Boeing Vertol ("Chinook")	CH-47C	10/13/76	Dulles Airport

TABLE I contains a table of the general characteristics of each helicopter.

Use of the Bell 47G and 206L and the Hughes 300C and 500C was arranged by the area representative of Bell Helicopter and Hughes Helicopter respectively. The Sikorsky S-61 (SH-3A) was provided by the NASA LaRC at Hampton, Virginia. The Bell 212 (UHIN) was provided by the U.S. Air Force from Andrews Air Force Base in Maryland, the Sikorsky S-64 "Skycrane" (CH-54B) was provided by the U.S. Army from Fort Eustis, Virginia, and the Boeing Vertol (CH-47C) was provided by the U.S. Army from New Cumberland, Pennsylvania. All helicopters were tested at or near their

maximum gross weight. In most instances this required the use of additional ballast. For the smaller helicopters this required the use of a few hundred pounds of ballast in the form of lead bars. However, for the larger helicopters the problem of ballast was solved in various ways. The Sikorsky S-61 provided by NASA was heavily instrumented because the helicopter is used for various research projects. The Sikorsky S-64 "Skycrane" carried an army truck for ballast which could be easily detached from the helicopter. As a result it was possible to test the S-64 "Skycrane" both with and without the army truck (a difference of approximately 13,500 lbs.). In the case of the Boeing Vertol CH-47C two empty 600 gallon fuel tanks were mounted inside the fuselage of the helicopter and filled with water to give additional ballast of approximately 10,100 lbs. Table II contains a detailed list of the weight components that comprised each helicopter's total gross weight during testing.

Photographs of the helicopter models tested are shown on Figures 9 to 16.

## 2.2 Helicopter Power Settings

Helicopter power settings for several test conditions are listed in Table III. The actual readings obtained in the cockpit are shown followed by the power referenced to that during the five foot hover. The power for the turbine powered helicopters was obtained from the standard on-board torquemeter. This instrument typically read in "percent" (psi for the 500C) and, since the rotors operate at constant rpm, torque is proportional to and gives an indication of the power used. Since the torquemeter uses an arbitrary reference, the percentage of hover power is shown for convenience. The piston engined helicopters used a manifold pressure gage to measure horsepower.

Helicopter power requirements show the "bucket" (i.e. a "U" shaped plot of power required versus airspeed) phenomenon with increasing airspeed. High power is required for hover. As forward airspeed increases the power requirements decrease until a "bucket" is reached at a fairly slow airspeed. The power required then increases with airspeed until the maximum airspeed is reached. Maximum airspeed is limited by available power or other limitations such as vibration or gearbox limitations which restrict the maximum airspeed with VNE (airspeed not to be exceeded at a given weight) placards. Generally the power required at the fastest airspeed is equal to or greater than the hover power except when VNE limitations are encountered. The UH1N and S-64 airspeed was restricted by VNE and the power at the fastest airspeed tested was less than during hover.

TABLE I

HELICOPTER CHARACTERISTICS

MANUFACTURER	HUGHES		HUGHES		BELL	
MODEL	300C		500C		47G	
MILITARY DESIGNATION	--		--		--	
POWER PLANT	AVCO-Lycoming HI0-360-DIA		Allison 250-C20A		AVCO-Lycoming TVO-435-G1A	
TYPE	4-Cylinder Reciprocating Engine		Turboshaft		6-Cylinder Reciprocating Engine	
RATED OUTPUT AT SEA LEVEL	190 shp at 3200 RPM		400 shp at 6000 RPM		220 shp at 3200 RPM	
EMPTY WEIGHT (lbs)	1025		1086		1892	
MAX. T.O. GROSS WEIGHT (lbs)	1900		2550		2950	
FUEL CAPACITY (gallons)	19		61.5		57	
MAXIMUM AIR SPEED (mph)	105 (91 Kts)		152 (132 Kts)		105 (91 Kts)	
ECONOMIC CRUISE SPEED (mph)	100 (87 Kts)		143 (124 Kts)		83 (72 Kts)	
MAXIMUM RANGE (miles)	255		377		250	
FUSELAGE LENGTH (ft.)	30.92		23		31.58	
PASSENGER CAPACITY	3		6		3	
	MAIN ROTOR	TAIL ROTOR	MAIN ROTOR	TAIL ROTOR	MAIN ROTOR	TAIL ROTOR
NUMBER OF BLADES	3	2	4	2	2	2
DIAMETER (ft.)	26.83	4.25	26.33	4.25	37.125	5.83
AREA DISK (sq.ft.)	563.5	14.2	544.6	14.2	1083	26.8
MAX. GROSS WT./AREA DISK (lb/sq.ft.)	3.36	--	4.7	--	2.72	--
CHORD LENGTH (inches)	6.75	4.86	6.75	4.86	11	4.94
AREA PER BLADE (sq.ft.)	7.55	.86	7.4	.85	17.14	1.20
BLADE LOADING (lb./sq.ft.)	1.12	--	1.17	--	1.36	--
ROTOR RPM	471	3094	484	3110	370	2160
BLADE PASSAGE FREQ. (Hz)	24	103	32	104	12	72
TIP SPEED (ft./sec)	661	690	667	692	719	658

TABLE I cont.

HELICOPTER CHARACTERISTICS

MANUFACTURER	BELL		BELL		SIKORSKY	
MODEL	206L		212		S-61	
MILITARY DESIGNATION	--		UHIN		SH-3A	
POWER PLANT	Allison 250-C20B		Pratt & Whitney PT6T-3 "Twin-Pac"		2-Gen. Electric T58-GE-8B	
TYPE	Turboshaft		Two PT6 Turboshaft Engines		Turboshaft	
RATED OUTPUT AT SEA LEVEL	420 shp at 6000 RPM		1800 shp at 6600 RPM		1250 shp at 19,500 RPM(ea. eng.)	
EMPTY WEIGHT (lbs.)	1894		6000		11,865	
MAX. T.O. GROSS WEIGHT (lbs.)	3900		10,000		20,500	
FUEL CAPACITY (gallons)	98		215		700	
MAXIMUM AIR SPEED (mph)	150 (130 Kts)		121 (105 Kts)		166 (144 Kts)	
ECONOMIC CRUISE SPEED (mph)	136 (118 Kts)		100 (87 Kts)		136 (118 Kts)	
MAXIMUM RANGE (miles)	370		296		625	
FUSELAGE LENGTH (ft.)	33.9		41.9		54.75	
PASSENGER CAPACITY	7		15		15	
	MAIN ROTOR	TAIL ROTOR	MAIN ROTOR	TAIL ROTOR	MAIN ROTOR	TAIL ROTOR
NUMBER OF BLADES	2	2	2	2	5	5
DIAMETER (ft.)	37	5.17	48	8.5	62	10.33
AREA DISK (sq. ft.)	1074.7	20.97	1809	56.7	3019	83.9
MAX. GROSS WT./AREA DISK (lb./sq.ft.)	3.63	--	5.53	--	6.79	--
CHORD LENGTH (inches)	13	5.25	21	11.5	18.25	5.7
AREA PER BLADE (sq. ft)	18.05	1.13	42	4.07	44.54	2.46
BLADE LOADING (lb./sq. ft.)	1.82	--	2.76	--	1.36	--
ROTOR RPM	394	2550	324	1662	293	1136
BLADE PASSAGE FREQ. (Hz)	13	85	11	55	17	95
TIP SPEED (ft./sec.)	763	690	814	740	659	614

TABLE I cont.

## HELICOPTER CHARACTERISTICS

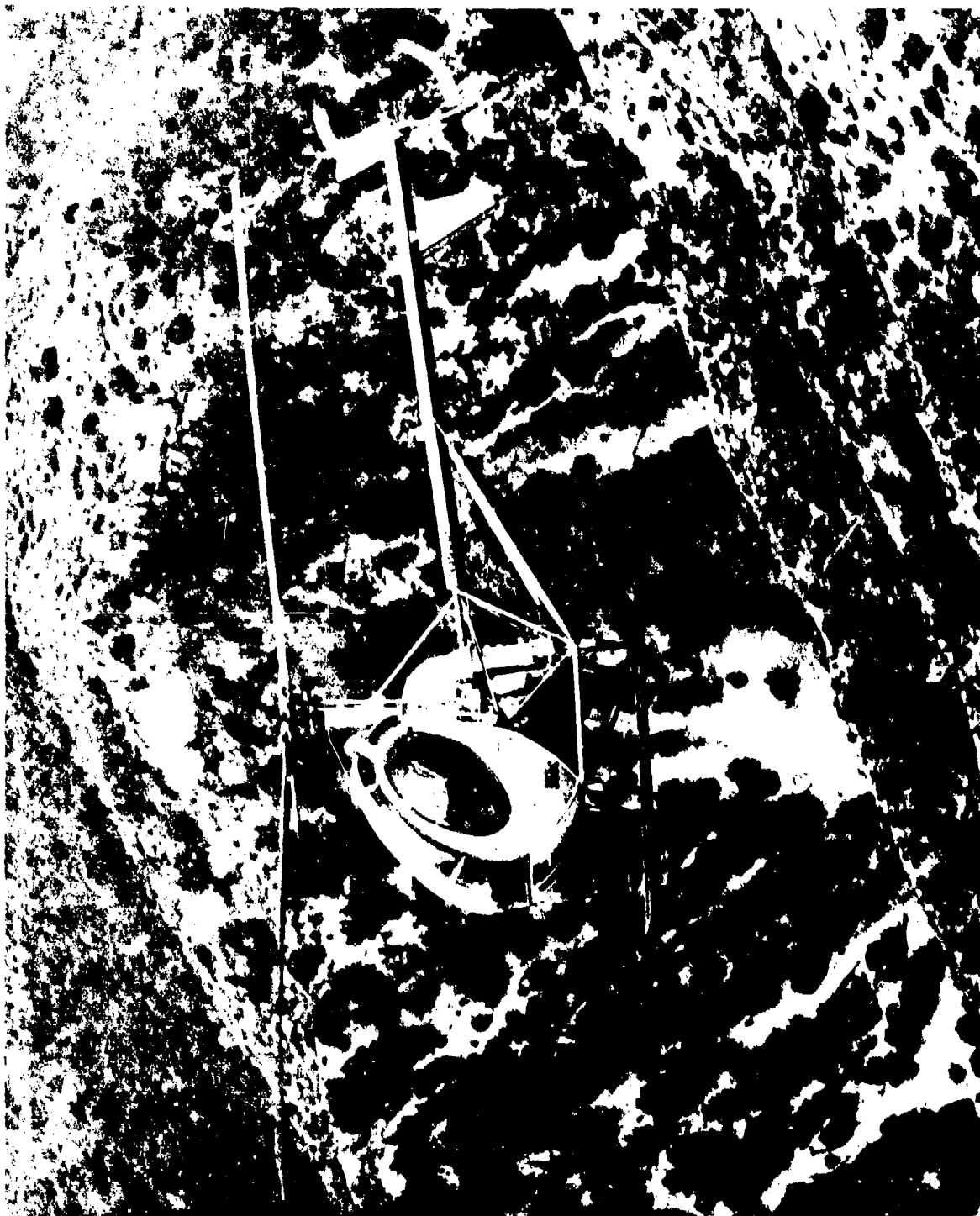
	SIKORSKY		BOEING VERTOL
	MAIN ROTOR	TAIL ROTOR	TANDEM ROTOR
MANUFACTURER	SIKORSKY		BOEING VERTOL
MODEL	S-64 "Skycrane"		114 "Chinook"
MILITARY DESIGNATION	CH-54B		CH-47C
POWER PLANT	2-Pratt & Whitney JFTD-12A-5A		2-AVCO-Lycoming T55-L-11
TYPE	Turboshaft		Turboshaft
RATED OUTPUT AT SEA LEVEL	4,800 shp (each eng.)		3750 shp at 15,680 RPM (ea. eng.)
EMPTY WEIGHT (lbs.)	19,234		20,378
MAX. T.O. GROSS WEIGHT (lbs)	47,000		45,000
FUEL CAPACITY (gallons)	880		1129
MAXIMUM AIR SPEED (mph)	127 (110 Kts)		190 (165 Kts)
ECONOMIC CRUISE SPEED (mph)	109 (95 Kts)		158 (137 Kts)
MAXIMUM RANGE (miles)	253		230
FUSELAGE LENGTH (ft.)	70.25		51
PASSENGER CAPACITY	4		33-44
NUMBER OF BLADES	6	4	3
DIAMETER (ft.)	72	16	60
AREA DISK (sq. ft.)	4070	201	2826/each
MAX. GROSS WT./AREA DISK (lb/sq.ft.)	10.3	--	7.96
CHORD LENGTH (inches)	26	15.4	25.25
AREA PER BLADE (sq.ft.)	78	10.27	63.1
BLADE LOADING (lb./sq.ft.)	1.71	--	1.33
ROTOR RPM	186	852	245
BLADE PASSAGE FREQ. (Hz)	18.6	57	3 Blades/Rotor $\Rightarrow$ 12 6 Blades/Helicopter $\Rightarrow$ 24
TIP SPEED (ft./sec.)	700	714	755
		16C	



TABLE II

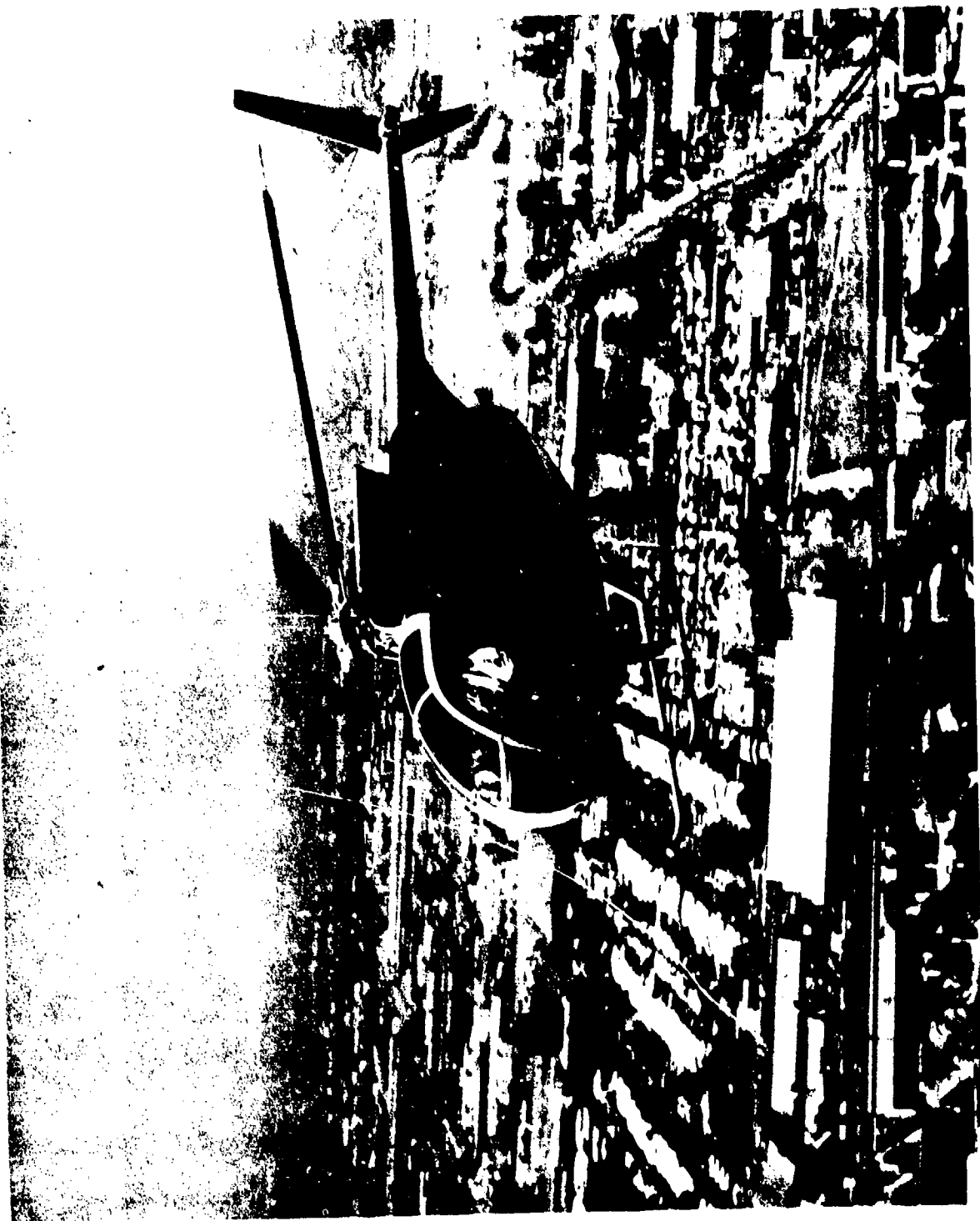
## HELICOPTER GROSS WEIGHT COMPARISONS

HELICOPTER MODEL	EMPTY WEIGHT	FUEL WEIGHT	BALLAST	INSTRUMENTATION AND CREW	MAXIMUM T.O. GROSS WEIGHT	GROSS WEIGHT DURING TEST
HUGHES 300 C	1025	130	200	450	1900	1800
HUGHES 500 C	1086	400	0	364	2550	2850
BELL 47-G	1892	370	200	388	2950	2850
BELL 206-L	1894	640	450	435	3900	3420
BELL 212 (UH1N)	6000	1400	400	1800	10,000	9600
SIKORSKY S-61 (SH-3A)	12,224	3000	0	3500	19,000	18,725
SIKORSKY S-64 (CH-54B) "SKYCRANE"	19,234	6600	13,500 (Army Truck)	3600	47,000	42,900
BOEING VERTOL (CH-47C) "CHINOOK"	20,400	6900	10,100 (1200 gal. water)	3600	45,000	41,000



HUGHES 300 C

FIGURE 9



HUGHES 500 C

FIGURE 10



BELL 47-G

FIGURE 11



BELL 206-L

FIGURE 12



FIGURE 13

BELL 212 (UH1H)



SIKORSKY S-61 (SH-3A)

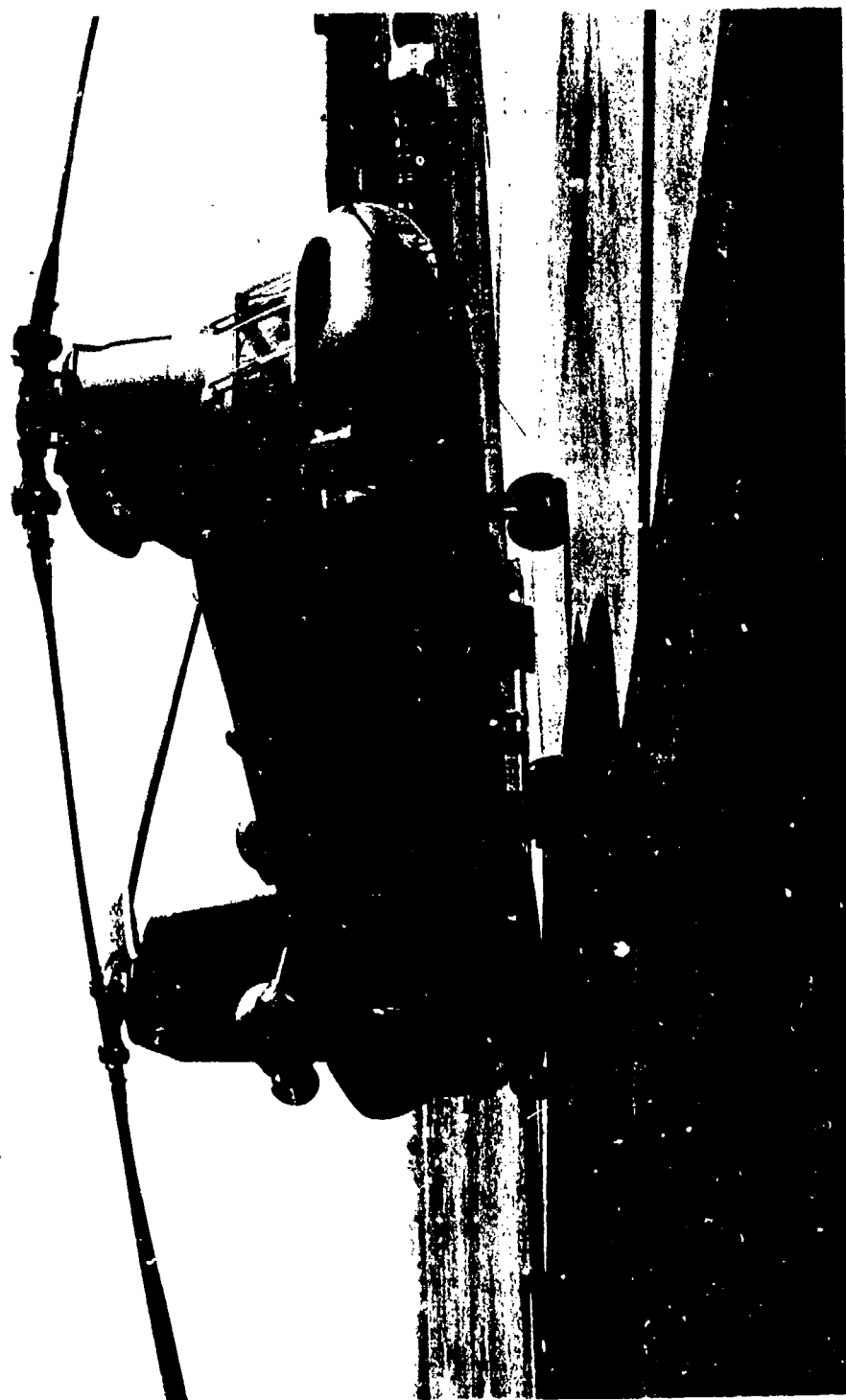
FIGURE 14



FIGURE 15

SIKORSKY S-64 "SKYCRANE" (CH-54B)





BOEING VERTOL "CHINOOK" (CH-47C)

FIGURE 16

TABLE III

## HELICOPTER POWER SETTINGS

HELICOPTER	HOVER			APPROACH			LEVEL FLYOVERS		
	5' HOVER	500' HOVER	3°	6°	9°	≈60KT.	V <sub>B/R</sub>	V <sub>MAX.</sub> @ SPEED	
S-64 (CH-54B) Heavy (Percent of Hover)	48-50% 100%	50-55% 104%	23% 22%	18% 35%	16% 32%	34-38% 69%	33-40% 70%	40% 77% @ 95KT	
S-64 (without Truck) (Percent of Hover)	27-30% 55%	26-30% 55%	--- ---	15% 29%	--- ---	24% 46%	30% 58%	35% 68% @ 105KT	
S-61 (SH-3) (Percent of Hover)	68-72% 100%	60-75% 97%	30-33% 44%	20-21% 29%	12-15% 19%	42-56% 70%	65-70% 97%	70-78% 104% @ 115KT	
CH-47C (Percent of Hover)	56% 100%	60-64% 110%	34% 60%	27% 48%	24% 43%	41% 73%	58-66% 114%	73% 130% @ 150KT	
Bell 212 (UHIN) (Percent of Hover)	69-72% 100%	65-78% 97%	35% 50%	34% 49%	20% 29%	40-41% 58%	55-63% 83%	60-64% 89% @ 114KT	
Bell 206L (Percent of Hover)	70-80% 100%	60-70% 91%	--- ---	15-18% 23%	11-13% 16%	35% 51%	78% 105%	80-89% 115% @ 145mph	
Hughes 500C (Percent of Hover)	42-44psi 100%	--- ---	22psi 50%	18-22psi 46%	9-12psi 25%	30psi 70%	42-46psi 104%	56psi 130% @ 150mph	
Hughe 300C (Percent of Hover)	24-26"Hg 100%	20-21"Hg 75%	--- ---	19"Hg 66%	14"Hg 36%	20"Hg 72%	21"Hg 78%	24"Hg 94% @ 90mph	
Bell 47G (Percent of Hover)	25"Hg 100%	25-26"Hg 102%	--- ---	16"Hg 40%	15-16"Hg 45%	21"Hg 78%	22-23"Hg 86%	24"Hg 94% @ 82mph	

### 3.0 TEST PROCEDURE

#### 3.1 Test Plan

The test procedure for each helicopter consisted of obtaining noise data during hover, level flyover, and approach conditions. During the hover portion of the test each helicopter was operated with a wheel clearance of about 5 feet and rotated with reference to the microphone array to record the noise levels at each 45° interval around the helicopter. Each angular location was marked so that the pilot could visually maintain the proper heading. Additional noise data was obtained at a 500 foot hover location. However, because of the windy conditions and the difficulty in keeping the helicopter positioned directly over the microphone array, only a limited amount of data was obtained at this altitude.

During the level flyover portion of the test, each helicopter was flown over the microphone array at an altitude of approximately 500 feet (150 meters) at airspeeds of 90, 100, and 110 percent of the best economical long range cruise speed and at an approach airspeed of about 60 Kts.

Approaches were flown at target glide slopes of 3, 6, and 9 degrees such that the altitude of the helicopter as it passed over the microphone array was held constant at 400 feet (120 meters). A portable theodolite was used to establish the approach glideslopes and verbal "fly-up/fly-down" commands were given to the pilot in order to keep the helicopter descending along the proper glide-slope. This procedure proved to be satisfactory and the approaches were performed with a high degree of accuracy. Figure 17 schematically describes the operation showing the relative location of the theodolite with respect to the microphone array for each of the different glideslopes. All approaches were flown at a constant airspeed of either 60 mph or 60 Kts (depending on the nomenclature of the on-board airspeed indicator--usually mph for civilian operated helicopters and Kts for military operated helicopters).

Most approaches and level flyovers were repeated several times to determine the degree of data repeatability achievable. The helicopter airspeed and altitude were monitored directly from the on-board instrumentation while photographic techniques were used to check the helicopters altitude as it passed directly over the microphone array.

#### 3.2 Microphone Instrumentation and Location

During hover the microphone array consisted of four microphones, two on each side of the hover location at distances of 246 feet

(75 meters) and 492 feet (150 meters). For the 500 foot hover, the level flyovers and approaches, the microphone array consisted of both sideline locations of 492 feet and two centerline microphones directly below the flight path of the helicopter. All microphones were mounted four feet (1.2 meters) above the ground (per FAR 36 requirements) along a line perpendicular to the flight path. Figure 18 shows the details of the microphone arrangement.

For this helicopter noise test program, four identical measuring systems were used. The microphone systems, data acquisition and data reduction was provided by the Department of Transportation (DOT) Transportation Systems Center (TSC) "Noise Measurement and Assessment Laboratory." Each system consisted of a General Radio Model 1962-9601, 1/2-inch pressure sensitive random incidence electret-condenser microphone with a B&K Model UA-0237 windscreen. In addition, a General Radio Model P42 Microphone Preamplifier was used to amplify the output of the microphone and provide impedance matching so that long cables could be used between the microphone/preamplifier combination and the recording system without signal loss or degradation in frequency response. The microphones were mounted four feet above the ground and oriented so that their diaphragm was essentially in the plane of the flight path of the aircraft (grazing incidence).

The data was recorded on two, two channel Nagra IV SJ Scientific Tape Recorders using Scotch-888 recording tape. The recorders were operated in a direct mode at a tape speed of 7.5 inches per second. A third track on each recorder was used for voice annotations which consisted of the run number, flight conditions before each run and a verbal marker used to identify the time at which the helicopter passed over the microphone array.

Field calibrations of the microphone/recorder system were performed every hour using a General Radio 1562-A Sound Level Calibrator which generates a 1000 Hz tone at a sound pressure level of 114 dB. In addition, a passive microphone simulator was substituted for the actual microphone to determine the minimum discernable sound pressure level (noise floor) of the system. The dynamic range of the measuring system was approximately 55 dB.

A Climatronics Model Electronic Weather Station (EWS) was used to continuously monitor and record the temperature, humidity, wind speed and direction. The wind sensors were located at a height of ten feet above the ground while the temperature and humidity sensors were located at a height of five feet. The weather station was located 250 feet from the flight path centerline in the plane of the sideline microphones.

### 3.3 Test Sites

The helicopter noise tests were conducted at two different sites. Five of the helicopters were tested at Dulles International Airport while the remaining three were tested at NASA Langley Research Center (LaRC) at Hampton, Virginia.

The test area at Dulles Airport was the old TRANSPO site north of the terminal and east of Runway 1 Left--19 Right (1L-19R). The test area was bounded on the west by the taxiway to the east of 1L-19R, on the south by the center of the terminal parking lot, on the east by the eastern edge of the terminal parking lot (north-south portion of the access road), and to the north by Route 606. The noise tests were conducted within these boundaries which provided a test area of approximately 3500 feet wide by 12,000 feet long. The surface of the test area consisted of a combination of decomposing asphalt, dirt and gravel. This surface was somewhat soft for a depth of about 2 inches and then become hard such that markers could only be driven in with some difficulty. Because of this surface, one of the centerline microphones (designated as-centerline west/hard surface) was installed over a hard plywood surface 16 feet long and 4 feet wide. The test site at Dulles Airport is described in Figure 19. All testing took place between the hours of 7:30 a.m. and 4:30 p.m. with occasional interference from commercial and general aviation activity at the airport. As a result, it was necessary to abort several runs because of the noise interference generated by the takeoff and landing of these aircraft.

The test site at NASA LaRC was located at the north end of Runway 17-35 with the flight path of the helicopters centered along the east edge of the runway. During the 5 foot hover portion of the test, three of the four microphones were located over concrete while the fourth microphone (designated 75m or east side-line/soft surface) was located over grass about three inches high. During the 500 foot hover, level flyovers and approaches the main centerline microphone used in most of the data analysis (designated-west centerline/hard surface) was located over concrete while the alternate centerline microphone was over grass. Figure 20 shows the test site in relation to the NASA LaRC airfield. Intermittant noise interference from military aircraft takeoff and landings from Langley Air Force Base (adjacent to the NASA LaRC) posed some delays.

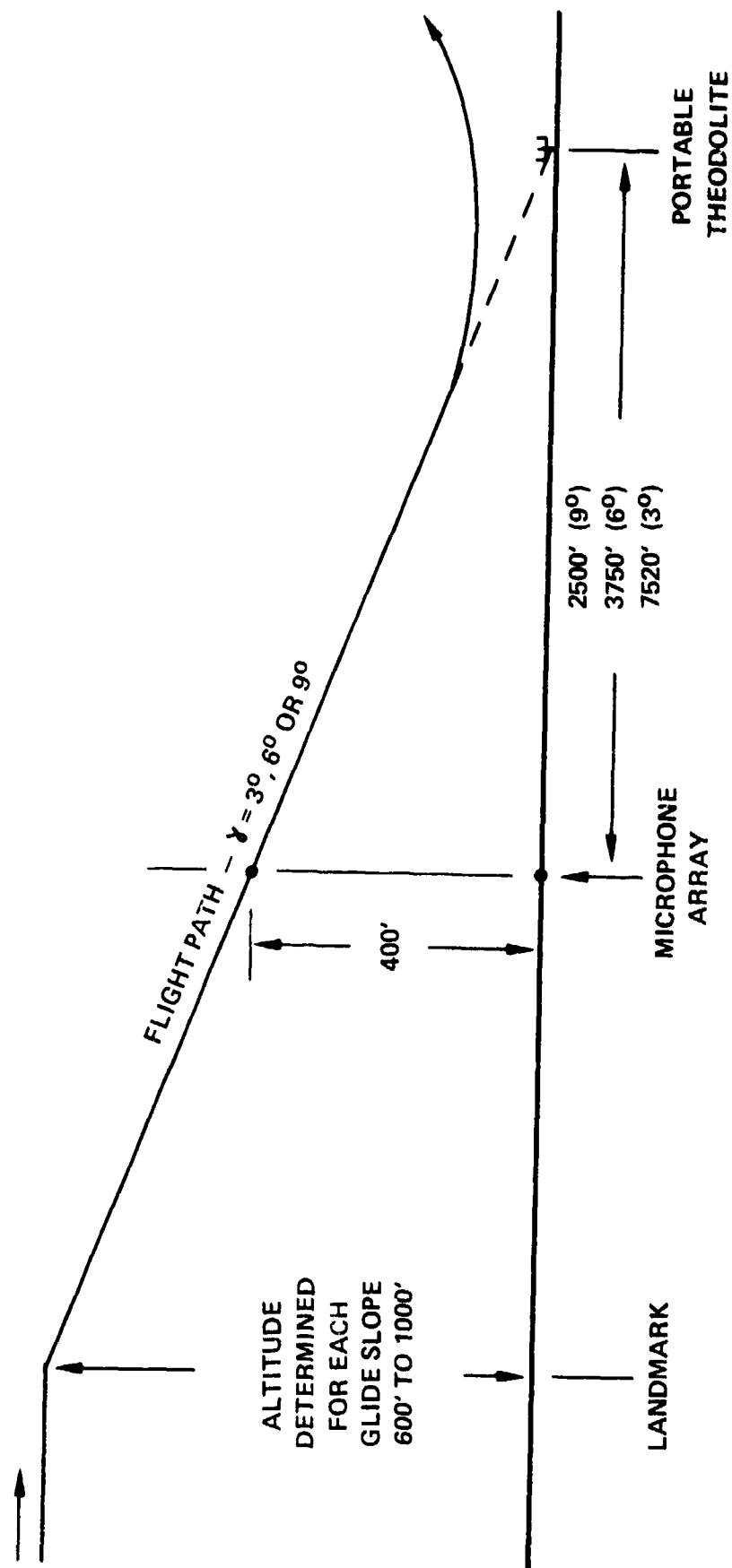


FIGURE 17. APPROACH PROCEDURE.

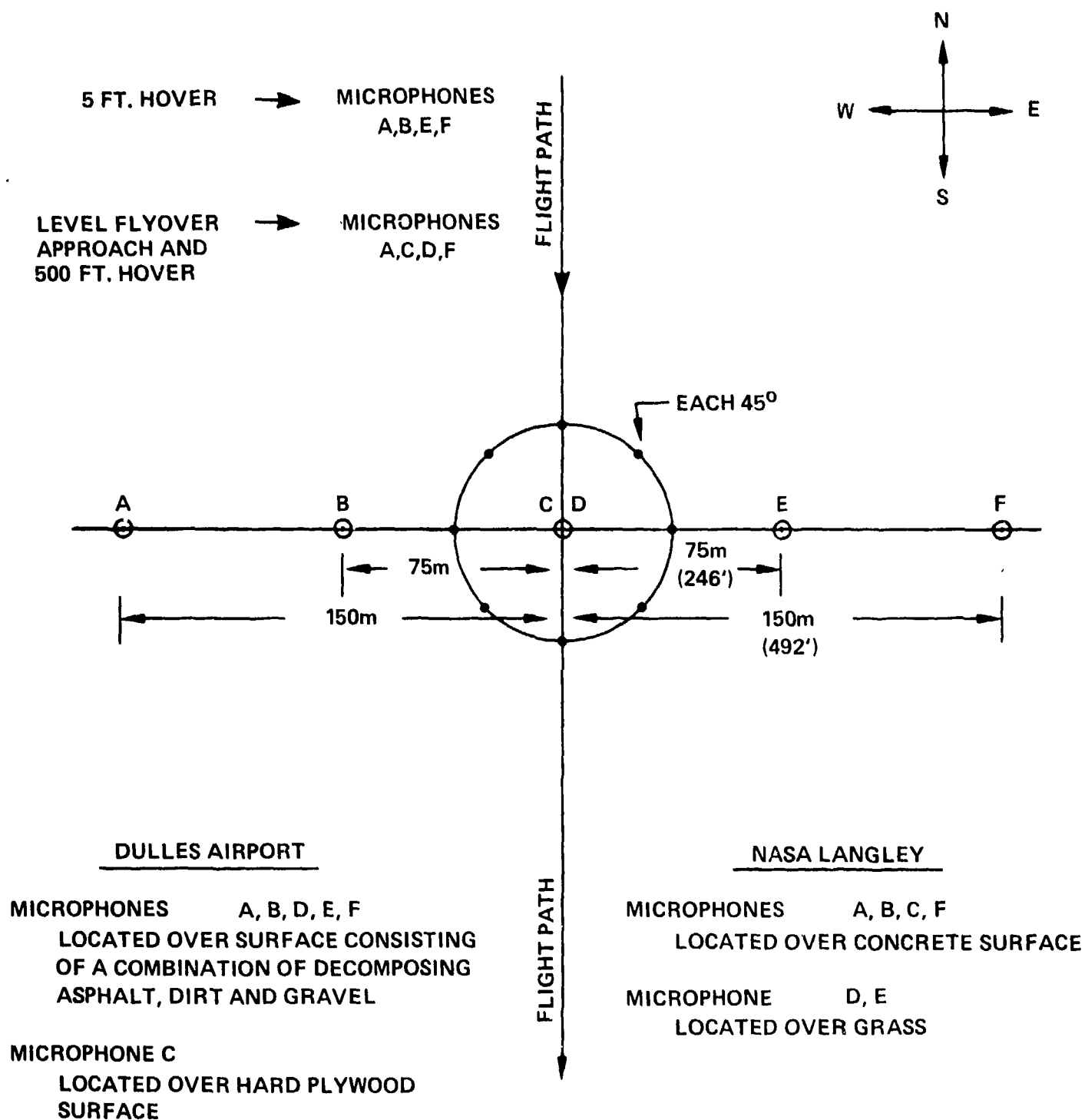


Figure 18. MICROPHONE ARRAY FOR  
HELICOPTER NOISE TEST.

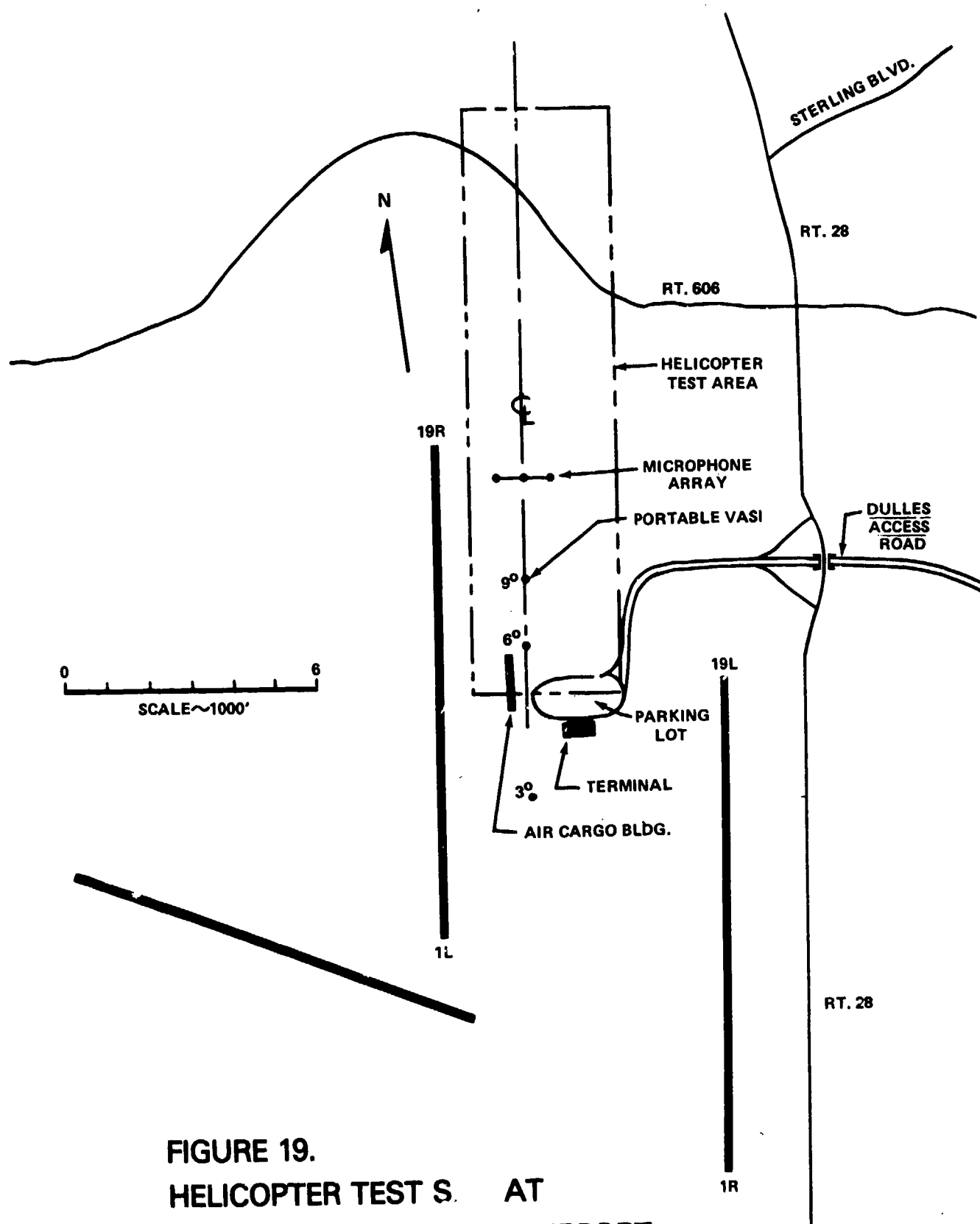


FIGURE 19.  
HELICOPTER TEST S. AT  
DULLES INTERNATIONAL AIRPORT.



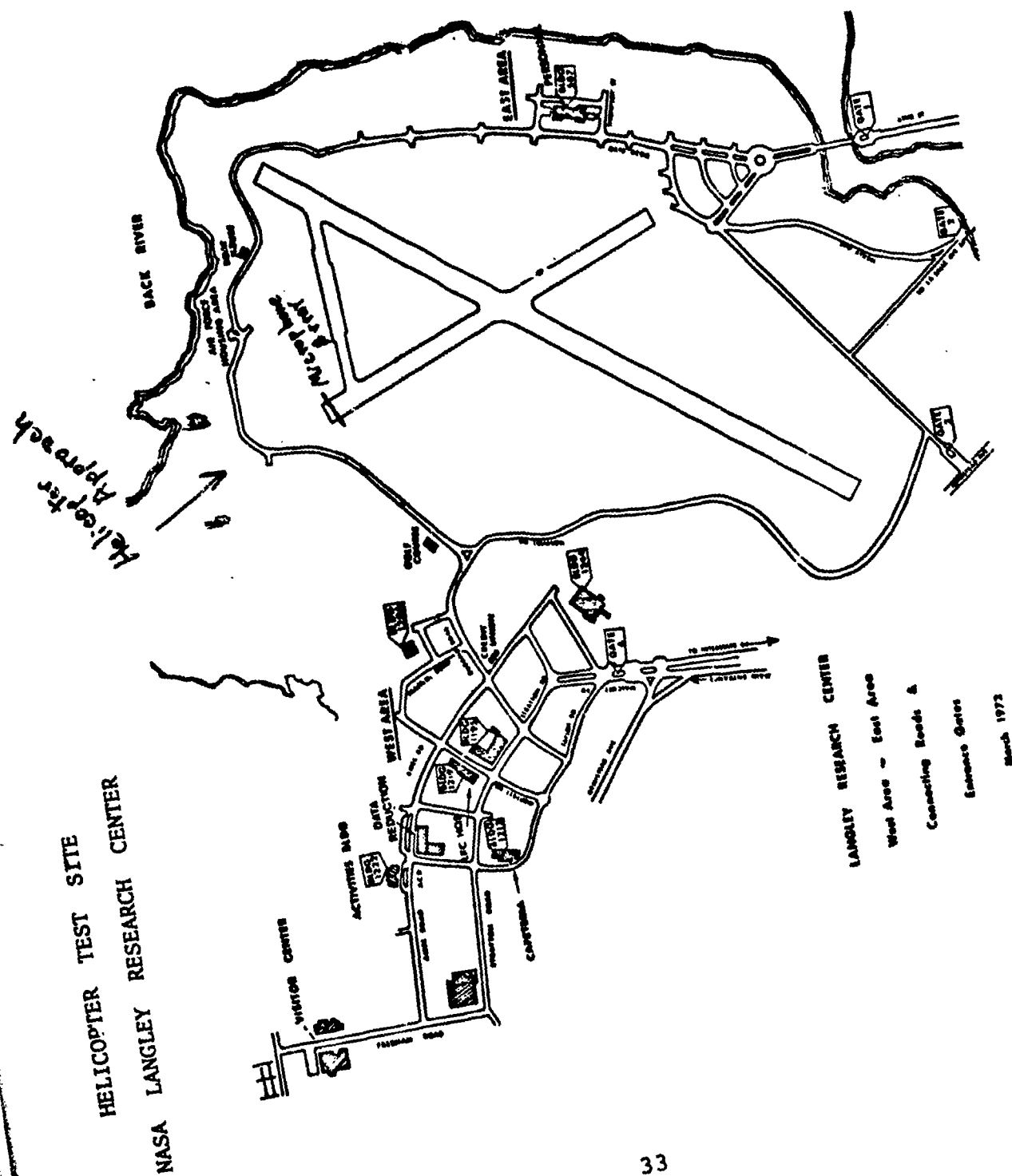


Figure 20

#### 4.0 DATA REDUCTION SYSTEM

The noise data plus the calibration signals that were recorded on the magnetic tape were fed into a modified General Radio 1921 Real Time Analysis System made up of a General Radio 1925 Multifilter and General Radio 1926 Multichannel RMS Detector. The necessary gain adjustments were made in the multifilter using the recorded calibration signals.

The GR-1925 Multifilter consisted of a set of parallel contiguous one-third octave filter channels from 25 Hz to 10 KHz plus a standard "A" weighted network, an accepted "D" weighted network and an unfiltered channel with a flat frequency response to provide Overall Sound Pressure Levels (OASPL). All outputs from the multifilter were fed into the GR-1926 Detector which sampled and computed the RMS level in dB for each channel for a 1/2 second measurement period. These levels were then converted to digital outputs and were fed into the Wang 720C computer which was programmed to store the digitized data in the Wang 730 Disc System. The analysis system has a dynamic range of 60 dB.

Data stored in the Wang 730 Disc System was processed as follows:

Hover Test -- Data from thirty-eight (38) 1/2 second integration periods were averaged together on an energy basis and data printed out for the average level, the maximum level and the minimum level versus 1/3 octave frequency bands (25 Hz to 10 KHz), plus the OASPL, PNL, PNLT and the "A" and "D" weighted noise levels.

Level Flyover and Approach Tests -- The data stored on the disc was processed according to FAR 36 procedures without corrections for temperature, humidity or aircraft position for each level flyover and approach condition. The processed noise levels consisted of the Effective Perceived Noise Level (EPNL), the Maximum Perceived Noise Level (PNL(M)), the Maximum Tone Corrected Perceived Noise Level (PNLT(M)), the maximum "A" weighted noise level (dBA(M)), the maximum "D" weighted noise level (dBD(M)) and the Maximum Overall Sound Pressure Level (OASPL). In addition, the processed data includes a time history of PNL, PNLT, dBA, dBD and OASPL at 1/2 second time intervals during flyover plus the 1/3 octave band spectra for about ten 1/2 second intervals during the flyover including the spectra at maximum PNL. The 1/3 octave band spectra are time referenced to the helicopter's visual overhead position.

## 5.0 FLYOVER AND APPROACH NOISE CHARACTERISTICS

### 5.1 Flyover Noise

During the level flyovers, each of the eight helicopters tested were flown over the microphone array at an altitude of 500 feet at airspeeds of 90, 100 and 110 percent of the best economical long range cruise speed and at a slower approach airspeed of about 60 mph. The time histories and 1/3 octave band spectra discussed in this section are from data obtained at the center-line microphone which was located over a hard (concrete) surface at NASA Langley Research Center (LaRC) and over the old TRANSPON site surface at Dulles Airport.

Before inspecting the flyover data it may be helpful to discuss some of the noise generating mechanisms associated with a helicopter. The noise signature of a helicopter is composed of contributions from several sources which include the main rotor, tail rotor, engine and transmission noise. In general it is the main rotor and tail rotor that dominate the noise generation mechanisms. The main rotor provides the lift and thrust forces for the helicopter and generates sound as a result of the inherent aerodynamic forces on the blades. These forces give rise to both periodic and random noise components which dominate the low to mid-frequency region of the 1/3 octave band spectra.

The main and tail rotor noise components are highly directional and radiate their peak noise levels near their plane of rotation. Consequently, as the helicopter approaches an observer the noise levels are determined at first by the main rotor at shallow observation angles relative to the helicopter flight direction. This noise, near the plane of rotation of the main rotor, tends to be impulsive in nature with the impulses corresponding to the blade passage frequency. The noise level and annoyance of this part of the flyover time history is a function of the advancing blade mach number and blade loading, i.e., weight per unit area of blade. For most helicopters (notable exceptions are the UHIN (Bell-212) and the CH-47C) this noise is well below the peak noise level of the flyover. As the helicopter approaches the overhead position the propagation path shortens and the angle of propagation moves away from the main rotor plane of rotation. The observer, however, is in the plane of rotation of the tail rotor and tail rotor noise tends to dominate the noise level at the overhead position and the maximum noise level for those helicopter without significant blade slap during a level flyover. After overhead passage the noise level falls rapidly and roughly with increasing distance from the tail rotor. When the helicopter is

well past the observer and again near the plane of rotation of the main rotor impulsive noise can again be heard but at a low noise level. An exception is the 47G which has an unmuffled reciprocating engine and, for this helicopter, the maximum noise occurs after overhead passage and falls rather slowly. This noise is believed to have a significant contribution from the engine exhaust.

Two helicopters were dominated by main rotor noise occurring well before the overhead passage. These were the UHIN (Bell 212) and the CH-47C. The UHIN had the highest tip speed of the tested helicopters and had a high level of "compressibility" slap due to its advancing tip mach number above 0.9. The CH-47C has a high tip speed and also an interaction between the tandem rotors.

#### 5.1.1 Time History Analysis

Time histories for level flyovers are shown in Figures 21 to 29. The plots show time history comparisons at several different airspeeds along with comparisons of the dBA, dBD and PNL weighted noise levels for the fastest airspeed. In general the different weighted noise levels track one another quite well. This indicates that any of the plotted subjective units can be used about equally well as a descriptor of helicopter noise time histories. The time histories use a "slow" meter response consistent with FAR Part 36. This meter response does not depict the peak levels of the impulsive portion of the flyover (See Section 7.0) because the approximately one-second averaging time in the meter response dilutes the impulsive spikes into a time averaged level.

The flyover time histories can be grouped roughly into three categories. The first category is the helicopters with a short triangular shaped time history such as the S-61, S-64, and 500C. The 300C should probably also fit into this category except that it was fairly slow and quiet and background noise tended to extend its flyover noise signature. The second category is the 47G with its unmuffled reciprocating engine exhaust. This caused the peak noise to occur after overhead passage and to be of fairly long duration. The piston engined (with muffler) 300C also showed this tendency but to a much lesser degree. The third category is the helicopters with main rotor blade slap. This category includes the UHIN (Bell 212), CH-47C and to a limited degree, the 206L. The peak levels of blade slap occur well before

overhead passage and are dependent upon airspeed. For example note the differences between 118 and 130 mph on the 206L, 99 Kts and 114 Kts on the UHIN and 100 and 141 Kts on the CH-47C. The 206L is an intermediate case because the peak noise occurred at overhead and was controlled by the tail rotor. The change in the noise characteristic and level of the UHIN and CH-47C as they passed the overhead position was remarkable.

The time histories of the helicopters with slap in the forward quadrant exhibit a rising and falling of the noise level before overhead. The reason for this could be the highly directional nature of the blade slap (ahead of the helicopter) and atmospheric turbulence combined with the long propagation paths of 2000 to 3000 feet from the microphone array. The UHIN and UHIN CH-47C show, as the helicopter approaches the microphone, a period of rapidly rising blade slap followed by a lessening of slap as the helicopter to microphone propagation path moved out of the plane of rotation. Tail rotor noise increases as the helicopter approaches the microphones. The CH-47C has compressibility bang followed by possibly a combination of compressibility and tandem rotor interactions. When comparing time histories at varying airspeed, it would be expected that, for a constant noise generation source, the slower airspeeds would have the longer time duration.

#### 5.1.2 One-Third Octave Band Spectra

Figures 30 to 37 show comparisons of the 1/3 octave band flyover spectra at several airspeeds with the helicopter located directly over the centerline microphone. By choosing the spectra at the overhead location, the data has consistent ground reflections making it possible to compare different airspeeds.

Except for the Boeing Vertol CH-47C which does not have a tail rotor, the overhead 1/3 octave band spectra of the other seven helicopters appear to be dominated by the tail rotor. All but the two Sikorsky Helicopters consisted of a two bladed tail rotor. The Sikorsky S-61 has a five bladed tail rotor while the S-64 "Skycrane" has a four bladed tail rotor. The static tail rotor blade passage frequencies of these helicopters ranged from a low of 55 Hz for the Bell 212 to a high of 104 Hz for the two Hughes helicopters. In general, the 1/3 octave band spectra consist of the blade passage frequency and harmonics of the tail rotor whose peaks dominated the low frequency region (50 Hz-400 Hz) of the spectra. Selected narrow-band spectra which more clearly identify the blade passage frequencies are shown in Section 7.2. The static blade passing frequencies must be adjusted in flight for doppler effects caused by the helicopter airspeed.

The 500C, UHIN, S-61 and S-64 show consistent trends of slightly higher overhead noise levels at faster airspeeds especially in the middle to higher frequencies. This could be caused by either the faster advancing tail rotor tip speeds or to increased trailing edge random noise from the main rotor. This latter noise source would be similar to "clean airfoil trailing edge noise" which is the noise caused when boundary layer fluctuations along the main rotor blades are convected past its trailing edge. This noise is broadband, highly dependent on velocity (here advancing rotor tipspeed), would be of fairly high frequency due to the small chord and thickness of the rotor blades and would propagate nearly perpendicular to the surface.

Figure 38 shows the 1/3 octave spectra for the S-64 Skycrane at a time before, at, and past overhead passage. For a uniform, non-directional noise source the 2.5 sec before overhead, spectra should be 2 dB lower than the overhead based solely on inverse spreading of sound and the 5.5 sec after overhead 6 dB lower. Comparing the -2.5 sec and the overhead on this basis of 2 dB apart we see the proper relationship at the 63 Hz band (tail rotor fundamental or fourth harmonic of main rotor) but a large increase in mid and high frequency noise as the helicopter passes overhead and the propagation angle changes from  $50^\circ$  below the flight direction to  $90^\circ$  from the flight path. A comparison of the overhead and 5.5 seconds after overhead shows, after allowing for the varying ground reflection, the 6 dB attributable to the inverse square law for a constant noise source. This would indicate a different noise mechanisms as the S-64 approaches overhead. The overhead noise on this helicopter was not impulsive nor is it attributable to blade slap. Possible explanations are that the tail noise was shielded by the fuselage before overhead passage or that main rotor trailing edge noise causes this phenomenon. Clearly, all aspects of helicopter noise are not well understood.

The changes in spectra for the UHIN during a flyover can be more easily understood (See Figures 39 and 40). Before overhead, at propagation angles of  $20^\circ$ - $30^\circ$  from the flight path the noise appears to be dominated by the main rotor, with the 160 to 500 Hz region controlled by the relative degree of "slap". At overhead the spectra abruptly changes with a drastic decrease in the very low frequencies. This would indicate a change from main rotor to tail rotor as the major noise contributor. After overhead the low frequencies again drop faster than indicated by the inverse square law indicating perhaps some main rotor contribution

even at overhead. The CH-47C exhibits the same trends as the UH1N even though it does not have a tail rotor. That is, there is a large drop in low frequency noise after overhead passage as shown on Figures 41 and 42. A 1/3 octave band analysis and "slow" meter response, while showing major overall trends, clearly lack the detail necessary for noise source and mechanism identification. Narrow band techniques and waveform identification are necessary to separate the sources such as main and tail rotor noise. This is briefly explored in Section 7.0.

## 5.2 Approach Noise

In order to evaluate the helicopter noise levels generated during landing, approaches were flown at target glideslopes of 3, 6, and 9 degrees such that the altitude of the helicopter as it passed over the microphone array was held constant at 400 feet (120 meters). A portable theodolite was used to establish the approach glideslopes and verbal "fly-up/fly-down" commands were given to the pilot in order to keep the helicopter descending along the proper glideslope. All approaches were flown at a constant airspeed of 60 mph or 60 knots depending on the nomenclature of the on-board airspeed indicator. The approach time histories and 1/3 octave band spectra discussed in this section are from data obtained at the centerline microphone.

### 5.2.1 Time History Analysis

During approach the helicopter is more or less descending through the blade wakes generated by the main rotor blades. As a result, the advancing rotor blade is cutting through the wake, generated by the preceding blade. This blade/wake interaction is responsible for generating blade slap during the landing procedure. Except for perhaps the Bell 212, whose main rotor tip speed is much higher than the other helicopters tested, we might expect that blade slap due to compressibility effects of the advancing blade would not be an important noise generation mechanism during low speed descent.

Figures 43 through 50 contain the time history comparisons at the different glideslopes along with comparisons of dBA, dBD, and PNL weighted noise levels for one of the glideslopes. Comparisons of these different weighted noise levels indicate that during descent all three track quite well with one another. In general, the time histories during approach show the maximum noise level occurring near the overhead position for all glideslopes. Blade slap, due to blade/wake interaction occurs somewhat randomly with glideslope and can be seen on the time histories as a "bump" of noise level before or after the overhead position. Some helicopters show a uniform increase in noise level throughout the entire time history for certain glideslopes. This could indicate that main rotor blade slap occurred continuously throughout the flyover.

Comparisons of the dBA noise levels at the various glideslopes show that the peak noise levels are generally obtained during the steeper 6 and 9 degree approaches. Only the S-61 shows a reverse trend with the peak dBA noise level obtained during the 3 degree approach. In particular, the A-weighted noise levels that define the flyover time histories of the two heavier helicopters (the Boeing Vertol CH-47C and the Sikorsky S-64 "Skycrane") show almost no differences in level with regard to glideslope.

In comparing the low speed level flyover time histories with those obtained during approach, the peak A-weighted noise levels during approach are slightly higher for the bigger helicopters (Bell 212, S-61, S-64 and Boeing Vertol CH-47C) even after adjusting the levels for the differences in altitude when directly over the microphone. Only in the case of the Bell 206L is the peak noise level higher during level flyover. The peak A-weighted noise level for both the Hughes 300C and the Bell 47G are roughly identical during both level flyover and approach while the Hughes 300C is higher during the approaches. The 300C at 9°, 206L at 6°, and S-61 at 3° glideslope show more slap than during level flyover at the "best range" airspeed. This slap is identified as a lift or bump in the forward part of the time history. Conversely, the UH1N and CH-47C, tend to have a triangular shaped time history during approach compared to the trapezoidal shape of the level flyover time history. This change is attributed to the reduction of compressibility slap during approach because of the slower airspeed.

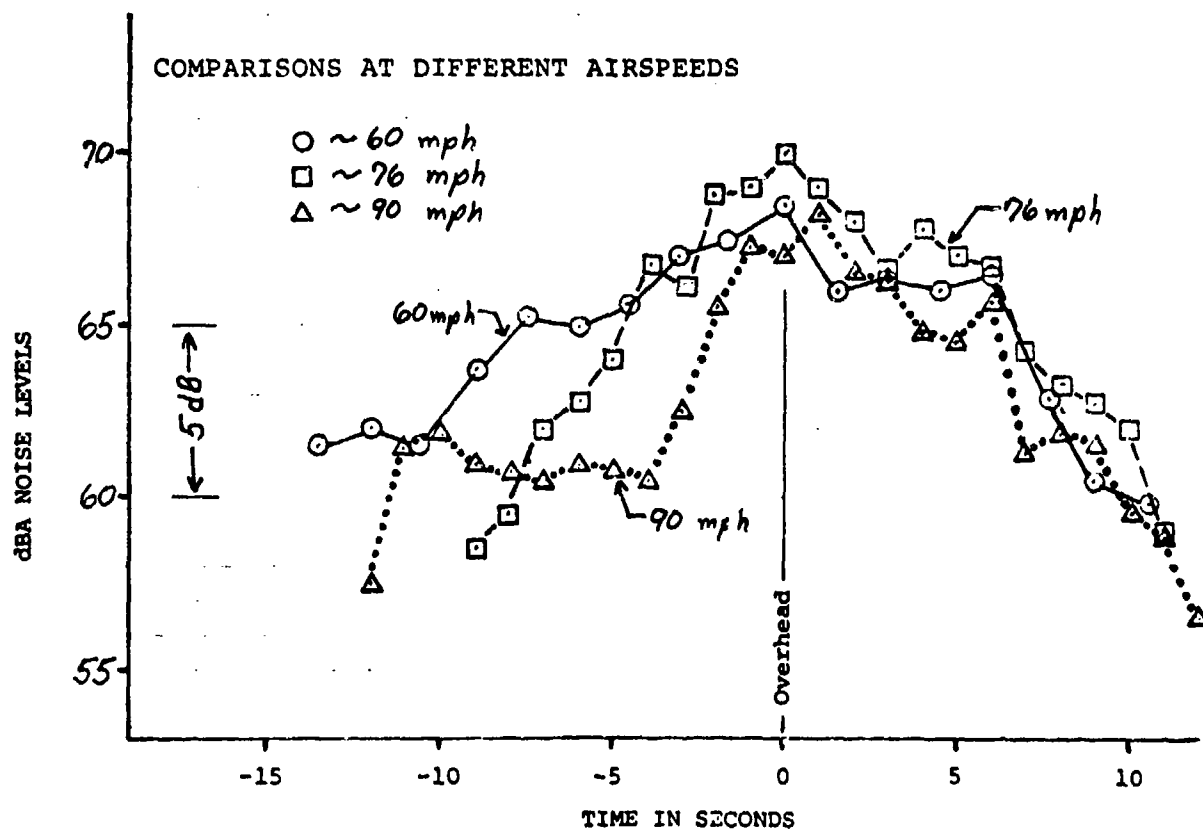
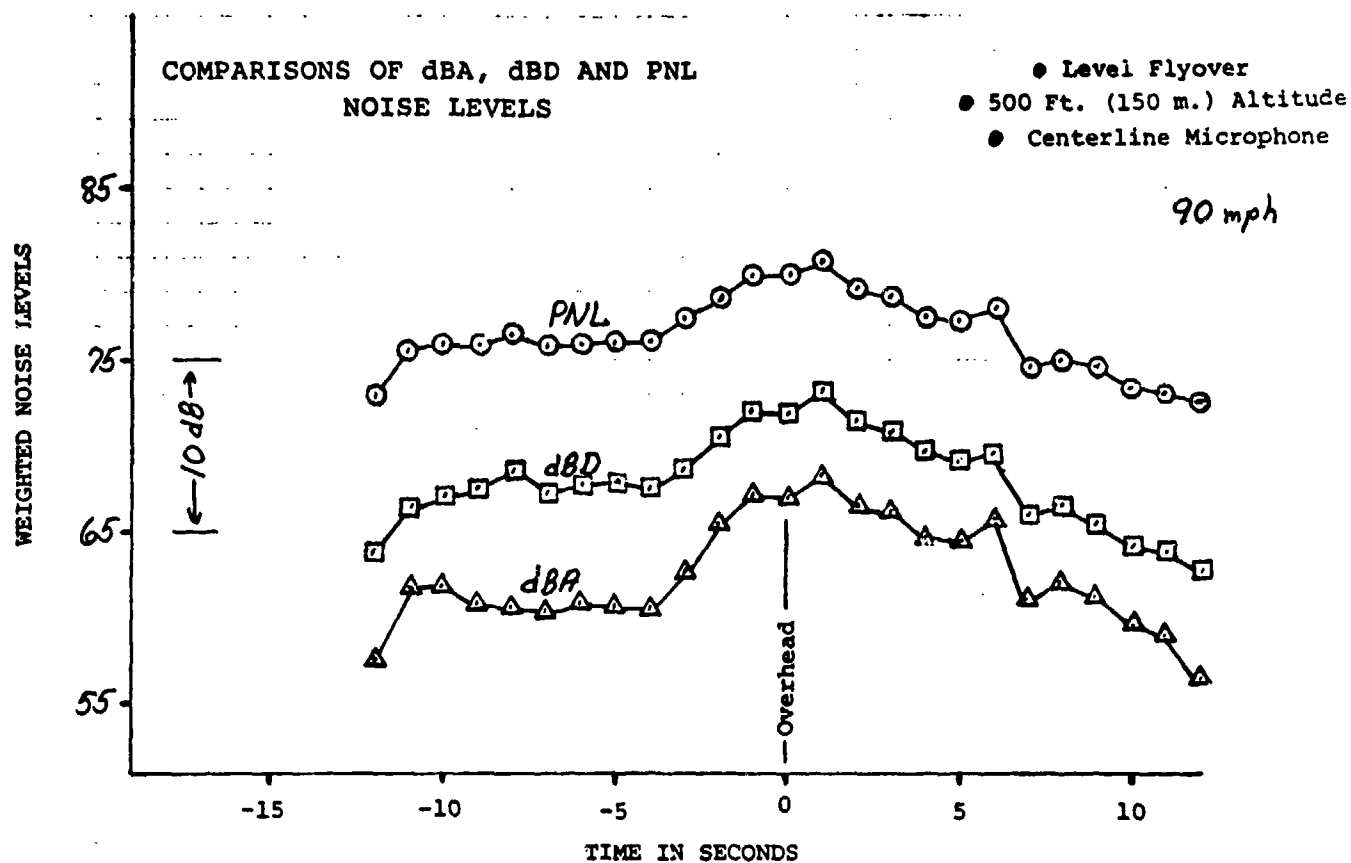
#### 5.2.2 One-Third Octave Band Spectra Analysis

Comparisons of the overhead 1/3 octave band spectra obtained during approach, Figures 51 to 58, show almost no variations in spectra shape with regard to glideslope. Only the Hughes 300C shows any real variation. However, the 6 degree approach is almost identical to that obtained during level flyover. In general, comparisons of the overhead spectra during approach are almost identical to those obtained during level flyover. However, this result probably should have been expected since when in the overhead location it is the tail rotor that dominates the 1/3 octave band spectra regardless of whether the helicopter is in level flight or descending for a landing.



FIGURE 21

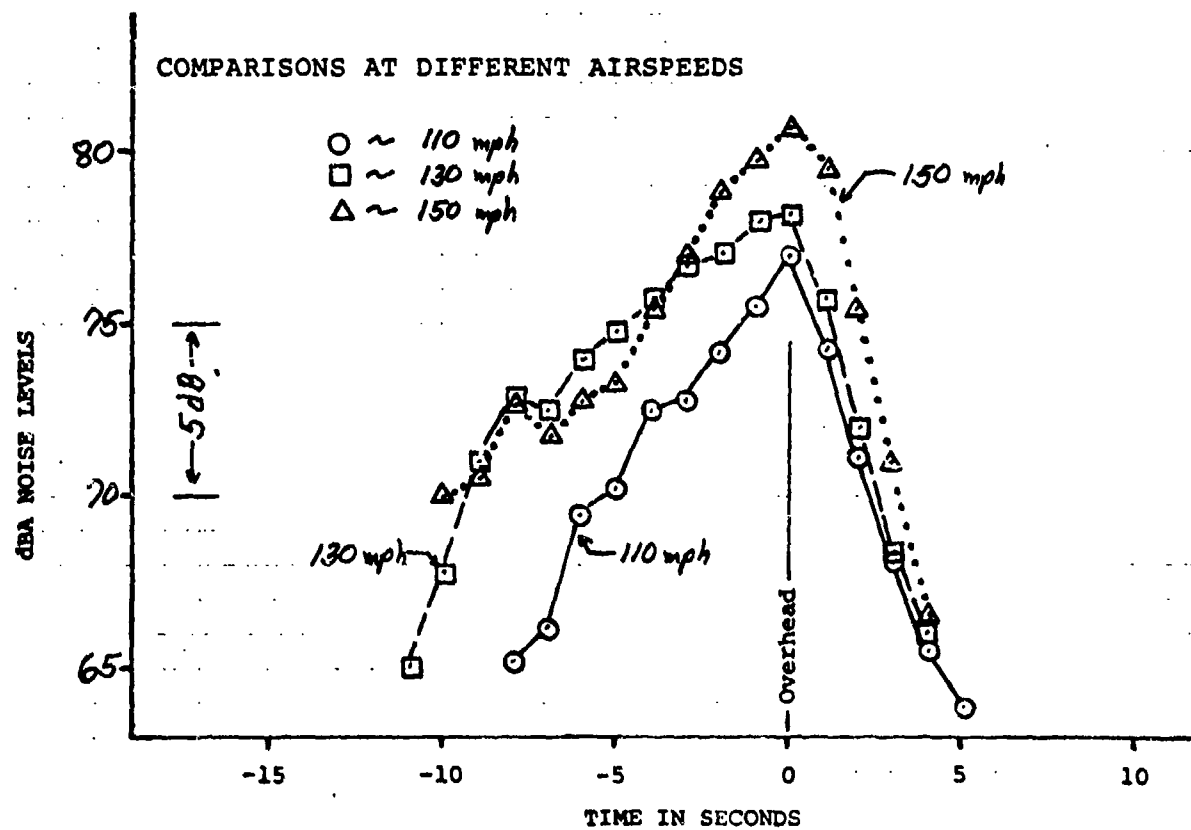
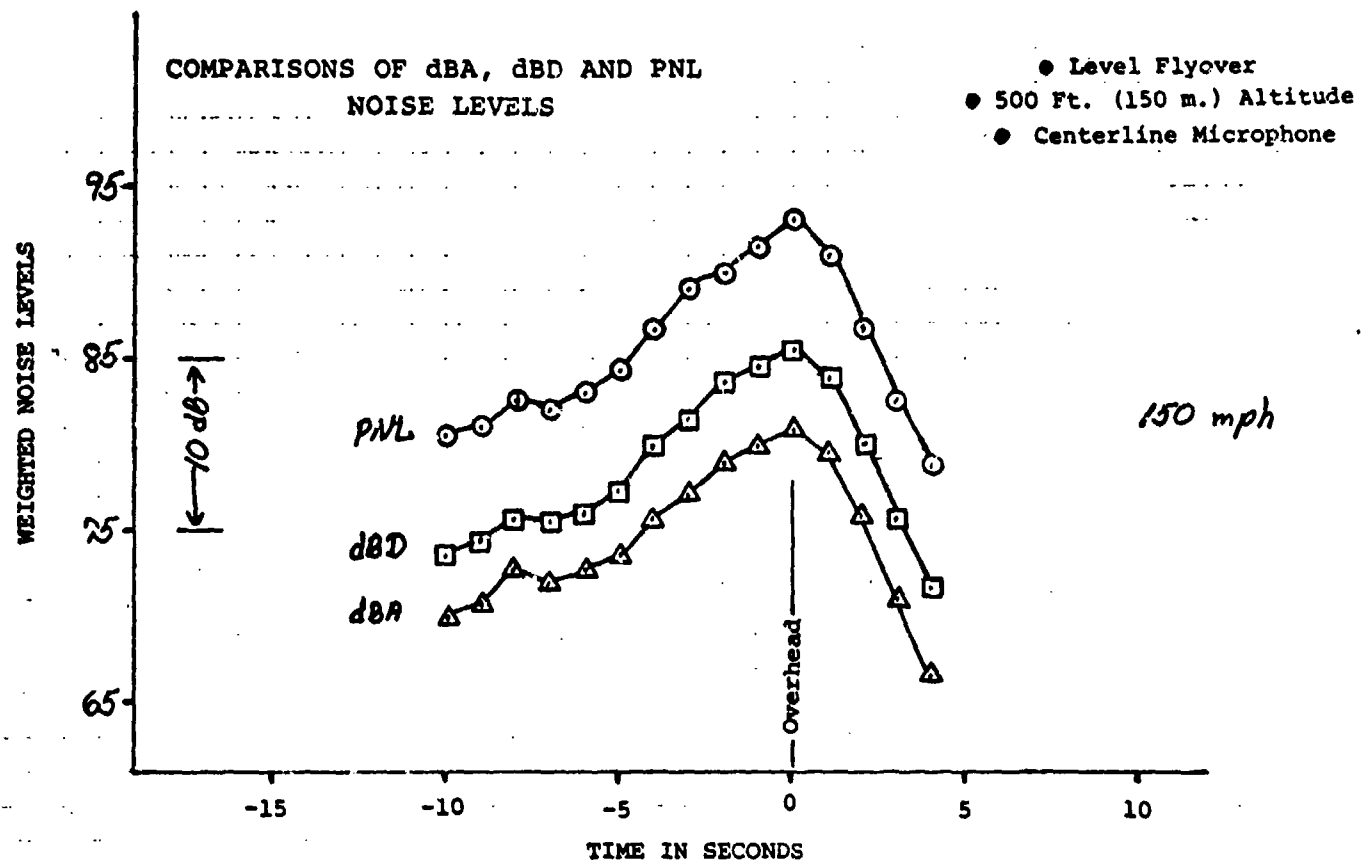
HUGHES 300-C  
FLYOVER TIME HISTORIES



# HUGHES 500-C

FIGURE 22

## FLYOVER TIME HISTORIES



# BELL 47-G

FIGURE 23

## FLYOVER TIME HISTORIES

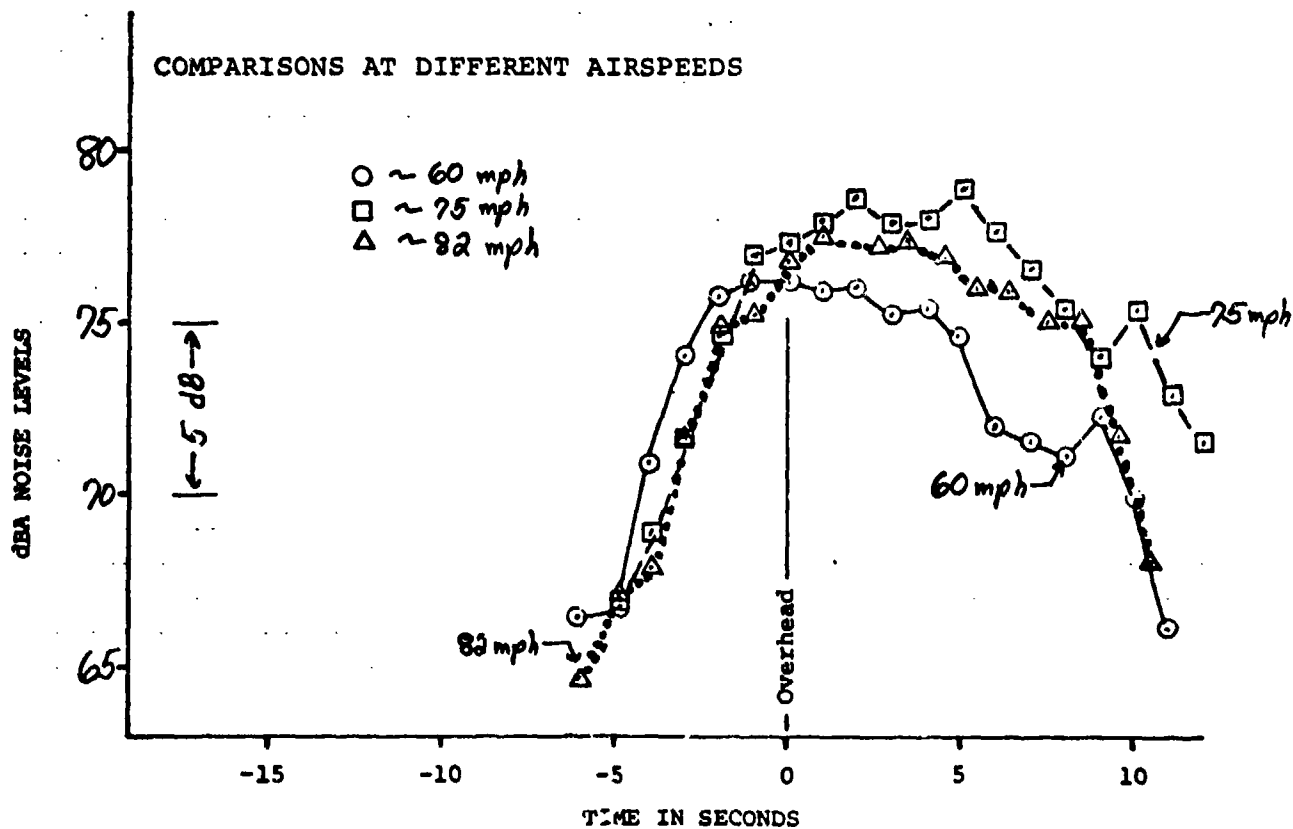
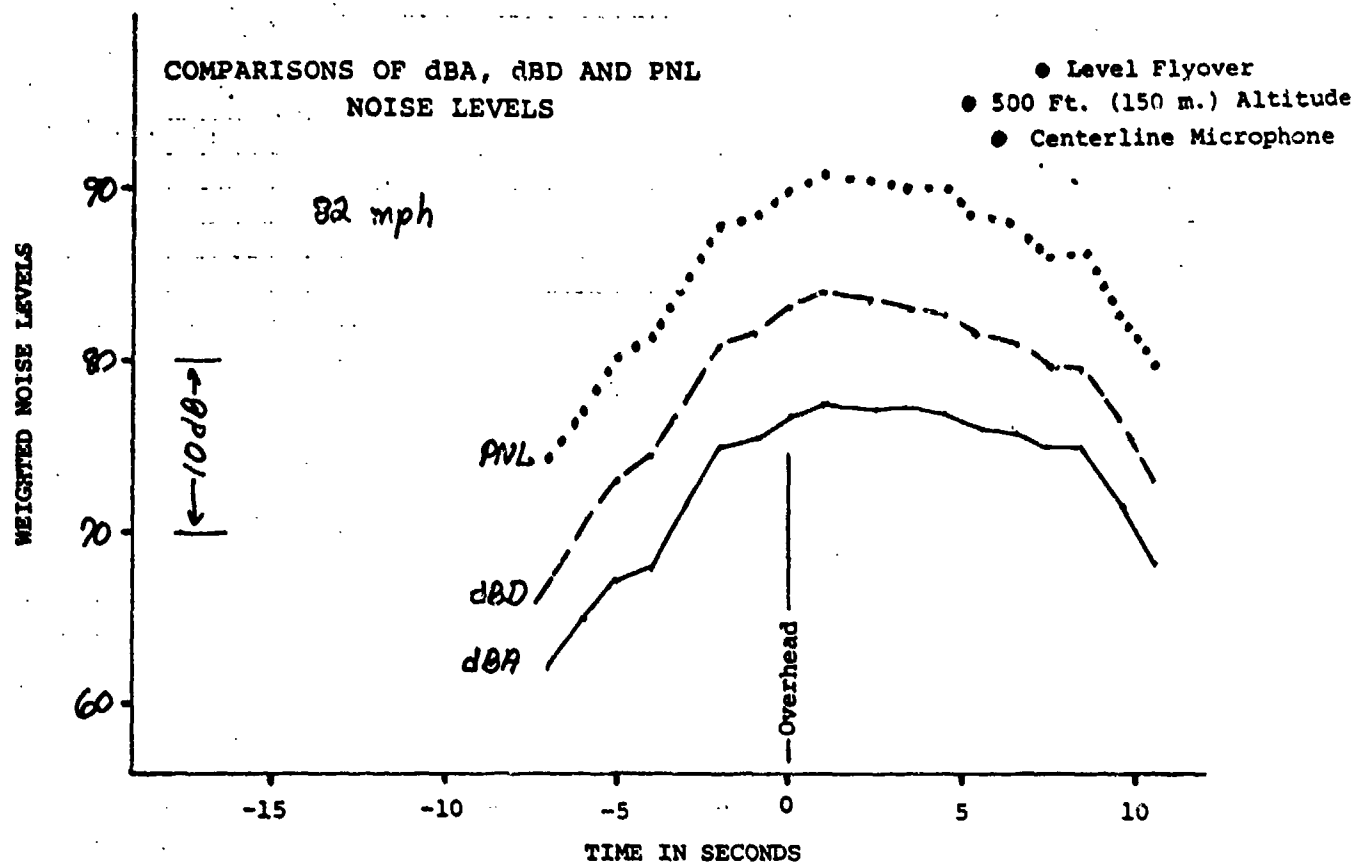


FIGURE 24

## FLYOVER TIME HISTORIES

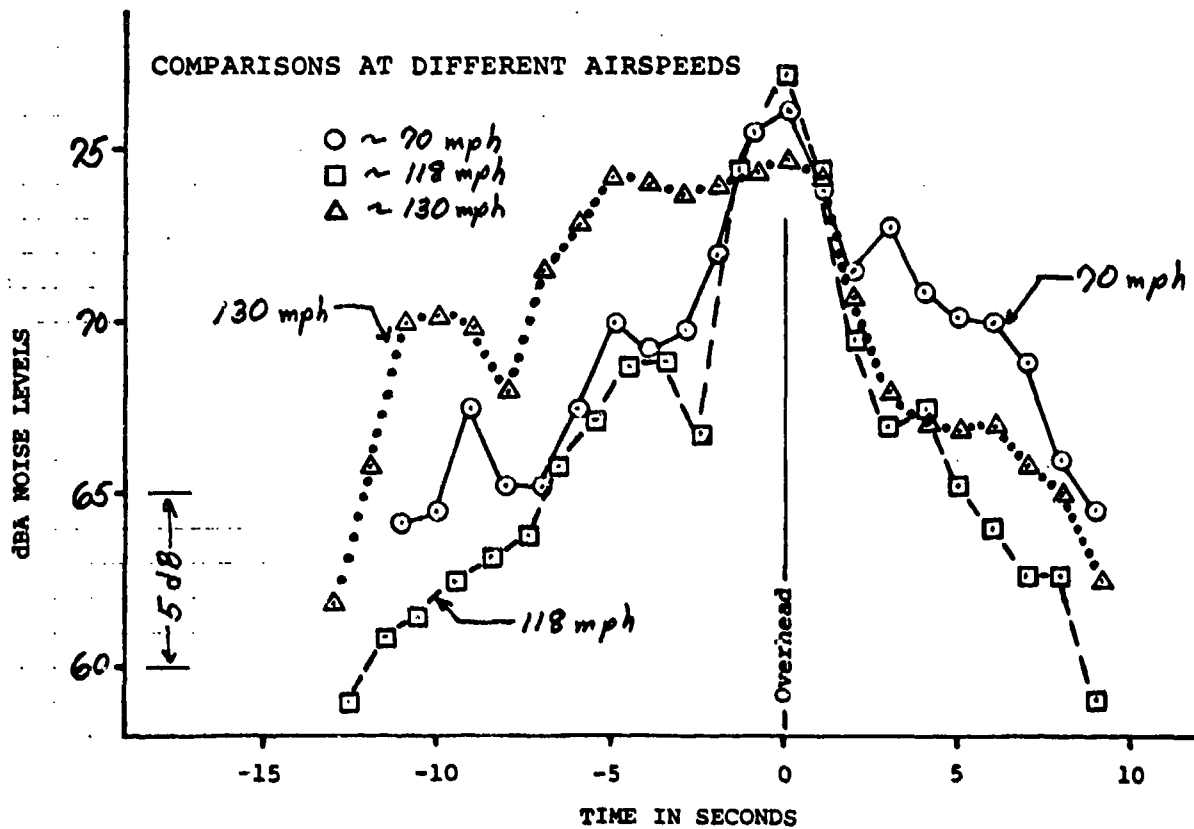
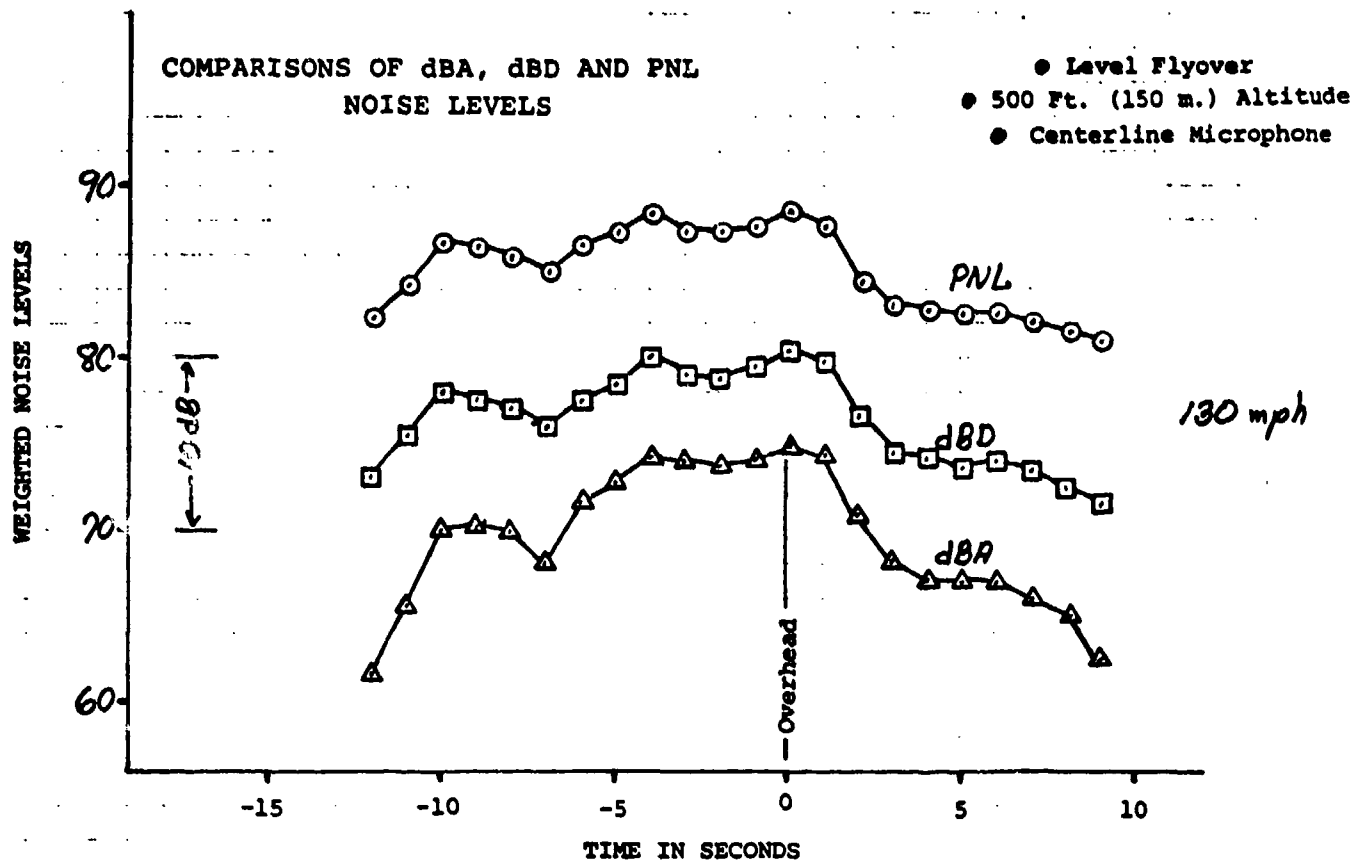
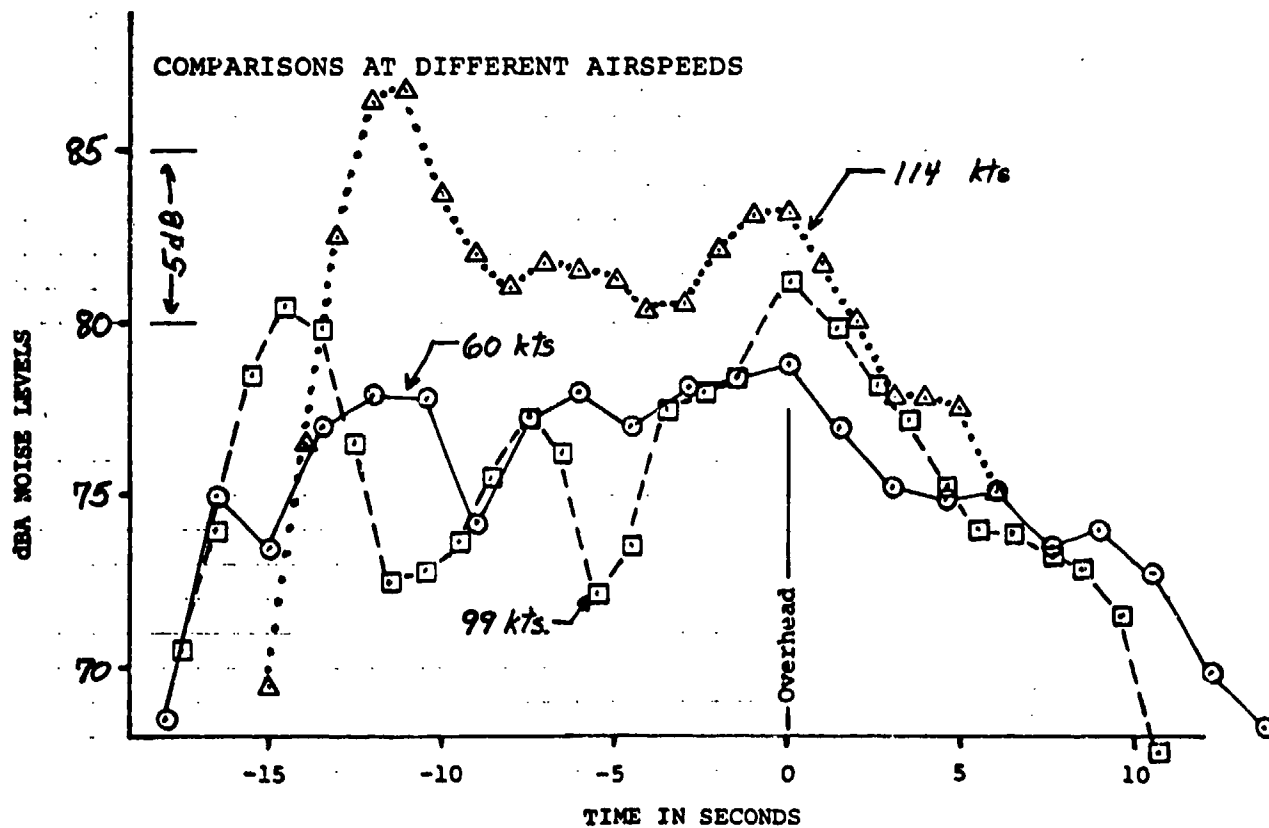
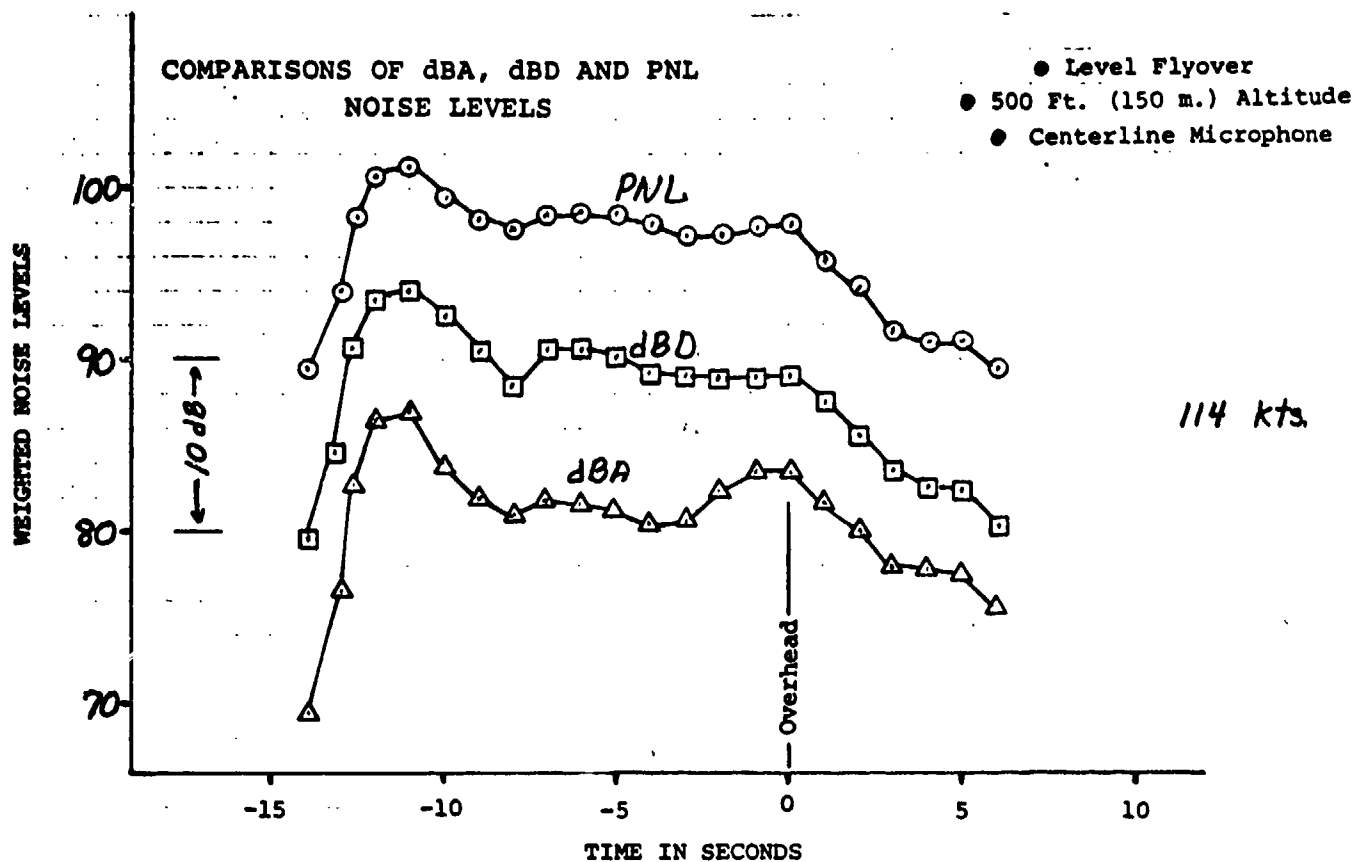


FIGURE 25

BELL 212 (UH1N)  
FLYOVER TIME HISTORIES



SIKORSKY S-61  
 FIGURE 26 FLYOVER TIME HISTORIES

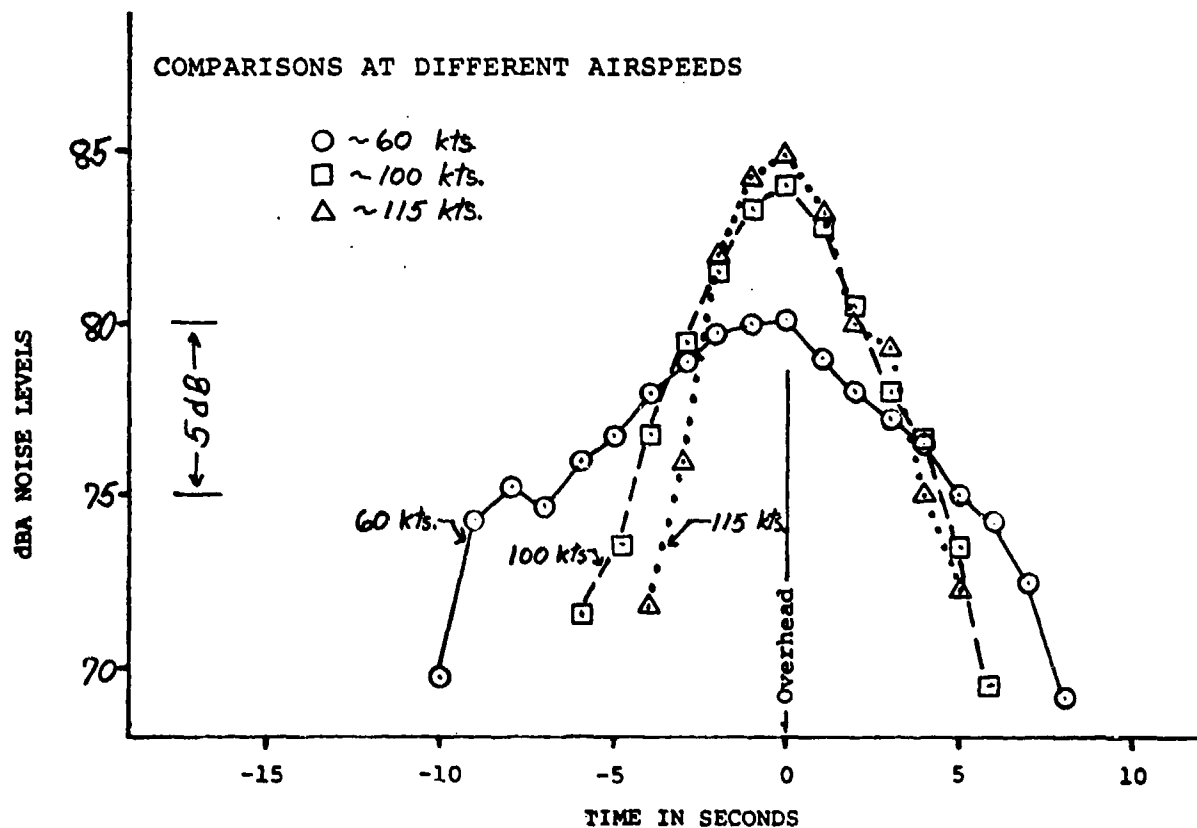
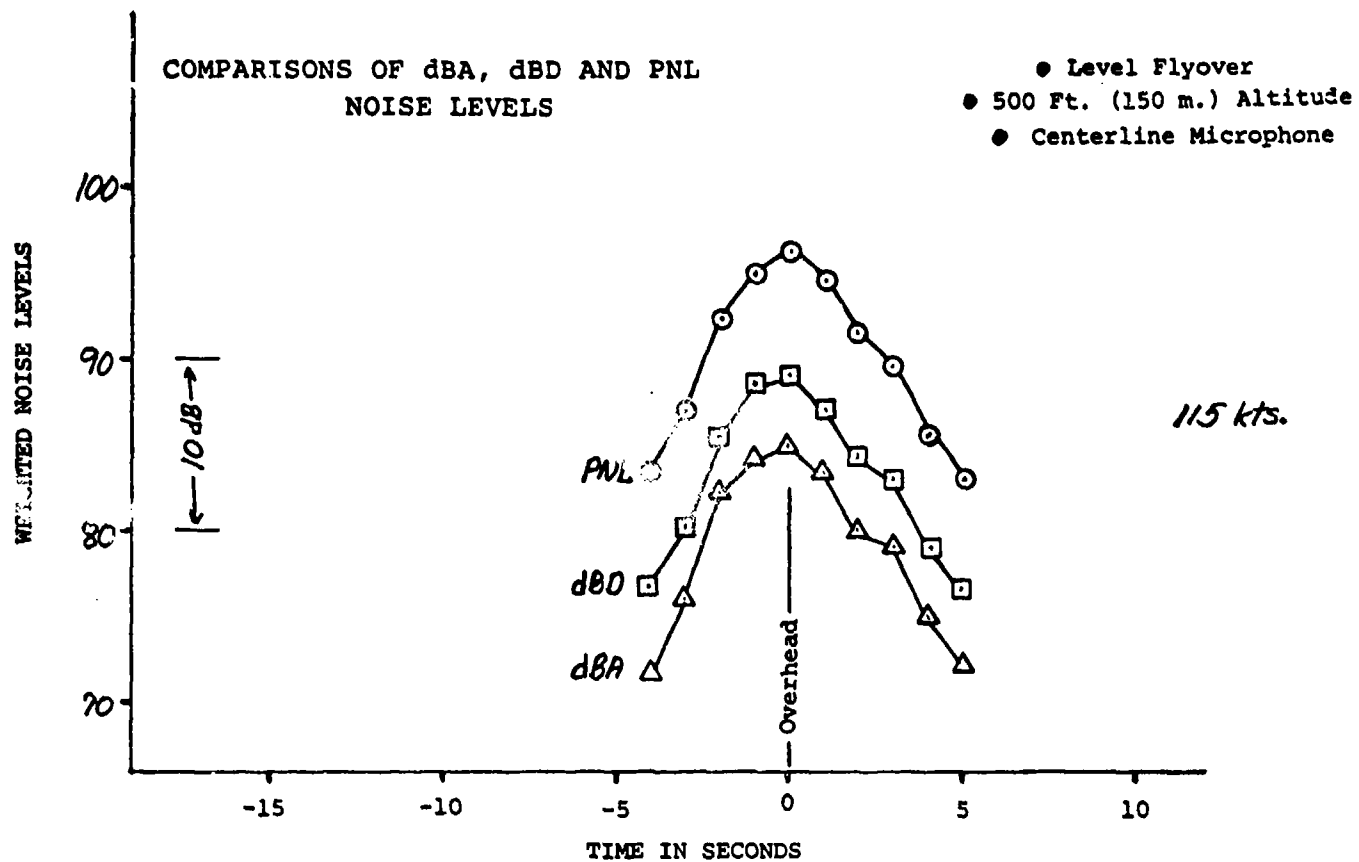


FIGURE 27

SIKORSKY S-64 "SKYCRANE"  
FLYOVER TIME HISTORIES

(with truck)

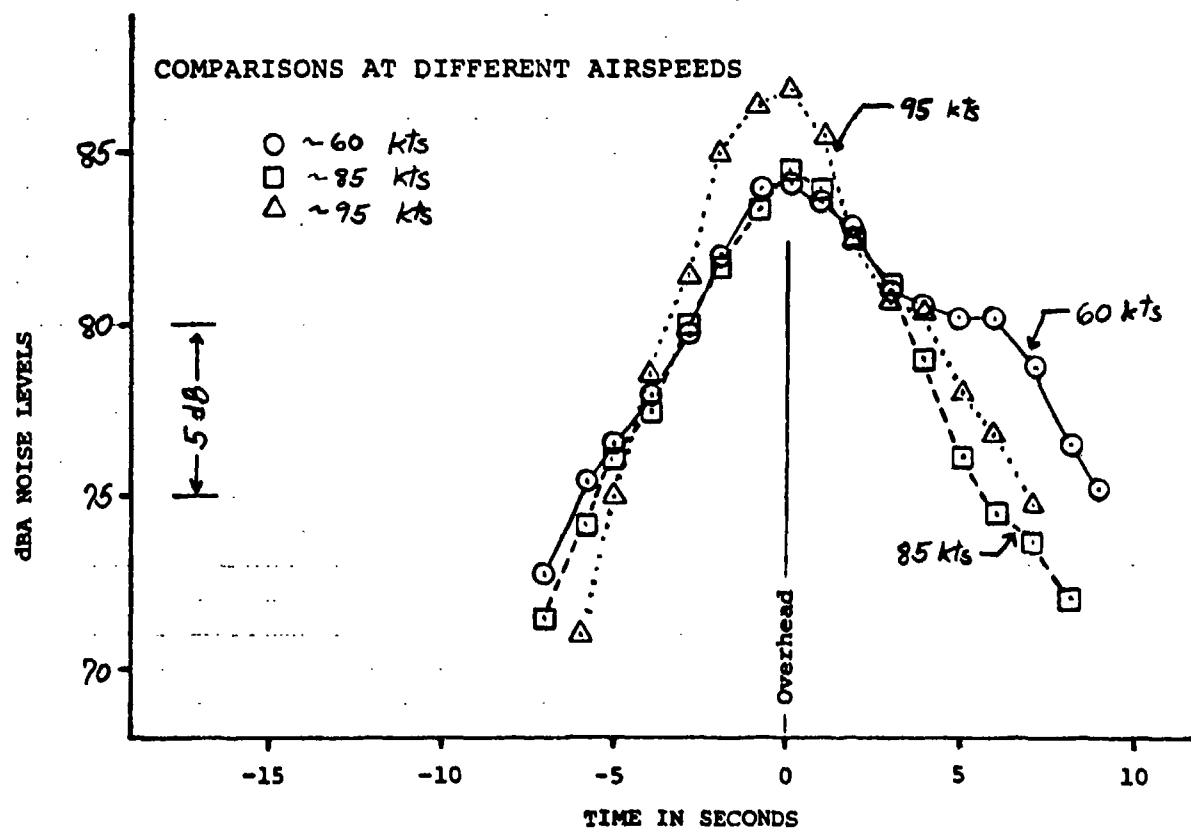
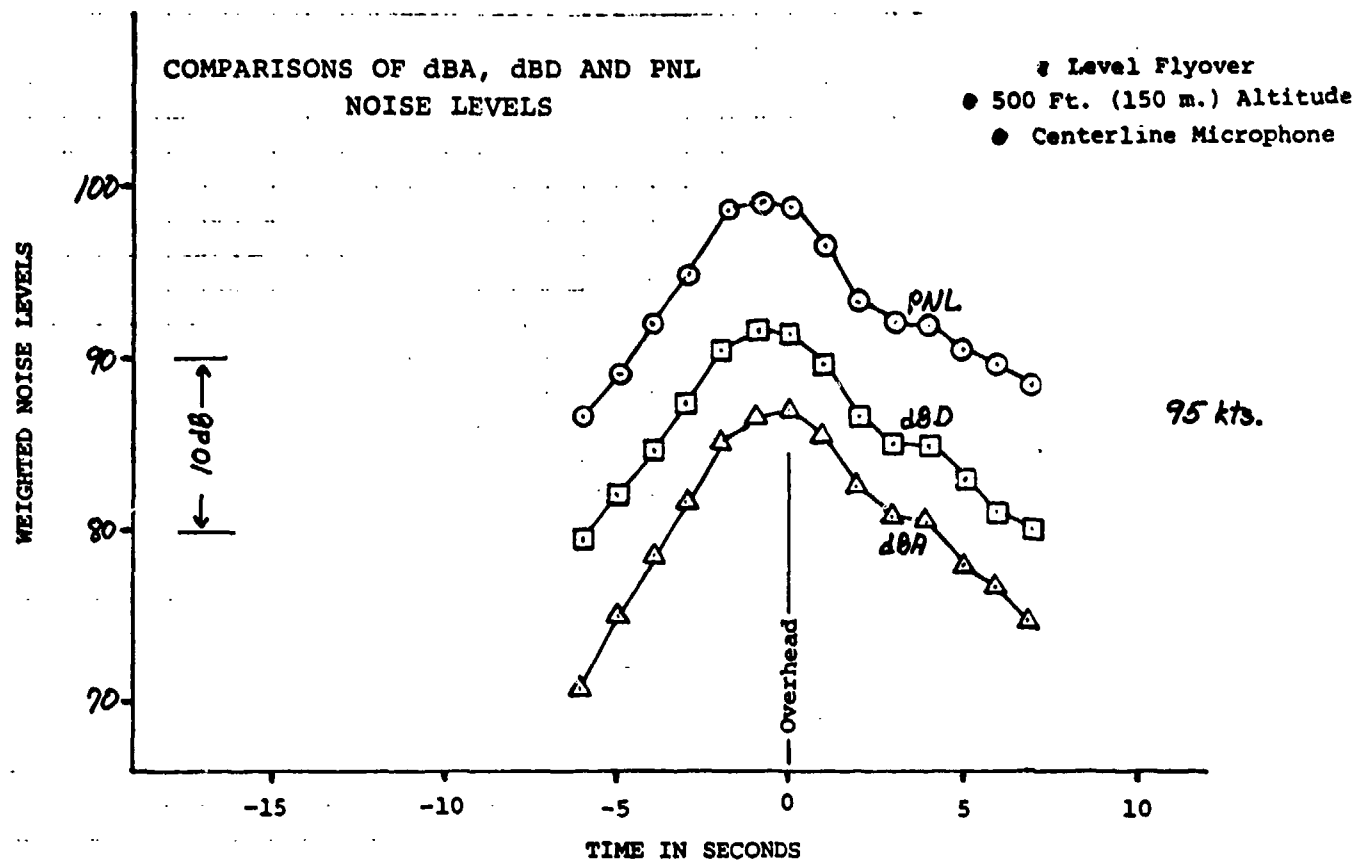


FIGURE 28

SIKORSKY S-64 "SKYCRANE"  
FLYOVER TIME HISTORIES

(without truck)

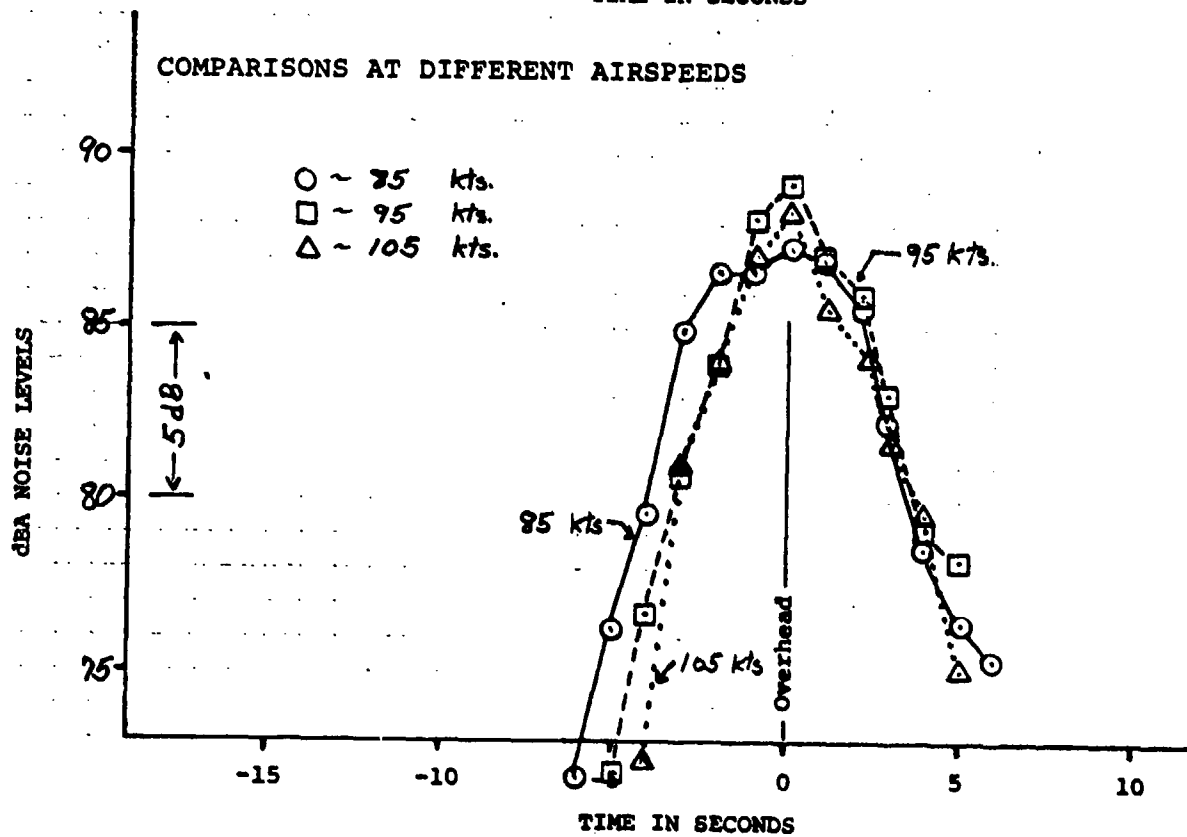
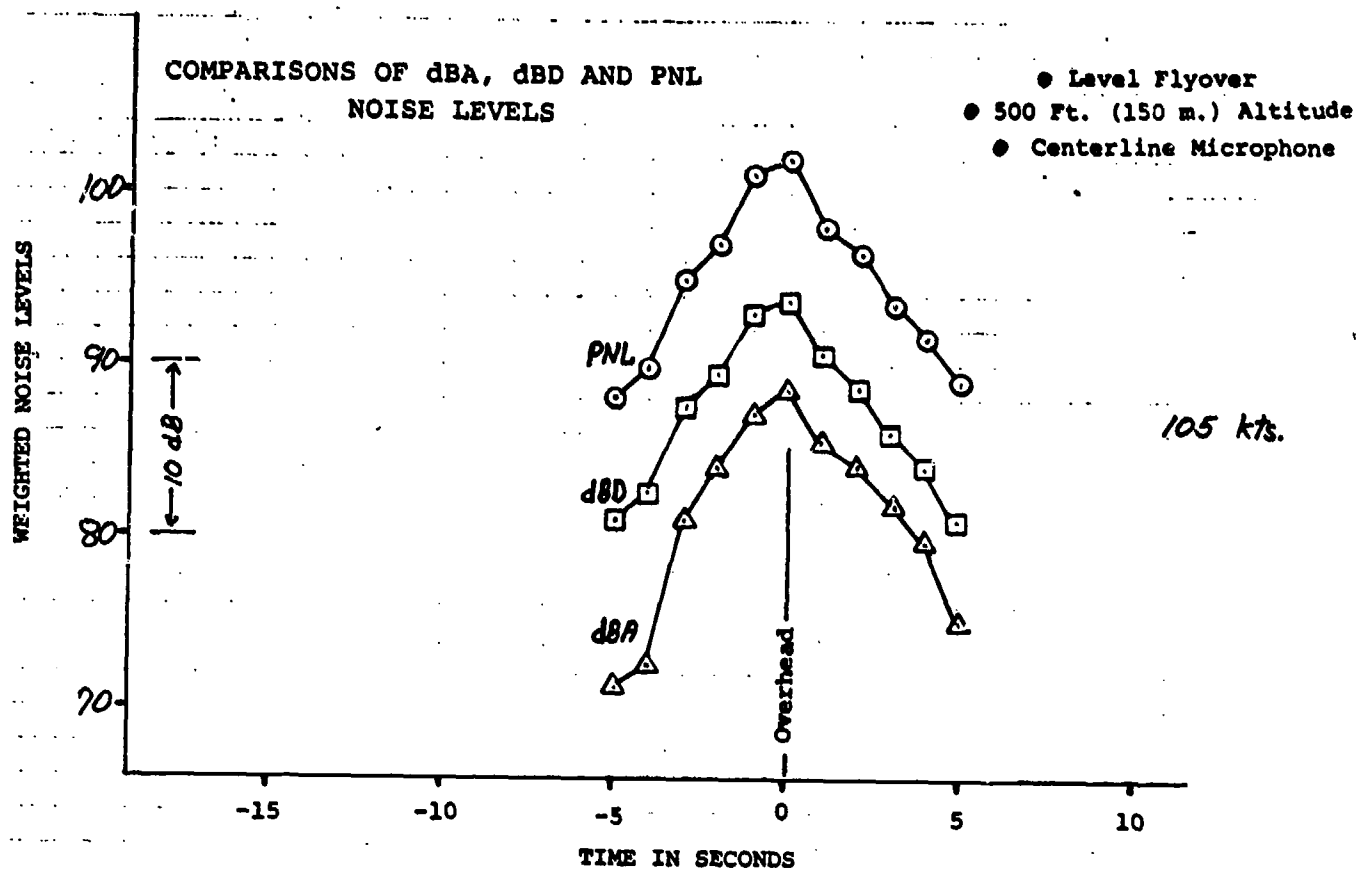
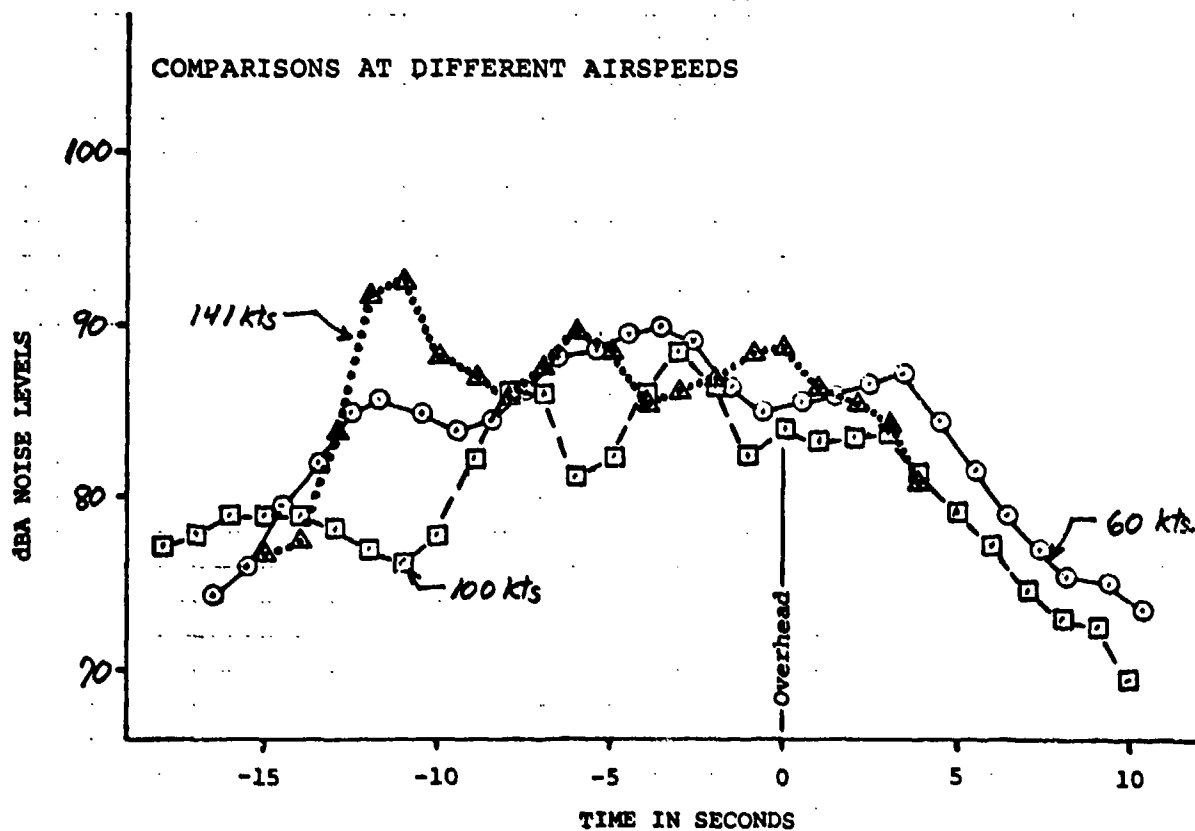
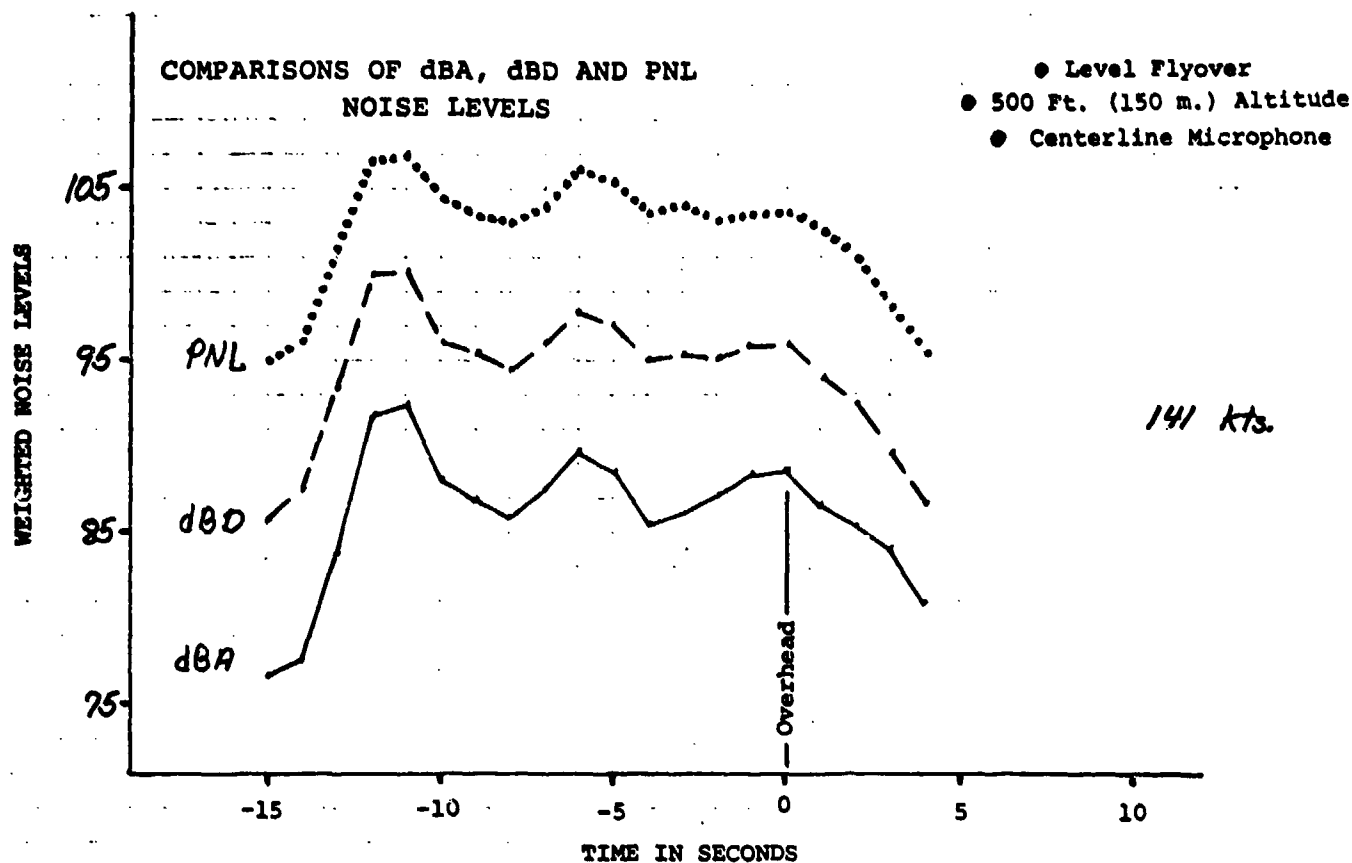




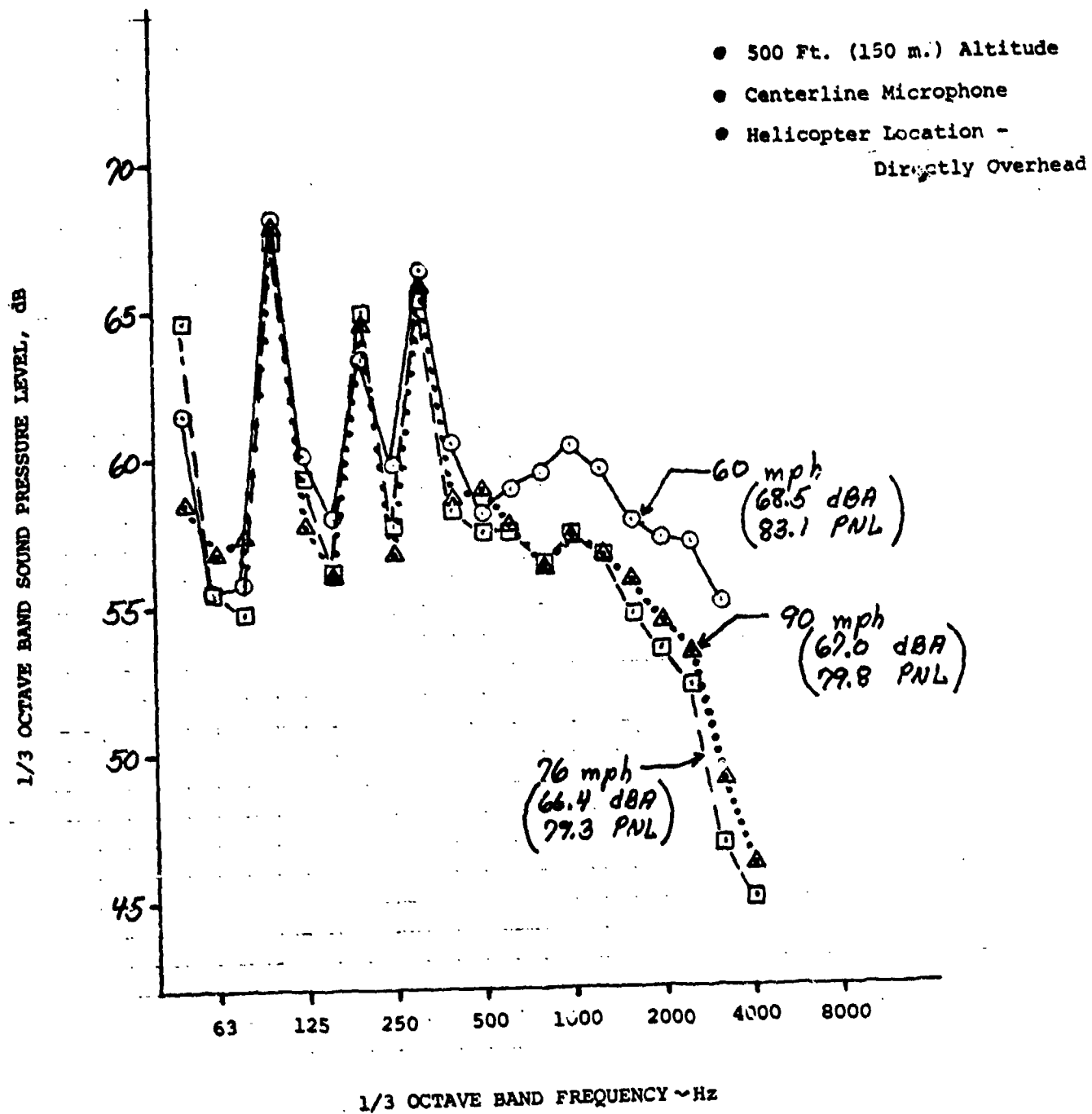
FIGURE 29

BOEING VERTOL CH-47C  
FLYOVER TIME HISTORIES



# HUGHES 300-C

FIGURE 30. LEVEL FLYOVER SPECTRA



# HUGHES 500-C

## FIGURE 31. LEVEL FLYOVER SPECTRA

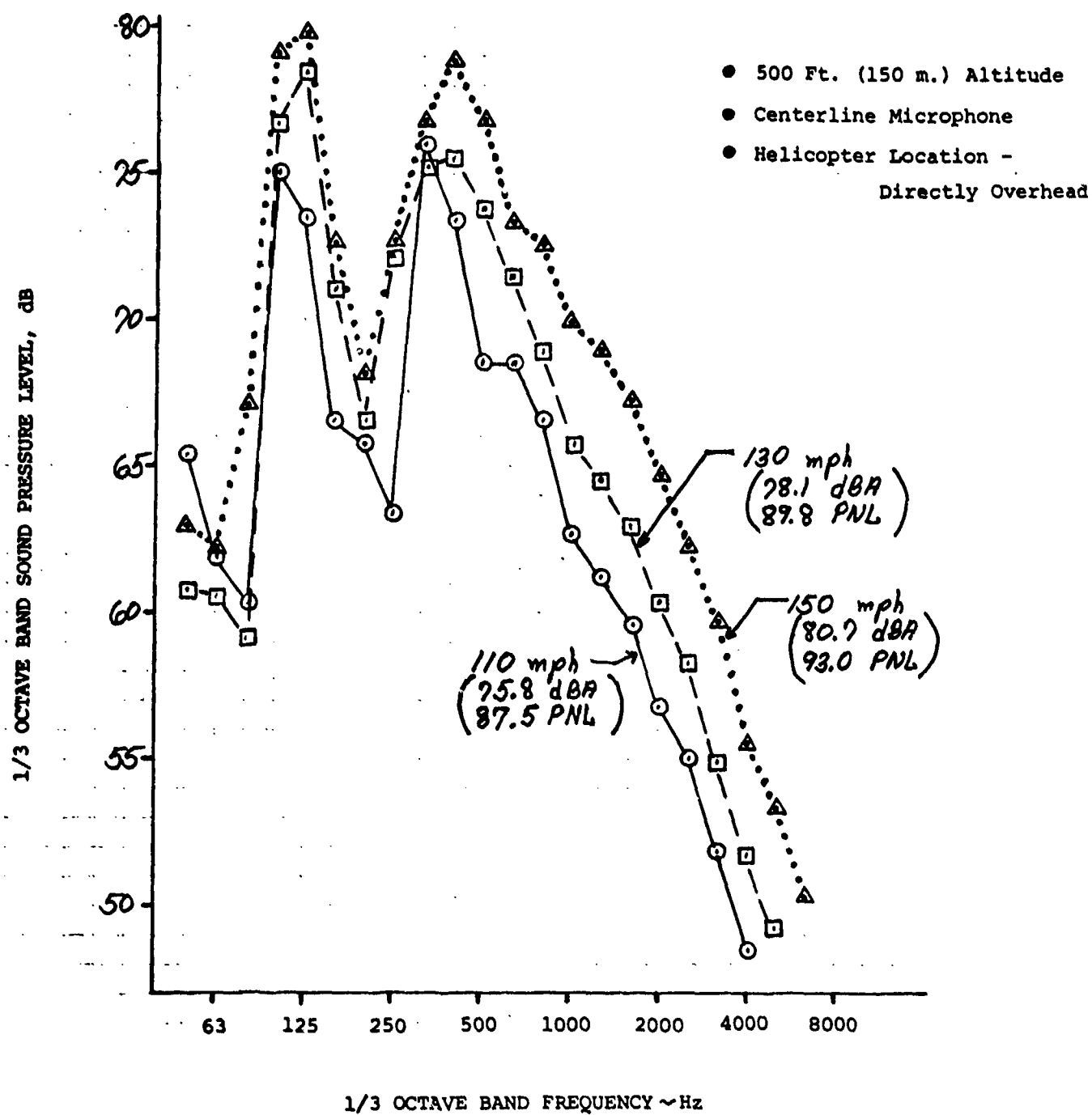
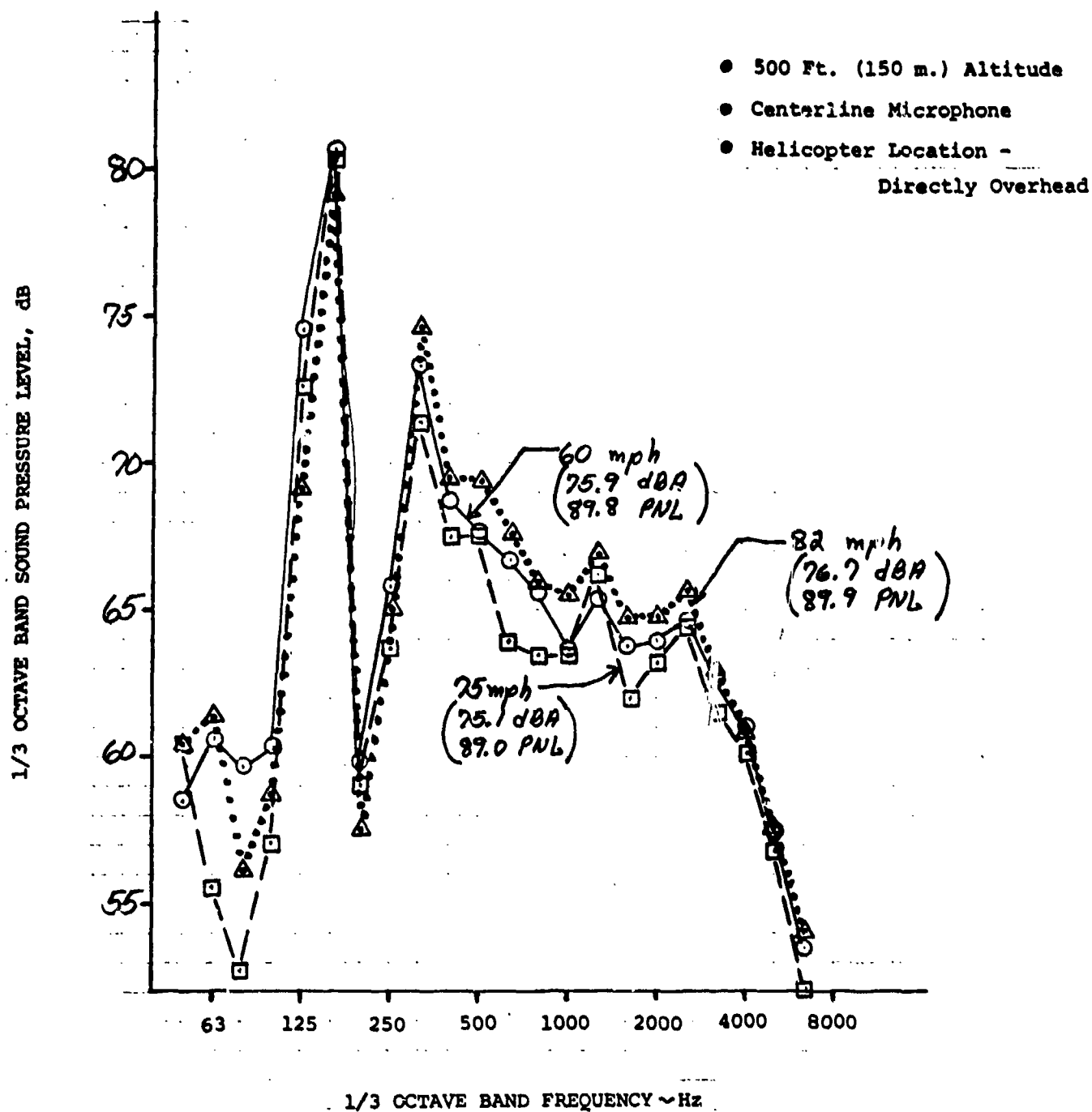
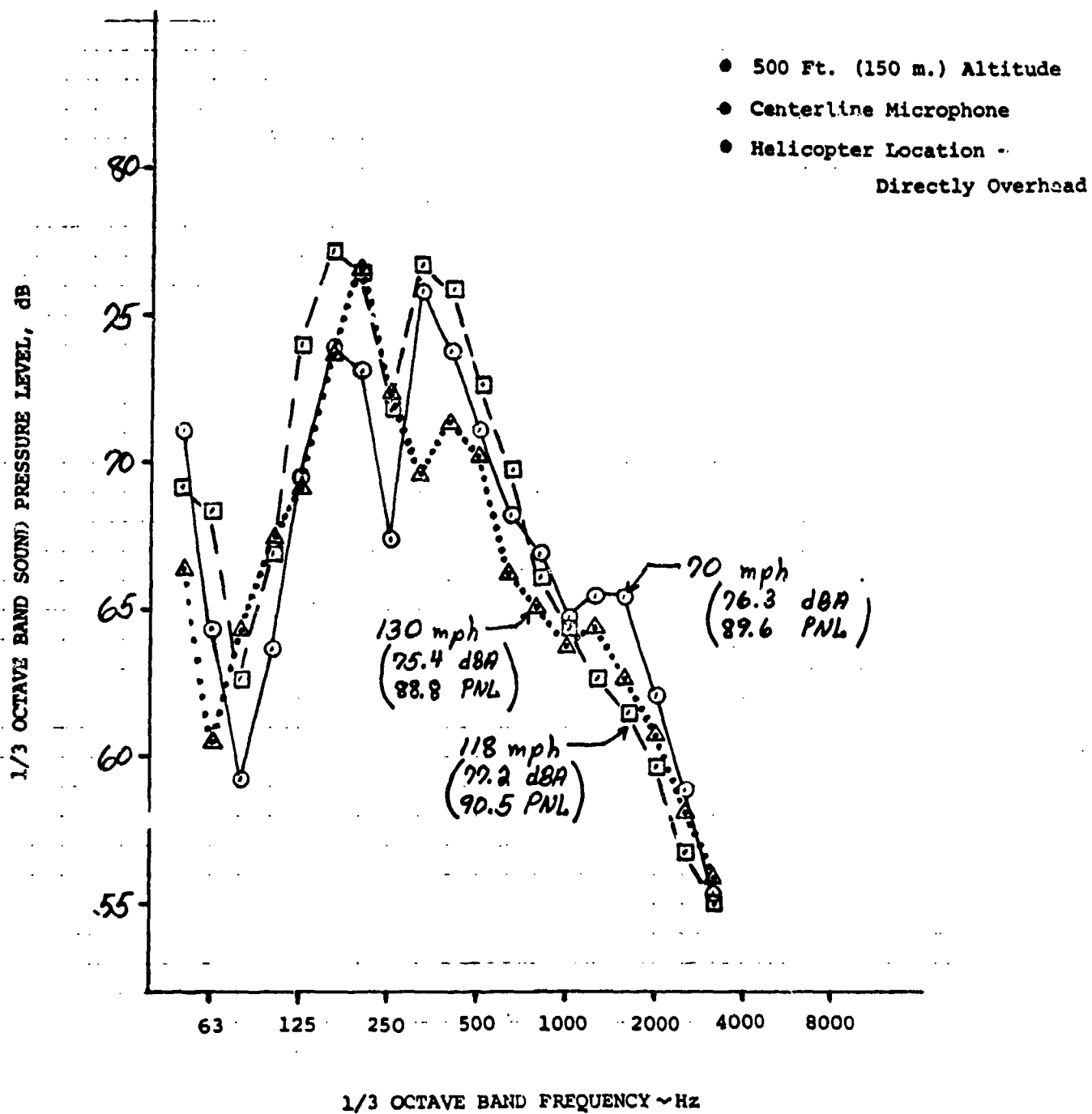


FIGURE 32. LEVEL FLYOVER SPECTRA



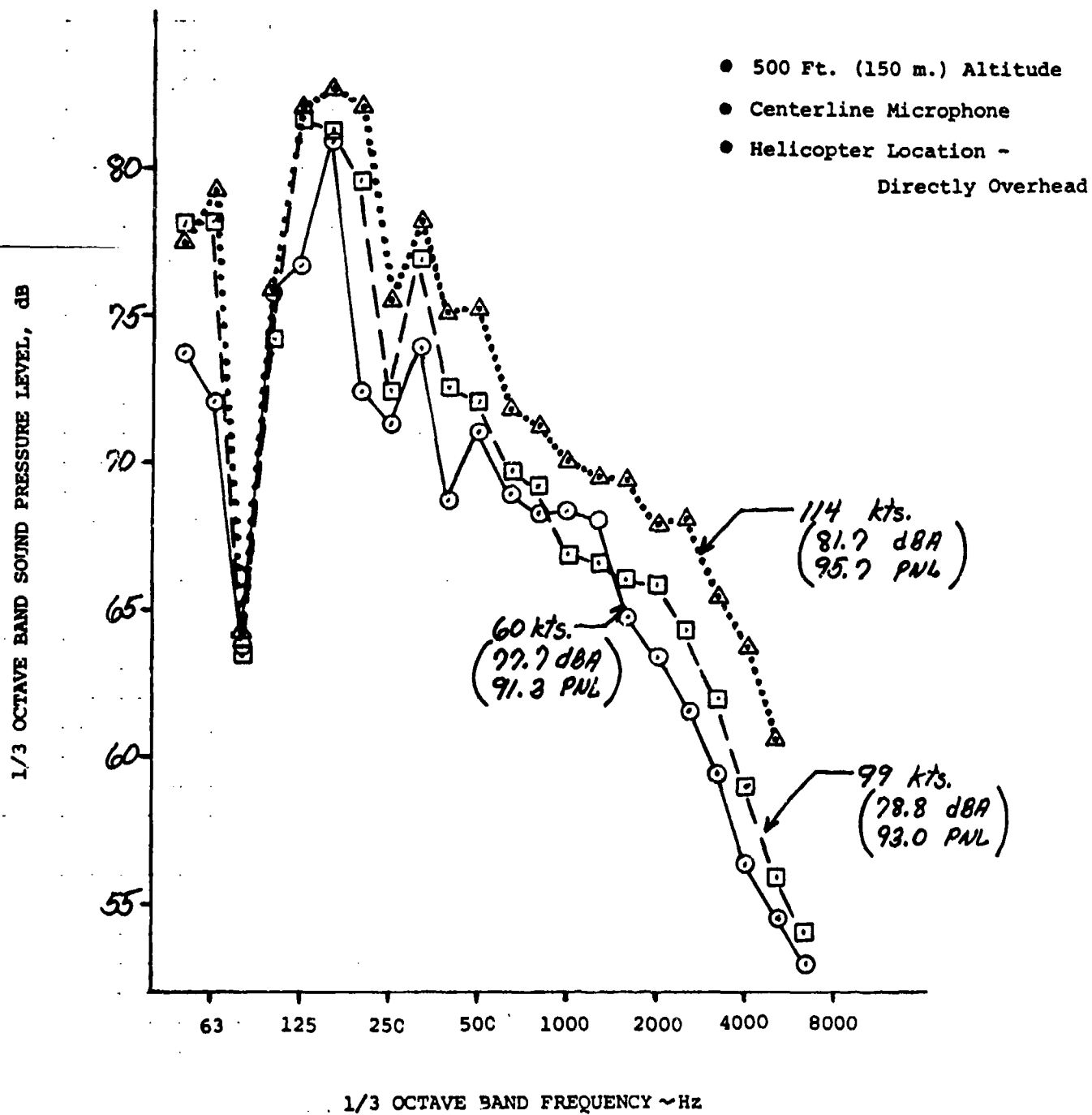
BELL 206-L

FIGURE 33. LEVEL FLYOVER SPECTRA



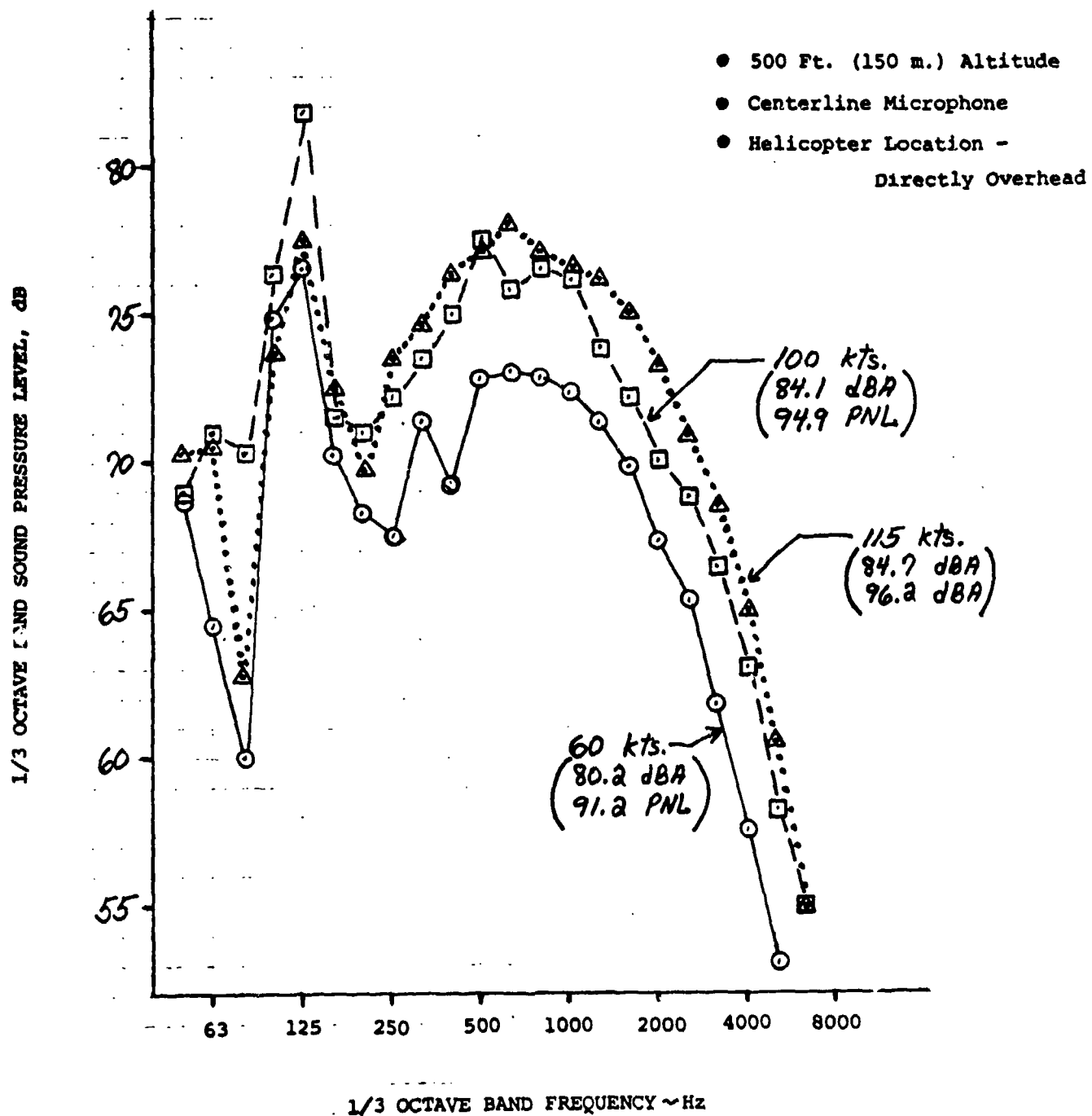
BELL 212 (UH1N)

FIGURE 34. LEVEL FLYOVER SPECTRA



# SIKORSKY S-61

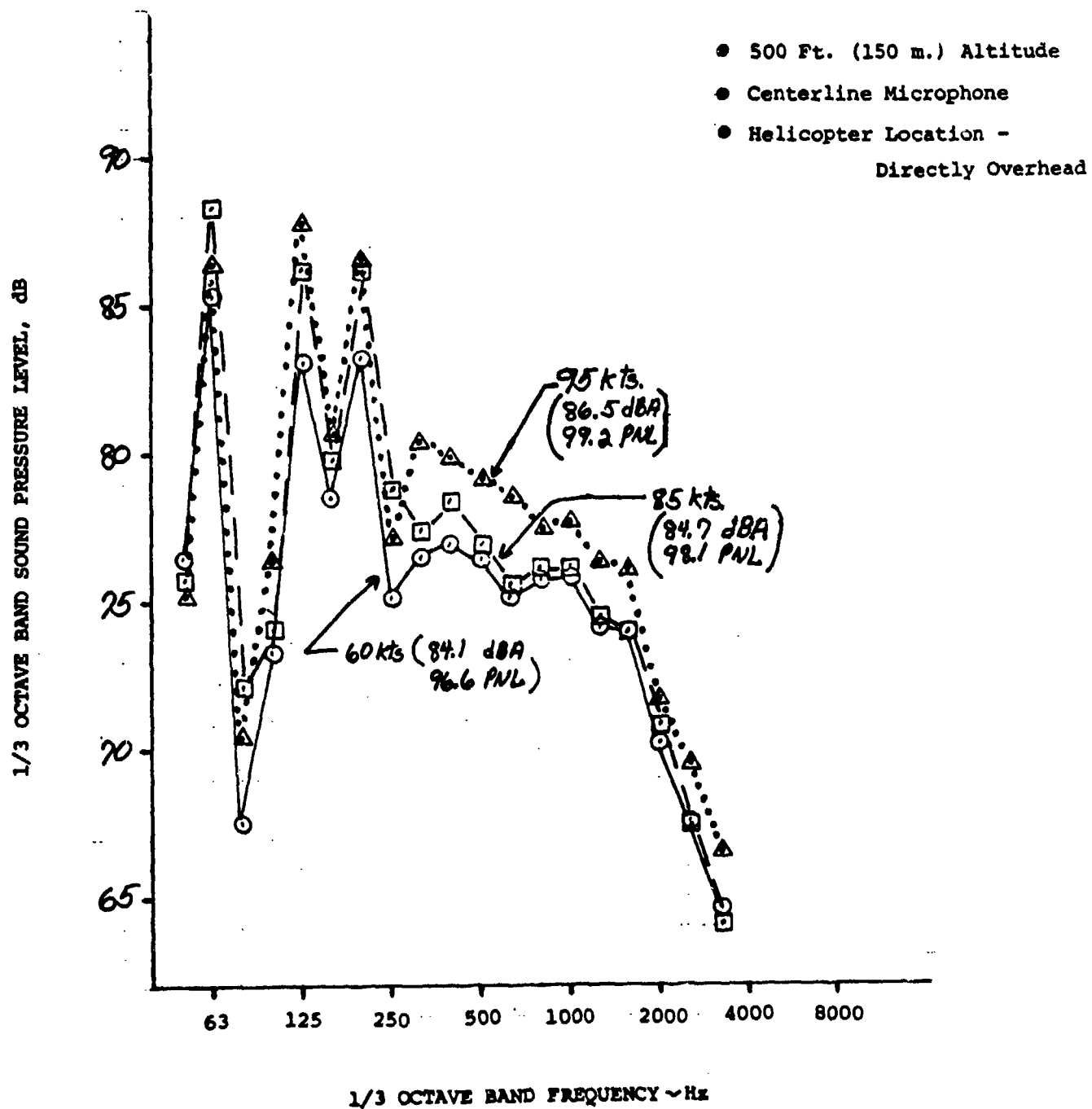
FIGURE 16. LEVEL FLYOVER SPECTRA



# SIKORSKY S-64 "SKYCRANE"

(with truck)

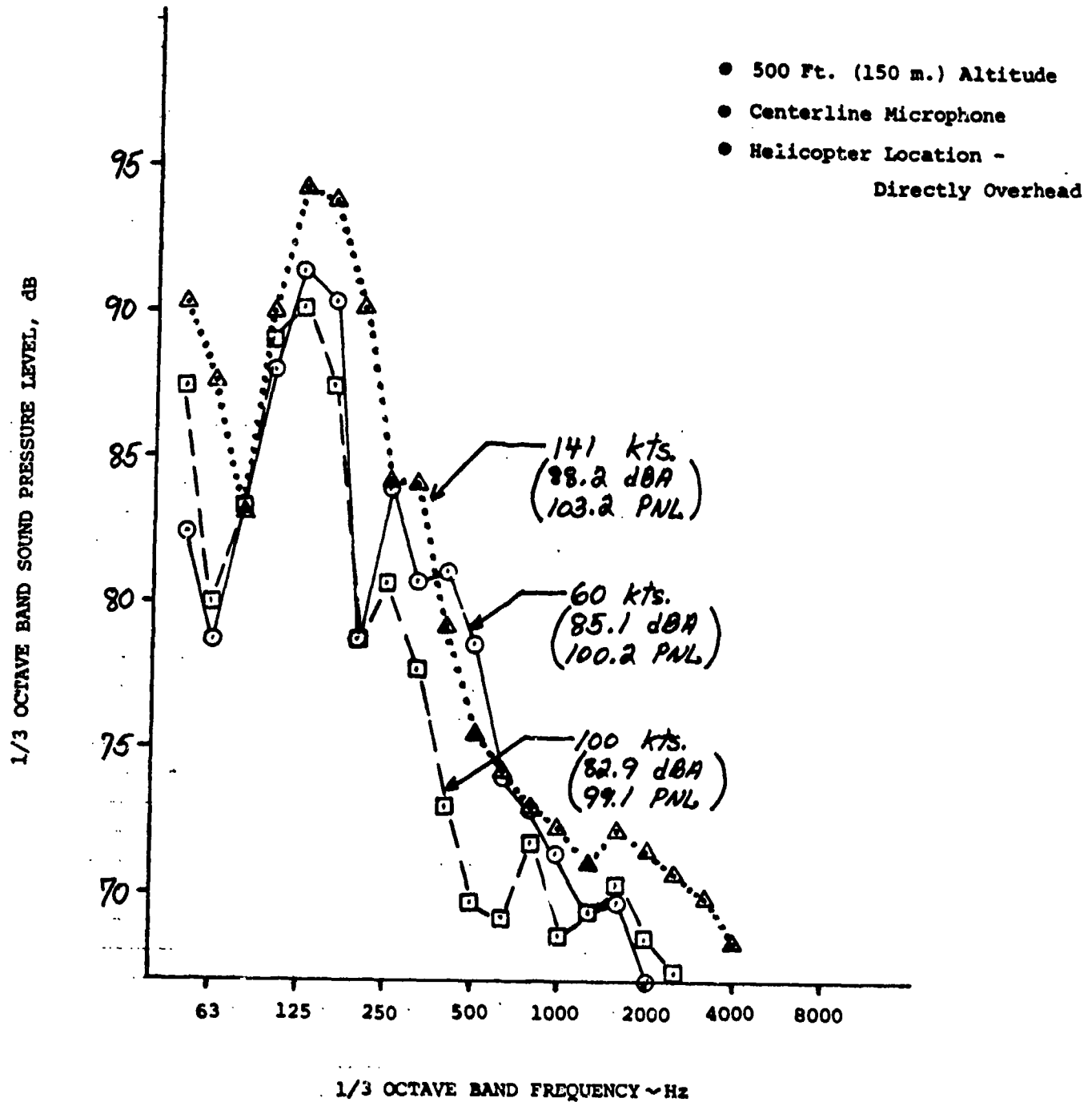
FIGURE 30. LEVEL FLYOVER SPECTRA





# BOEING VERTOL CH-47C

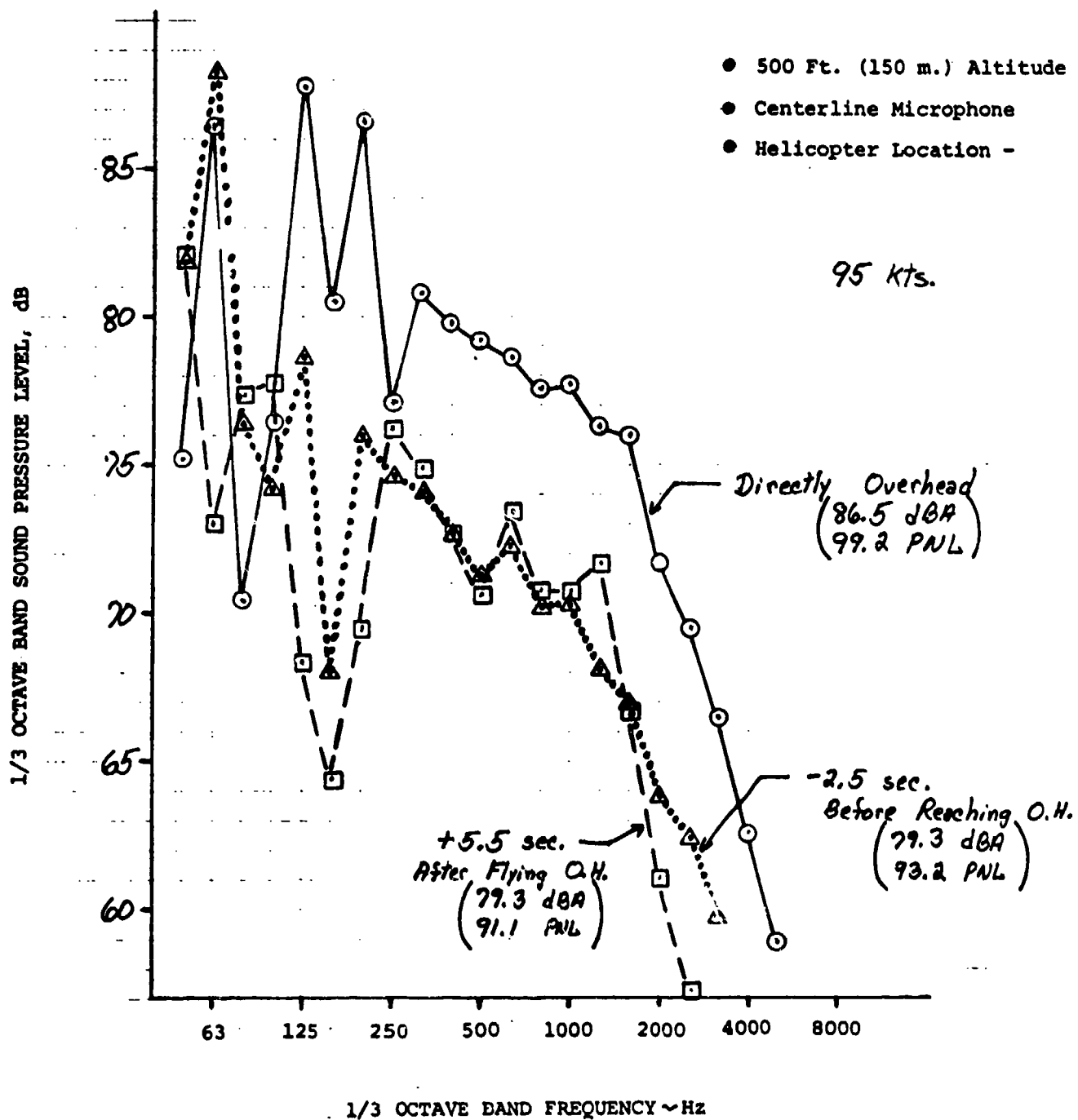
## FIGURE 37. LEVEL FLYOVER SPECTRA



# SIKORSKY S-64 "SKYCRANE"

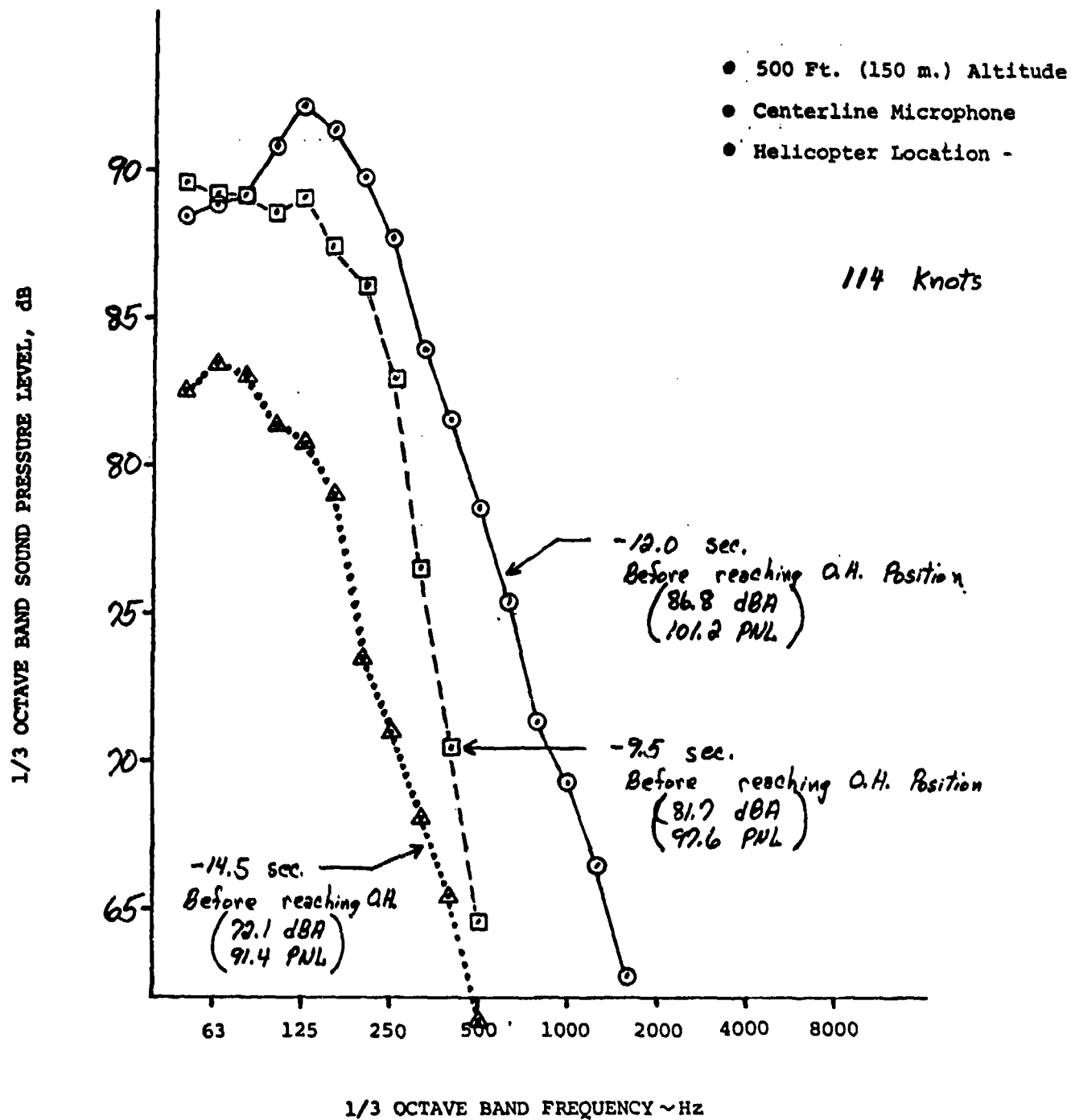
(with truck)

FIGURE 38. LEVEL FLYOVER SPECTRA



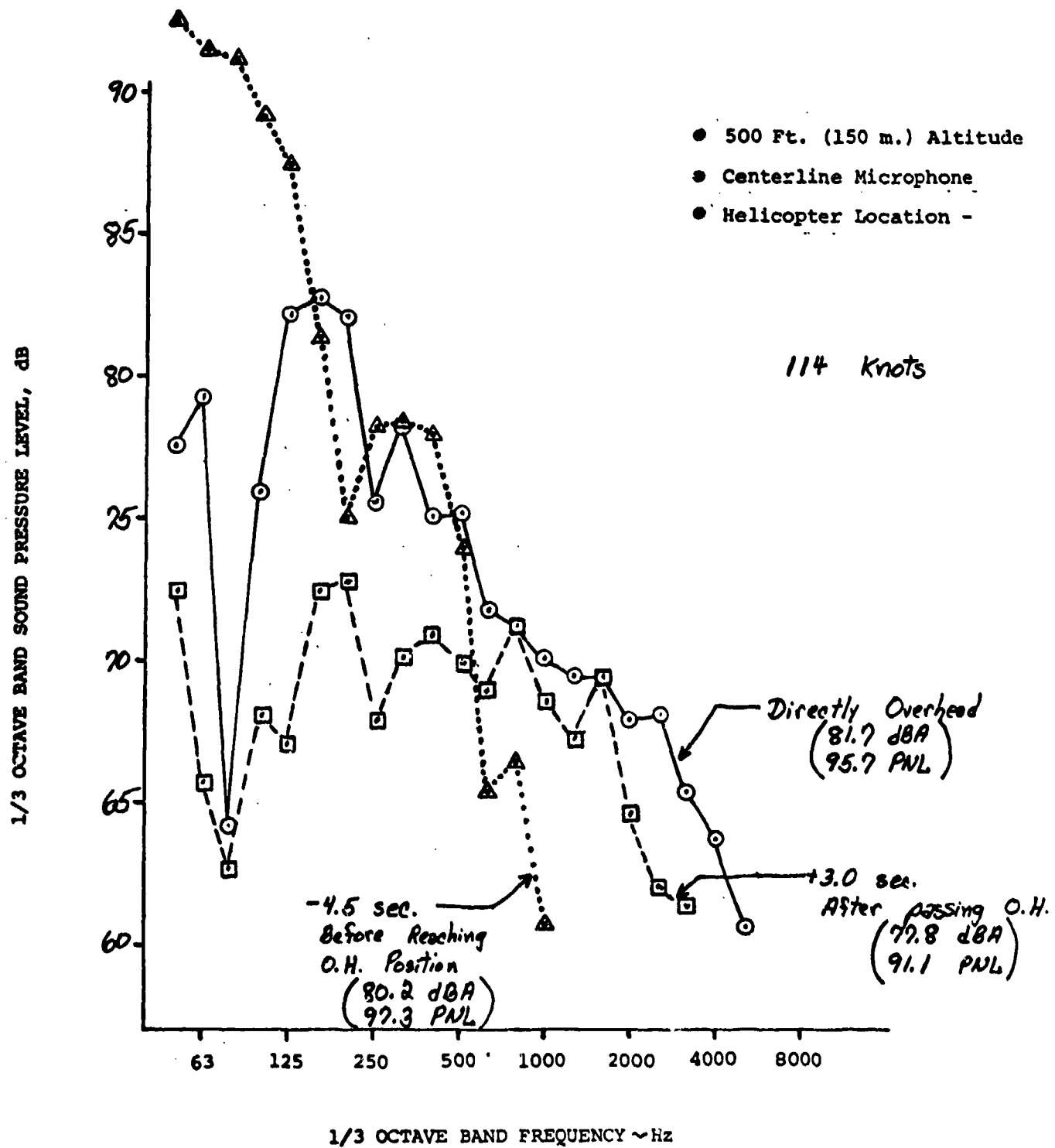
BELL 212 (UH1N)

FIGURE 39 . LEVEL FLYOVER SPECTRA



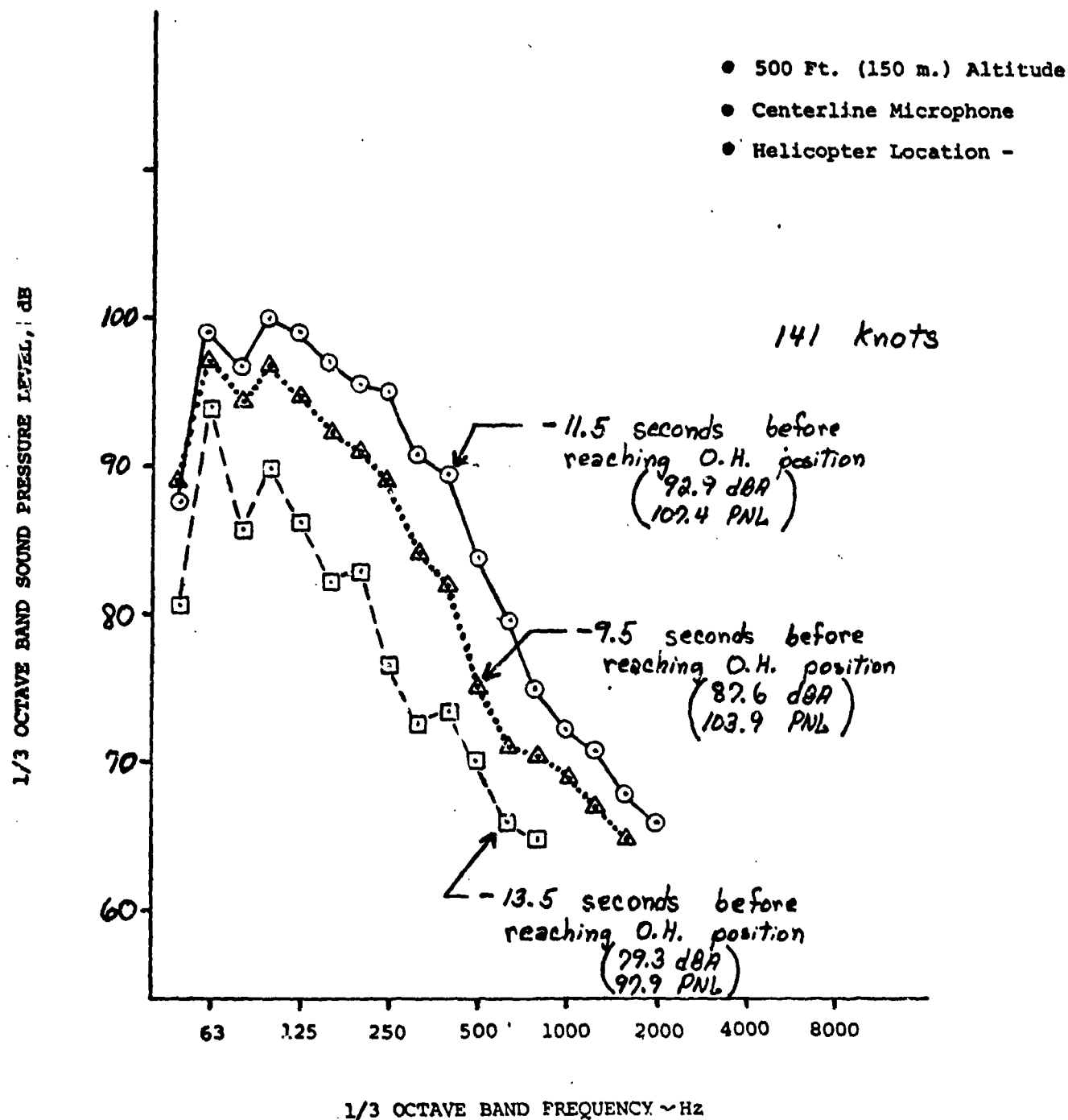
BELL 212 (UH1N)

FIGURE 40. LEVEL FLYOVER SPECTRA



# BOEING VERTOL CH-47C

## FIGURE 41 . LEVEL FLYOVER SPECTRA



# BOEING VERTOL CH-47C

FIGURE 4A. LEVEL FLYOVER SPECTRA

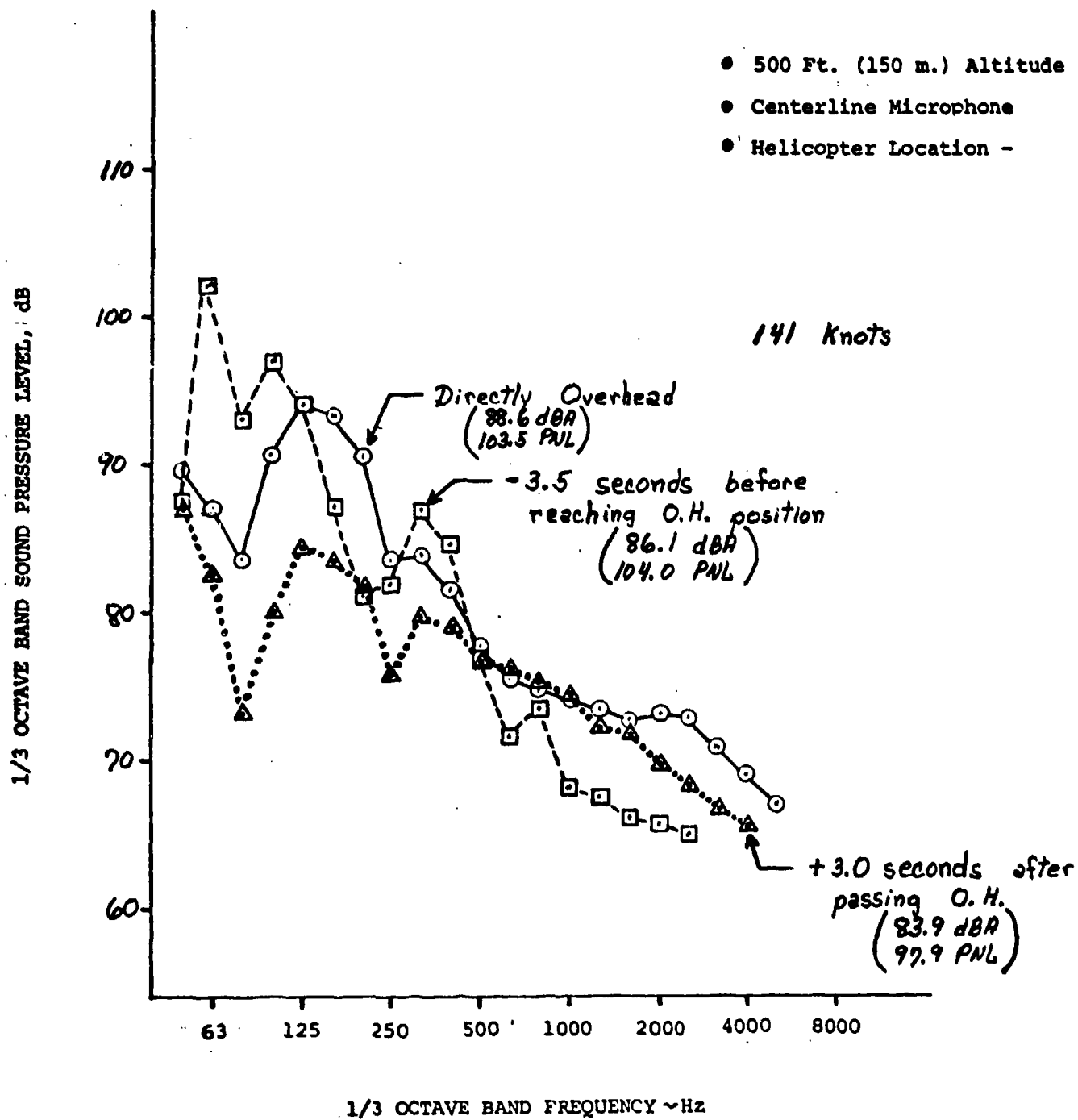
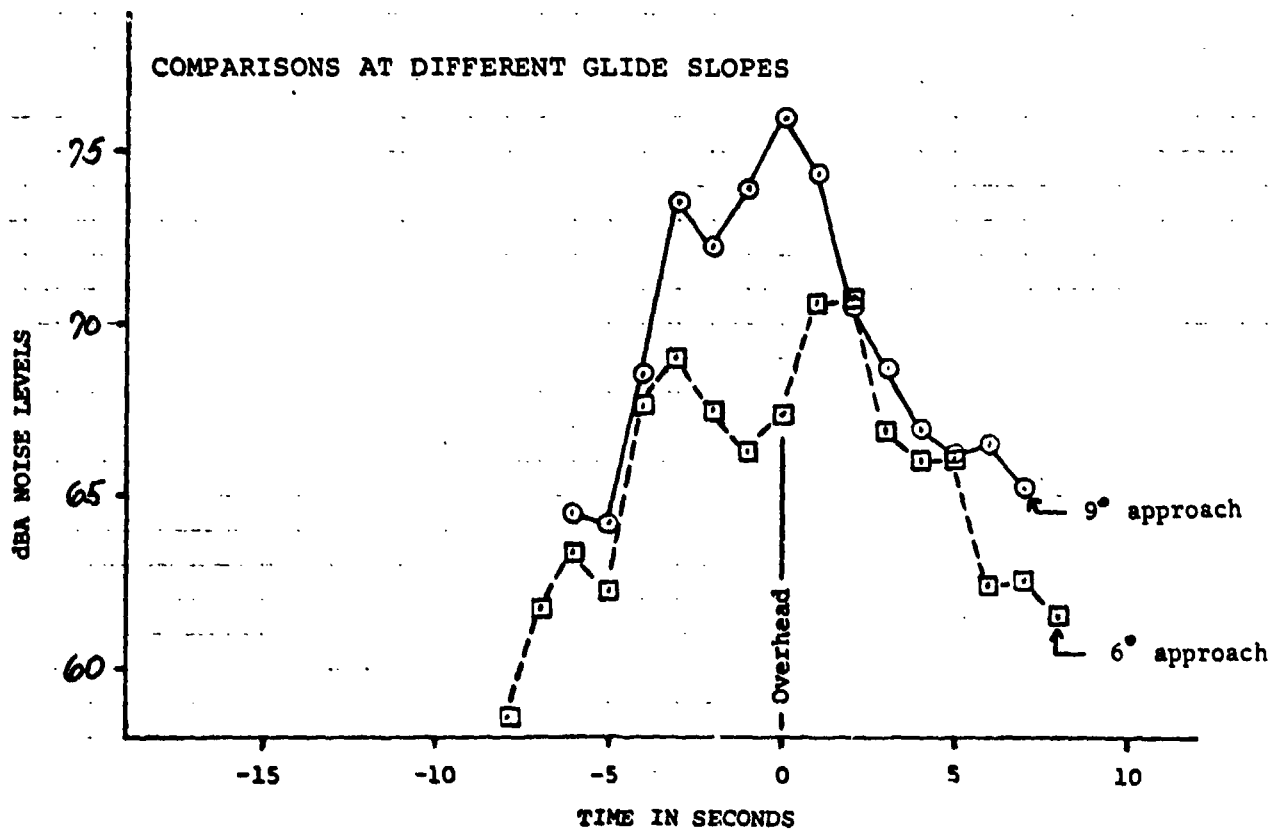
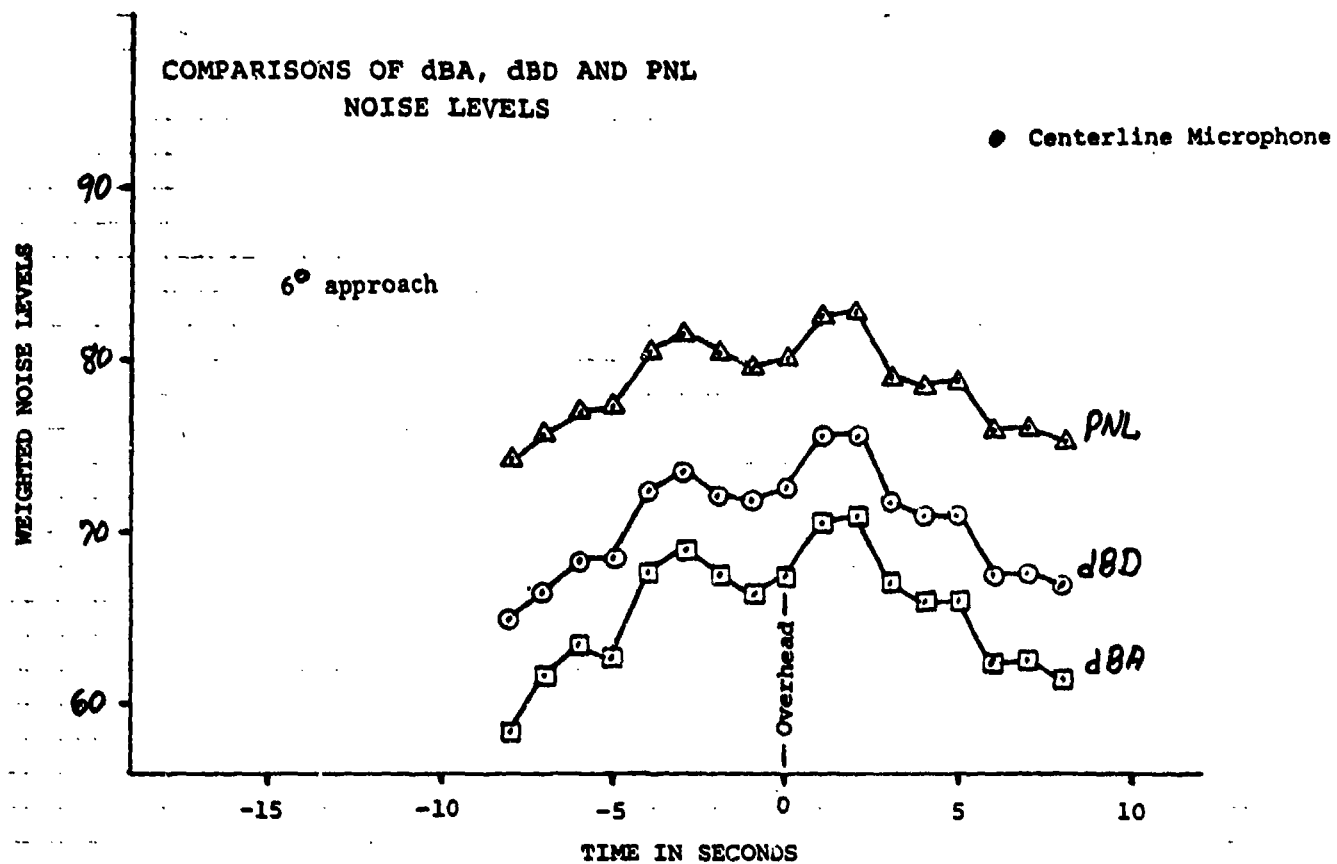


FIGURE 43

HUGHES 300-C  
APPROACH TIME HISTORIES



HUGHES 500-C  
 FIGURE 44 APPROACH TIME HISTORIES

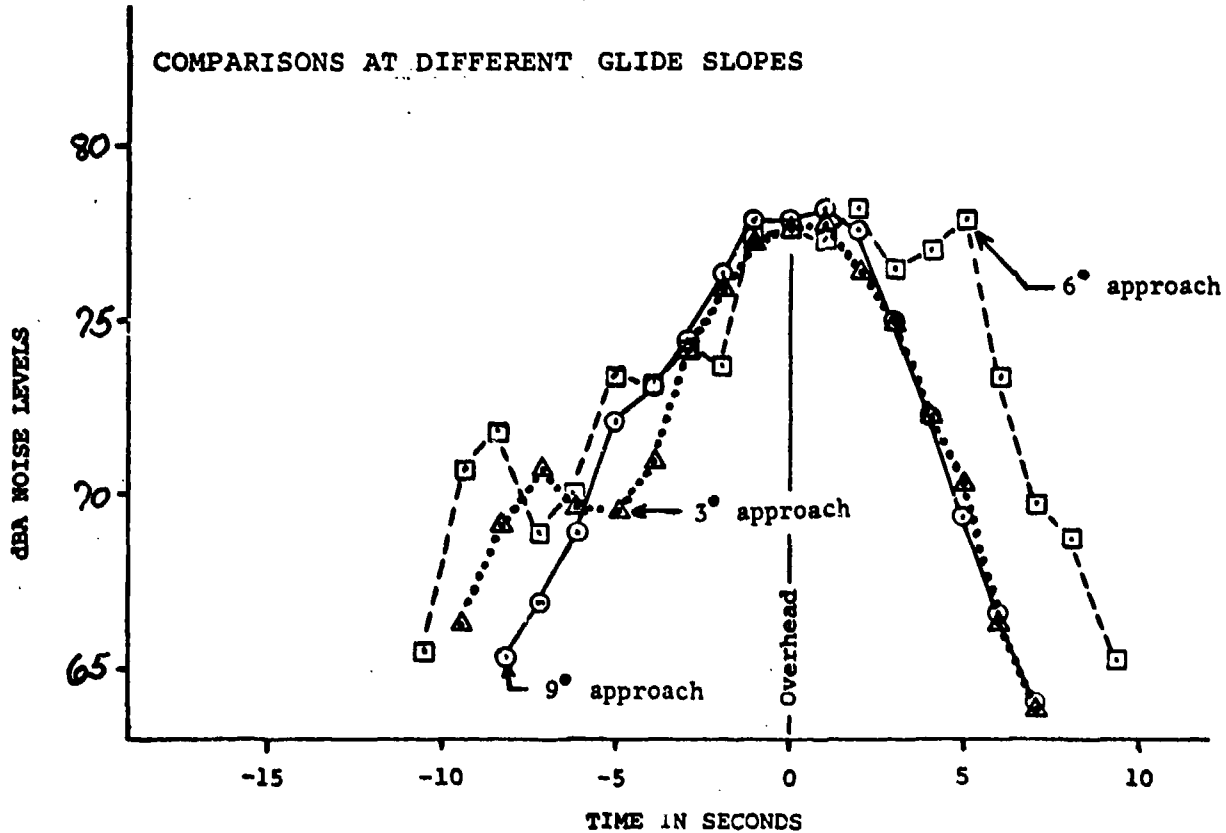
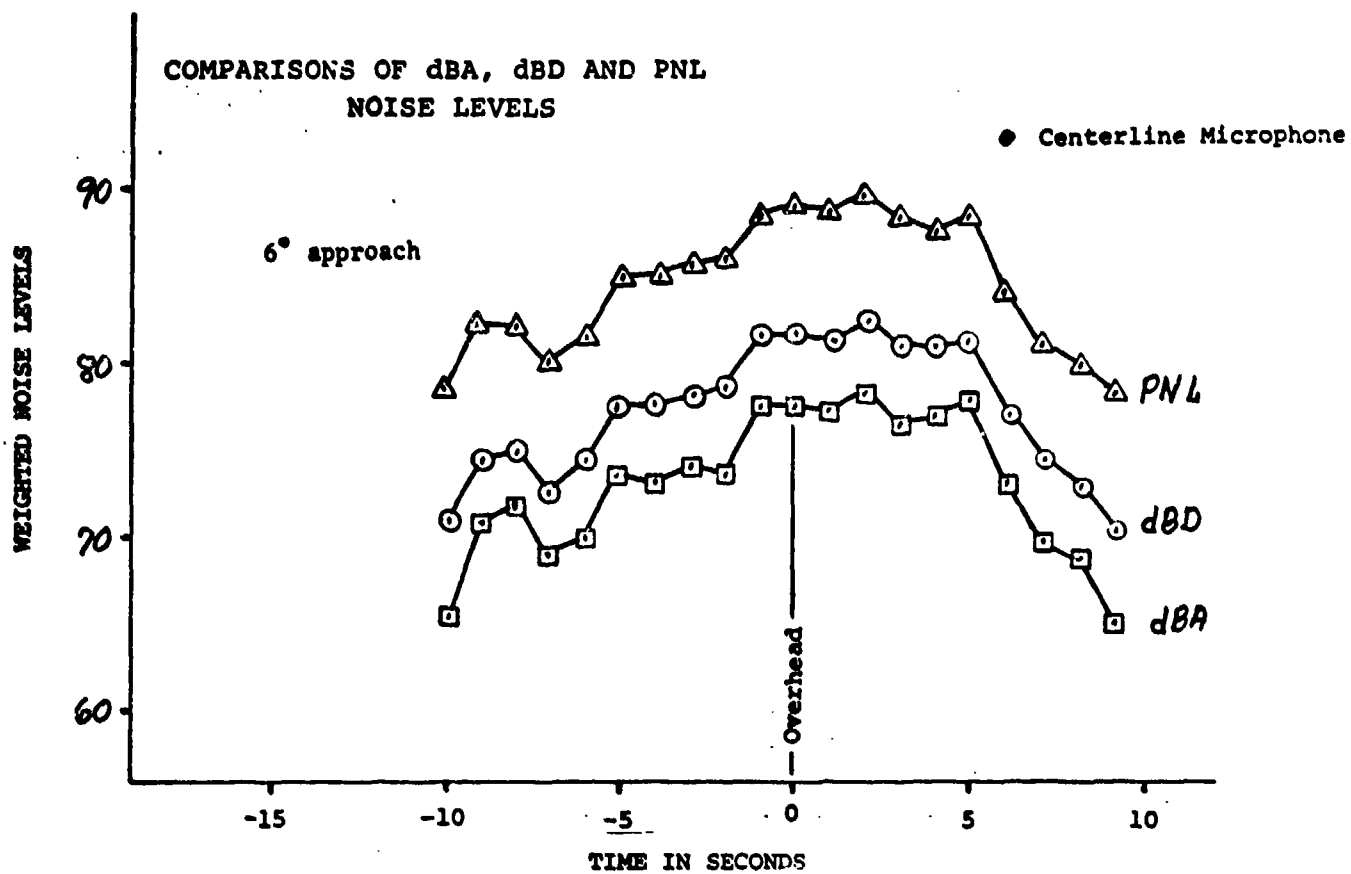
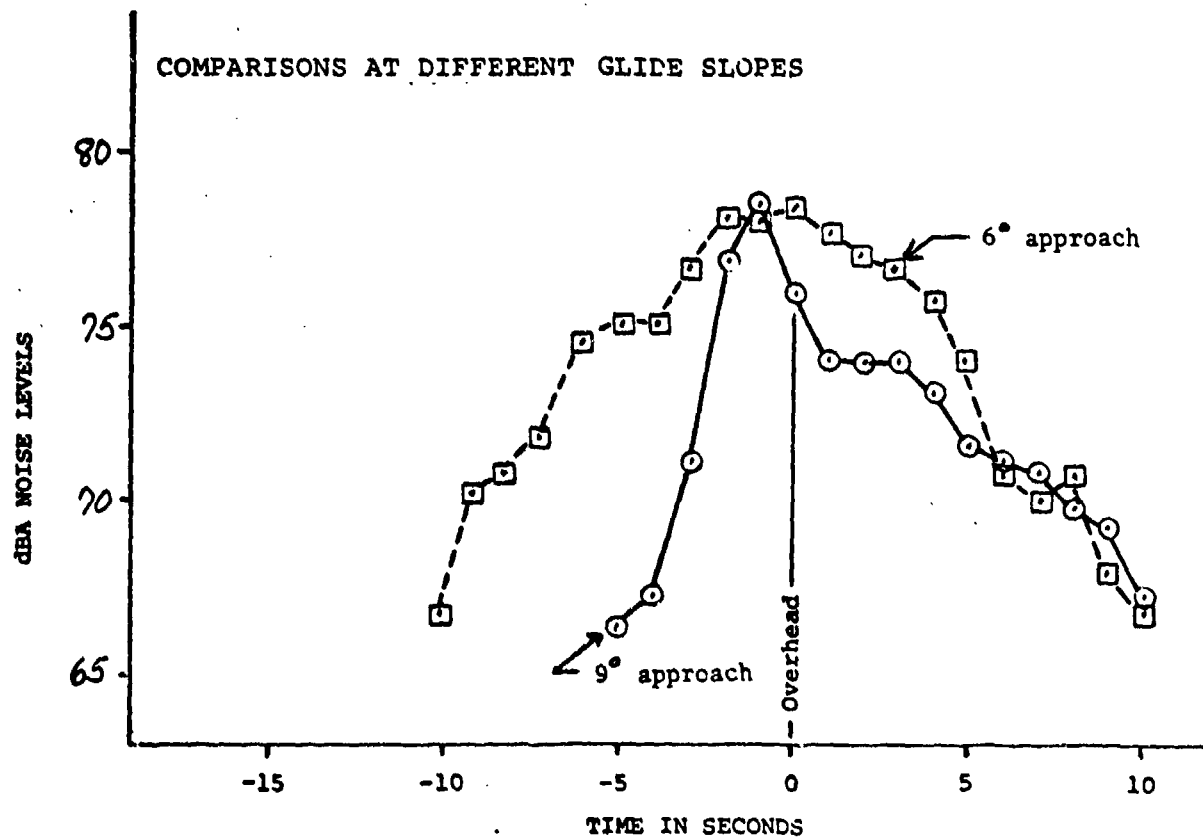
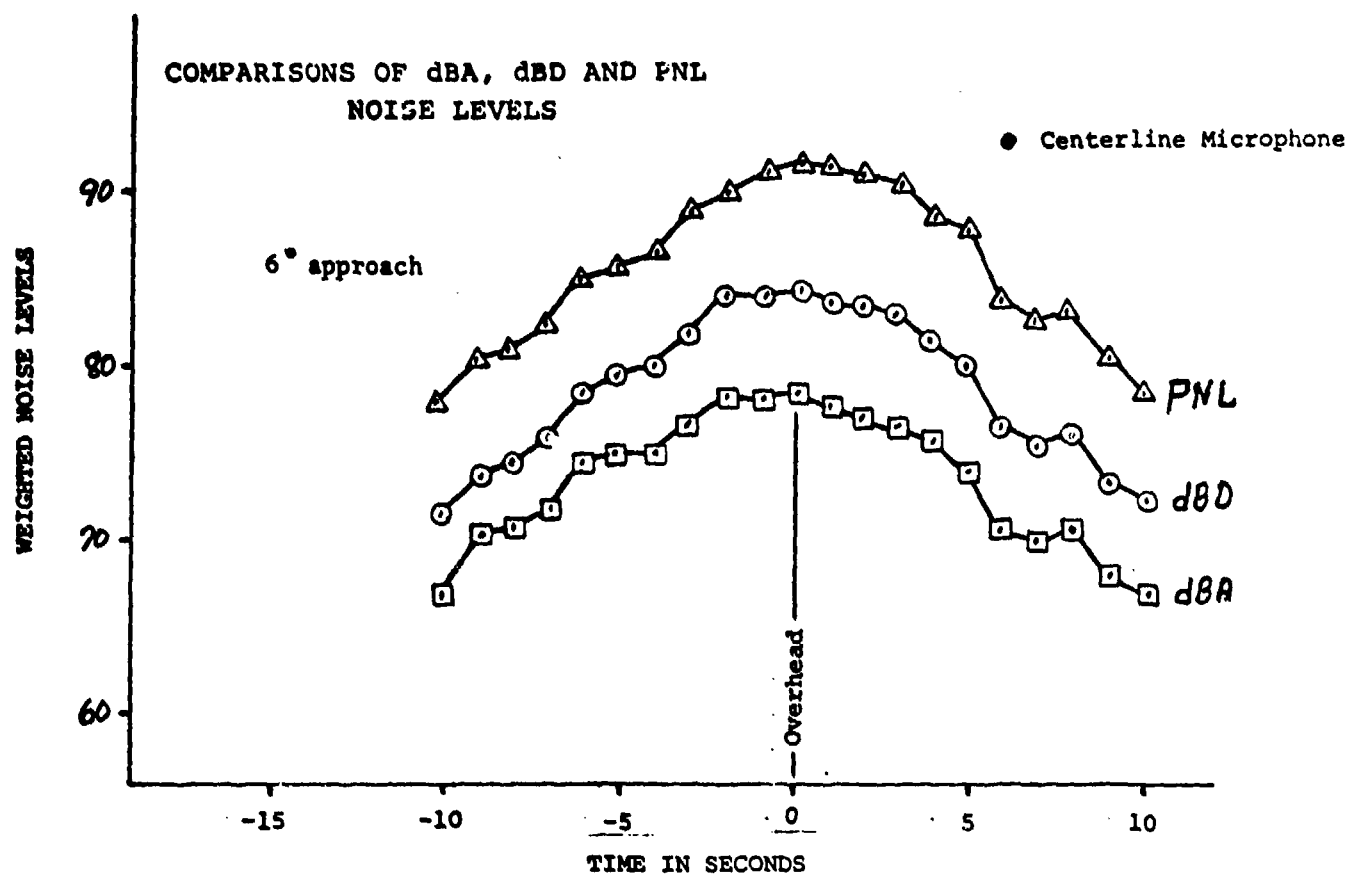


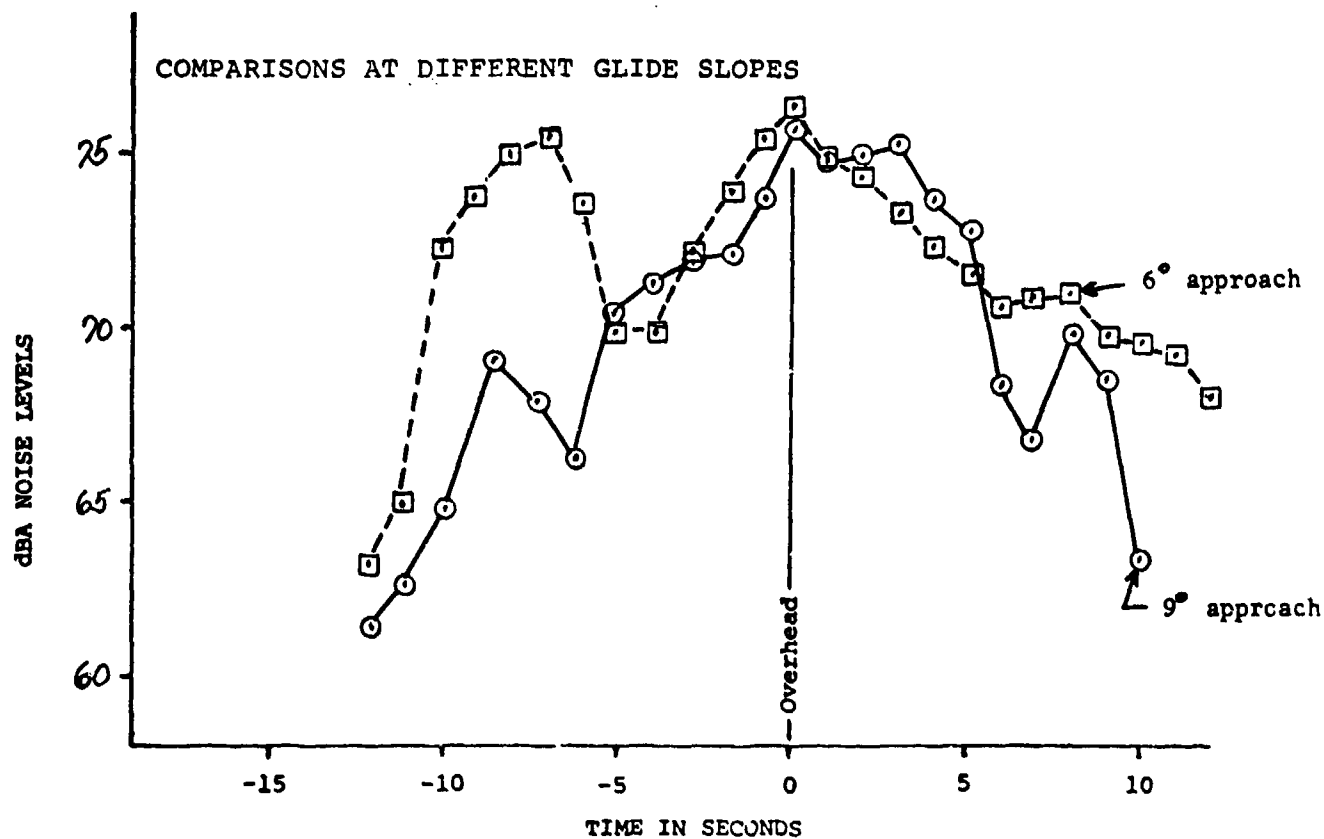
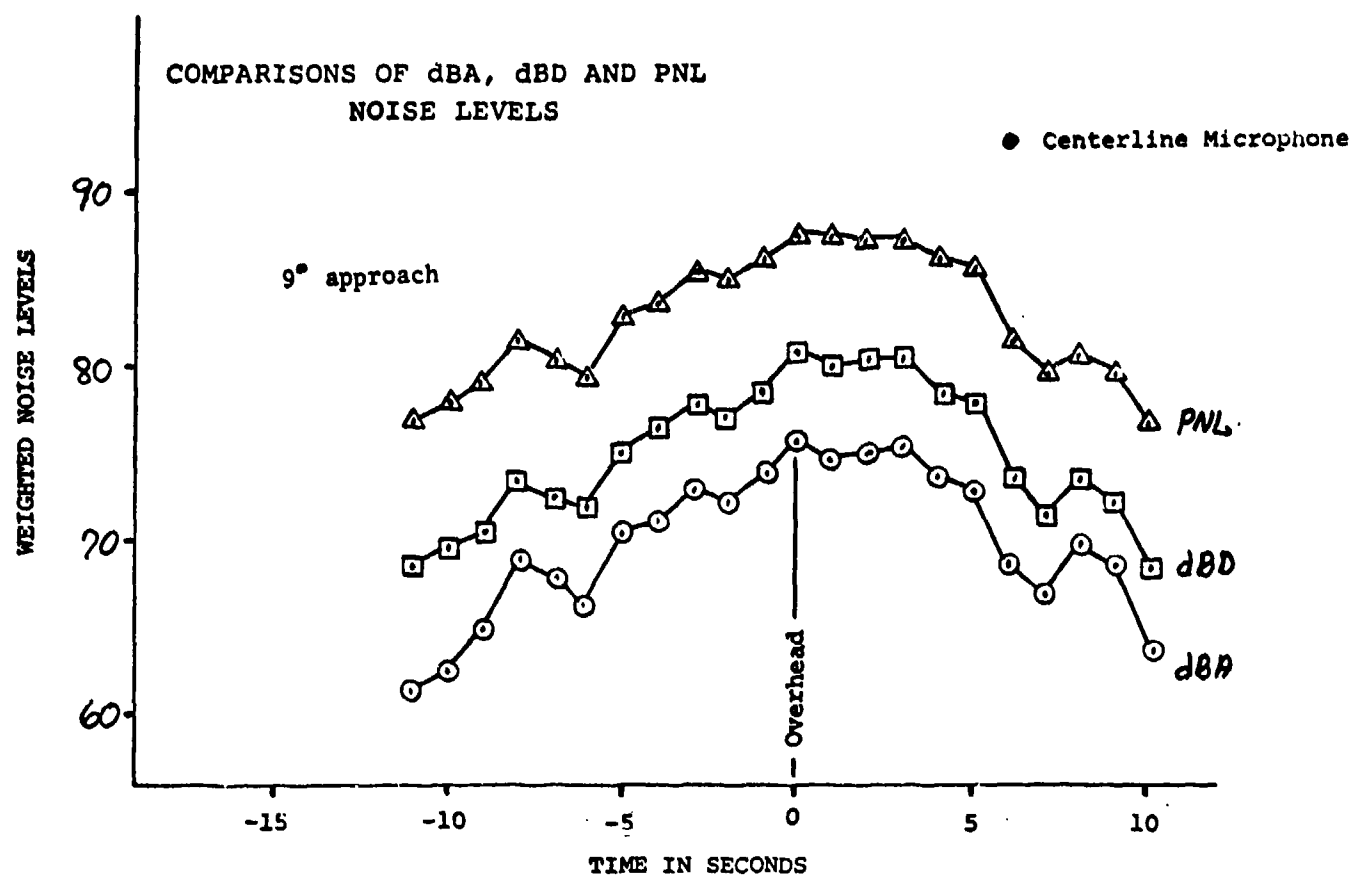


FIGURE 45

BELL 47-G  
APPROACH TIME HISTORIES

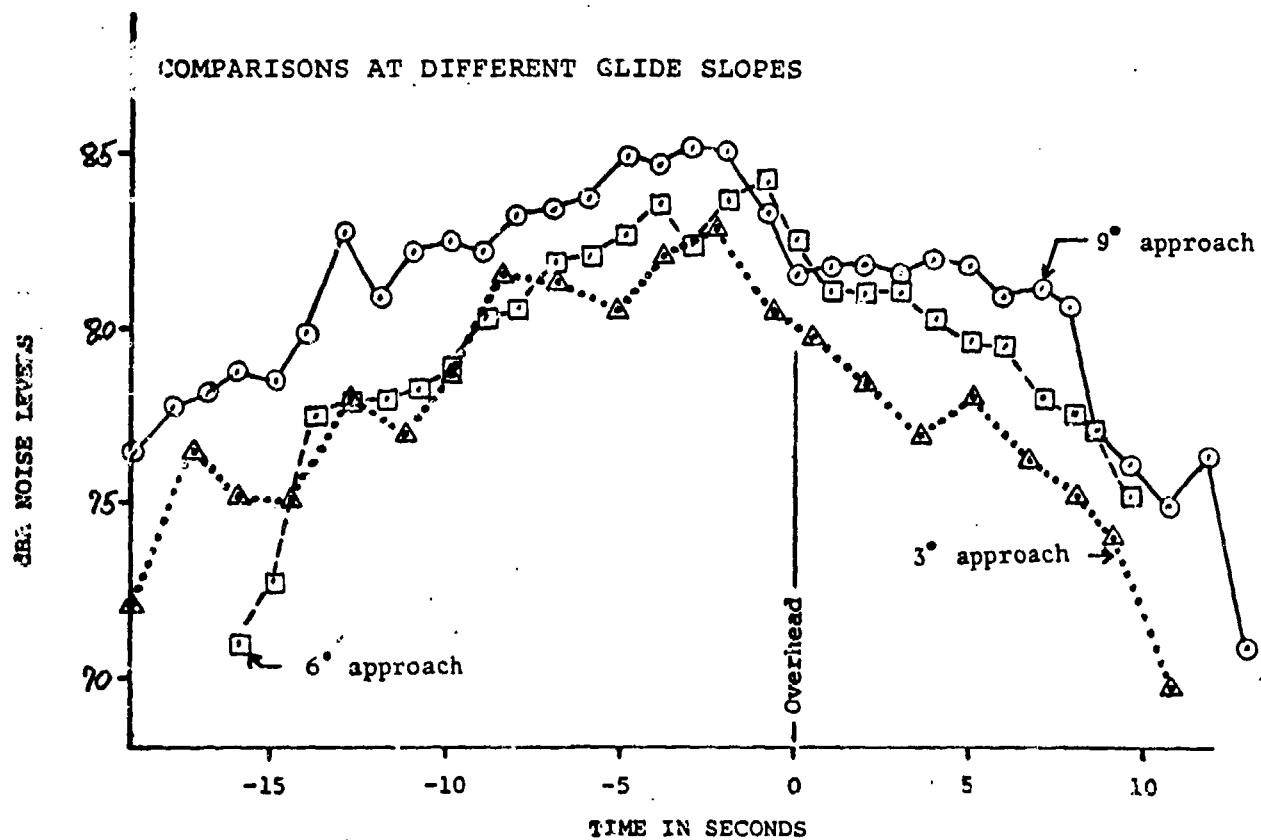
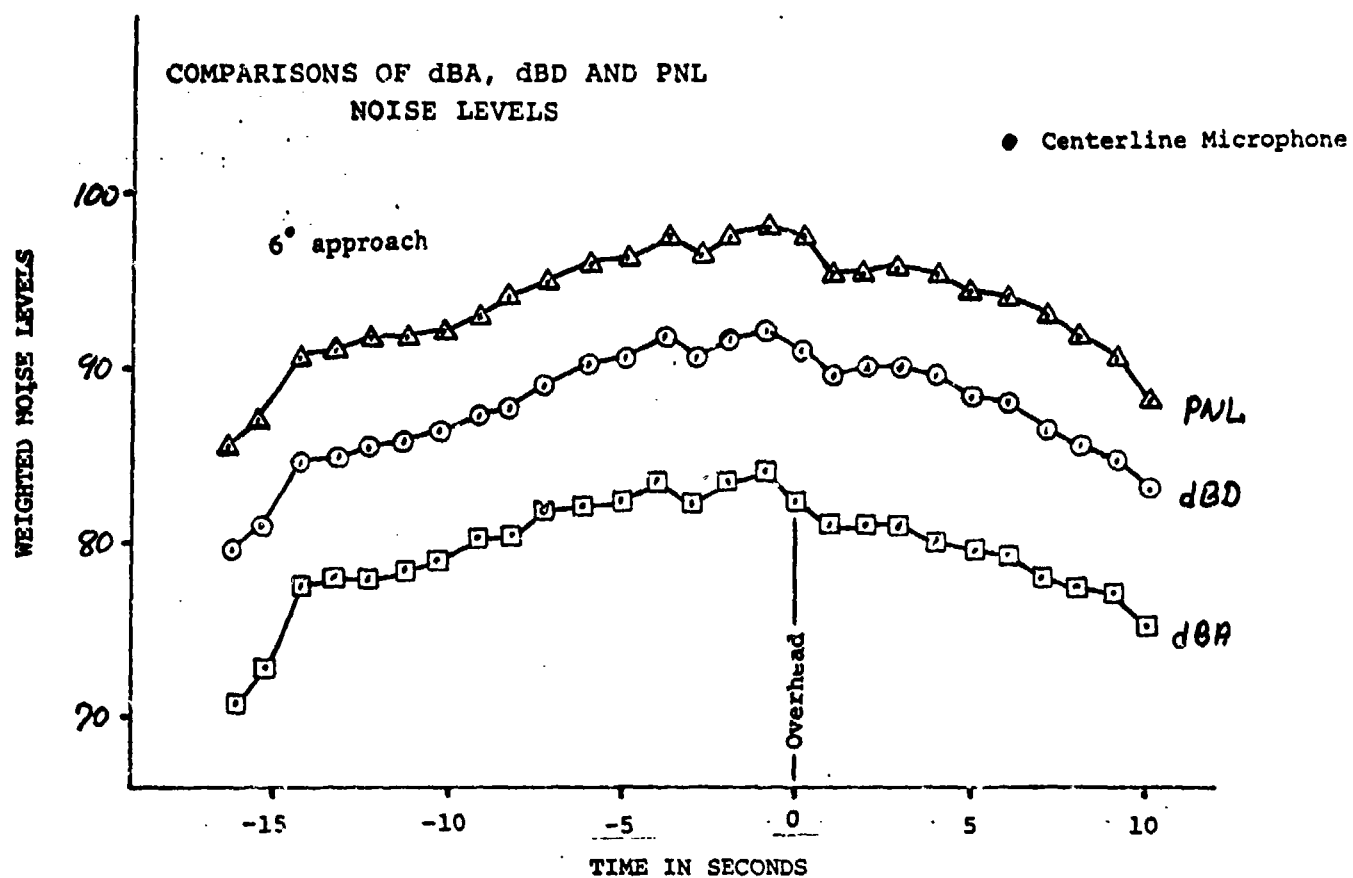


BELL 206-L  
FIGURE 46 APPROACH TIME HISTORIES



BELL 212 (UH1N)  
 APPROACH TIME HISTORIES

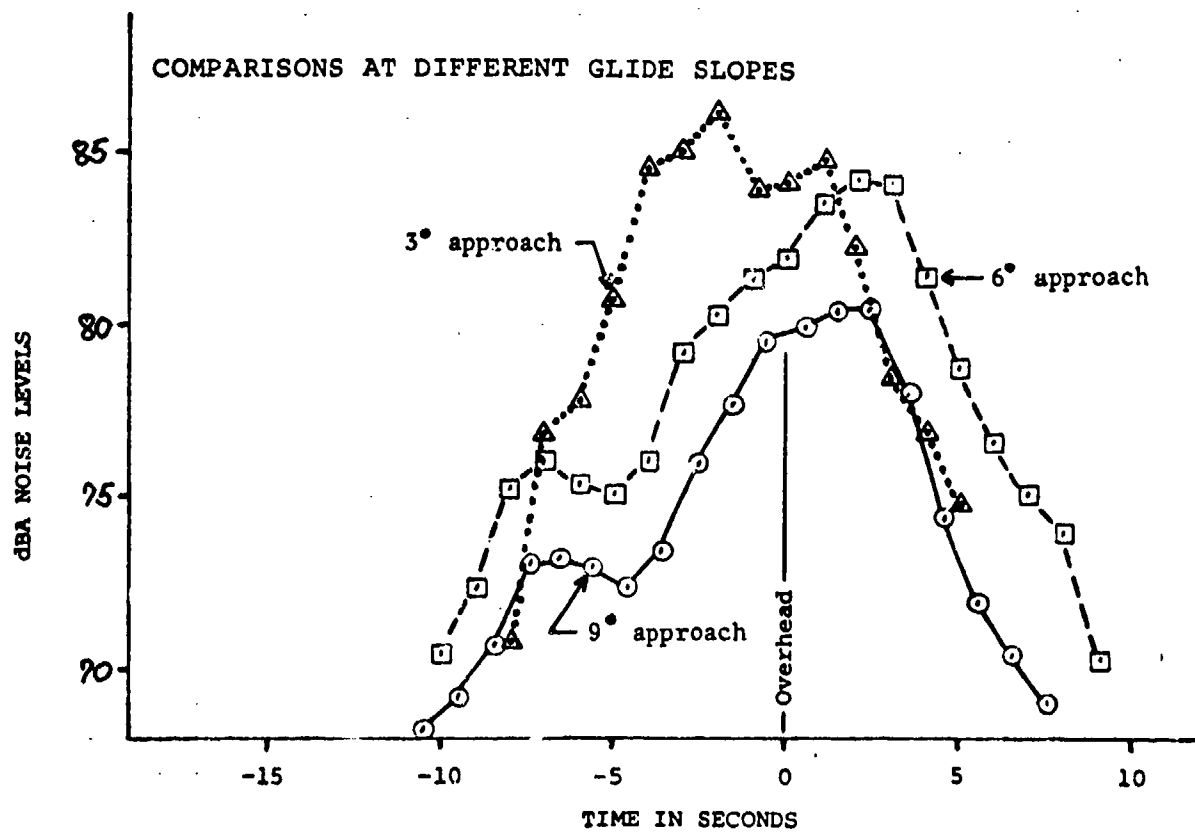
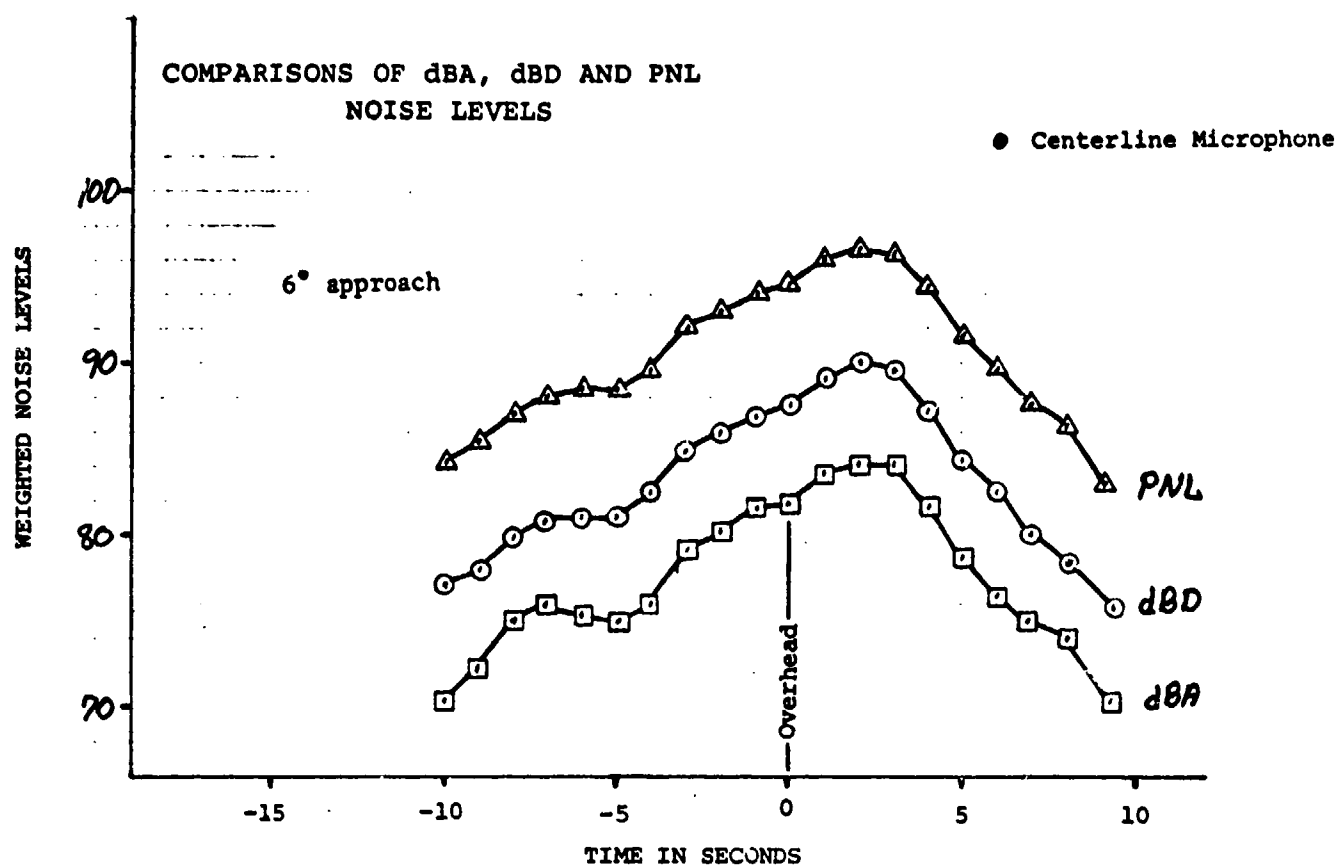
FIGURE 47



# SIKORSKY S-61

FIGURE 46

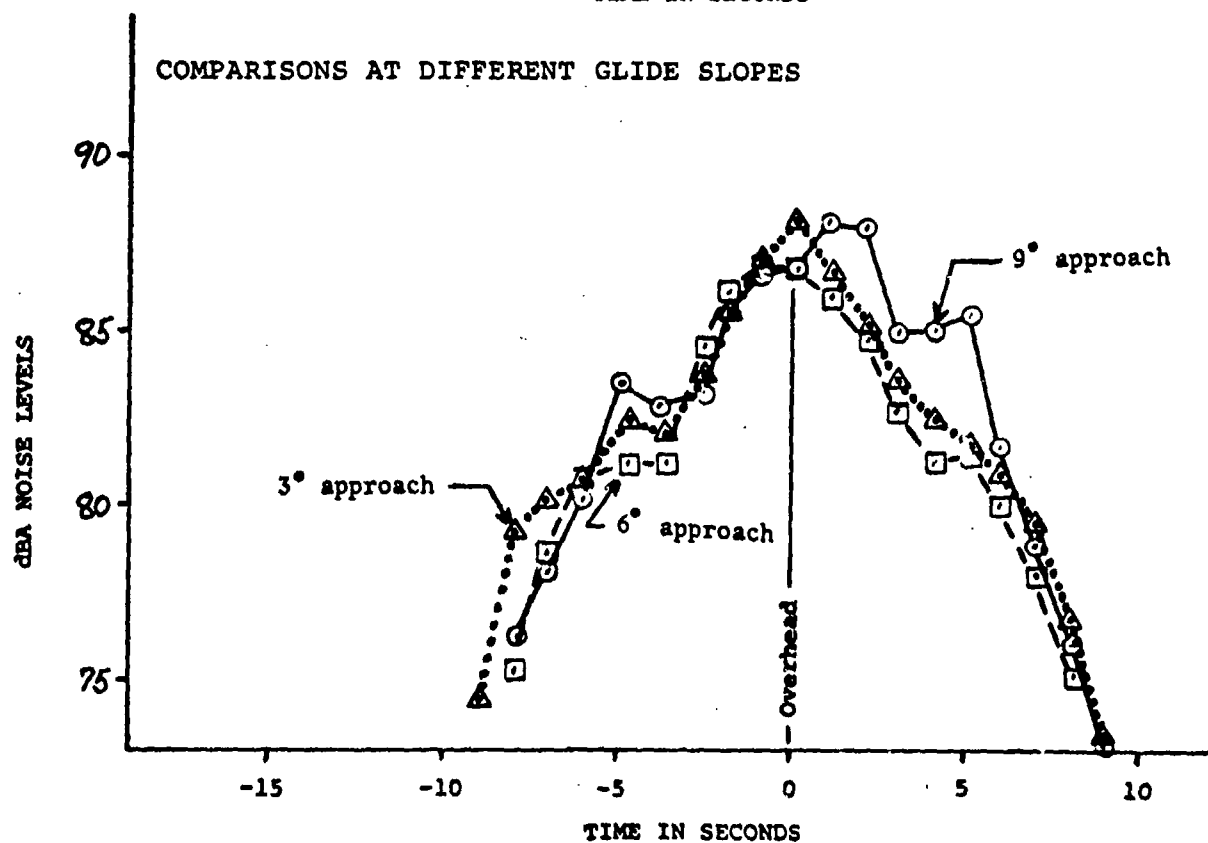
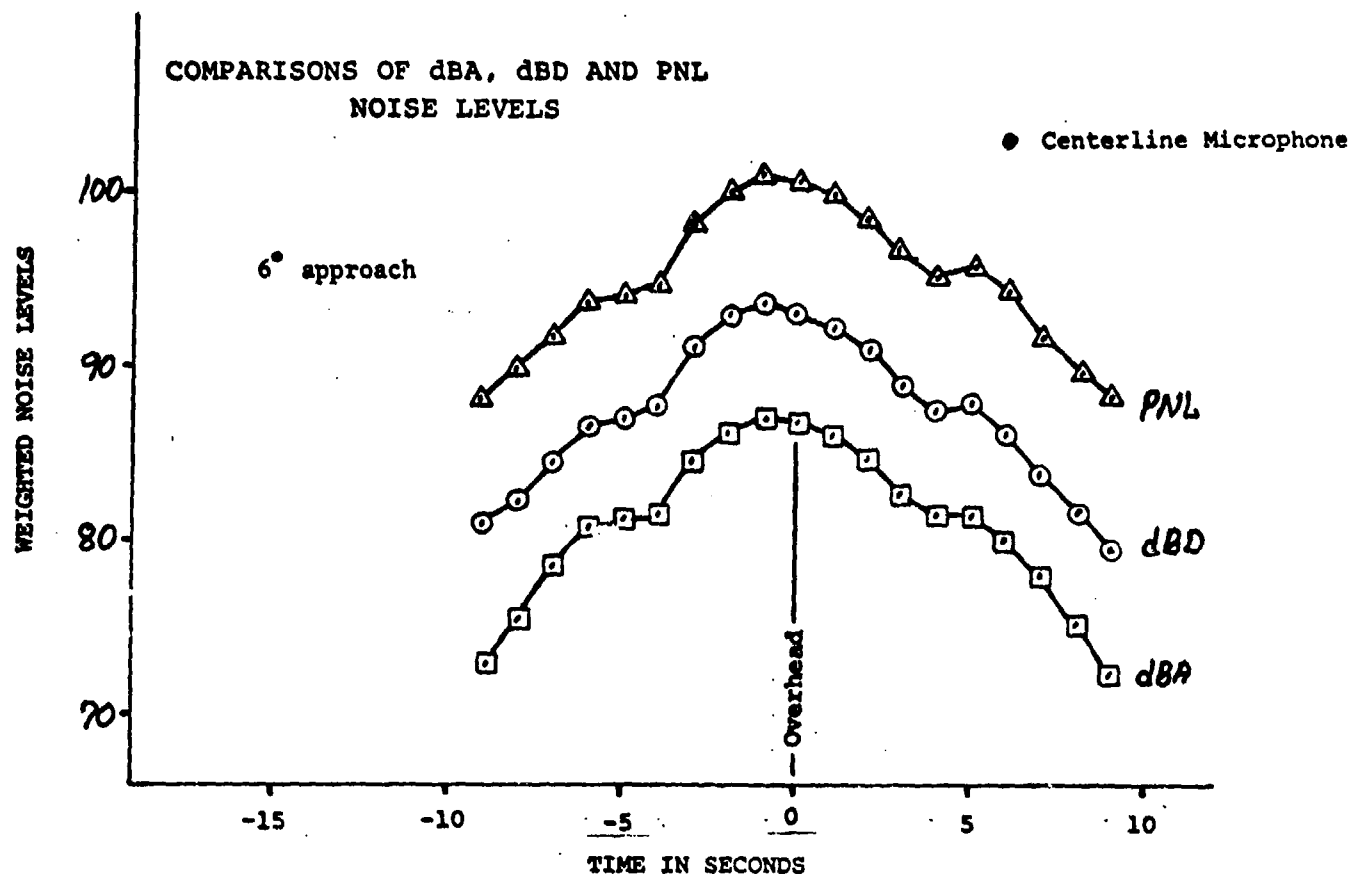
## APPROACH TIME HISTORIES



SIKORSKY S-64 "SKYCRANE"  
APPROACH TIME HISTORIES

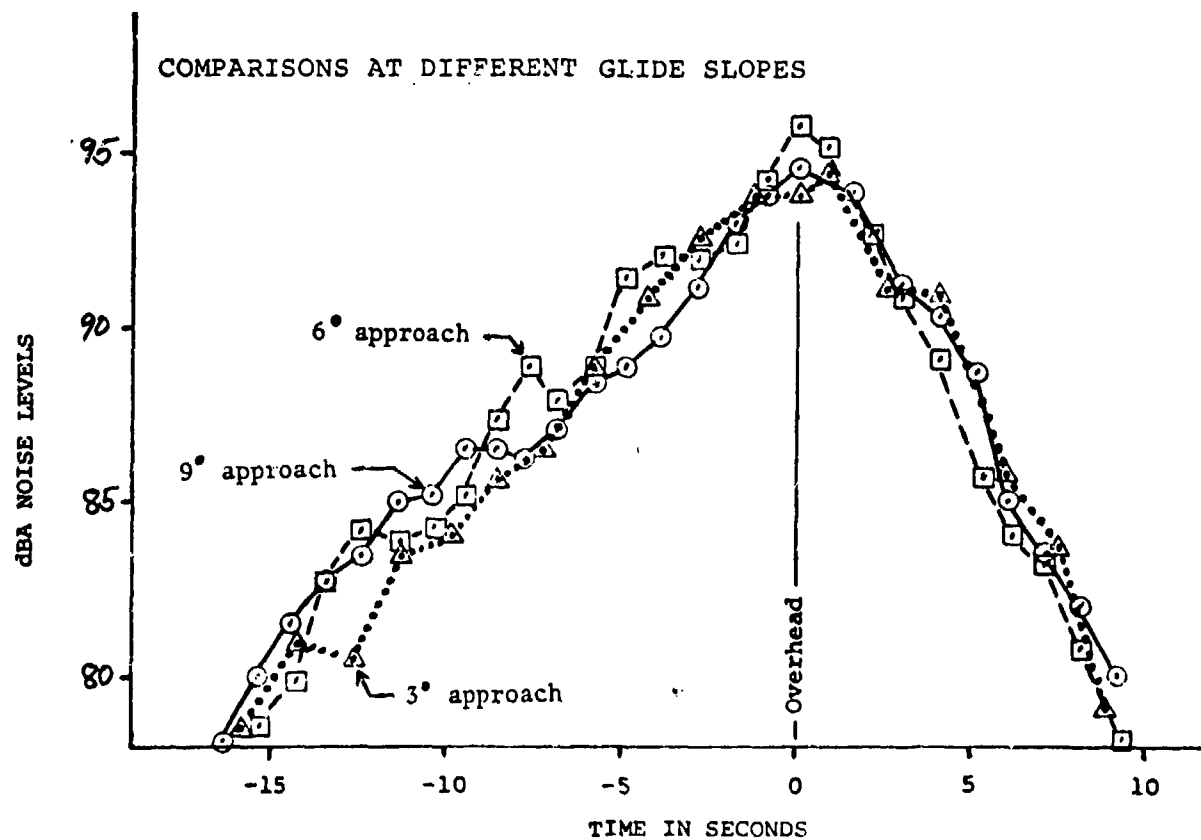
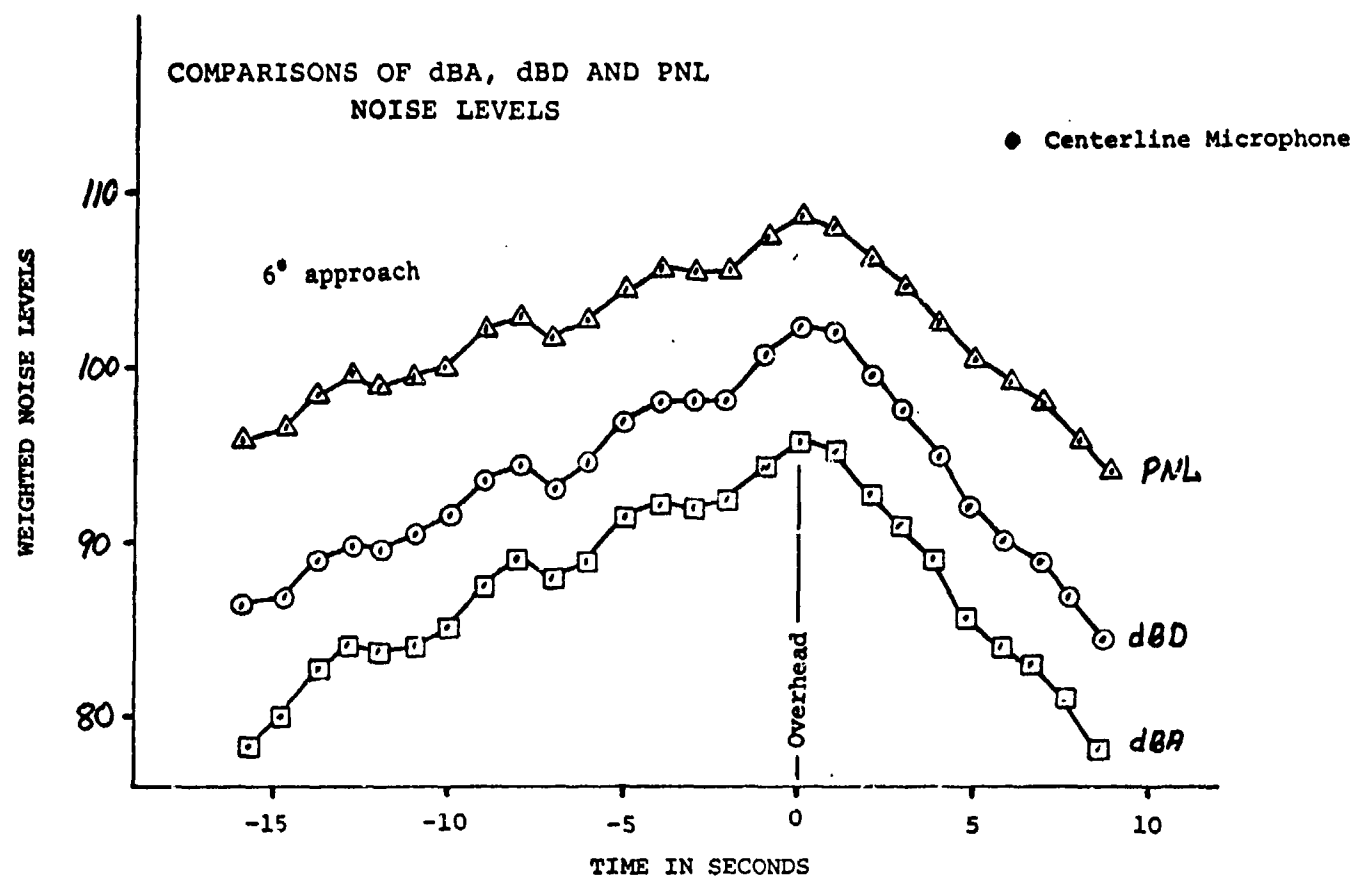
(with truck)

FIGURE V7



BOEING VERTOL CH-47C  
APPROACH TIME HISTORIES

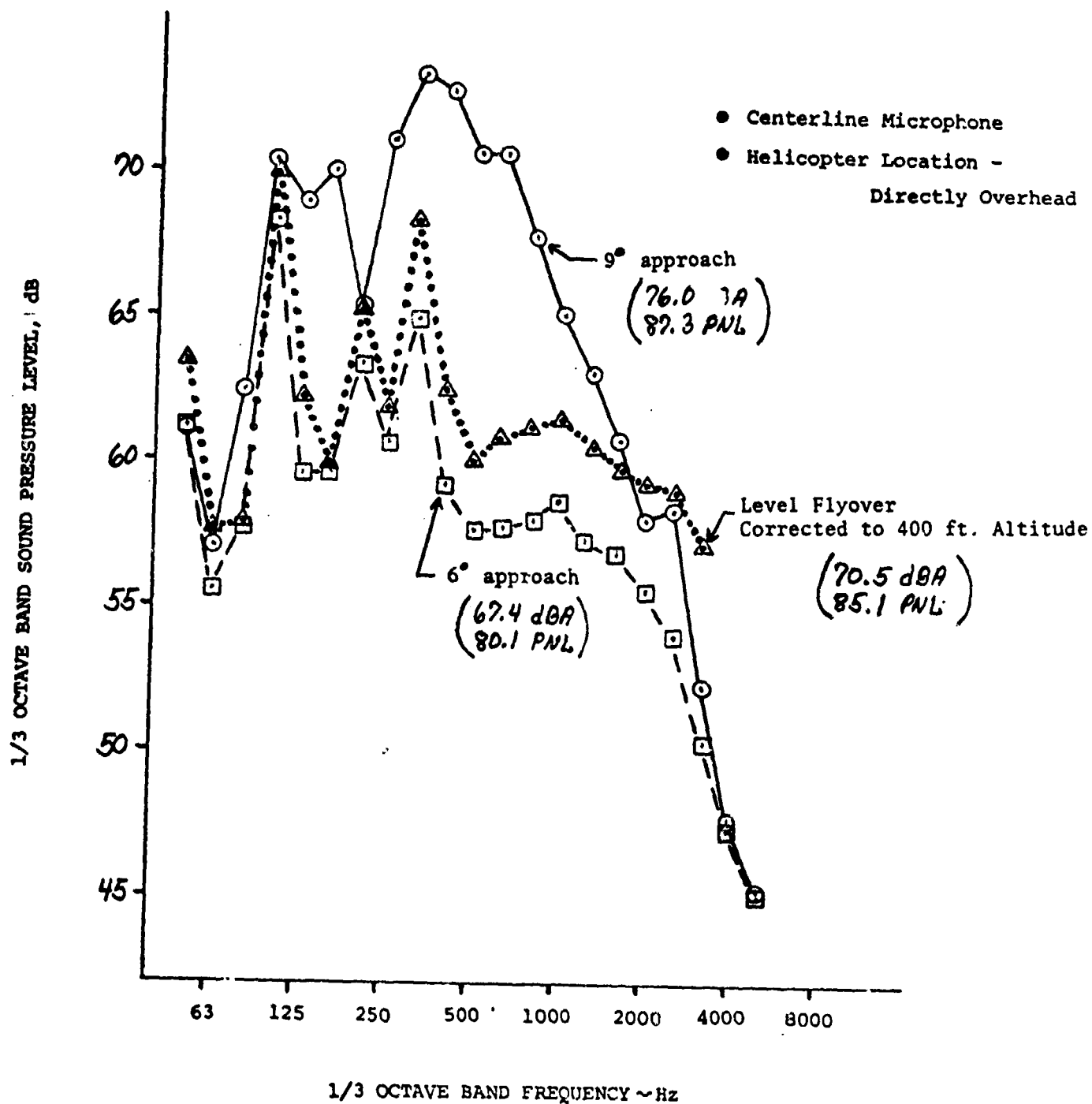
FIGURE 50



# HUGHES 300-C

FIGURE 51

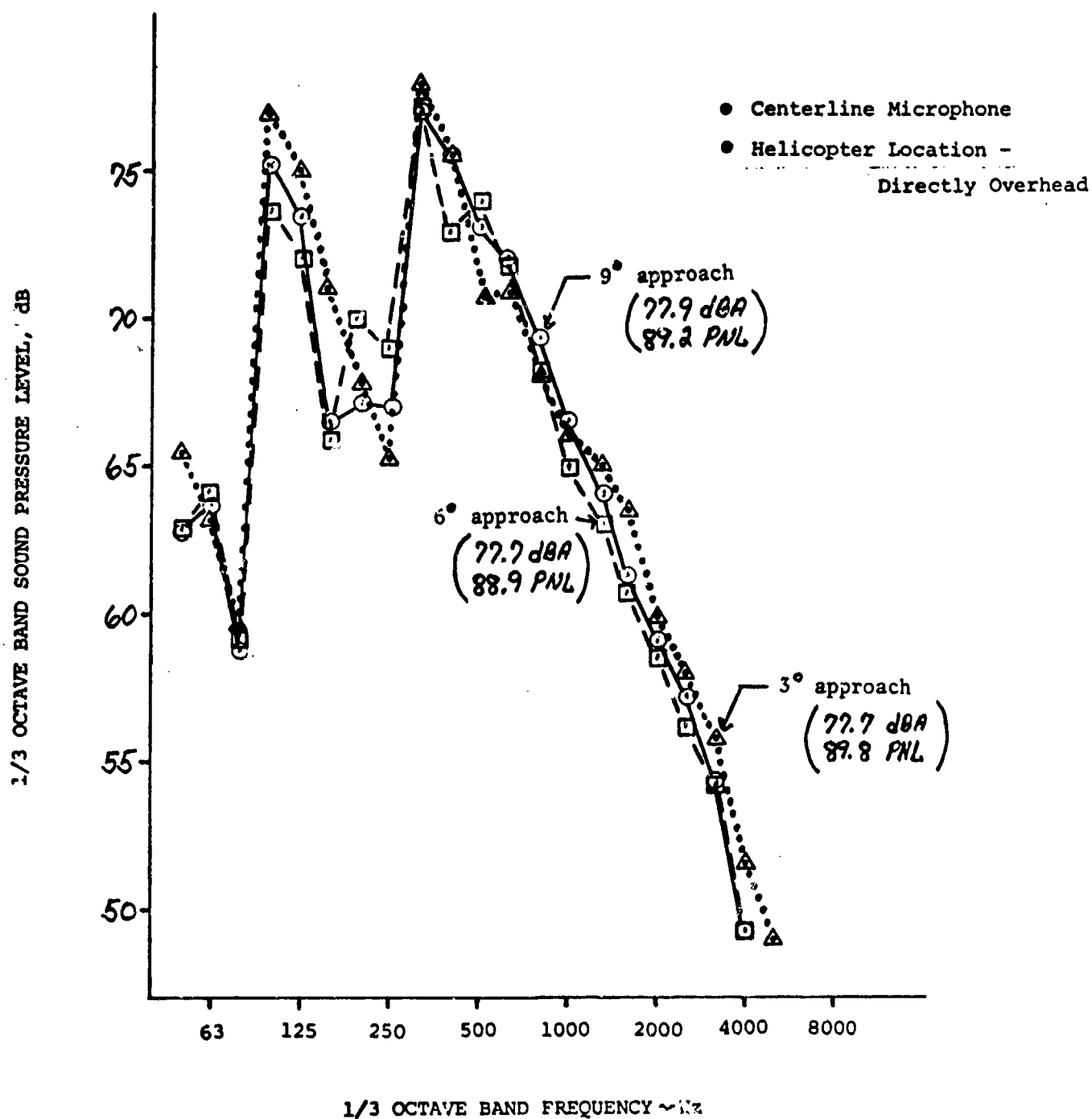
## SPECTRA DURING APPROACH



# HUGHES 500-C

FIGURE 52

## SPECTRA DURING APPROACH

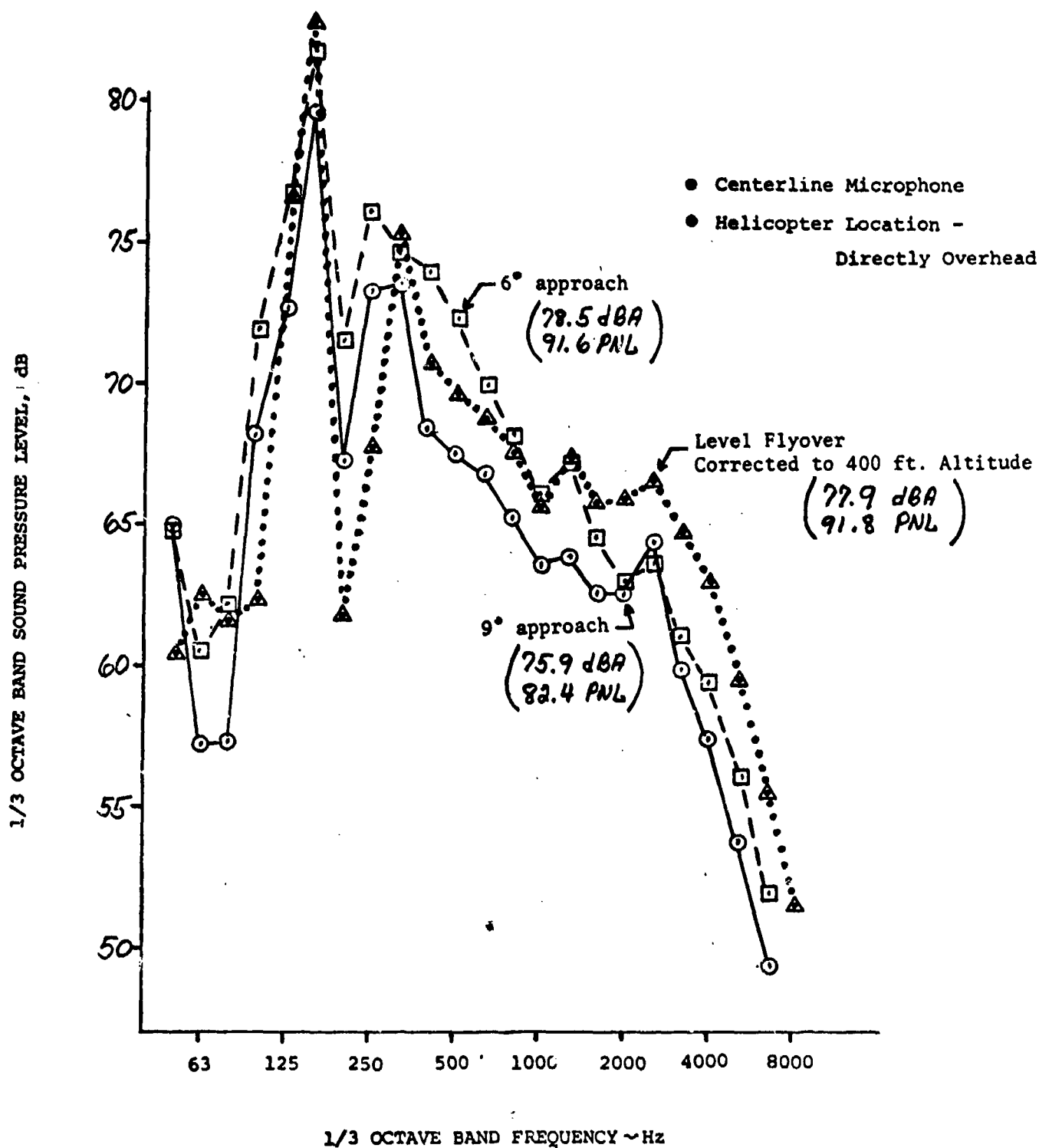




BELL 47-G

FIGURE 53

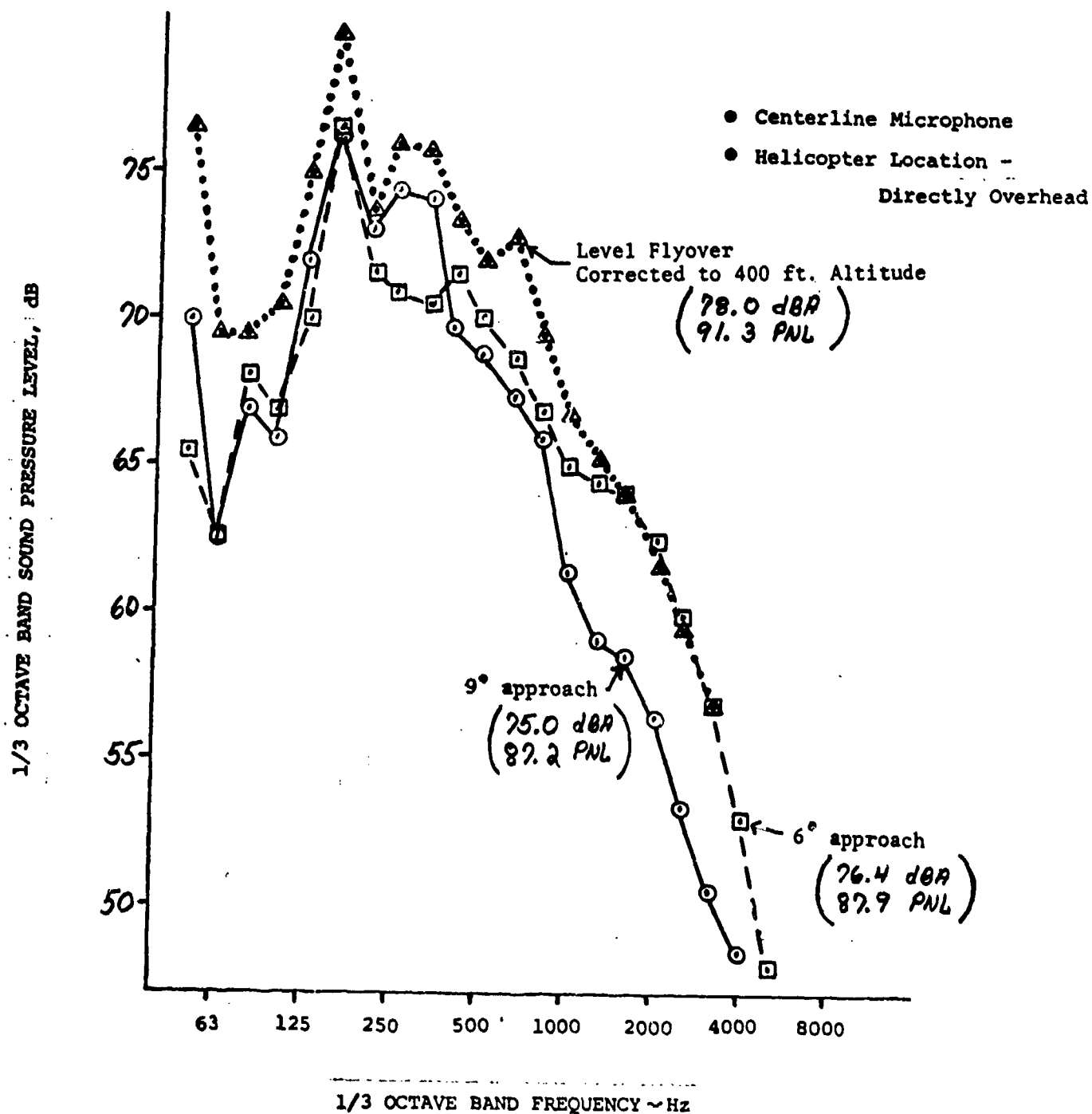
SPECTRA DURING APPROACH



BELL 206-L

FIGURE 54

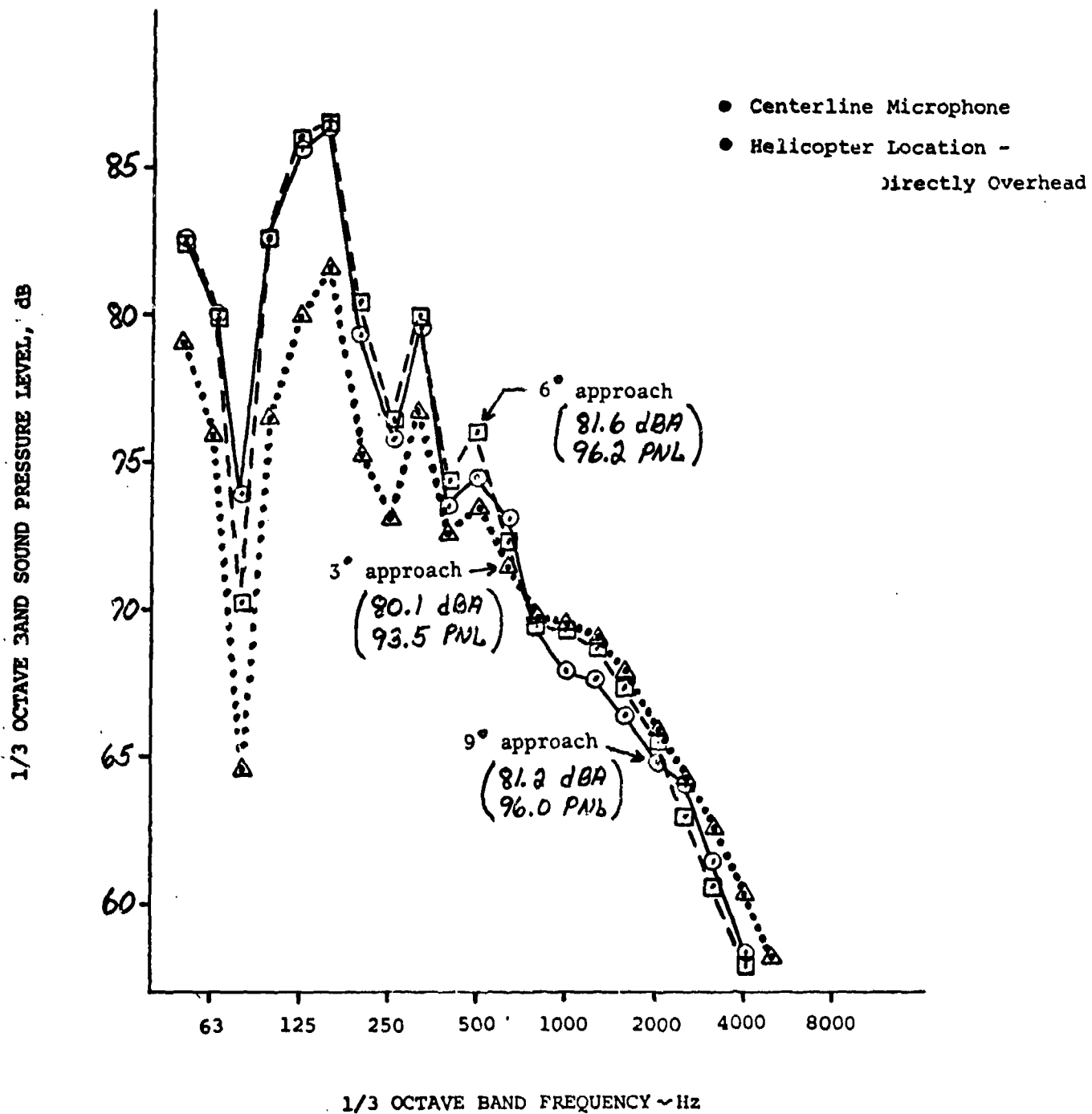
SPECTRA DURING APPROACH



BELL 212 (UH1N)

FIGURE 55

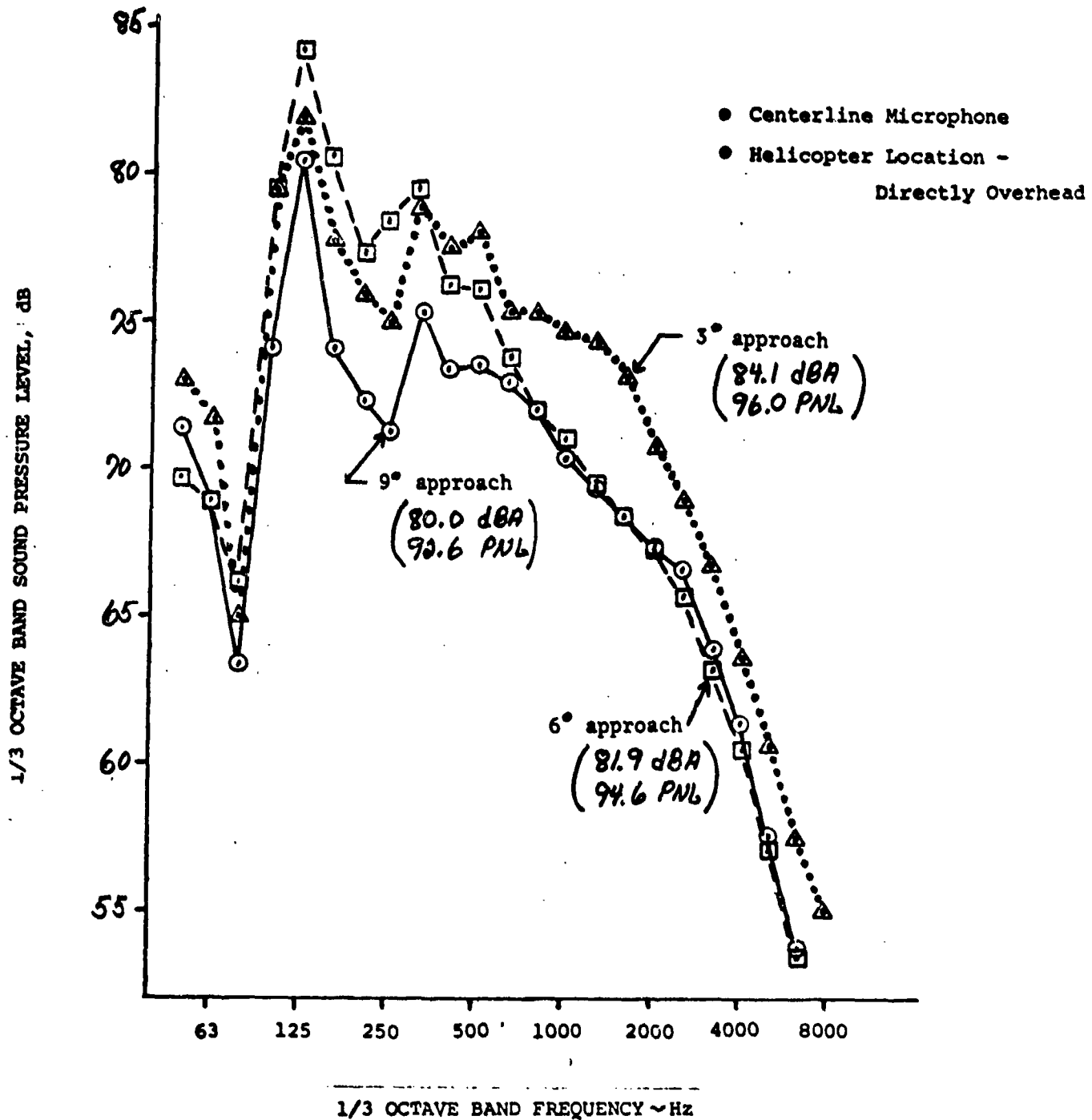
SPECTRA DURING APPROACH



# SIKORSKY S-61

FIGURE 56

## SPECTRA DURING APPROACH

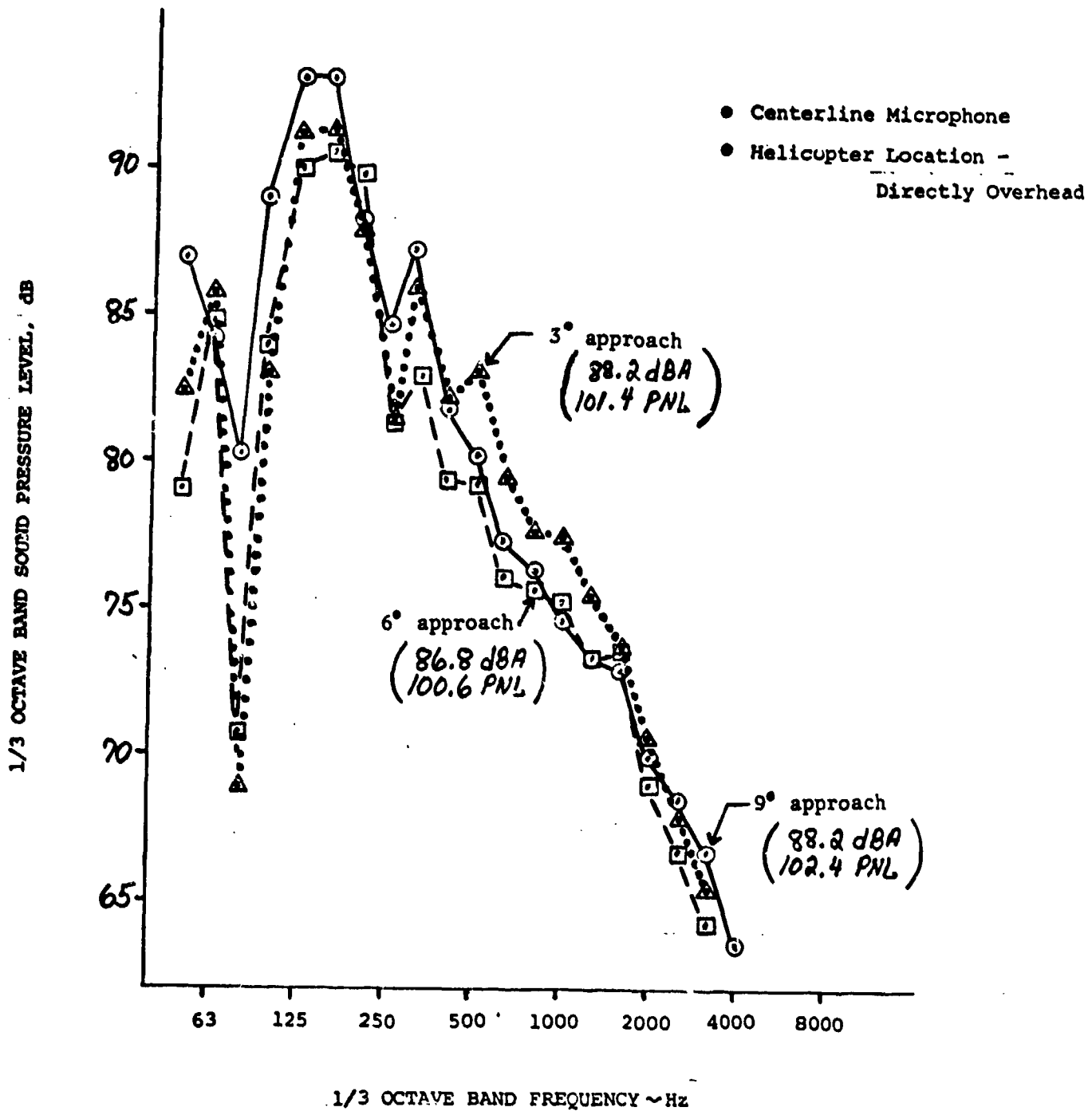


# SIKORSKY S-64 "SKYCRANE"

(with truck)

FIGURE 57

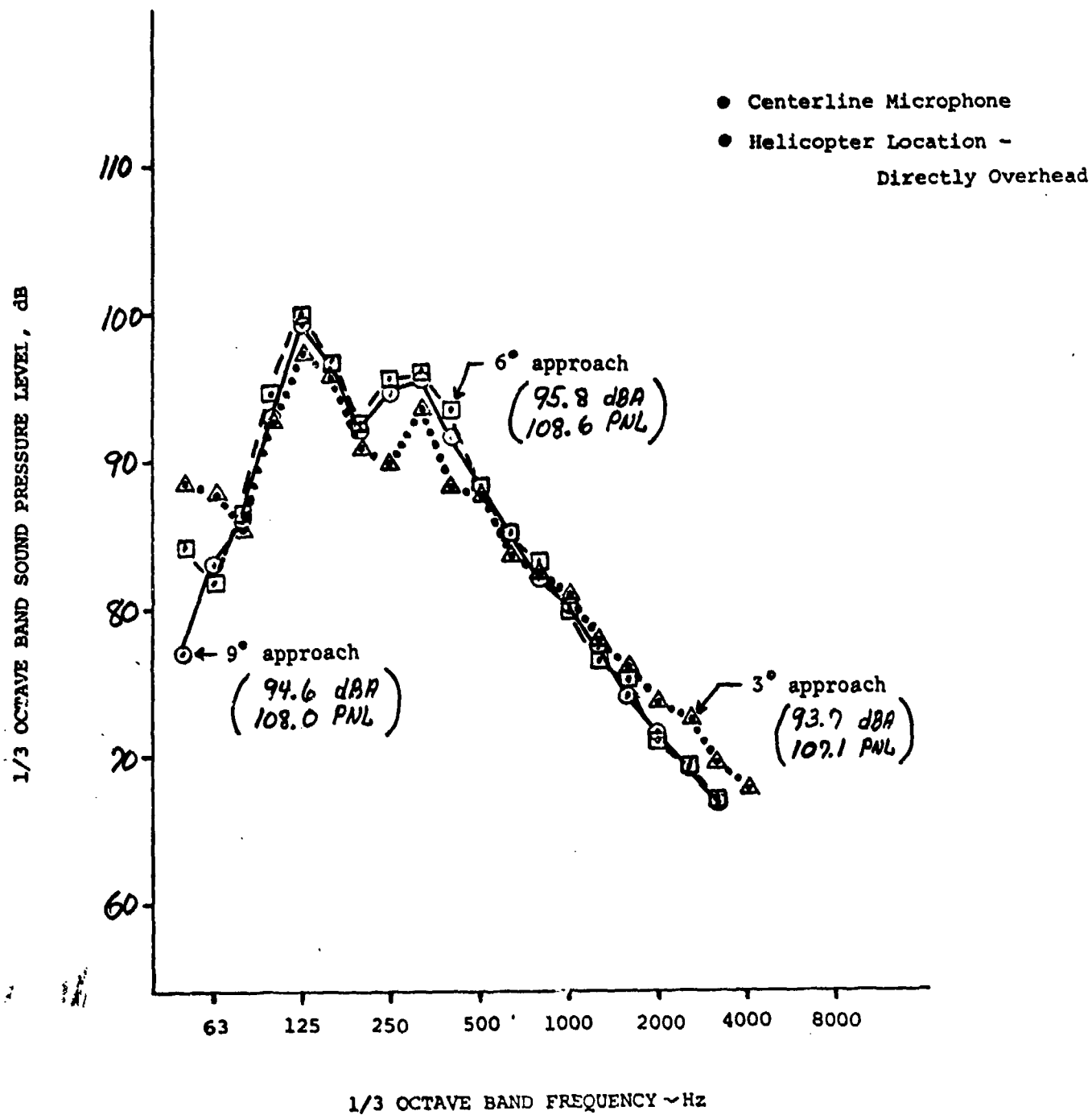
SPECTRA DURING APPROACH



# BOEING VERTOL CH-47C

FIGURE 54

## SPECTRA DURING APPROACH



### 5.3 Statistical Analysis Of Flyover Noise Data

An analysis has been made of the statistical repeatability (standard deviation) of the level flyover noise data obtained from the helicopter noise test. The unit of evaluation is the standard deviation,  $\sigma$ , which is equal to:

$$\sigma = \frac{\sqrt{\sum (y - \bar{y})^2}}{N-1}$$

where "y" is the noise level in a given unit and " $\bar{y}$ " is the average for several runs at the same airspeed. Since only 2-4 runs were made at a given condition in order to include the required variables in the limited test time, the technique of "pooled" variance is used. This technique, which assumes that the causes of variance are independent of the test condition, (i.e. airspeed) is calculated by:

$$\sigma_{\text{pool}} = \frac{\sqrt{\sum (y - \bar{y})^2_{\text{pool}}}}{\sum (v)}$$

where the " $\sum$ " refers to the summation of the components and degrees of freedom ( $v = N-1$ ) of the individual test conditions. The degree of freedom is generally equal to the number of flyover runs less the number of airspeeds tested except for the 47G. All the flyover runs were lumped together for this helicopter because of the limited airspeed range and exhaust noise contribution.

The pooled standard deviations are listed on Table IV for the centerline and sideline microphones. Nearly all of the runs were reduced for a centerline microphone but usually only the "best range" velocity runs were reduced for the sideline microphones. The rather large variance for the Bell 206L was caused by the series of runs at 118 mph. Deleting this velocity reduces the standard deviation significantly. Only the A-level standard deviations are shown for the 300C and 206L because of the difficulty in determining the 10 PNdB downpoints for EPNL.

EPNL generally has a smaller deviation than does the peak A-level. This was expected and is caused by the moderating effect of duration on the peak level. Those runs within a set with a

higher peak level generally have a shorter duration. The standard deviation for the sideline microphones is somewhat conservative because only the sideline data for 1 or 2 flight velocities was reduced for most helicopters. An observation can be made that the helicopters which "slap", i.e. the CH-47C and Bell 212 (UHIN), tend to have more scatter than the other helicopters.

The purpose of "pooling" the data is to increase the degrees of freedom,  $V$ , in order to increase the confidence level of the data. An inherent assumption is that the causes of scatter in the data are independent of the test variables, in this case, airspeed. Table V lists the standard deviations for each flight speed. There does not appear to be any consistent trends of standard deviation with airspeed.

The CH-47C and 47G were tested under nearly ideal conditions with calm winds. It is interesting that their standard deviation (peak A-level) is the same, 1.5 dBA, on a pooled basis, as the other six helicopters tested under windy conditions. This could indicate that the effect of wind was less than expected or the impulsive nature of the CH-47C, with its inherently higher variation due to the impulsiveness distorts the low wind case.

#### 5.4 Effect of Ground Reflecting Surface

This describes the effect of the centerline microphone reflecting surface on the flyover noise levels obtained during the Helicopter Noise Test. The tests were conducted in October 1976 at Dulles International Airport and Langley Field. The comparisons are between the "transpo dirt" and plywood (2-8'x4' sheets end to end) at Dulles and Between short grass (about 3 inches high) and concrete at Langley. Most of the data was analyzed (standard condition) for the microphone over dirt at Dulles and over concrete at Langley.

An initial assessment of the effects of microphone reflecting surface was made using the strip chart-maximum A-level data in November 1976. This showed that there were small differences between the dirt and plywood at Dulles but significant differences between the grass and concrete at Langley. At Dulles, the centerline noise level measured over plywood was, on the average, 0.25 dBA higher for 92 runs than the dirt centerline. At Langley the concrete gave an average noise level 1.9 dBA higher than grass for 51 runs.



TABLE IV POOLED STANDARD DEVIATION

<u>HELICOPTER MODEL</u>	<u>MICROPHONE</u>	<u>N RUNS</u>	<u>V</u>	<u><math>\sigma</math> EPNL</u>	<u><math>\sigma</math> MAX LA</u>
BELL 47G	Centerline	8	7	1.18	1.12
	Sideline	10	8	1.35	1.31
S-64	Centerline	16	9	.55	.50
	Sideline	10	6	.48	1.06
S-61	Centerline	11	7	.96	1.51
	Sideline	6	4	.60	1.24
500C	Centerline	10	5	.21	.87
	Sideline	8	4	.46	1.03
BELL 212	Centerline	14	10	1.20	1.48
	Sideline	7	5	1.10	1.43
CH-47C	Centerline	14	9	1.08	1.76
	Sideline	16	10	1.28	2.37
500C	Centerline	11	7	N.A.	1.17
	Sideline	6	4	N.A.	.85
206L	Centerline	15	10	N.A.	2.40
	Sideline	6	4	N.A.	1.04
206L w/o 118mph	Centerline	11	7	N.A.	1.31

NOTE: Sideline runs were at only 1 or 2 airspeeds.  
Centerline runs for 4-5 airspeeds.

TABLE V      STANDARD DEVIATIONS BY AIRSPEED

<u>HELICOPTER</u>	<u>MICROPHONE</u>	<u>AIRSPEED</u>	<u>N/RUNS</u>	<u>V</u>	<u>T EPNL</u>	<u>LA MAX</u>
S-64 Heavy	Grass	60 KT	2	1	.7	.25
		85 KT	2	1	.65	.56
		95 KT	3	2	.7	.10
	Grass	95 KT	3	2	.26	.56
	W-Sideline	95 KT	3	2	.56	1.16
	E-Sideline	95 KT	3	2	.35	1.18
S-64 Light	Grass	85 KT	2	1	.78	0
		95 KT	2	1	0	.78
		105 KT	2	1	.24	.78
	W-Sideline	105 KT	2	1	.42	.78
	E-Sideline	105 KT	2	1	.56	.78
S-61	Grass	60 KT	2	1	.22	.78
		100 KT	3	2	1.46	1.56
		115 KT	3	2	.85	1.98
	Grass	115 KT	3	2	.56	1.15
	W-Sideline	115 KT	3	2	.44	1.54
	E-Sideline	115 KT	3	2	.72	.84
300C	Grass	60 mph	3	2	NA	.93
		69 mph	2	1		1.55
		76 mph	3	2		1.48
	W-Sideline	82 mph	3	2		.16
		76 mph	3	2		.36
		76 mph	3	2		1.15
206L	Grass	70 mph	3	2	NA	1.41
		106 mph	3	2		1.73
		118 mph	4	3		3.91
		130 mph	3	2		1.00
	W-Sideline	145 mph	2	1		.28
		130 mph	3	2		1.01
		130 mph	3	2		1.07

**TABLE V** STANDARD DEVIATIONS BY AIRSPEED (Cont'd)

HELICOPTER	MICROPHONE	AIRSPEED	N RUNS	V	σ EPNL	σ LA MAX
CH-47C	Ce	60 KT	2	1	.92	1.06
	Ce	126 KT	2	1	.50	.64
	Ce	141 KT	4	3	1.18	2.05
	Ce Plywood	141 KT	4	3	.91	2.02
	Ce	150 KT	2	1	1.63	1.24
	W-Sideline	100 KT	2	1	.36	1.98
	E-Sideline	100 KT	2	1	2.54	4.53
	W-Sideline	141 KT	4	3	.73	2.12
	E-Sideline	141 KT	4	3	1.65	2.44
	W-Sideline	150 KT	2	1	.36	.42
	E-Sideline	150 KT	2	1	0	.28
BELL 212	Ce	60 KT	3	2	1.1	.25
	Ce	99 KT	3	2	.26	1.26
	Ce	110 KT	4	3	1.12	2.20
	Ce	114 KT	4	3	1.63	1.15
	W-Sideline	110 KT	3	2	.38	.65
	E-Sideline	110 KT	4	3	1.40	1.77
500C	Ce	69 mph	2	1	.36	0
	Ce	110 mph	2	1	.28	.7
	Ce	144 mph	2	1	0	1.0
	Ce	150 mph	2	1	.14	.85
	Ce Grass	144 mph	2	1	0	1.27
	W-Sideline	144 mph	2	1	0	1.27
	E-Sideline	144 mph	2	1	.36	.85
	W-Sideline	150 mph	2	1	.85	1.27
	E-Sideline	150 mph	2	1	0	.56
47G	Ce	60-90 mph	8	7	1.18	1.12
	Ce	68 mph	2	1	.64	0
	Ce	75 mph	3	2	1.31	1.51
	W-Sideline	75 mph	3	2	1.67	1.58
	E-Sideline	75 mph	3	2	1.88	1.71

In order to obtain realistic levels and to be consistent between the sideline (dirt at Dulles, concrete at Langley) and centerline microphones it was decided to use the dirt microphone at Dulles and the concrete microphone at Langley. The Dulles "transpo dirt" was not actually soil but a low-grade asphalt surface decomposing into a dusty/gravel surface on the top 1-2 inches after which it became fairly hard. Therefore, this surface can be considered "semi-impervious" and the 0.25 dBA difference in level between it and the plywood is considered negligible.

Digital data was obtained with both reflecting surfaces for the level flyover at the "best range" velocity for the three helicopters tested at Langley to investigate the characteristics between the grass and concrete. These results are described below where each value is an average of two or three runs:

AVERAGE NOISE LEVEL OVER CONCRETE MINUS LEVEL OVER GRASS

<u>HELICOPTER MODEL</u>	<u>EPNL</u>	<u>PNLTM</u>	<u>PNLM</u>	<u>MAX A-LEVEL</u>	<u>OASPL</u>
500C	.8	.8	.8	.5	1.3
S-61	2.6	2.9	2.9	3.0	1.6
S-64	.8	.6	.6	.8	1.1

The larger difference for the S-61 appears to be a function of the particular runs chosen for the analysis because the strip Chart "A" level data showed fairly random differences between concrete and grass with the level for the concrete minus grass varying from 0.5 to 3.5 dBA maximum for all three helicopters. The overhead spectra is compared on Figures 59 and 60 for the S-61 and 500C. The overhead position gives the maximum noise level for these helicopters.

Differences between the transpo dirt and plywood at Dulles are shown for the CH-47C using 4 level flyovers at 141 Kt. The average noise level over plywood minus the noise level over dirt is 0.3 EPNdB, 0.05 dBA, 0.6 dB Overall and 0.4 PNdB. Figures 61 and 62 show the spectral comparisons for a forward angle (maximum level) and the overhead position. The difference due to reflecting surface is generally quite small.

FIGURE 59

MICROPHONE REFLECTING SURFACE COMPARISON

Helicopter Noise Measurement Program

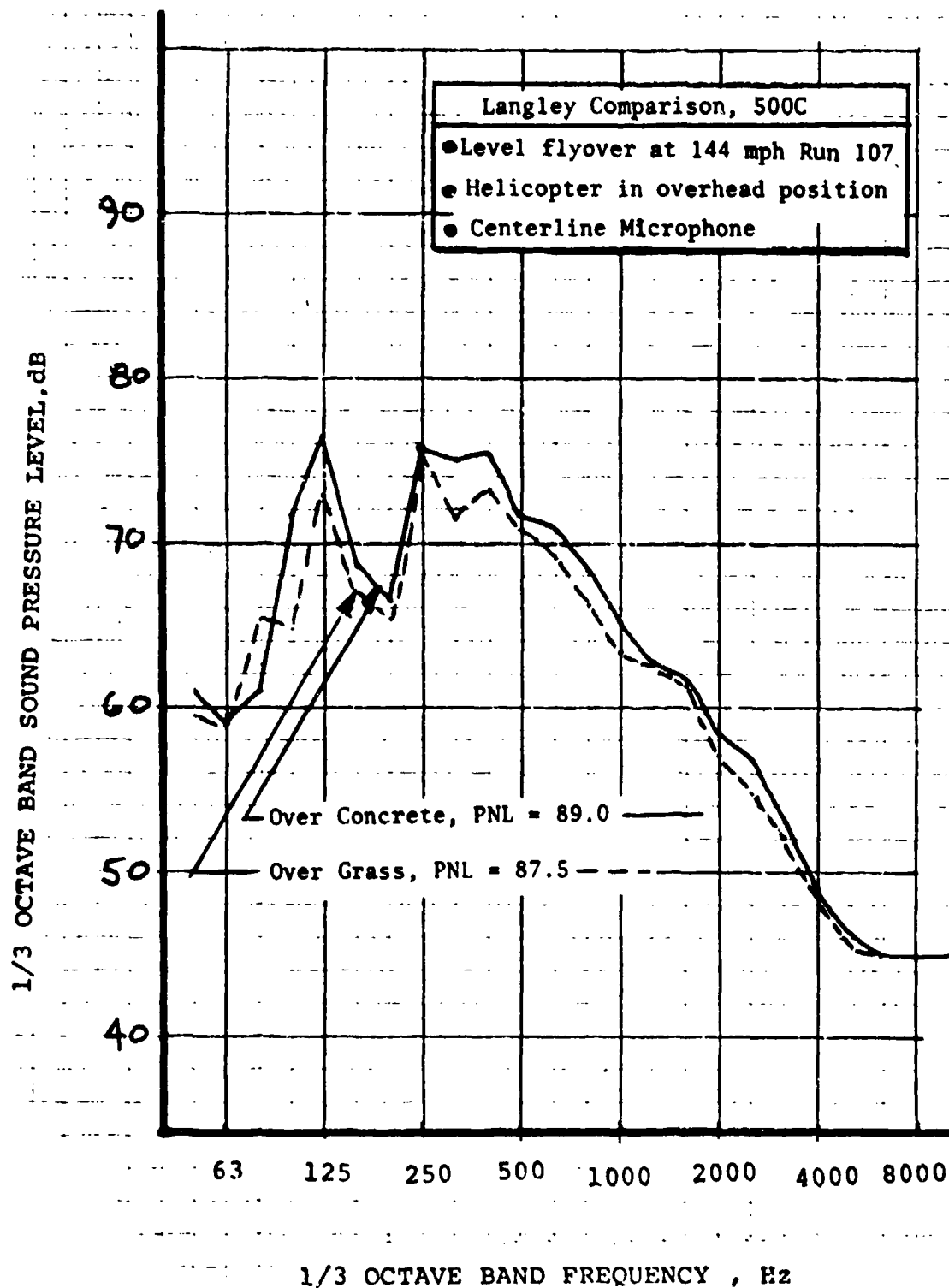


FIGURE 60

MICROPHONE REFLECTING SURFACE COMPARISON

Helicopter Noise Measurement Program

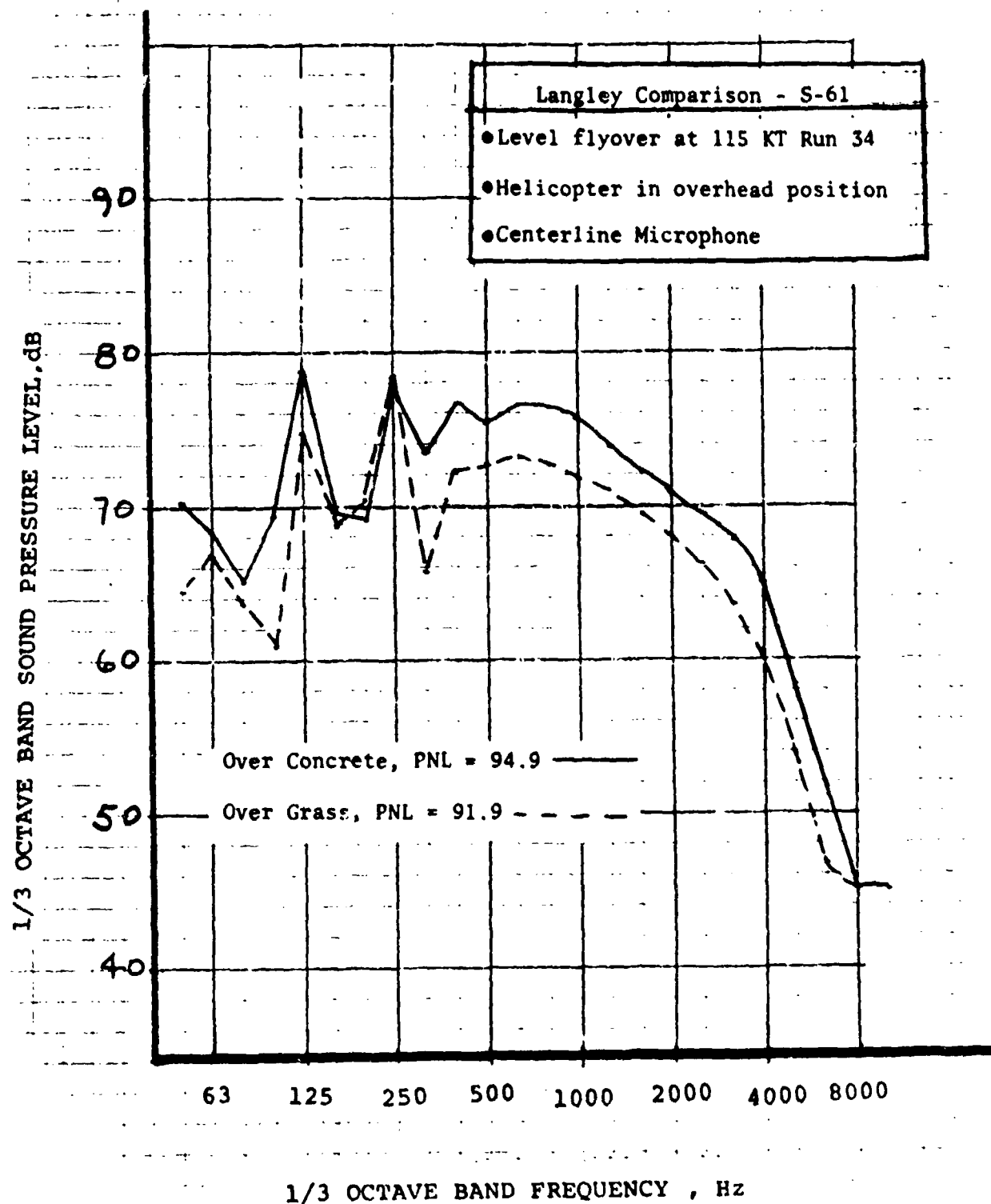
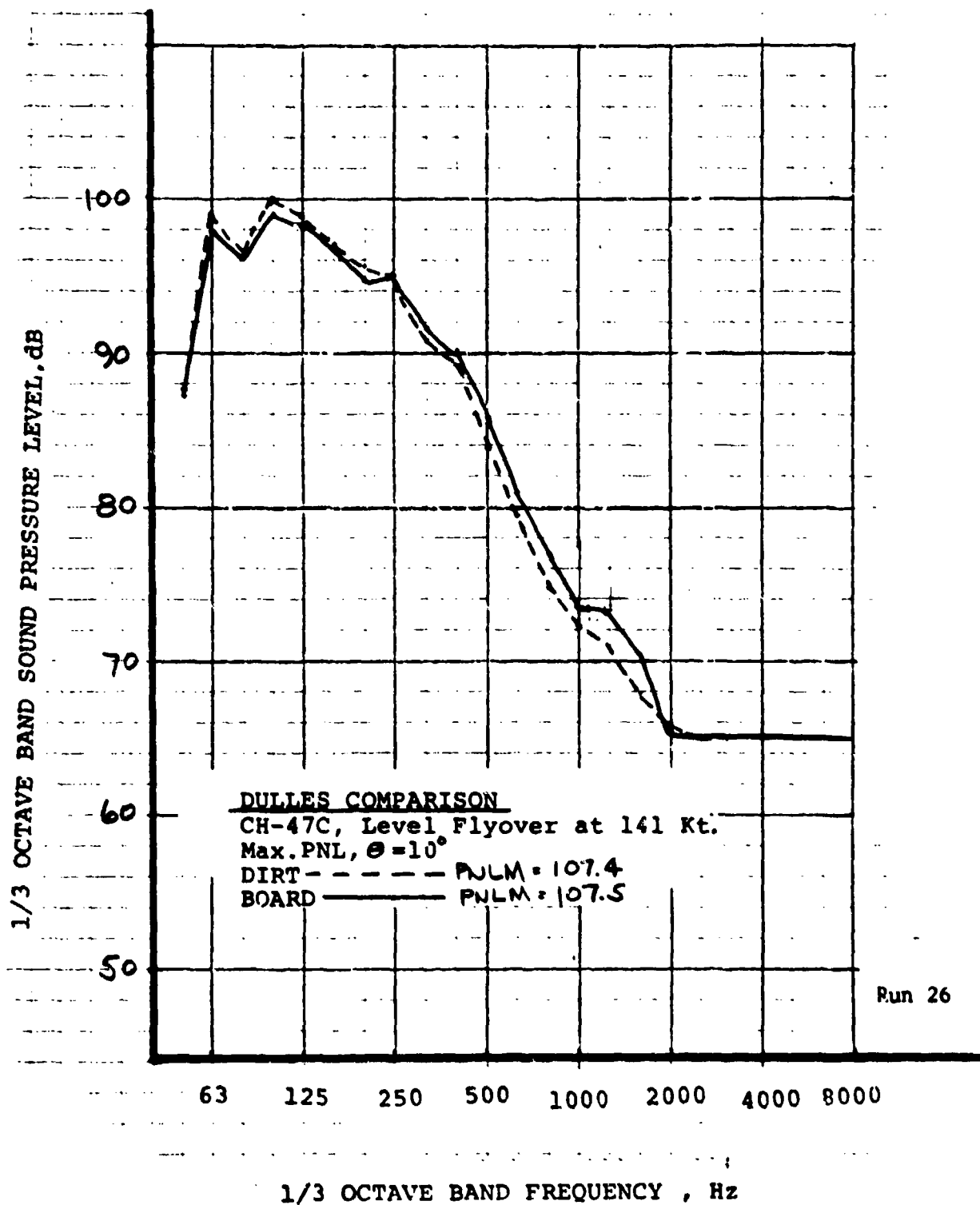


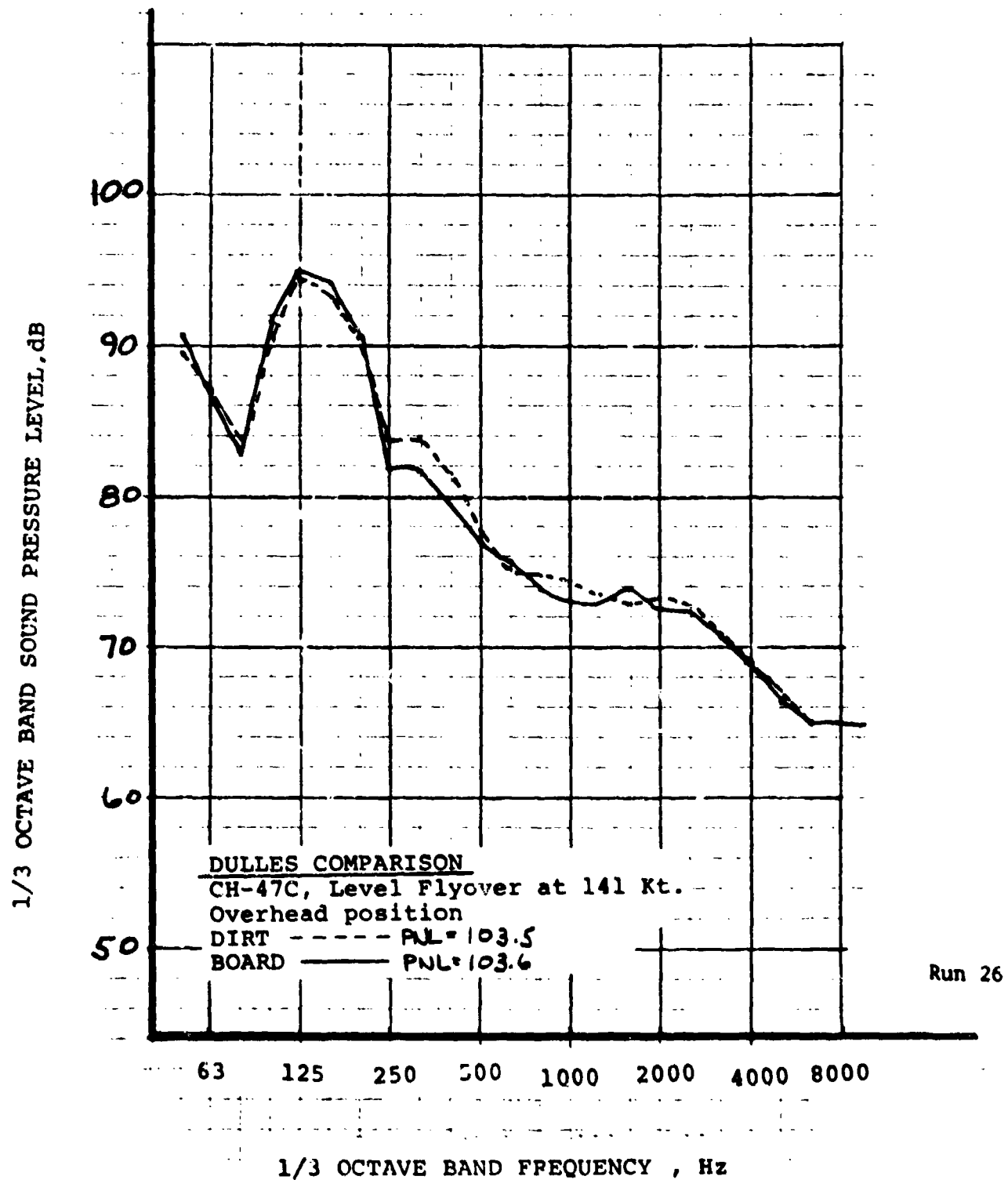
FIGURE 61

MICROPHONE REFLECTING SURFACE COMPARISON

Helicopter Noise Measurement Program



**FIGURE 62**  
**MICROPHONE REFLECTING SURFACE COMPARISON**  
**Helicopter Noise Measurement Program**



Run 26



## 6.0 HOVER NOISE DATA

### 6.1 Hover Test Program

The hover tests were conducted at a target wheel clearance of five feet. Four (4) microphones were placed at a 1.2 meter height at 150 and 75 meters on opposite sides of the hover point. The helicopter was hovered around a complete circle with data recorded for 30 seconds at each 45 degree location. The data presented was digitized and based on 19 one-second energy averages. The maximum and minimum level in each band and weighted overall level as well as the standard deviation was also determined. Visual techniques were used to align the helicopter. Wheel clearance tended to be 10 feet rather than 5 feet for the largest helicopters to minimize the adverse affects of downwash on the test personnel and instruments.

A unique nomenclature was used to define the helicopter heading. The heading angle is the direction the helicopter was facing clockwise from North as the reference. Acoustic data is referenced by the angle from the nose clockwise to the microphone as shown on Figure 63. Printouts of the hover data are available in Report No. FAA-RD-77-57.

### 6.2 Hover Test Results

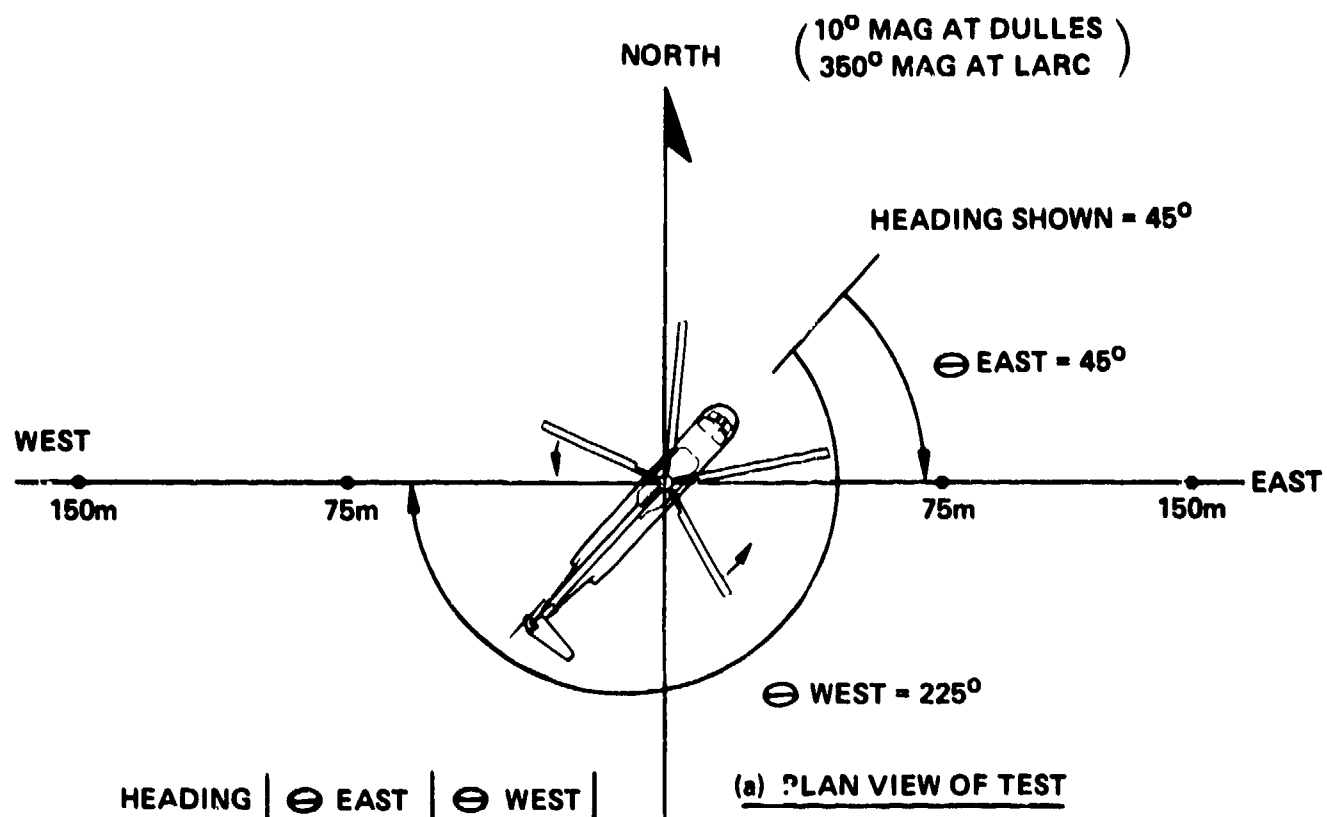
The most striking characteristic of the hover data is its variability over time with the helicopter in a fixed position. Figure 64 shows typical A-level time histories for several helicopters and a total spread of 10 dBA is quite common. Ambient wind was a problem during most of the hover tests and the windy tests tended to have a larger standard deviation than did the tests conducted with light winds. A larger problem associated with the high wind during the hover tests is an asymmetry of the data between the microphones on either side of the helicopter. That is, with the helicopter in a given angular position relative to the microphone, the upwind microphone would be significantly quieter than the downwind microphone at certain angular positions. These corresponded to the helicopter tail rotor being upwind of the downwind microphone as shown on Figure 65. This noise difference was frequency dependent and the implication is that a new noise source was generated by the wind. The low frequencies associated with rotor blade passage are nearly equal on both sides but a large difference exists in the mid-frequencies from 250 to 1600 Hz as schematized on Figure 66. The difference in upwind and downwind noise level can be correlated with the wind velocity as shown on Figure 67. The trend lines show a zero dB difference at about 3 mph and this wind velocity could be considered an upper limit for ideal hover noise testing.

The large increase in mid-frequency noise level at the downwind microphone is hypothesized to be a directional blade slap possibly caused by interactions between the main and tail rotor wakes. The smaller difference in the low frequencies could be due to wind propagation effects alone which would create a shadow zone upwind and possibly more noise propagated downstream. Figure 68 shows the average noise level as a function of helicopter gross weight. The peak level at any angle was plotted and the upwind microphone was used to avoid the blade slap problem associated with the downwind microphone. It is interesting that the two noisiest helicopters during hover relative to the trend lines (CH-47C, 47G) were tested under nearly calm conditions. This indicates that the windy conditions on the other helicopters may have propagated the noise away from the upwind microphone and that these levels are 1-2 dB too low. PNL tends to have a steeper slope than dBA probably because PNL emphasizes low frequencies more heavily than A-weighting and the heavier helicopters tend to have higher tipspeeds and thus more low frequency noise at the rotor harmonics. The larger size of the blades would also tend to generate lower frequencies due to Strouhal Number effects.

Figures 69-92 show directivity patterns and one-third octave band spectra for selected angles for the eight helicopters tested. The angles for the spectra were chosen to provide examples of both similar noise levels at the east and west microphones and the asymmetry due to wind effects. The difference at 135° for the CH-47C could be due to a highly direction pattern and misalignment during the 360° rotation. In general though the CH-47C and 47G, which were tested under light winds show a good repeatability between the east and west microphones. The winds during hover were as follows:

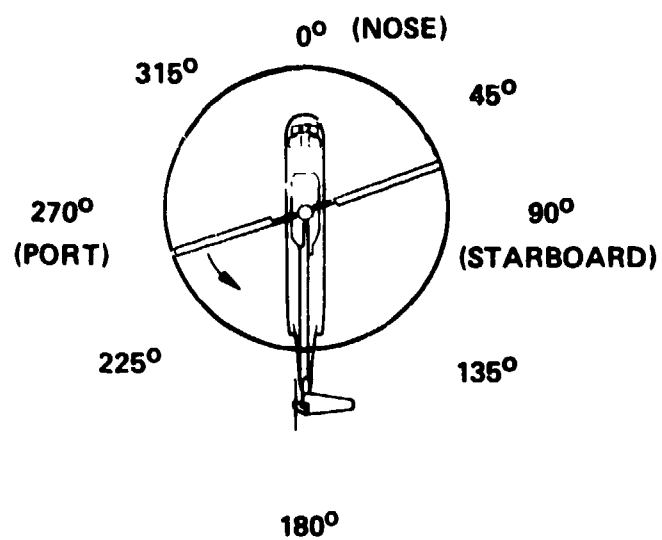
HELICOPTER	WIND VELOCITY	DIRECTION REL. TO TEST (N = 0°)
CH-47C	3-4 mph	180° (from South)
Bell 47G	2-4 mph	10° - 330° (N to NW)
300C	6 G 12 mph	300° (from NW)
206L	8 G 14 mph	300°
UHIN	8-10 mph	185°
S-61	10-16 G 23 mph	30° (From NE)
S-64 Heavy	10-14 G 18 mph	20° - 40°
S-64 Light	8-11 mph	65°
500C	2-5 G 9	50°

The high frequency tone at angles within 45° of the nose on the CH-47C and S-64 (Skycrane) appears to be due to compressor inlet "whine". This tone does not appreciably affect the overall noise level. No turbomachinery noise was evident for the other helicopters. PNL tends to have a smaller standard deviation during hover than A-weighted level because the low frequencies, which are more heavily weighted by PNL, tend to vary less than the middle frequencies.



HEADING	⊖ EAST	⊖ WEST
0°	90°	270°
45°	45°	225°
90°	0°	180°
135°	315°	135°
180°	270°	90°
225°	225°	45°
270°	180°	0°
315°	135°	315°

(b) ANGULAR TRANSFORMATION



C. HELICOPTER PLAN VIEW

FIGURE 63. HOVER NOTATION FORMAT

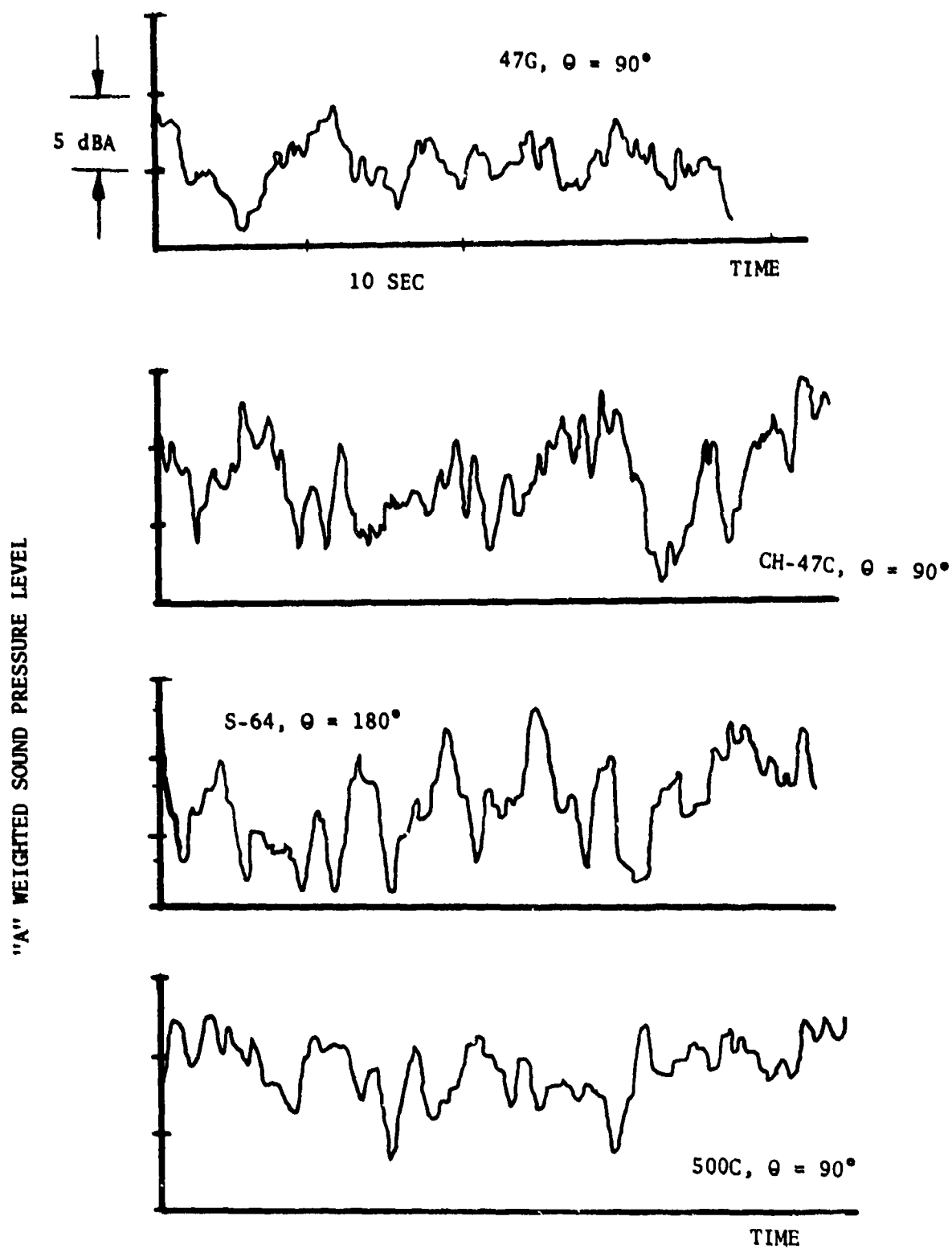
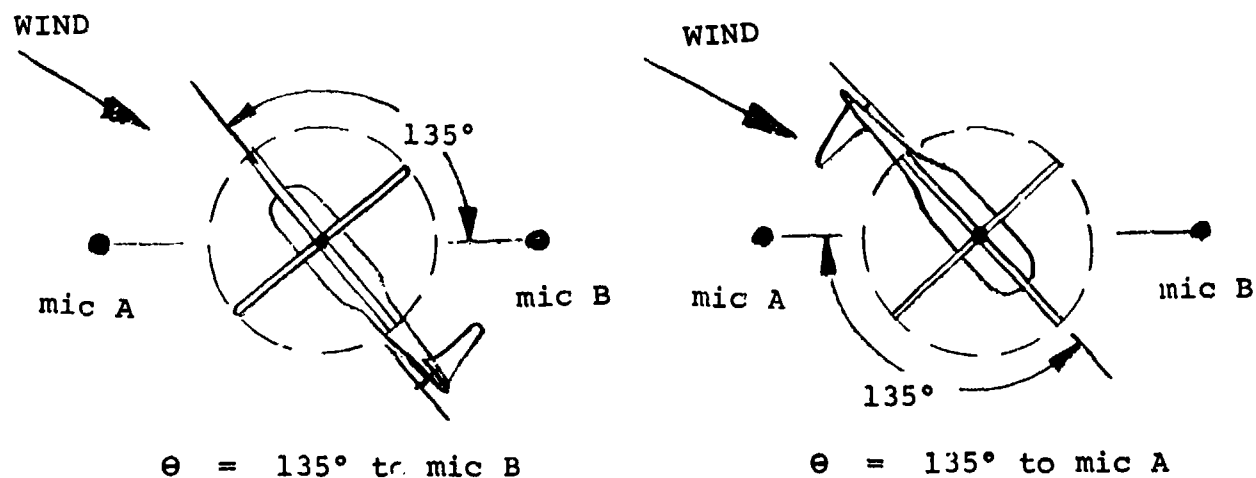
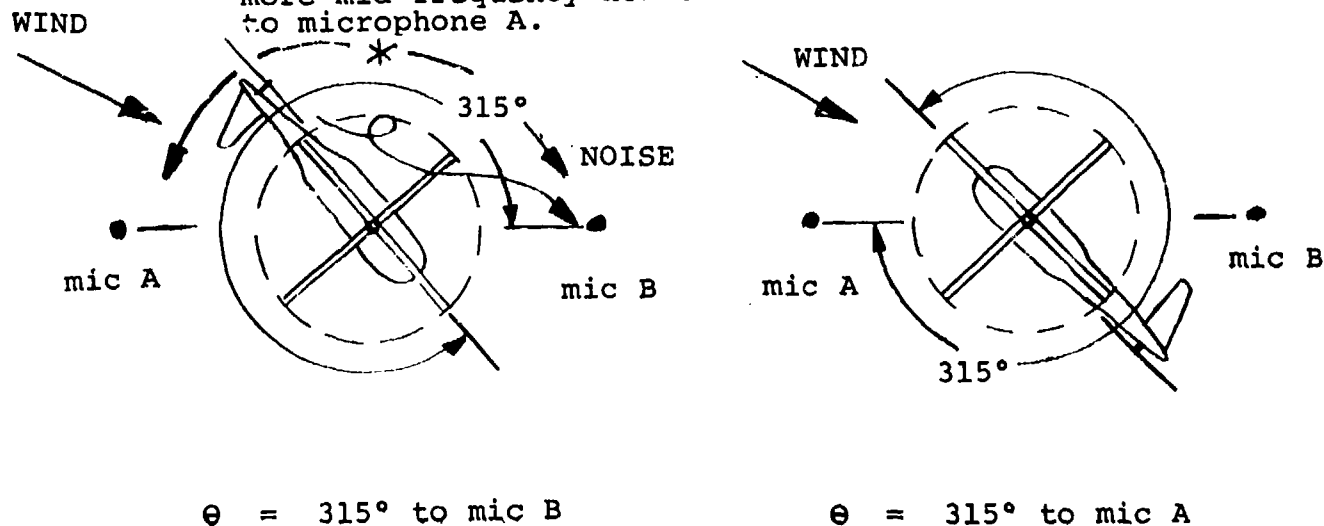


FIGURE 64 TYPICAL HOVER TIME HISTORIES



a. Similar Noise Propagated To Microphones A & B,  $\theta = 135^\circ$

\*When tail is in this location, the downwind microphone, B, receives more mid-frequency noise relative to microphone A.



b. Increased Noise To Downwind Microphone B,  $\theta = 315^\circ$

FIGURE 65. RELATIONSHIP OF HELICOPTER HEADING TO MICROPHONE NOISE LEVEL ASSYMETRY

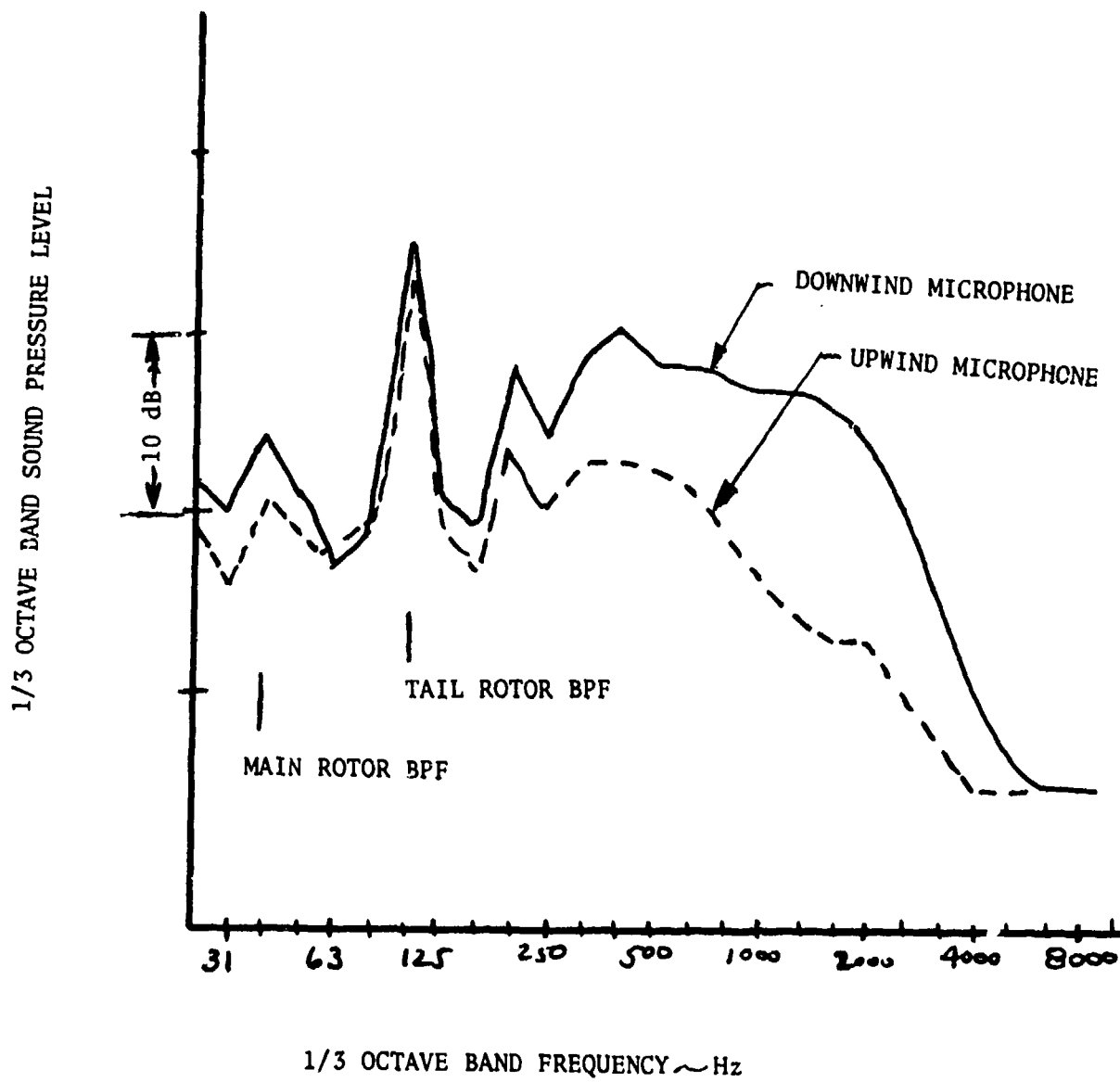


FIGURE 66. SPECTRAL CHARACTERISTICS OF HOVER NOISE ASSYMETRY

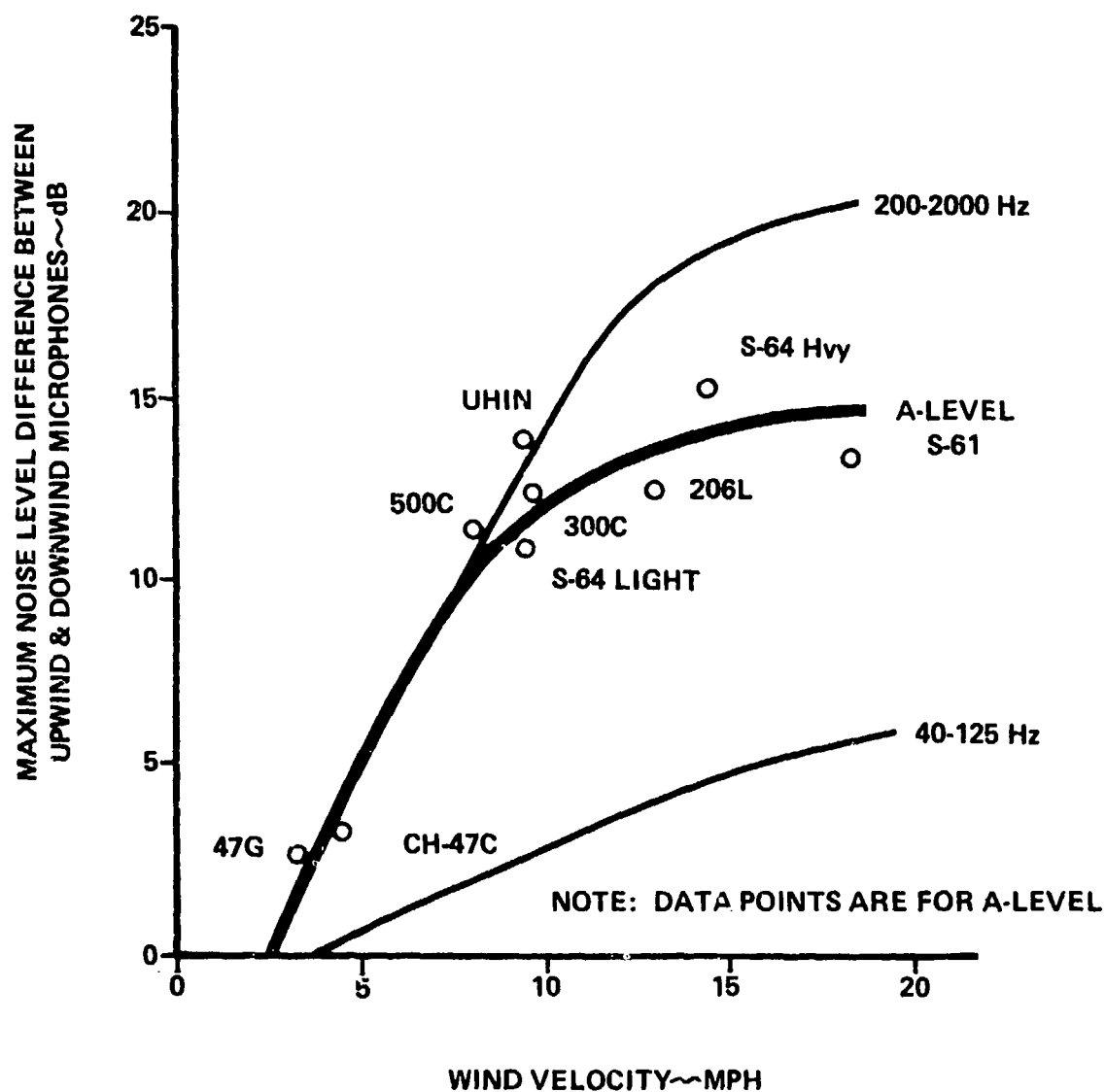
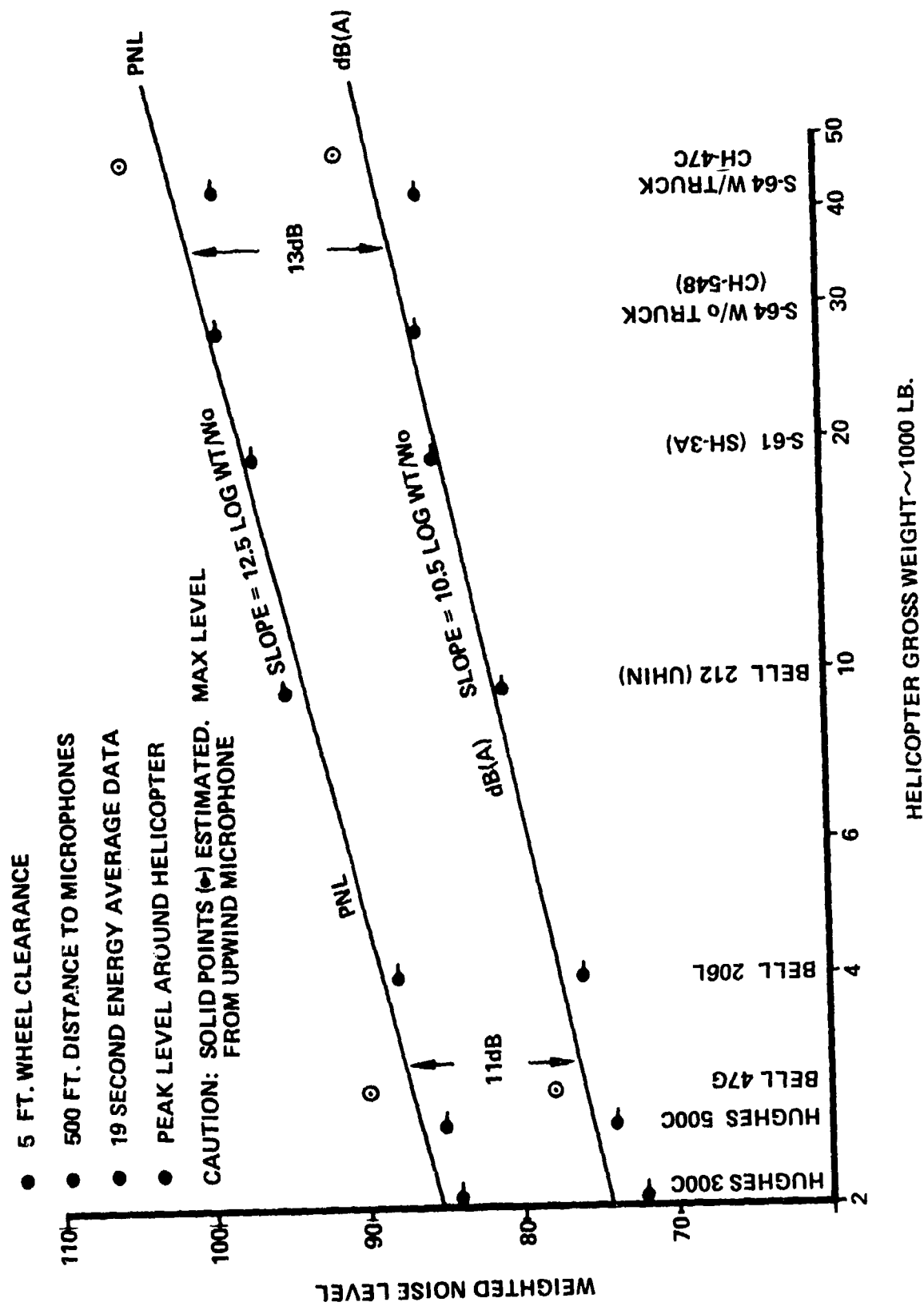


FIGURE 67. CORRELATION OF HOVER NOISE LEVEL  
ASYMMETRY WITH WIND VELOCITY.



**FIGURE 68. HOVER NOISE LEVELS AS A FUNCTION OF WEIGHT.**



FIGURE 69. HELICOPTER HOVER DIRECTIVITY

● 500 FT. (150m) DISTANCE TO MICROPHONES

● HOVER 5.0 FEET ABOVE GROUND

⊕ Energy Average  $\pm 1.0$  Std. Deviation

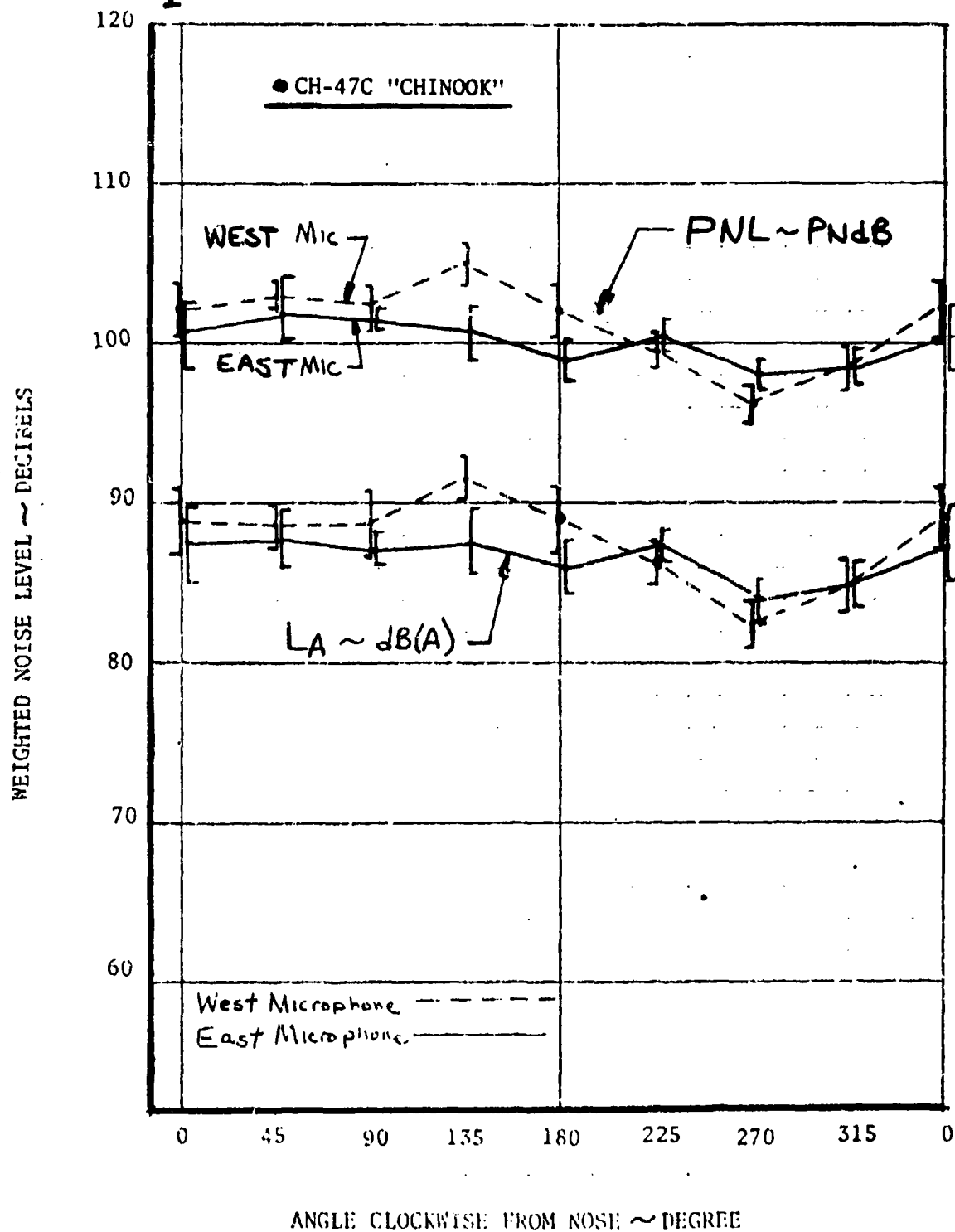


FIGURE 70. FIVE FOOT HOVER SPECTRA

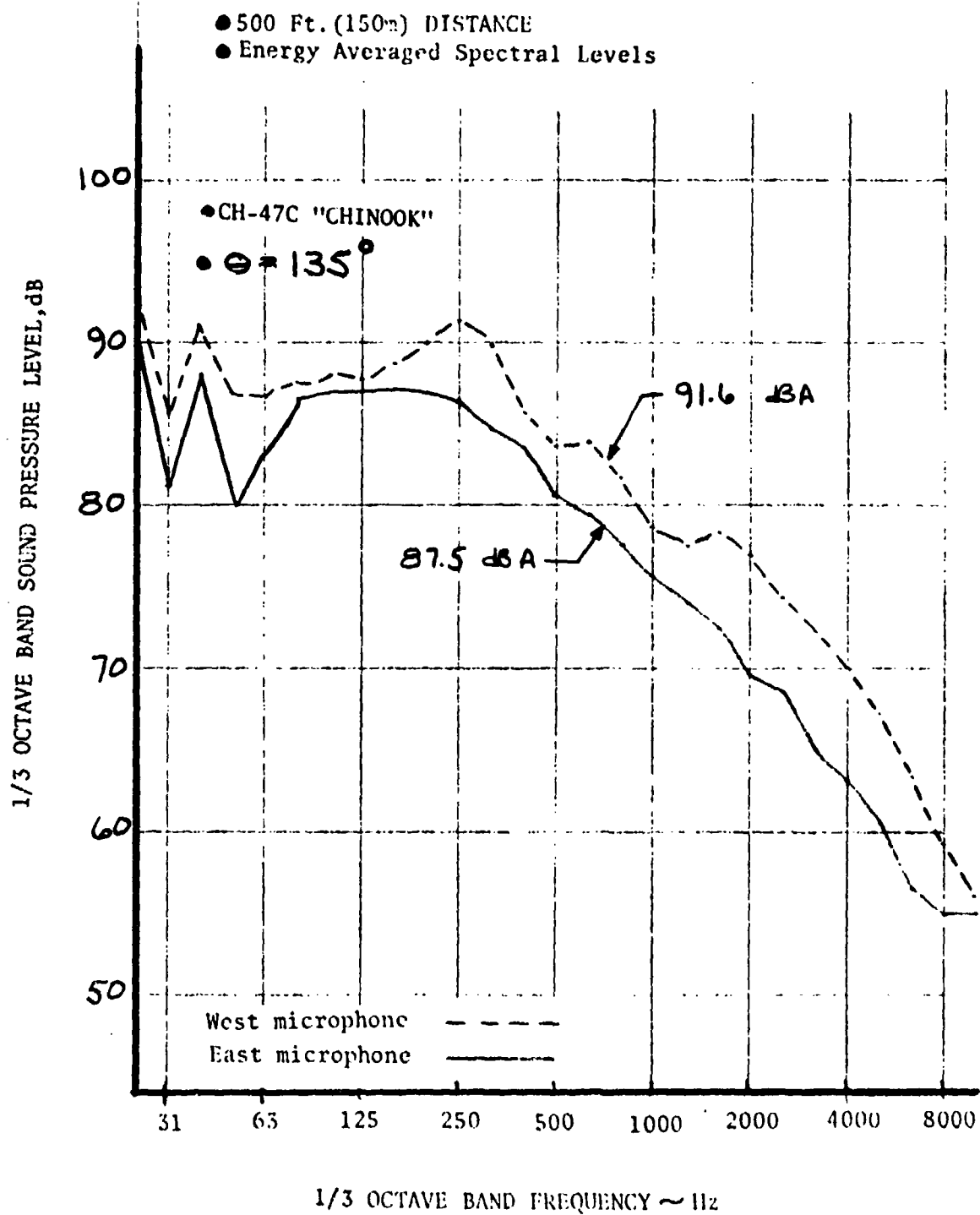


FIGURE 71. FIVE FOOT HOVER SPECTRA

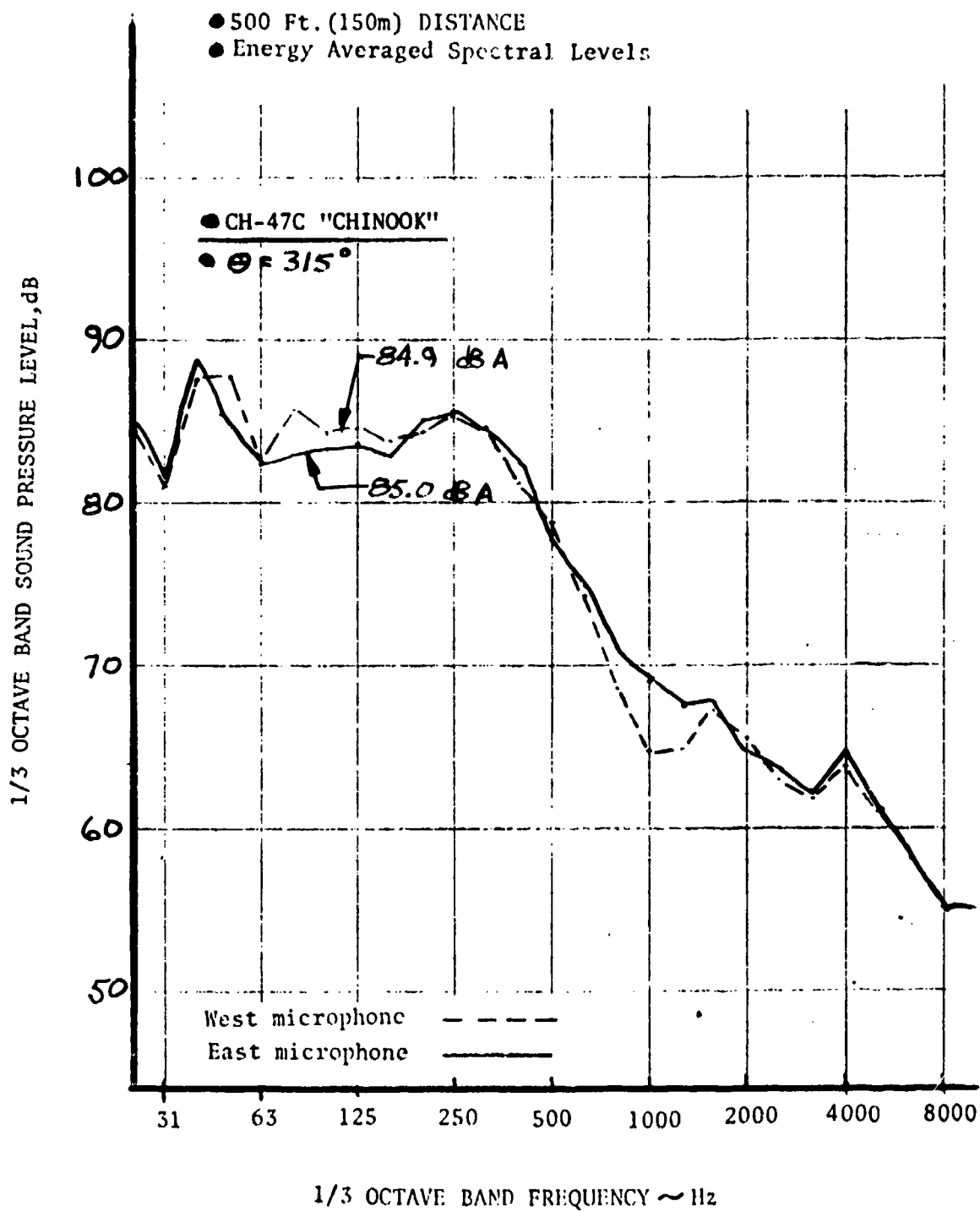


FIGURE 7A HELICOPTER HOVER DIRECTIVITY

● 500 FT. (150m) DISTANCE TO MICROPHONES

● HOVER 5.0 FEET ABOVE GROUND

⌋ Energy Average  $\pm 1.0$  Std. Deviation

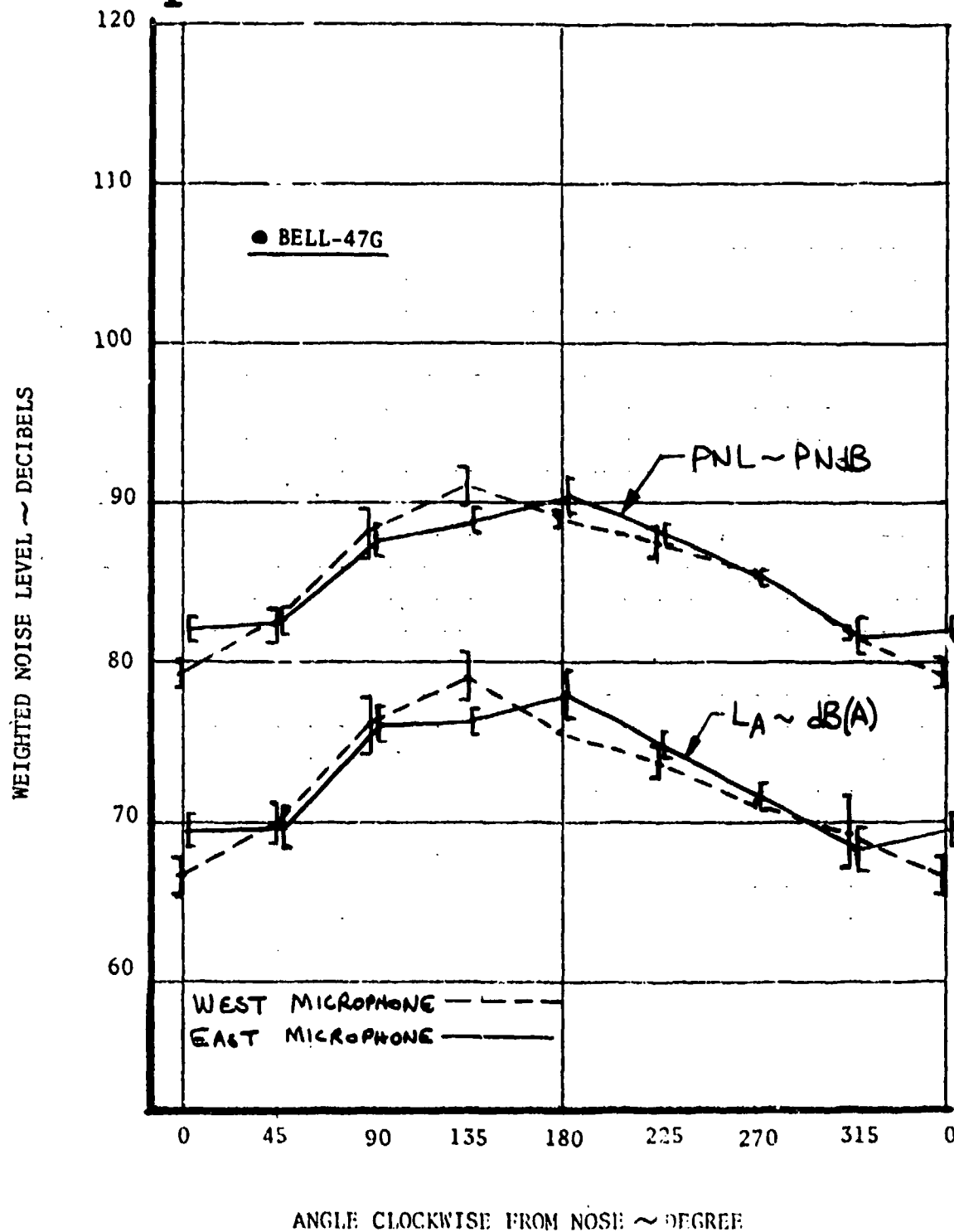


FIGURE 23. FIVE FOOT HOVER SPECTRA

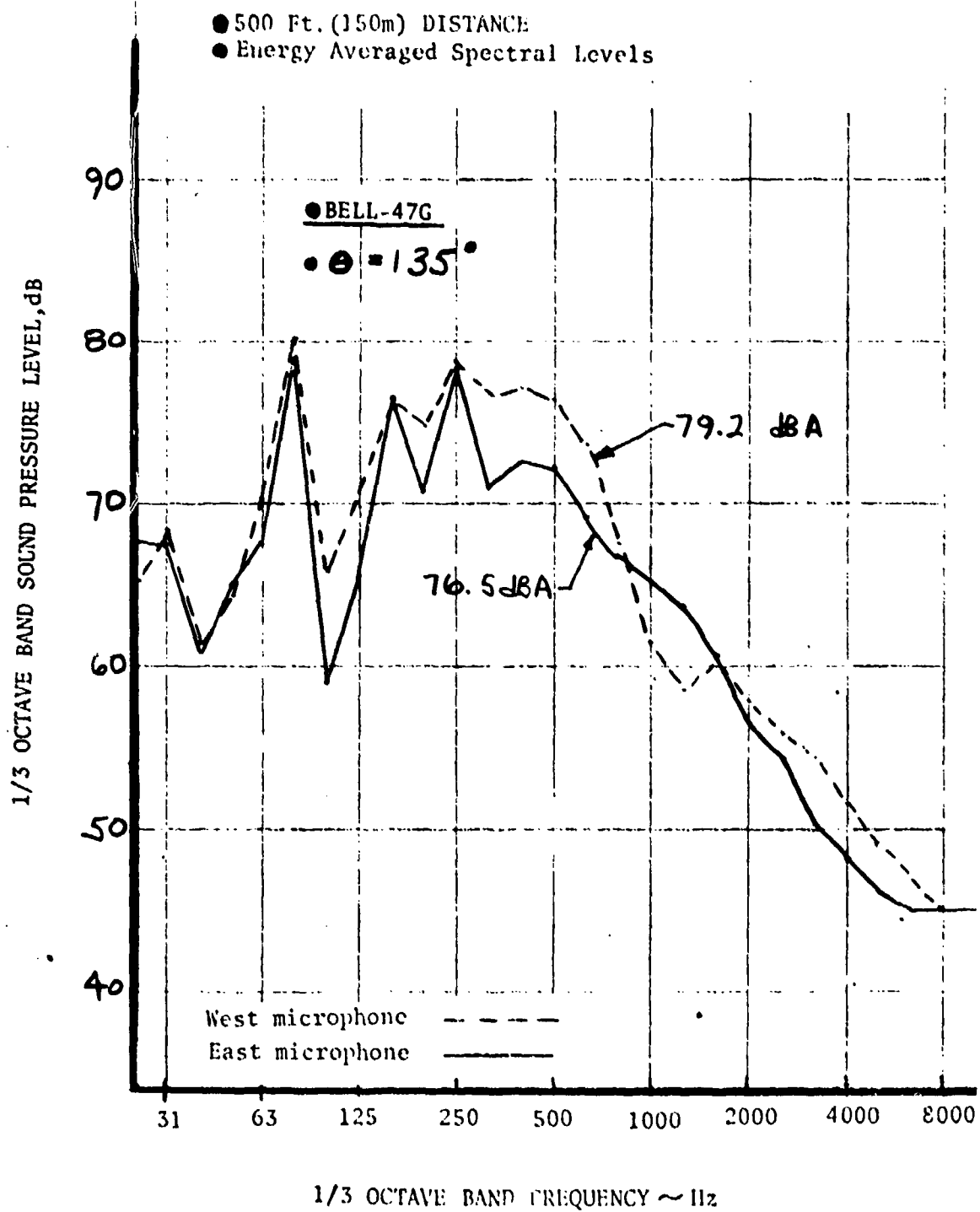


FIGURE 74. HELICOPTER HOVER DIRECTIVITY

● 500 FT. (150m) DISTANCE TO MICROPHONES

● HOVER 5.0 FEET ABOVE GROUND

⊥ Energy Average  $\pm 1.0$  Std. Deviation

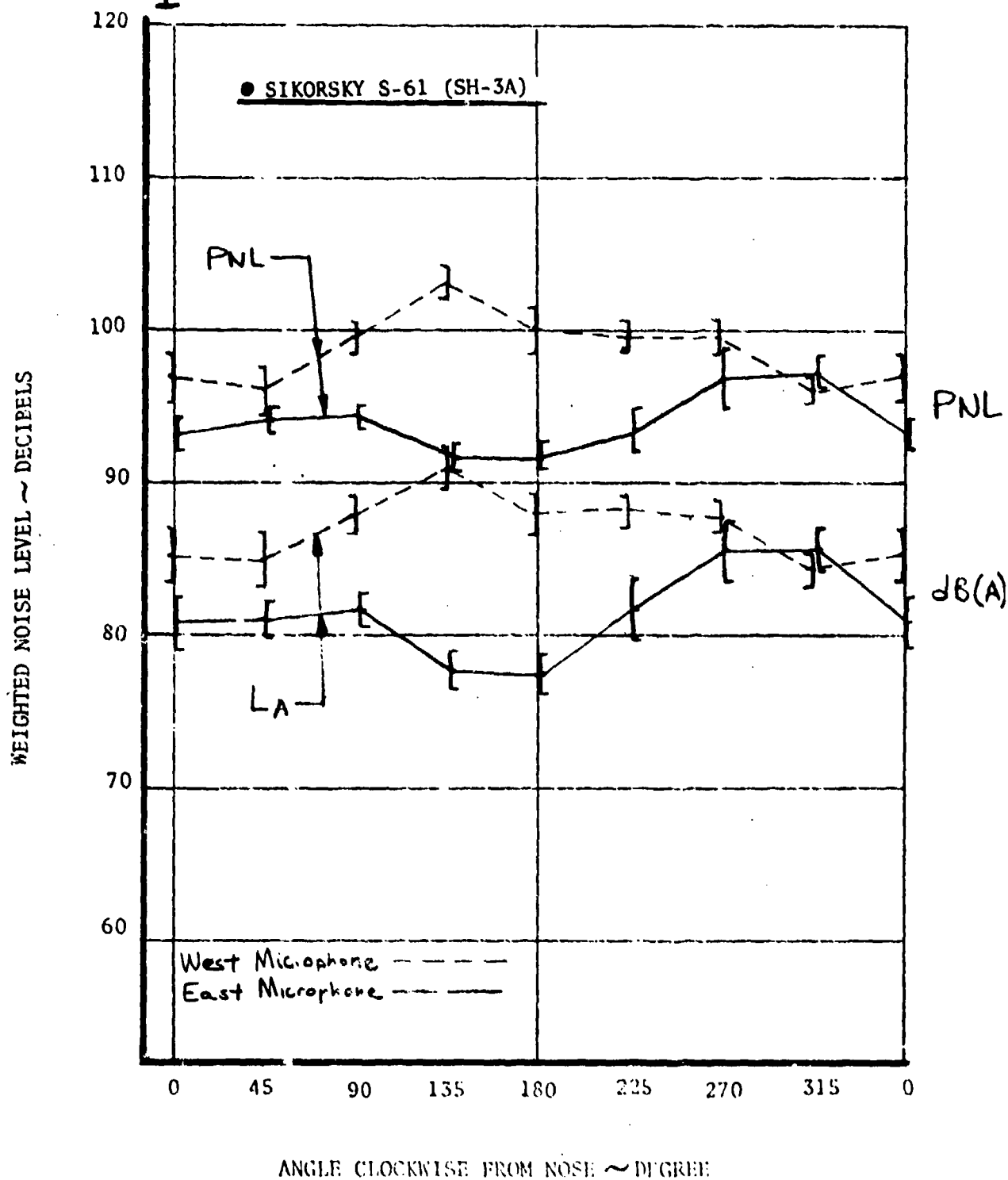


FIGURE 25. FIVE FOOT HOVER SPECTRA

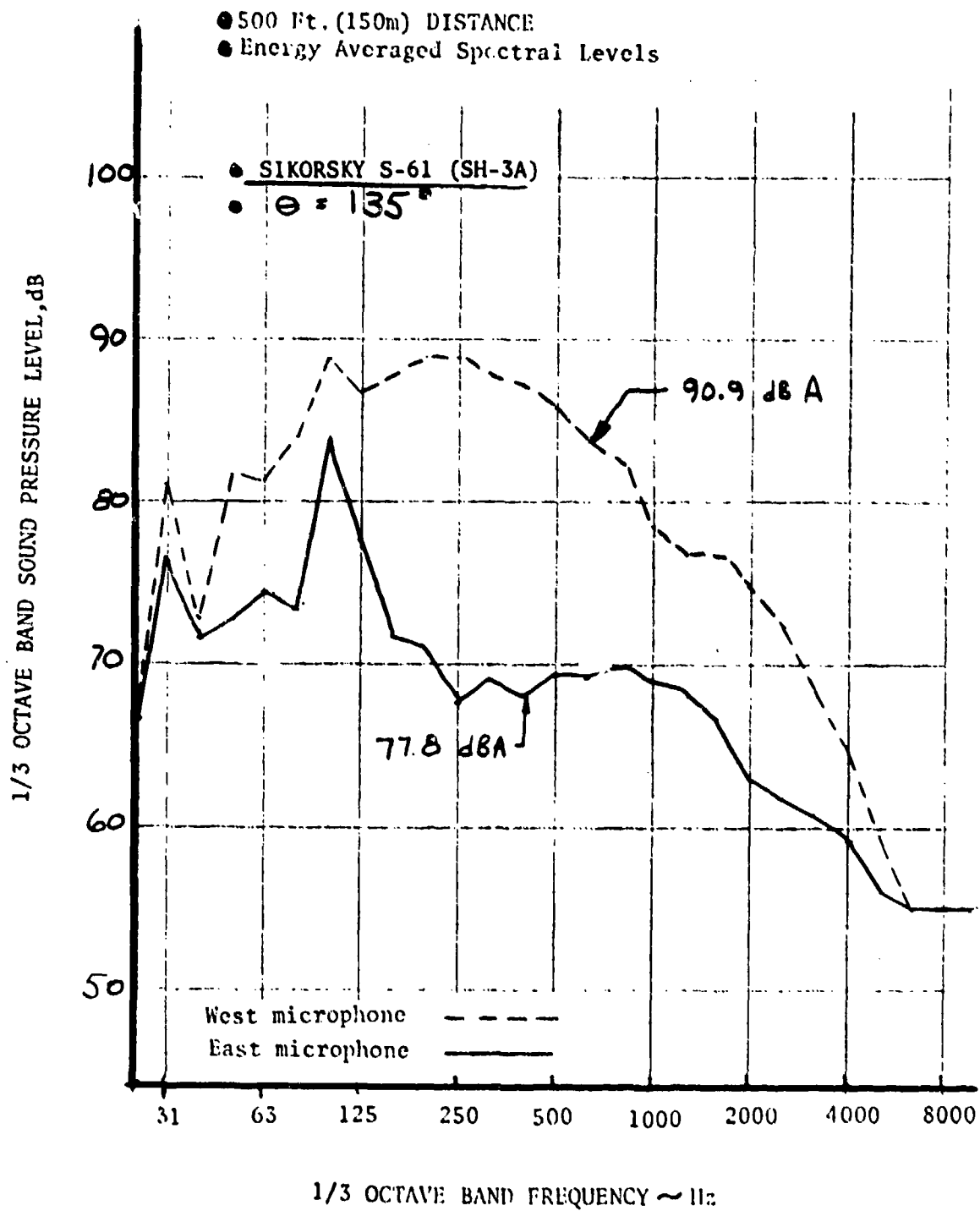


FIGURE 76. FIVE FOOT HOVER SPECTRA

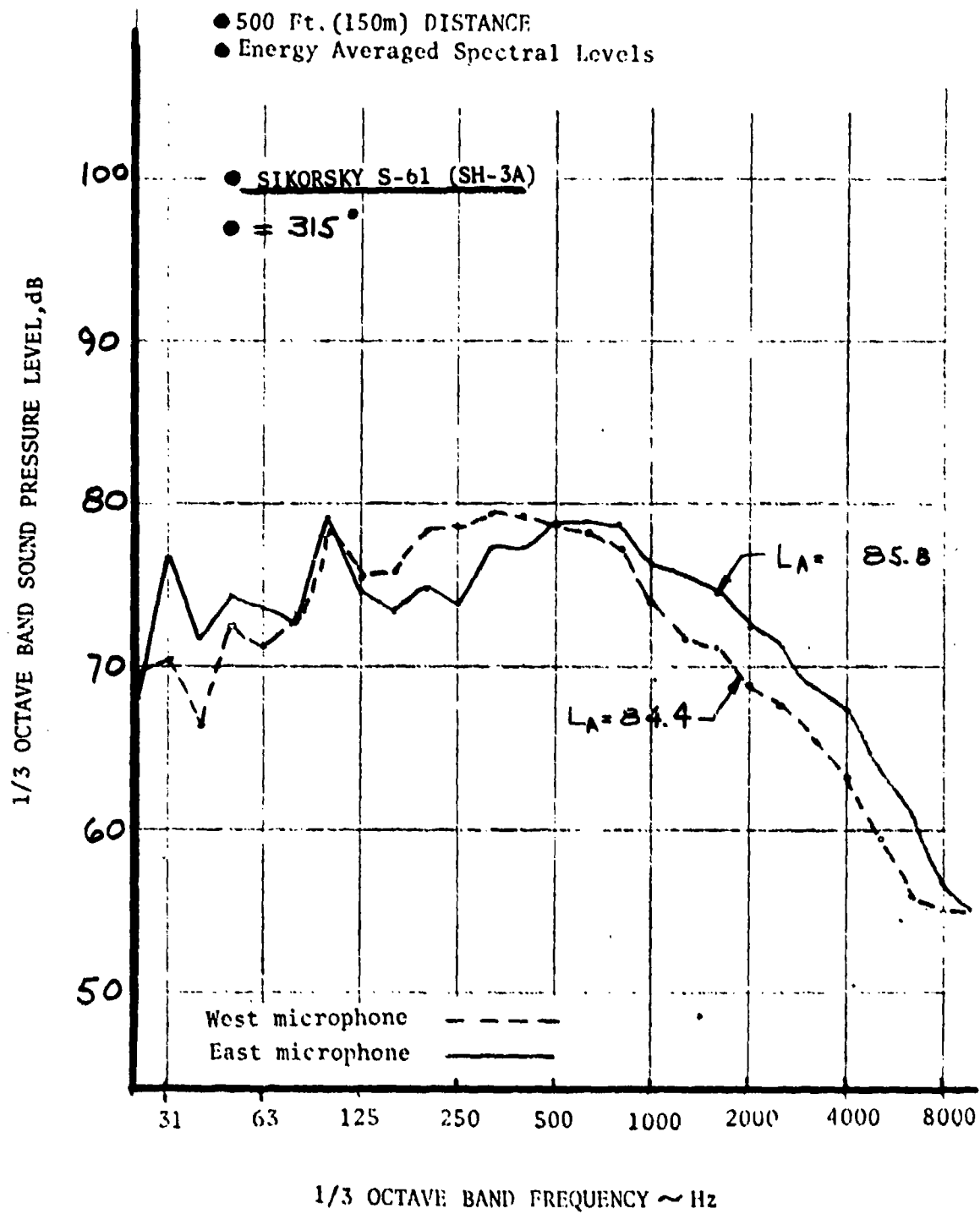




FIGURE 77. HELICOPTER HOVER DIRECTIVITY

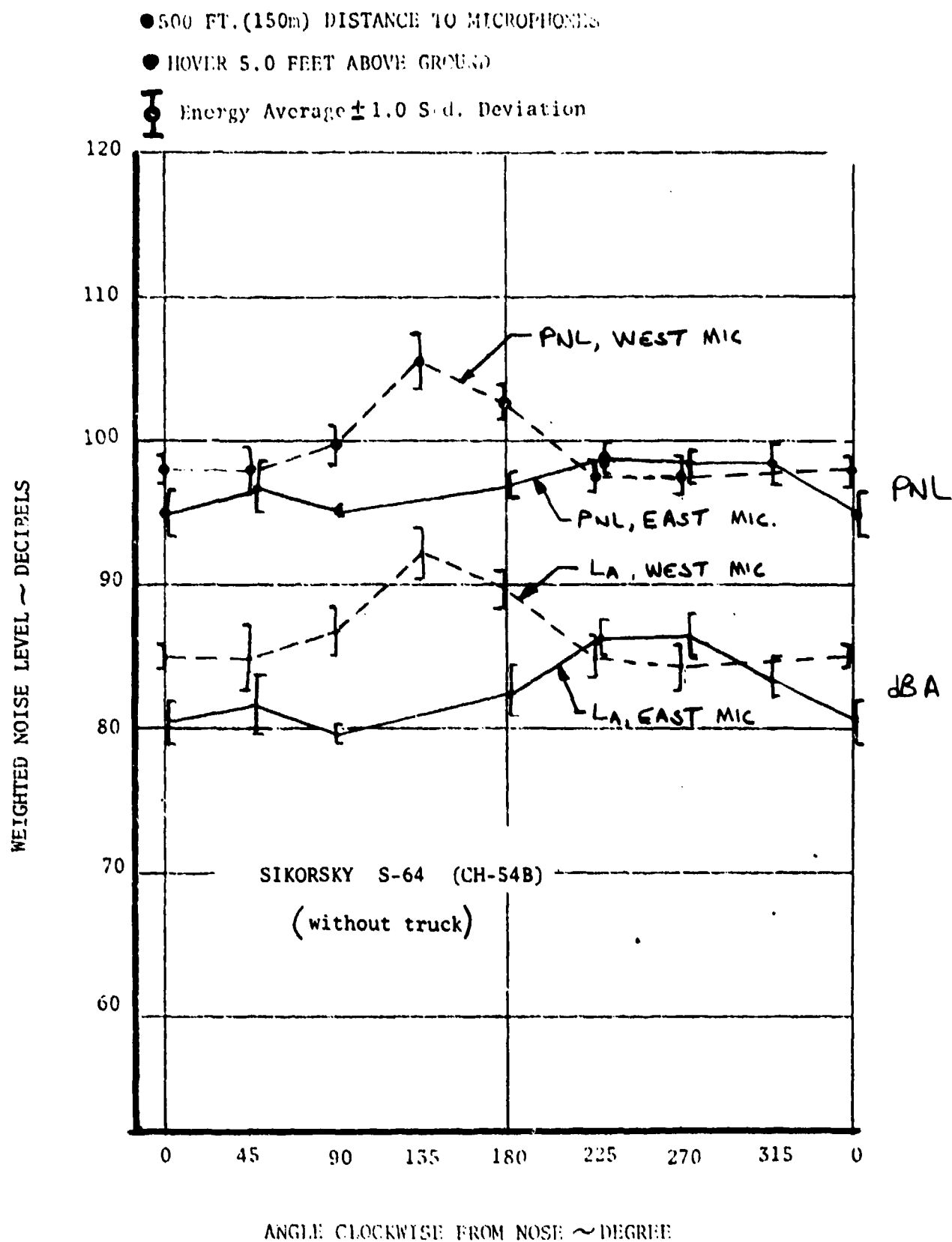


FIGURE 79. HELICOPTER HOVER DIRECTIVITY

● 500 FT. (150m) DISTANCE TO MICROPHONES

● HOVER 5.0 FEET ABOVE GROUND

⌋ Energy Average  $\pm 1.0$  Std. Deviation

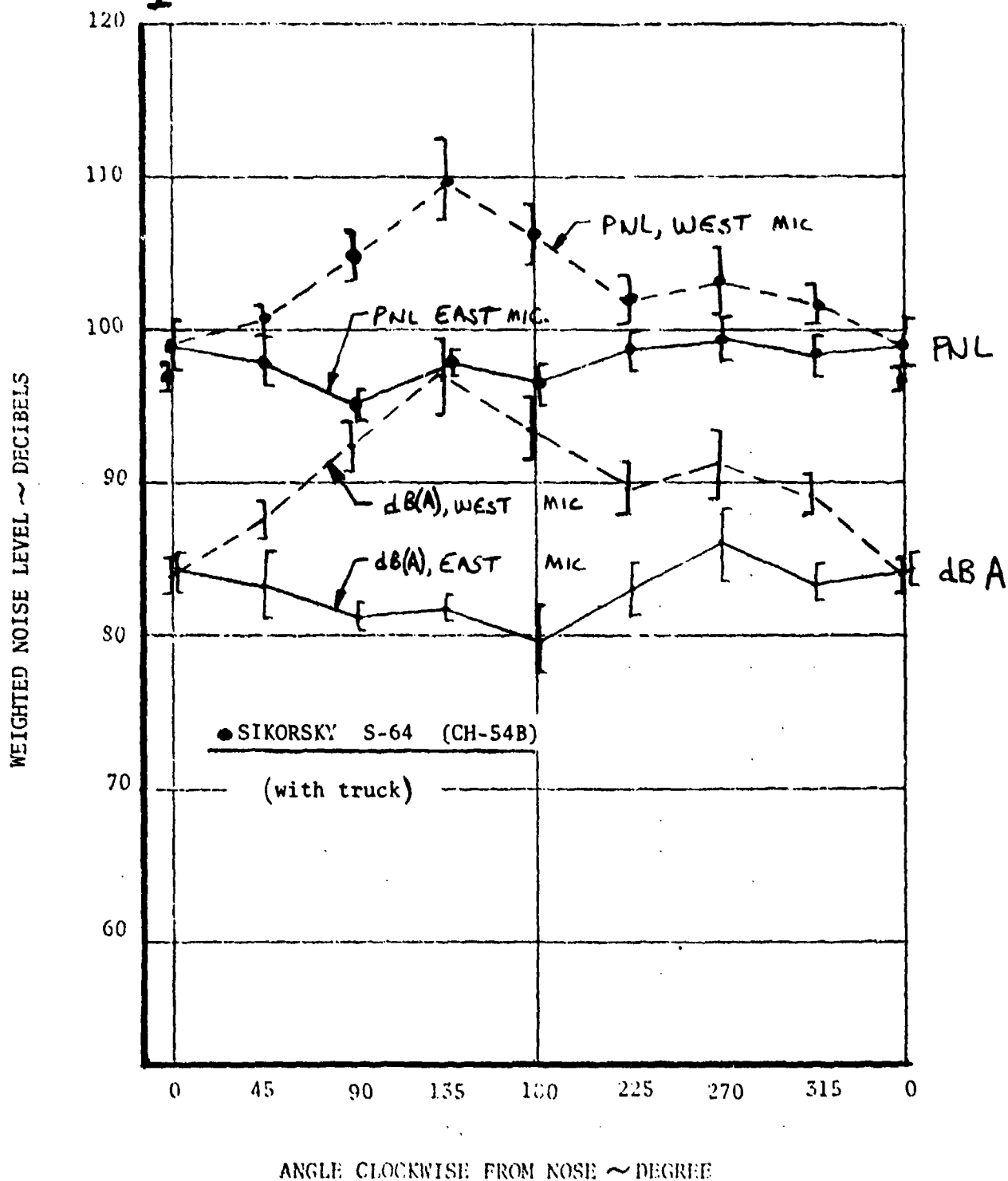


FIGURE 79. FIVE FOOT HOVER SPECTRA

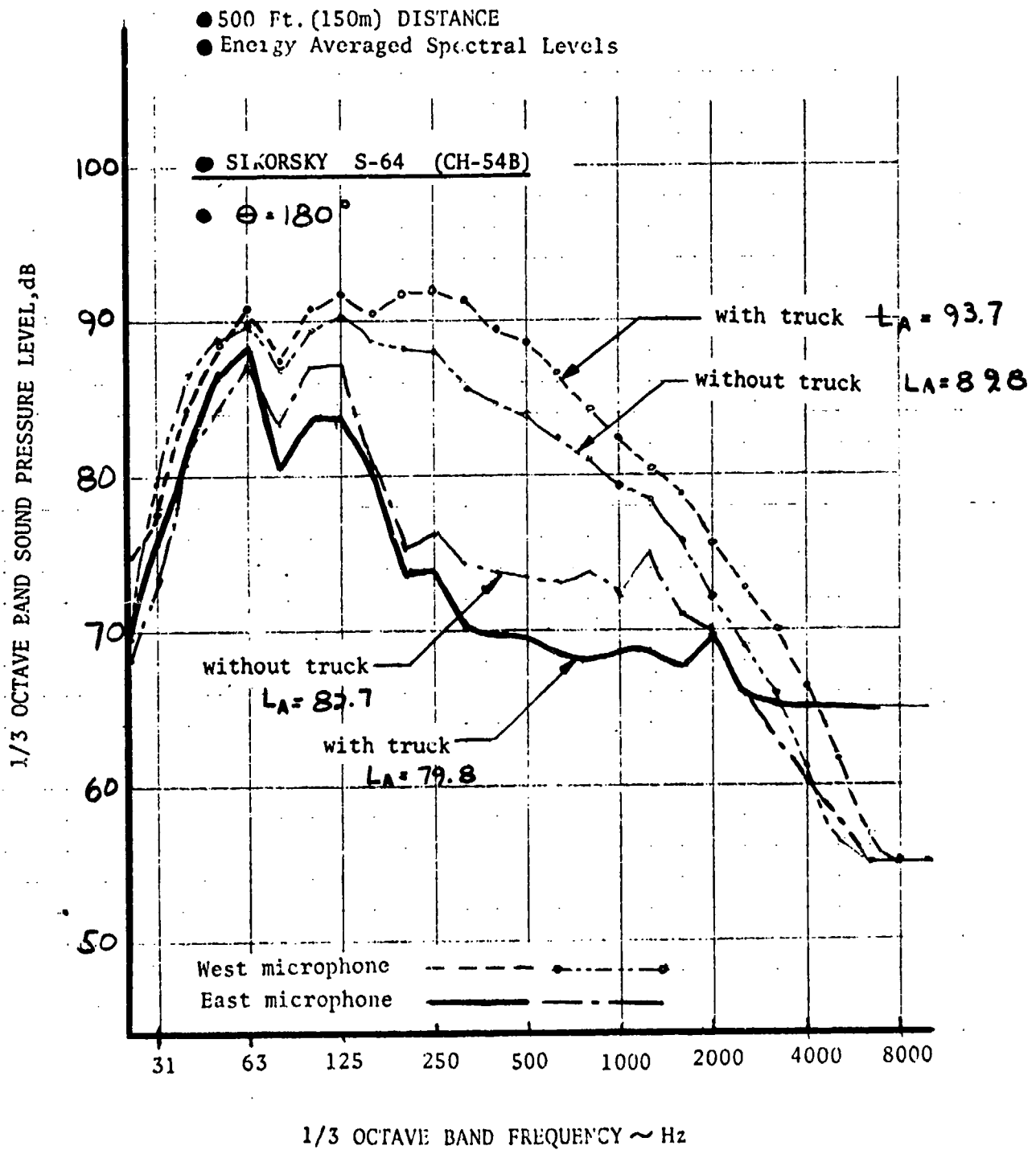


FIGURE 90. FIVE FOOT HOVER SPECTRA

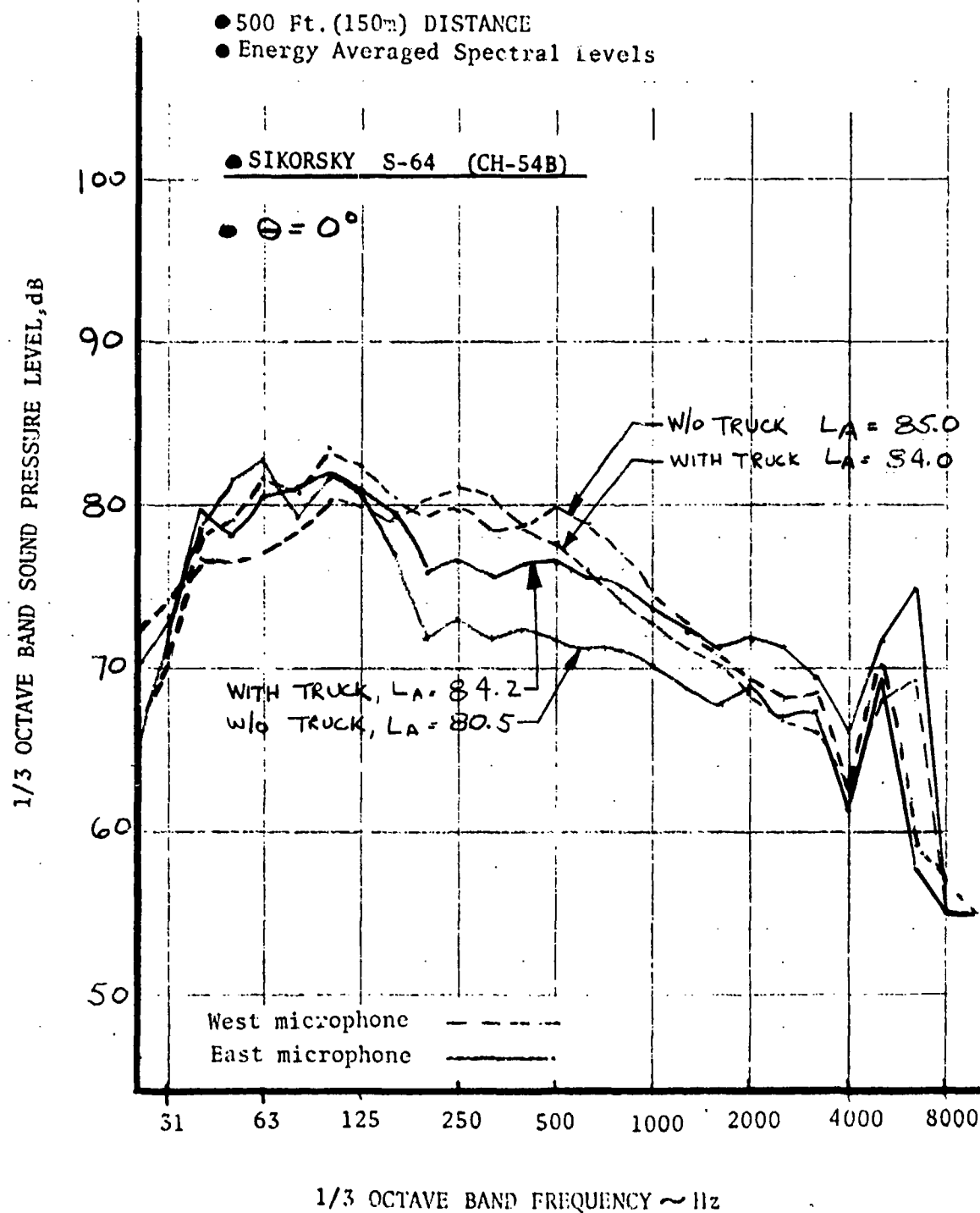


FIGURE 7. HELICOPTER HOVER DIRECTIVITY

● 500 FT. (150m) DISTANCE TO MICROPHONES

● HOVER 5.0 FEET ABOVE GROUND

⊥ Energy Average  $\pm 1.0$  Std. Deviation

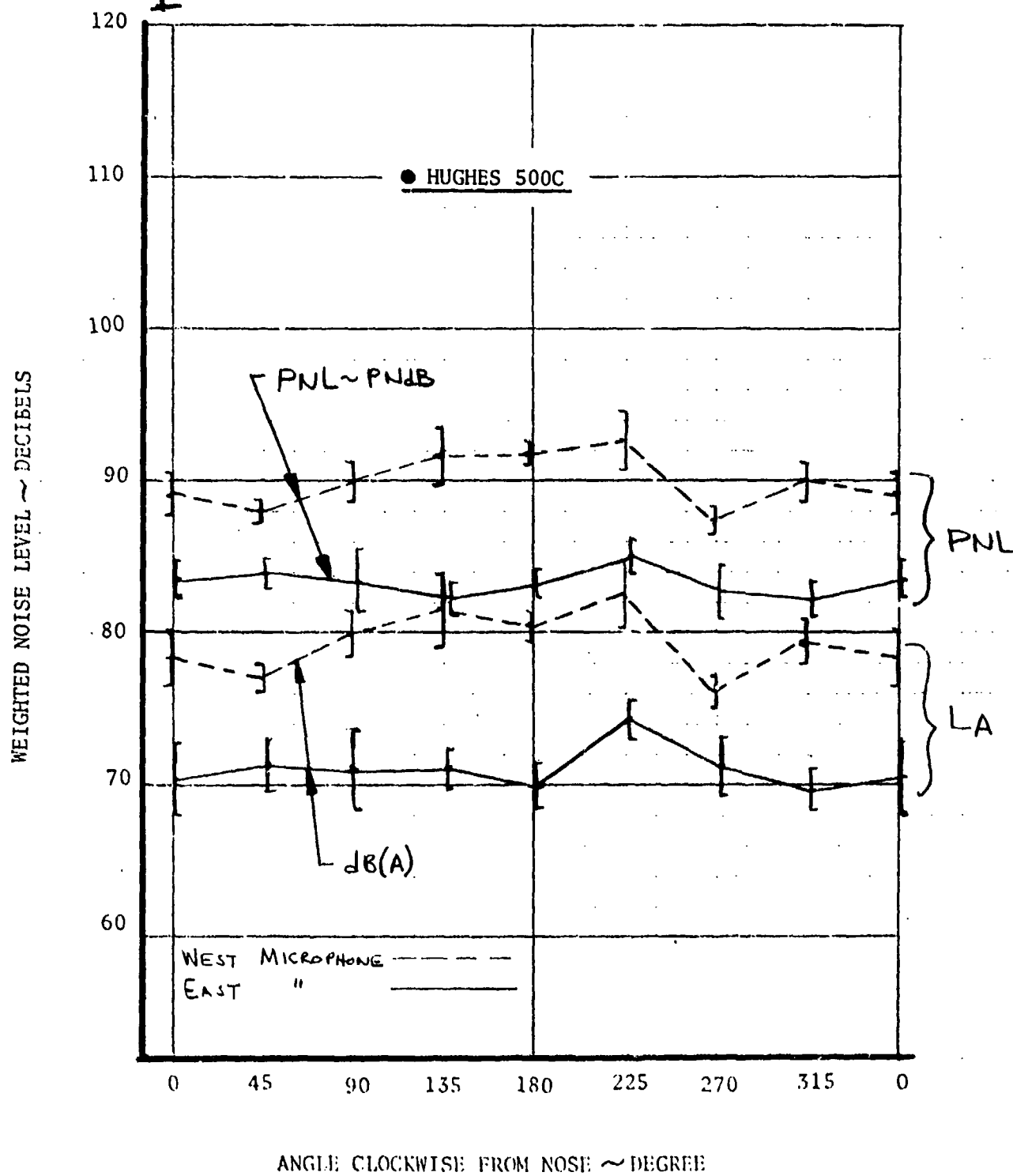


FIGURE 22. FIVE FOOT HOVER SPECTRA

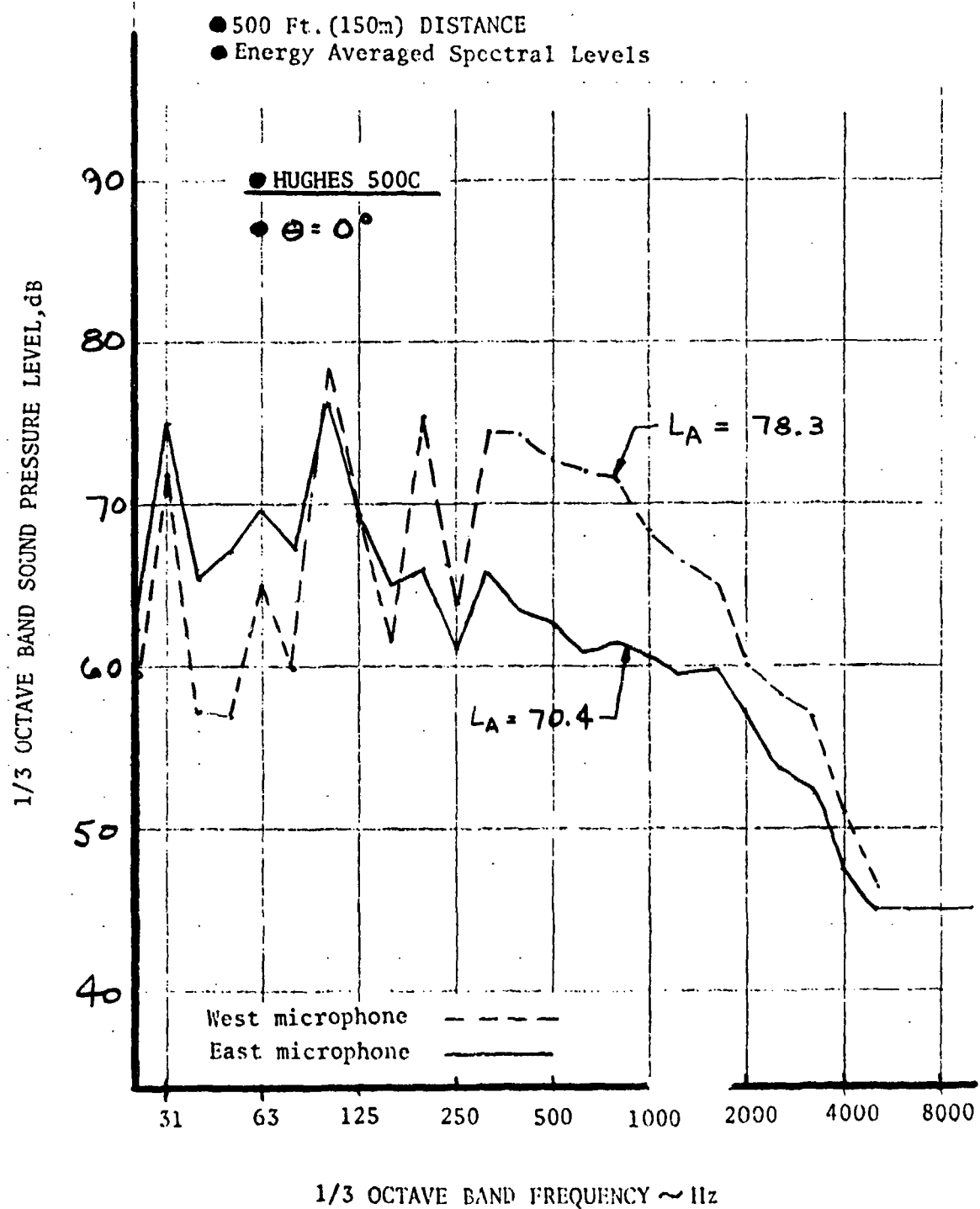


FIGURE 93. FIVE FOOT HOVER SPECTRA

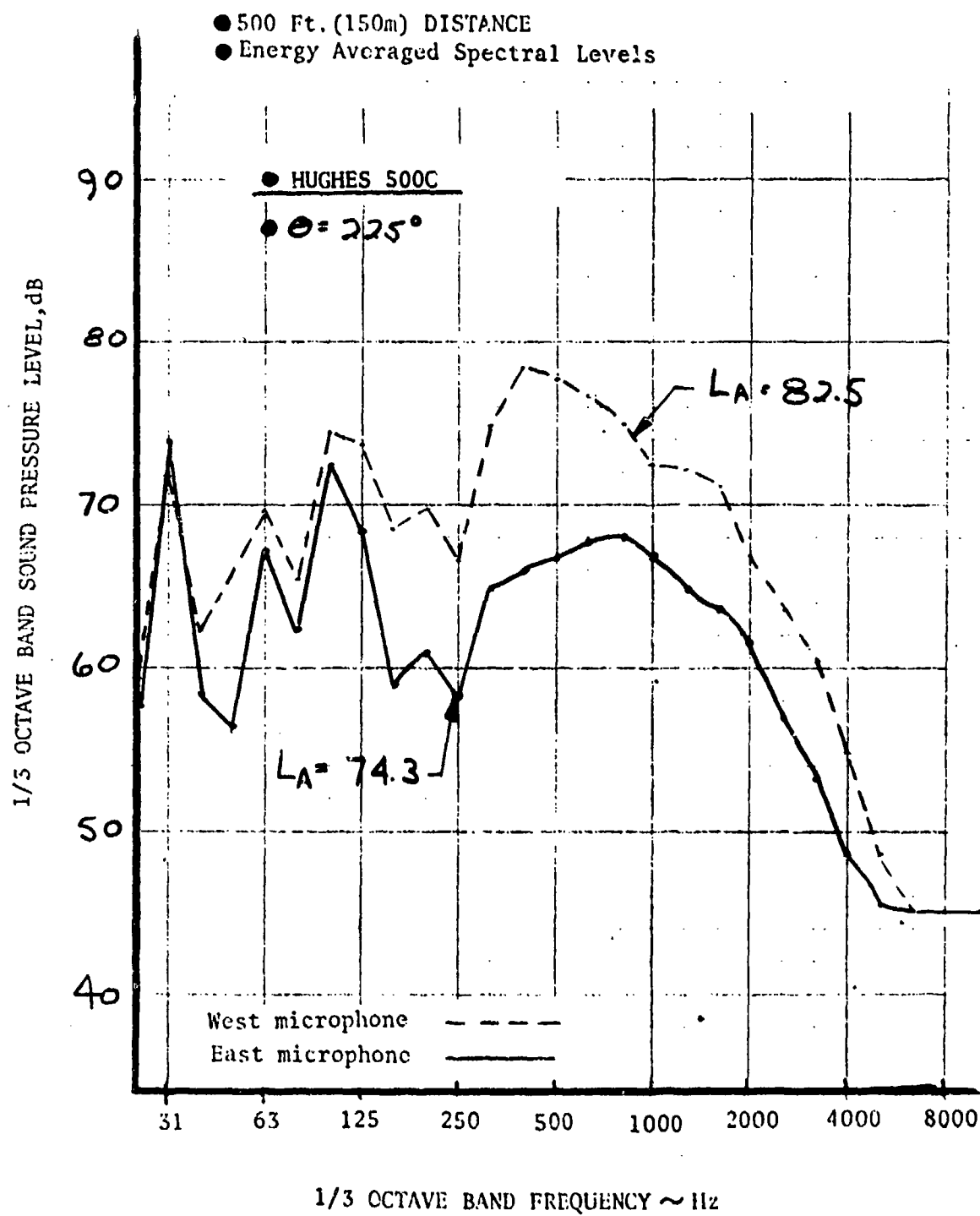


FIGURE 84. HELICOPTER HOVER DIRECTIVITY

● 500 FT. (150m) DISTANCE TO MICROPHONES

● HOVER 5.0 FEET ABOVE GROUND

⊥ Energy Average  $\pm 1.0$  Std. Deviation

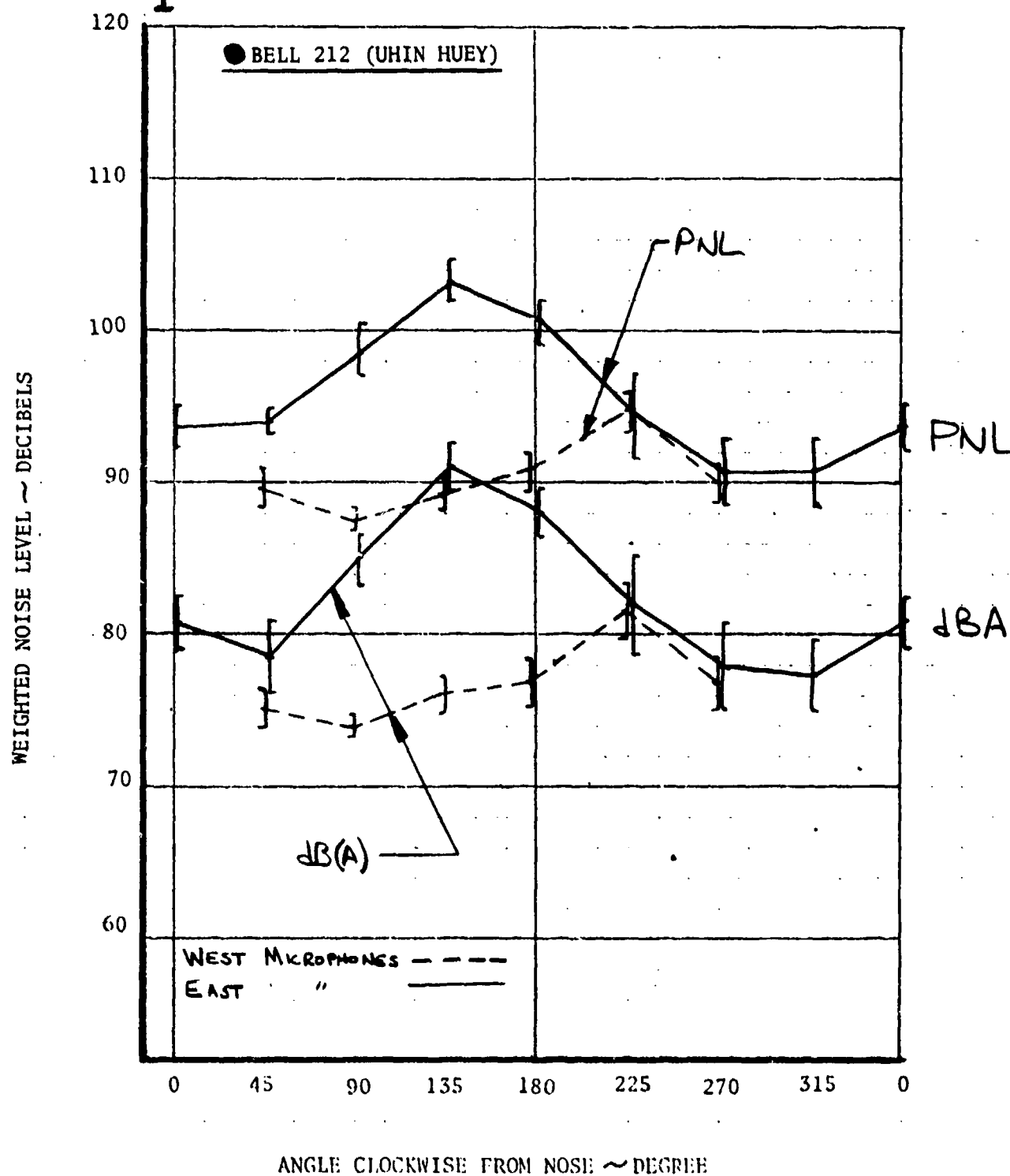




FIGURE 25. FIVE FOOT HOVER SPECTRA

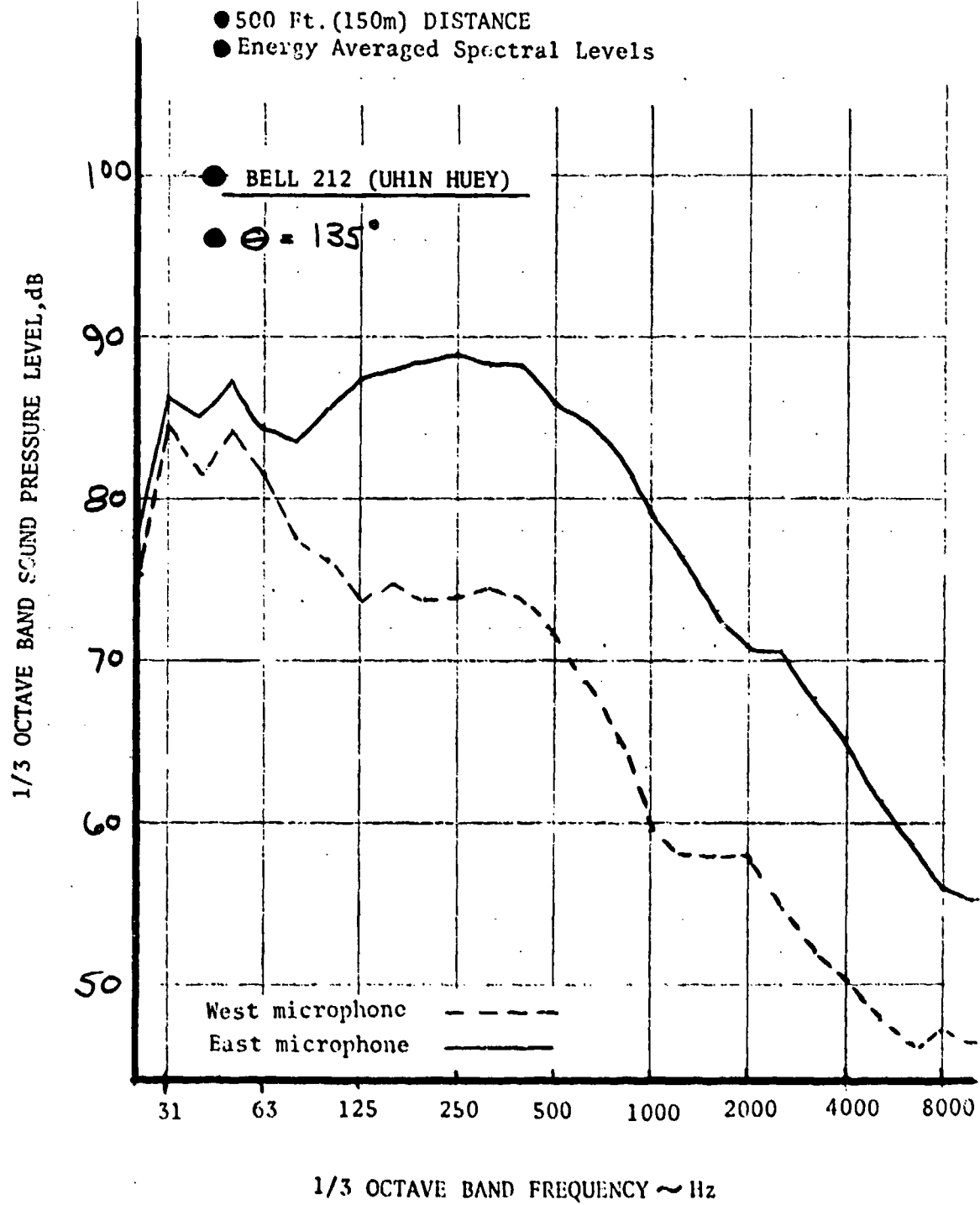


FIGURE 86. FIVE FOOT HOVER SPECTRA

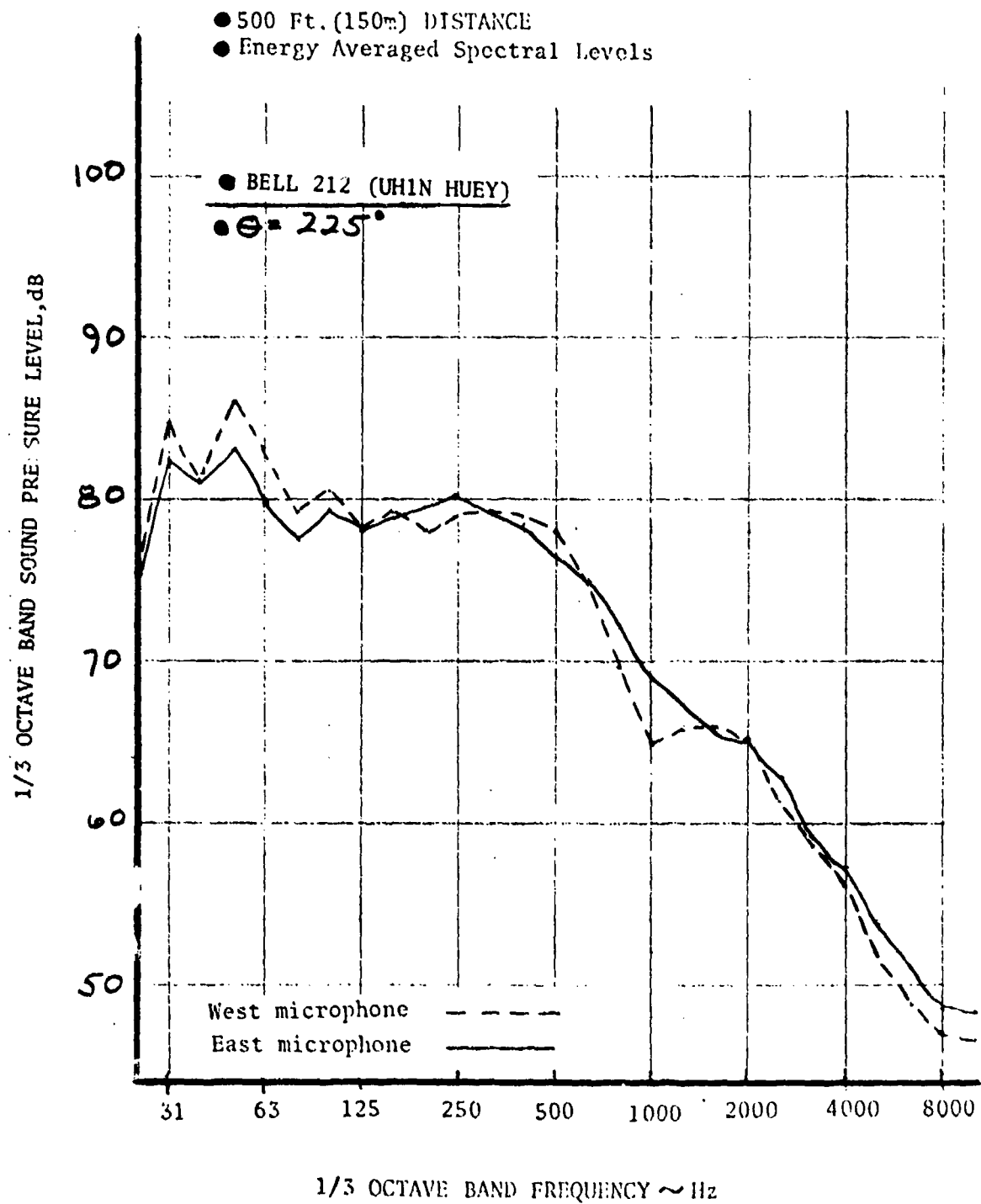


FIGURE 89. HELICOPTER HOVER DIRECTIVITY

● 500 FT. (150m) DISTANCE TO MICROPHONES

● HOVER 5.0 FEET ABOVE GROUND

⊕ Energy Average  $\pm 1.0$  Std. Deviation

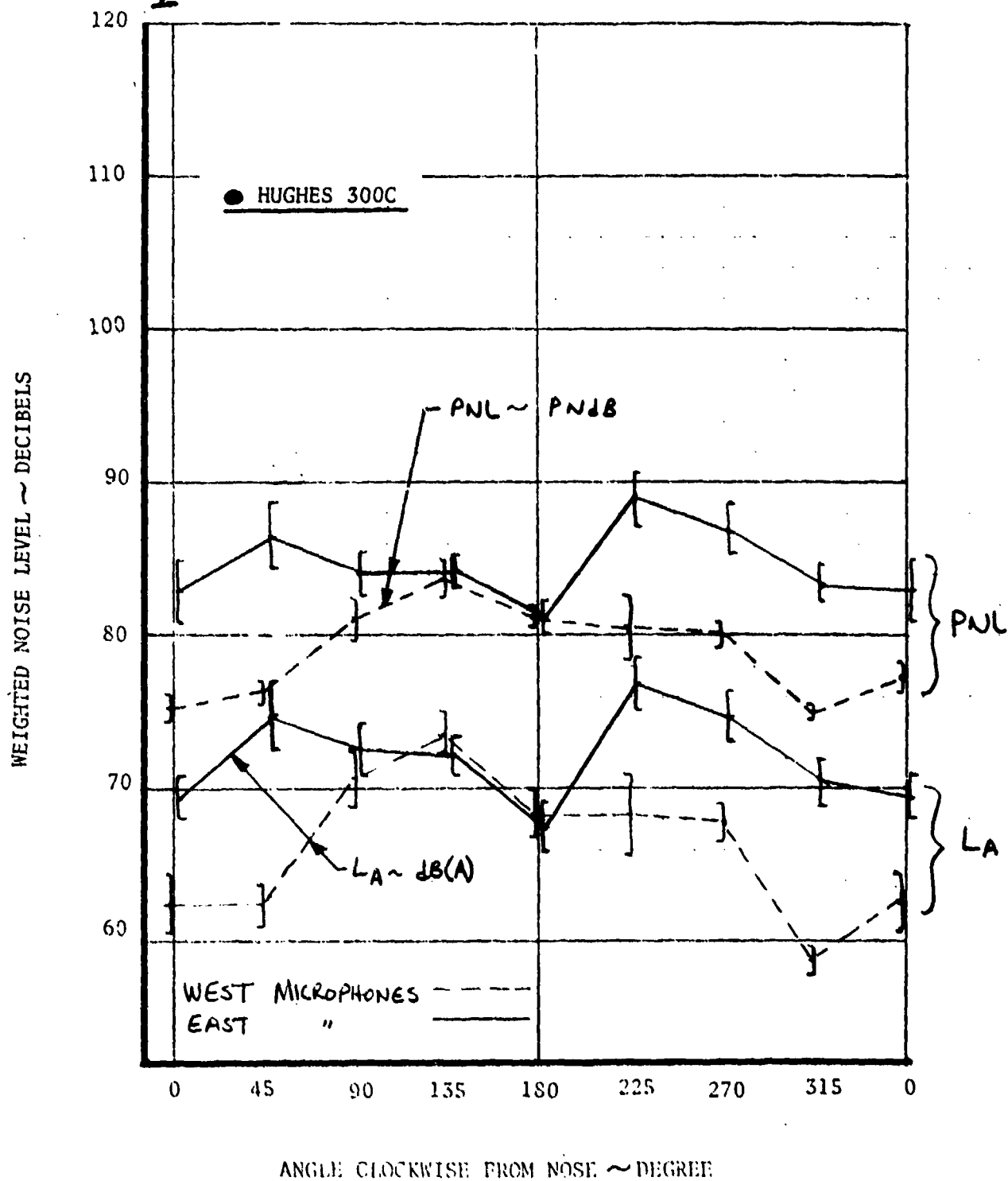


FIGURE 88. FIVE FOOT HOVER SPECTRA

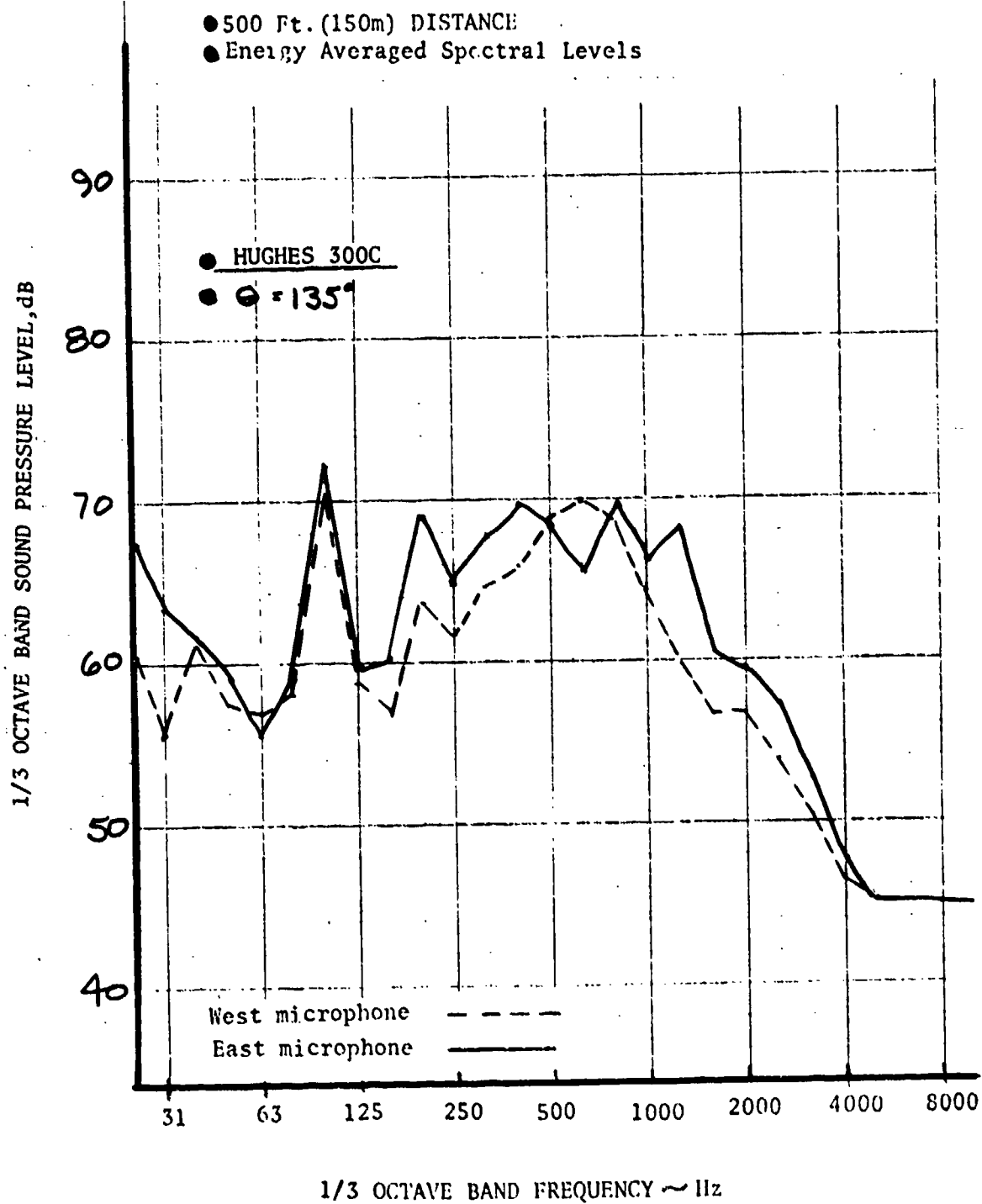


FIGURE 89. FIVE FOOT HOVER SPECTRA

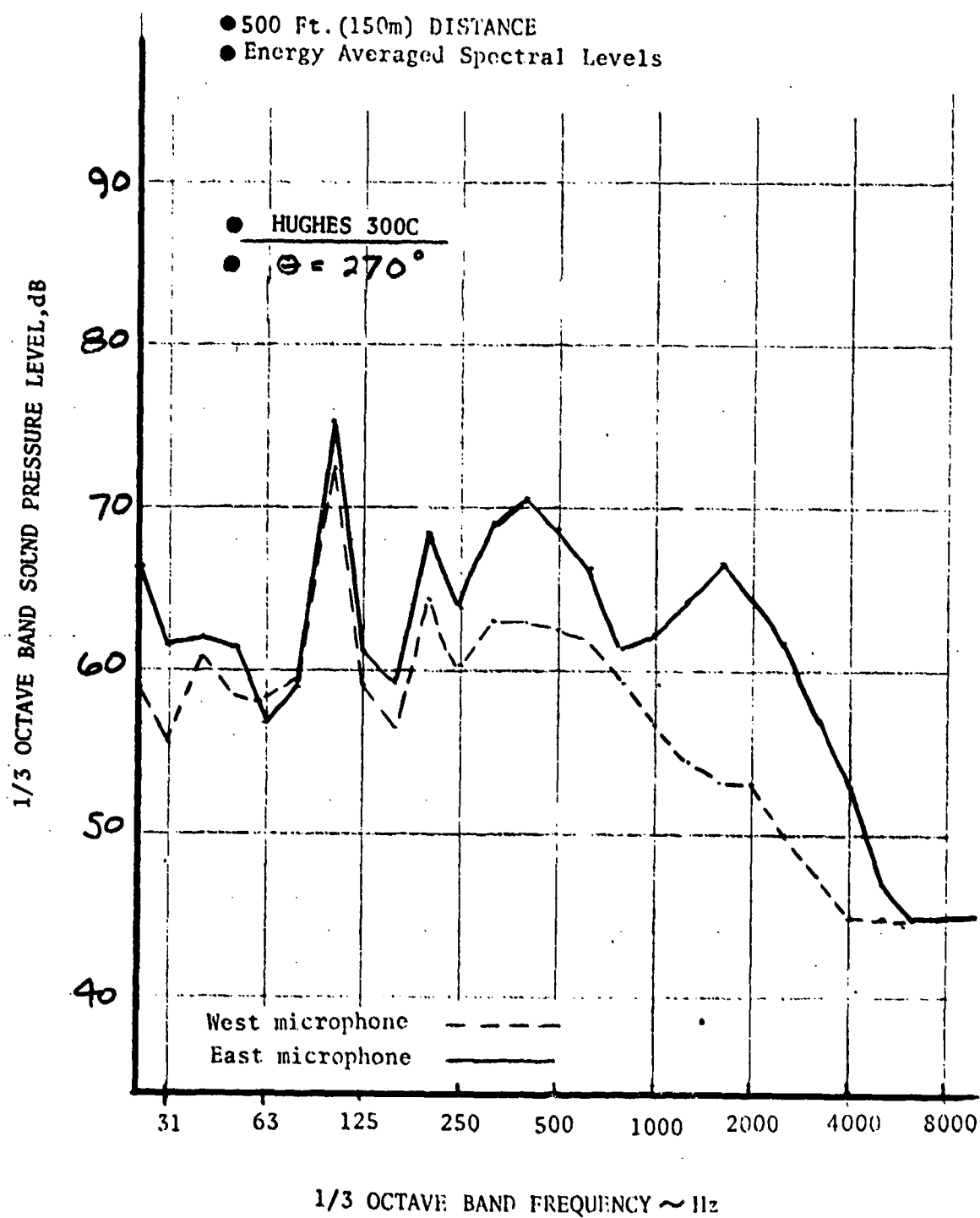


FIGURE 90. HELICOPTER HOVER DIRECTIVITY

● 500 FT. (150m) DISTANCE TO MICROPHONES

● HOVER 5.0 FEET ABOVE GROUND

⊥ Energy Average  $\pm 1.0$  Std. Deviation

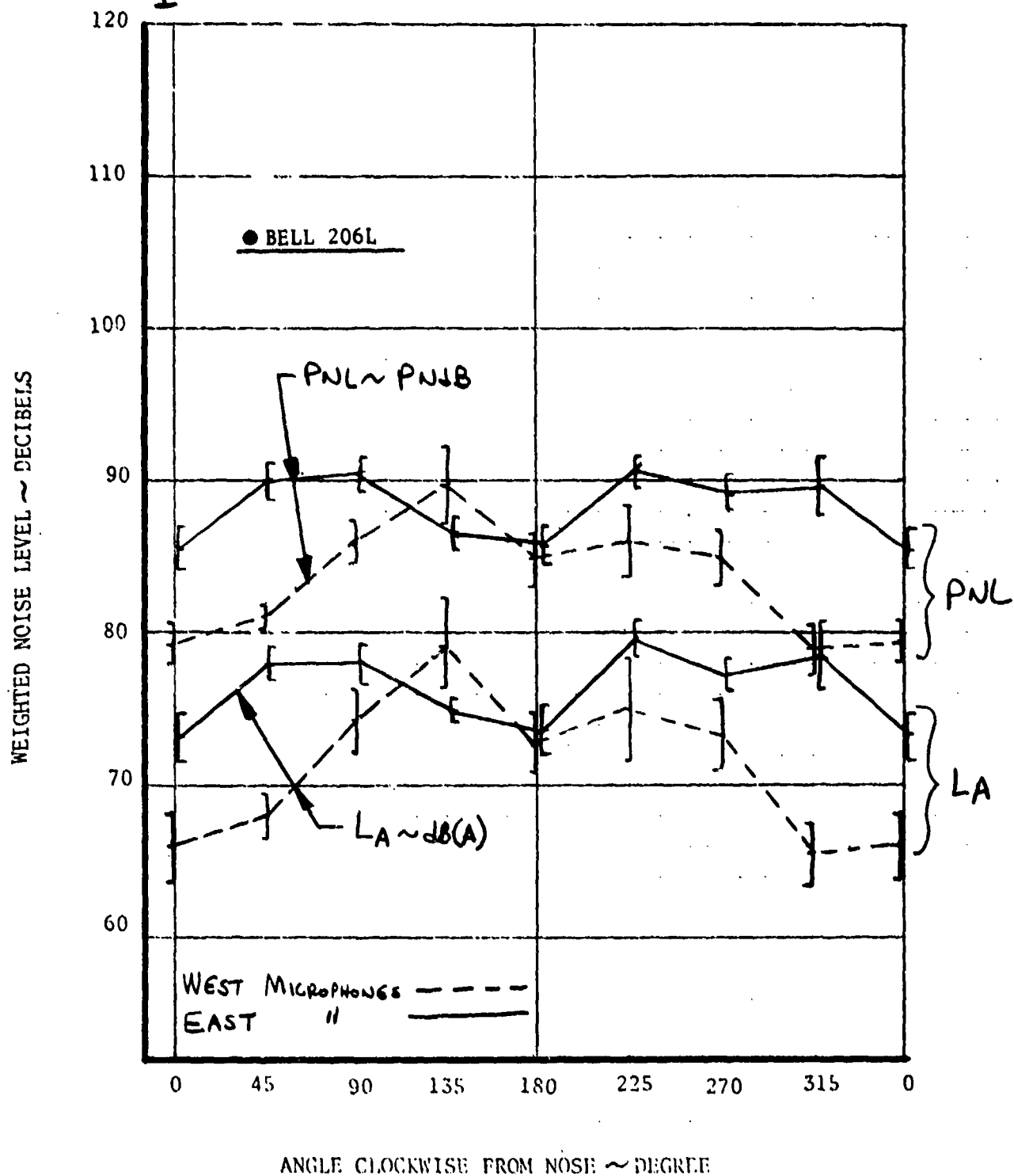


FIGURE 97. FIVE FOOT HOVER SPECTRA

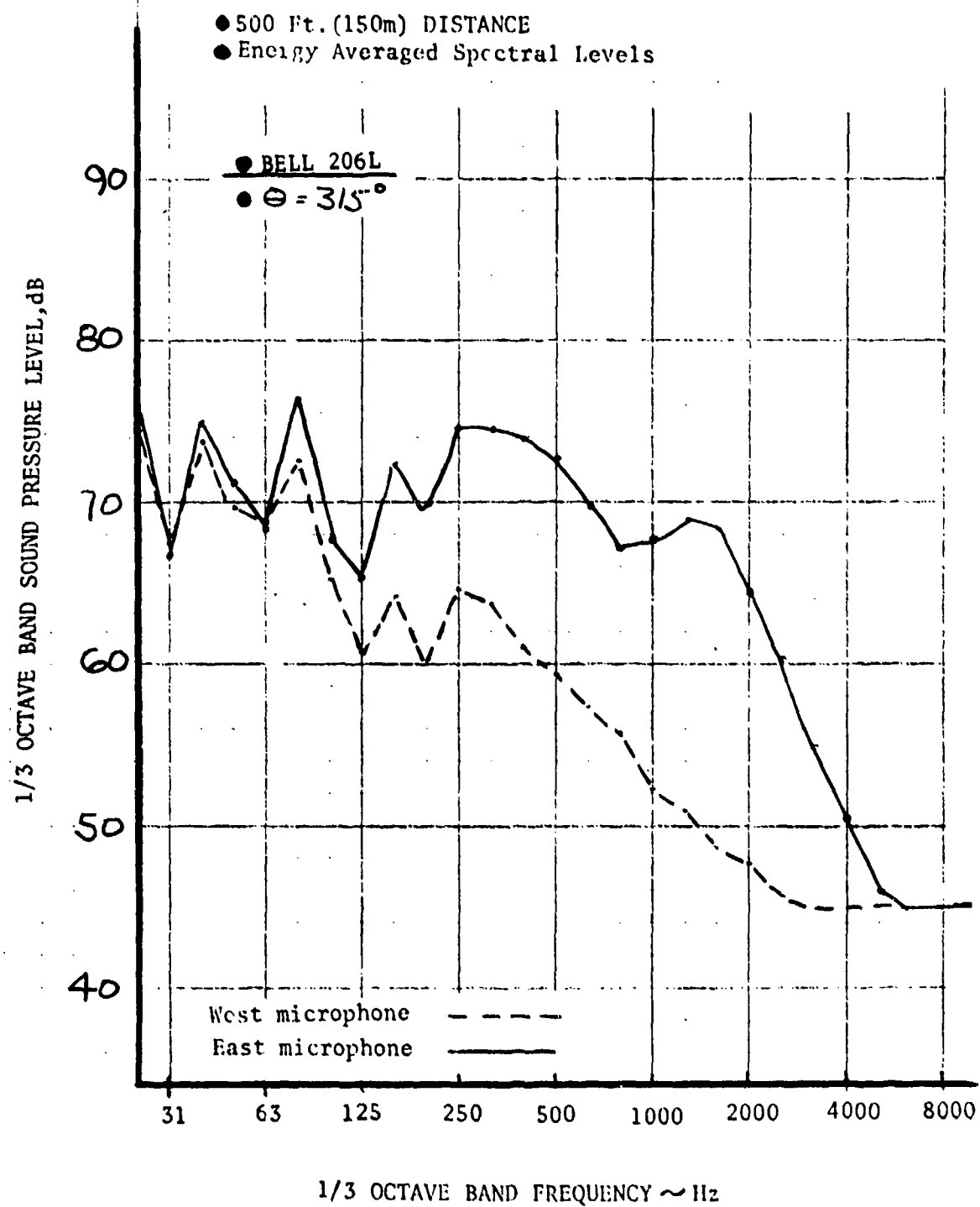
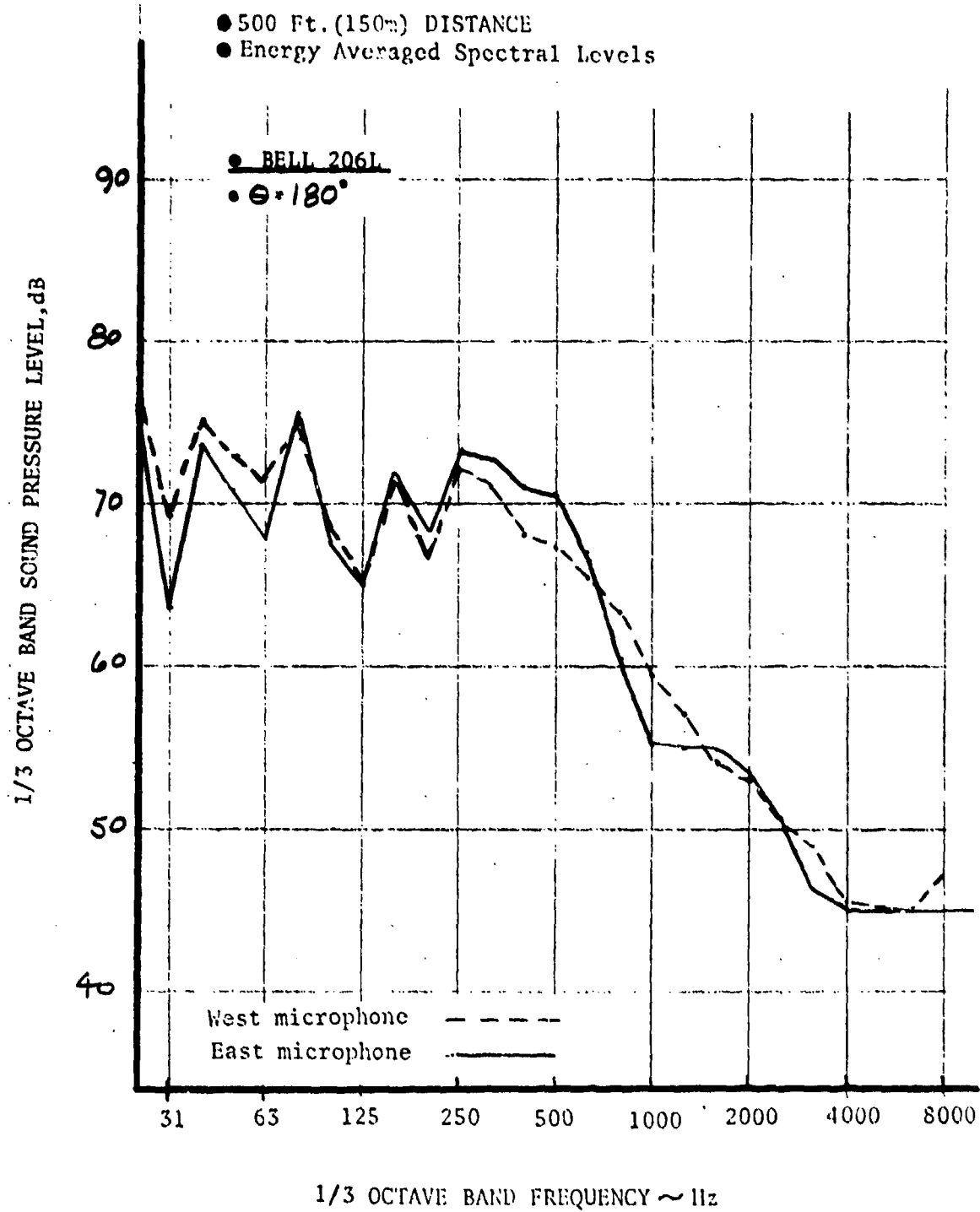


FIGURE 72. FIVE FOOT HOVER SPECTRA





## 7.0 IMPULSIVE AND NARROW BAND ANALYSIS

### 7.1 Waveform Analysis

Selected waveforms (pressure vs. time) were analyzed early in the program to examine visually the striking differences in noise characteristics between different types of helicopters. The noise signature for 300 milliseconds of data at the peak A-weighted noise level during the flyover was obtained using the signal enhancement operation mode of the Nicolet Scientific FFT Analyzer Model O-FFT-400.

Impulsive type waveforms are evident for the UHIN (Bell 212) Figures 93 and 94, and the CH-47C, Figure 95. These signatures are characterized by sharp, impulsive rises in sound pressure at time intervals corresponding to the passage of each main rotor blade with the frequency adjusted for doppler effects. Figure 93 shows compressibility slap for a UHIN during level flyover with the helicopter approaching the microphone. During approach, the UHIN generates a more complex but lower peak level signature. The "multiple peaks" could be due to blade vortex interaction combined with compressibility slap. The CH-47C, during a high speed level flyover, generates a pattern with the tall set of spikes (70 msec) at the blade passage of a single rotor and the tall and short spikes together at the combined blade passage of both rotors.

The 500C and S-61 exhibit a waveform signature more similar to that generated by conventional jet powered transports. The 500C, Figure 96, shows main rotor noise at intervals of 25 msec. intervals with the intervening spikes at the tail blade passage frequency of about 10 msec. The S-61 signature has a complex and somewhat inexplicable pattern (Figure 97). The main rotor blade passage is at 50-60 msec and the tail rotor at about 10 msec.

The level of impulsiveness at the time of peak A-weighted noise was estimated by playing several recordings, A-weighted, through a B&K-2209 SLM and recording the peak A-level on "slow" response,

peak impulse hold and rms impulse hold. The difference between peak impulse hold and slow approximates the crest factor and is a measure of impulsiveness. Typical results were as follows:

AIRCRAFT	PEAK IMPULSE HOLD - SLOW	RMS IMPULSE HOLD - SLOW
Typical Jet Transports i.e.(727, Concorde)	13-15 dBA	1.0 - 1.5 dBA
Helicopters with Slap (CH-47C, UHIN)	16-29 dBA	3.5 - 6.5 dBA
Helicopters with Little or no slap at peak noise	12-14 dBA	1.0 - 2.0 dBA

Helicopters with little or no slap have crest factors at peak noise during a flyover of the same magnitude as jet transports. This would indicate that slow weighting such as specified by FAR Part 36 would be appropriate for the measurement of the noise from these helicopters. Helicopters with dominant slapping characteristics, however, have substantially higher crest factors and "slow" rms averaging would not give an accurate indication of the peak sound pressure these helicopters produce.

## 7.2 Narrow-Band Spectral Analysis

Figures 98-107 show narrow band spectra for the CH-47C, UHIN, Bell 206L, 500C, and S-61. These spectra were produced using the Nicolet Scientific FFT Analyzer Model O-FFT-400. Two figures are shown for each of the five helicopters. The first represents the helicopter approaching the microphone and the second is at the time of overhead passage. Two plots are shown on each figure. The upper plot shows 0 to 1000 Hz and the lower plot expands the first 200 Hz for clarity. Doppler effects often increase the apparent blade passage frequencies.

The CH-47C, Figures 98 and 99, has no tail rotor and the pulses due to main rotor blade passage are clearly evident. Figure 98 shows a slapping condition and Figure 99 the overhead where the slap is greatly diminished. The slapping generally affects the portion of the spectra from 200 to 700 Hz. The expanded waveforms show the sharp impulsive nature of the spectra on Figure 98 with a more rounded shape on Figure 99 as the helicopter passes overhead. The ground reflection interference pattern at overhead is also present. The noise increase during slap for the UHIN, Figure 100, compared to Figure 101, overhead, appears primarily to be from 20 to 400 Hz at the sideline microphone. During slap the main rotor noise dominates the spectrum well beyond 200 Hz

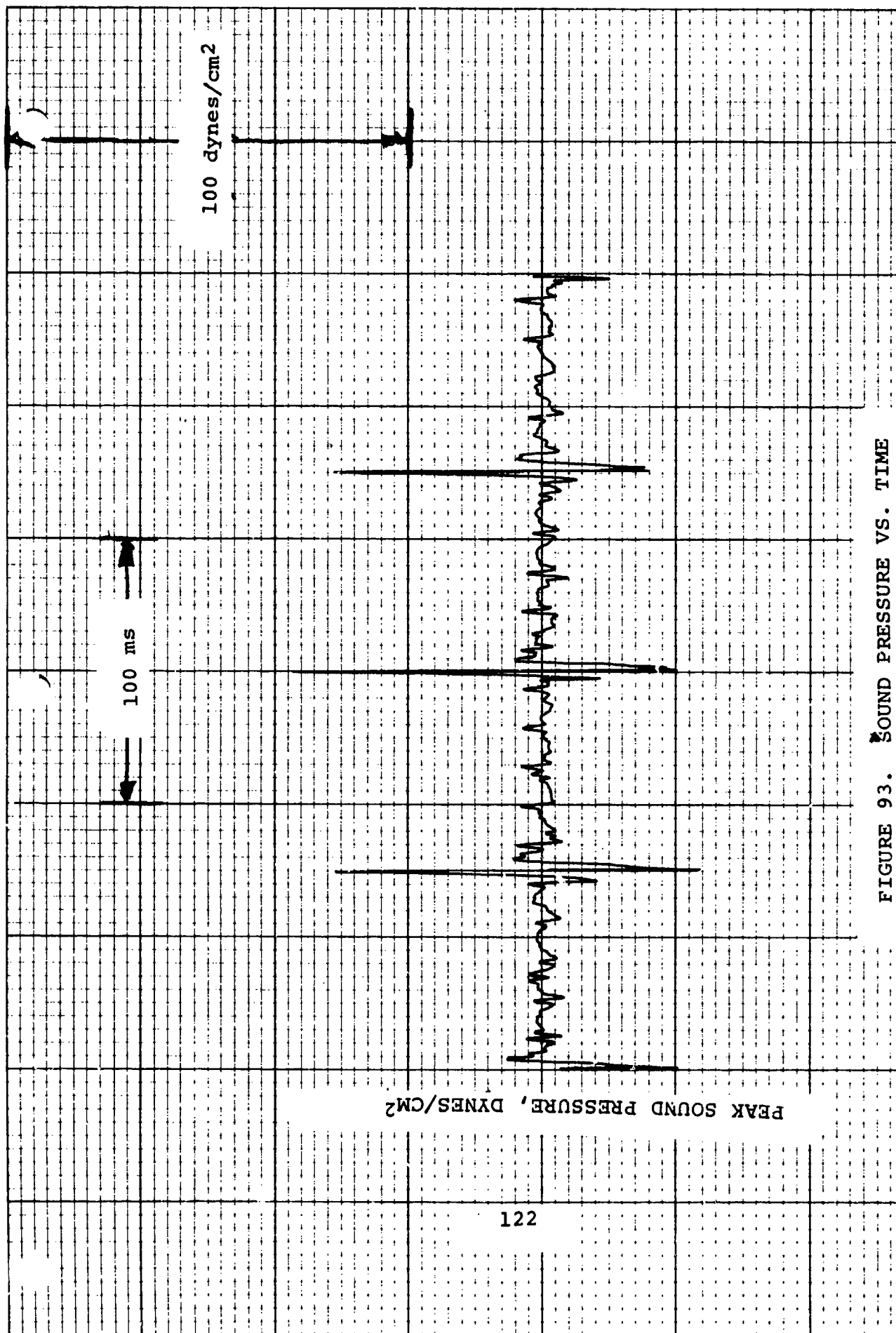


FIGURE 93. SOUND PRESSURE VS. TIME  
 BELL 212 (UHIN), LEVEL FLYOVER AT  
 114 KNOTS, 500 FOOT ALTITUDE, WAVE-  
 FORM AT PNLM, RUN 38

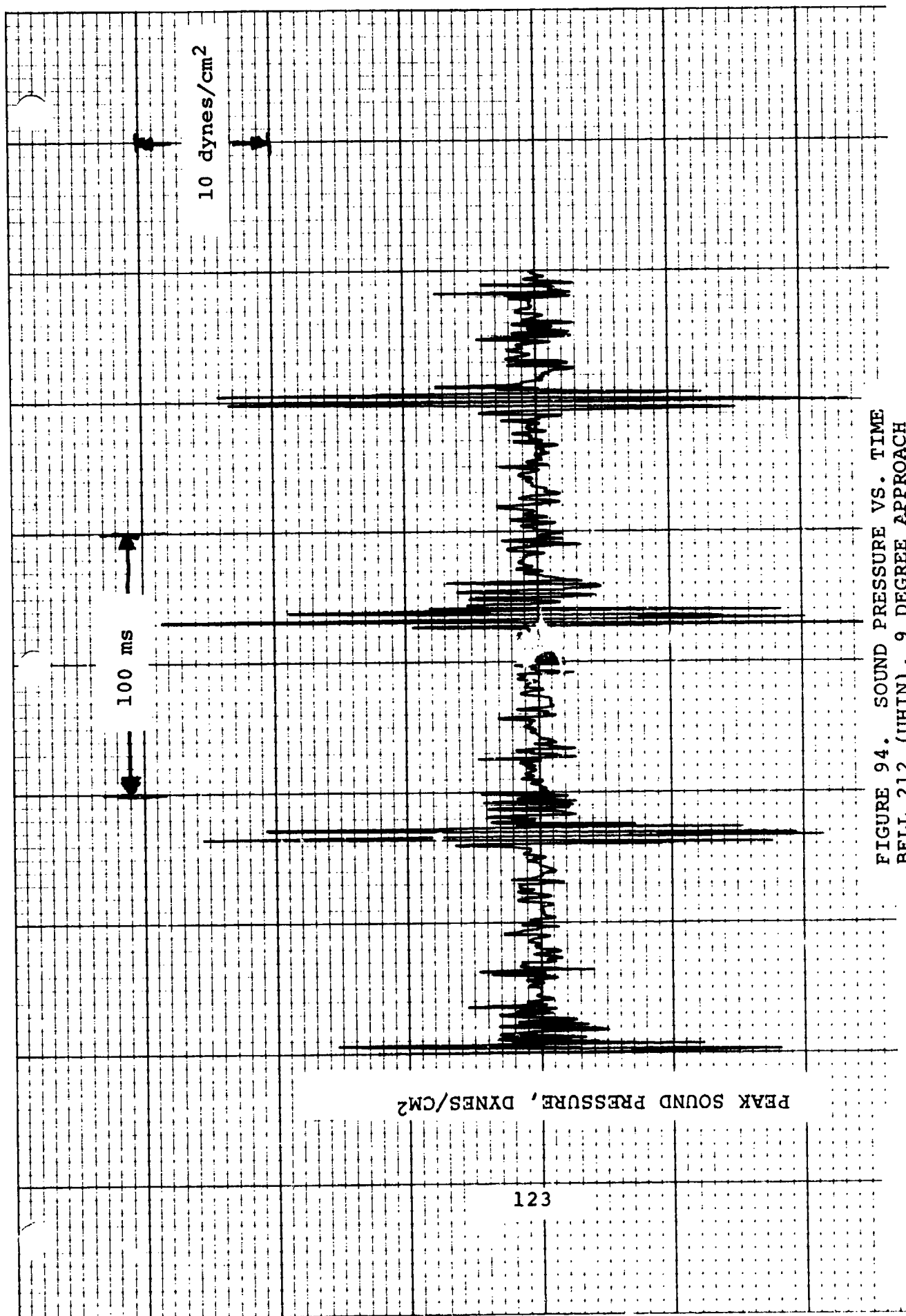


FIGURE 94. SOUND PRESSURE VS. TIME  
BELL 212 (UHIN), 9 DEGREE APPROACH  
AT 60 KNOTS, 400 FOOT ALTITUDE,  
WAVEFORM AT PNLM, RUN 26

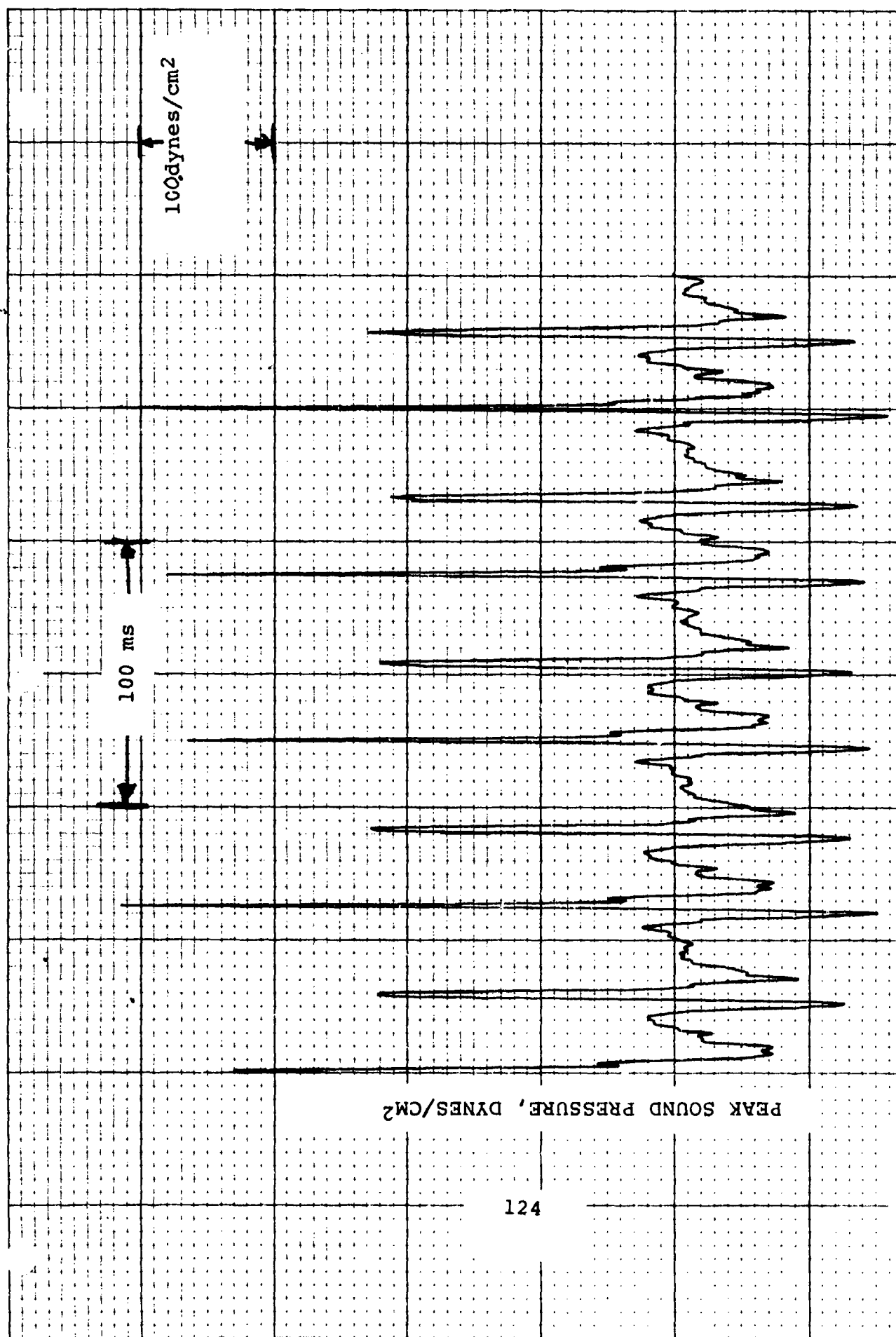


FIGURE 95. SOUND PRESSURE VS. TIME  
 VERTOL CH-47C, LEVEL FLYOVER AT  
 150 KNOTS, 500 FOOT ALTITUDE, WAVE-  
 FORM AT PNLM, RUN 28

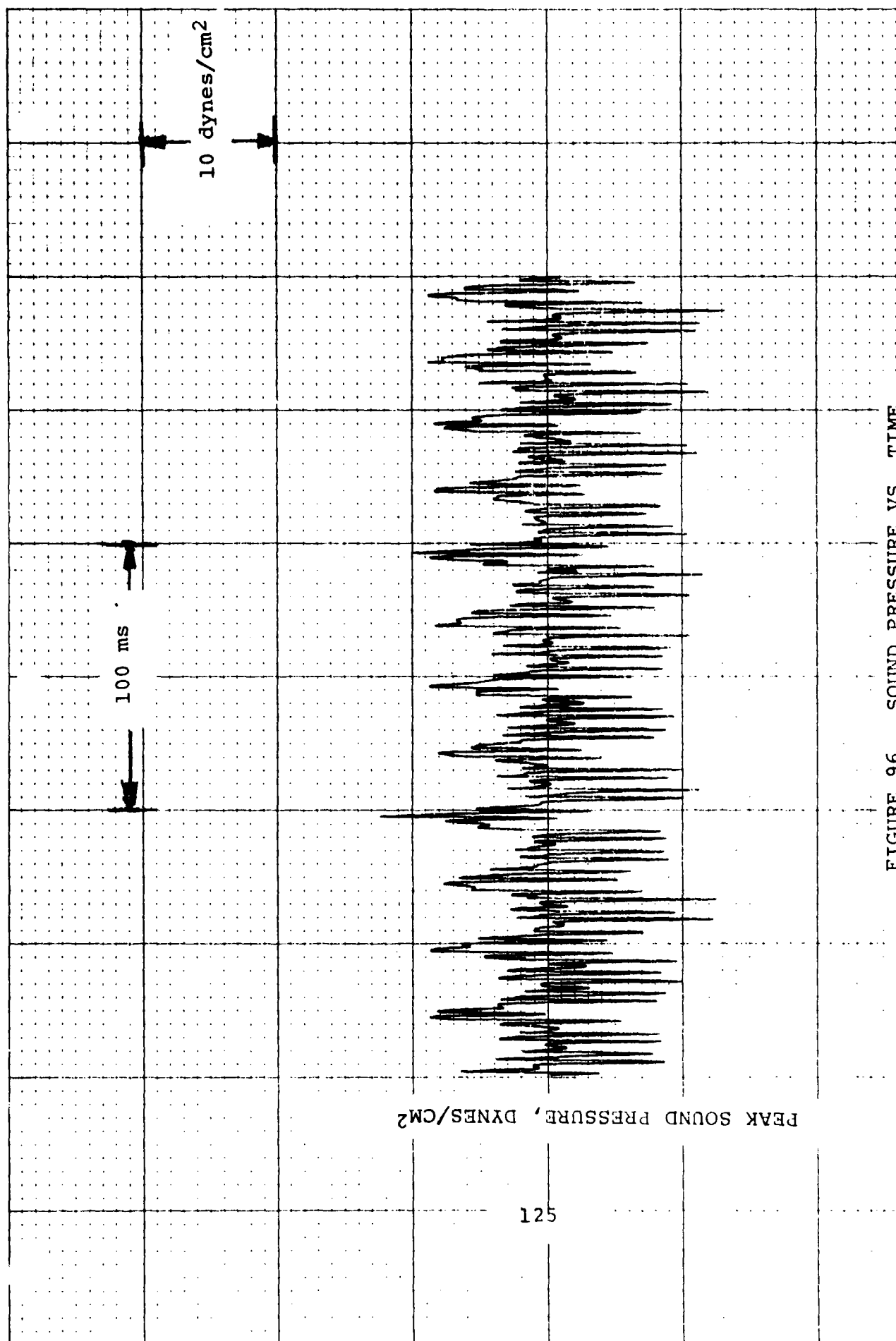


FIGURE 96. SOUND PRESSURE VS. TIME  
HUGHES 500C, LEVEL FLYOVER AT 150mph,  
500 FOOT ALTITUDE, WAVEFORM AT PNLM,  
RUN 109

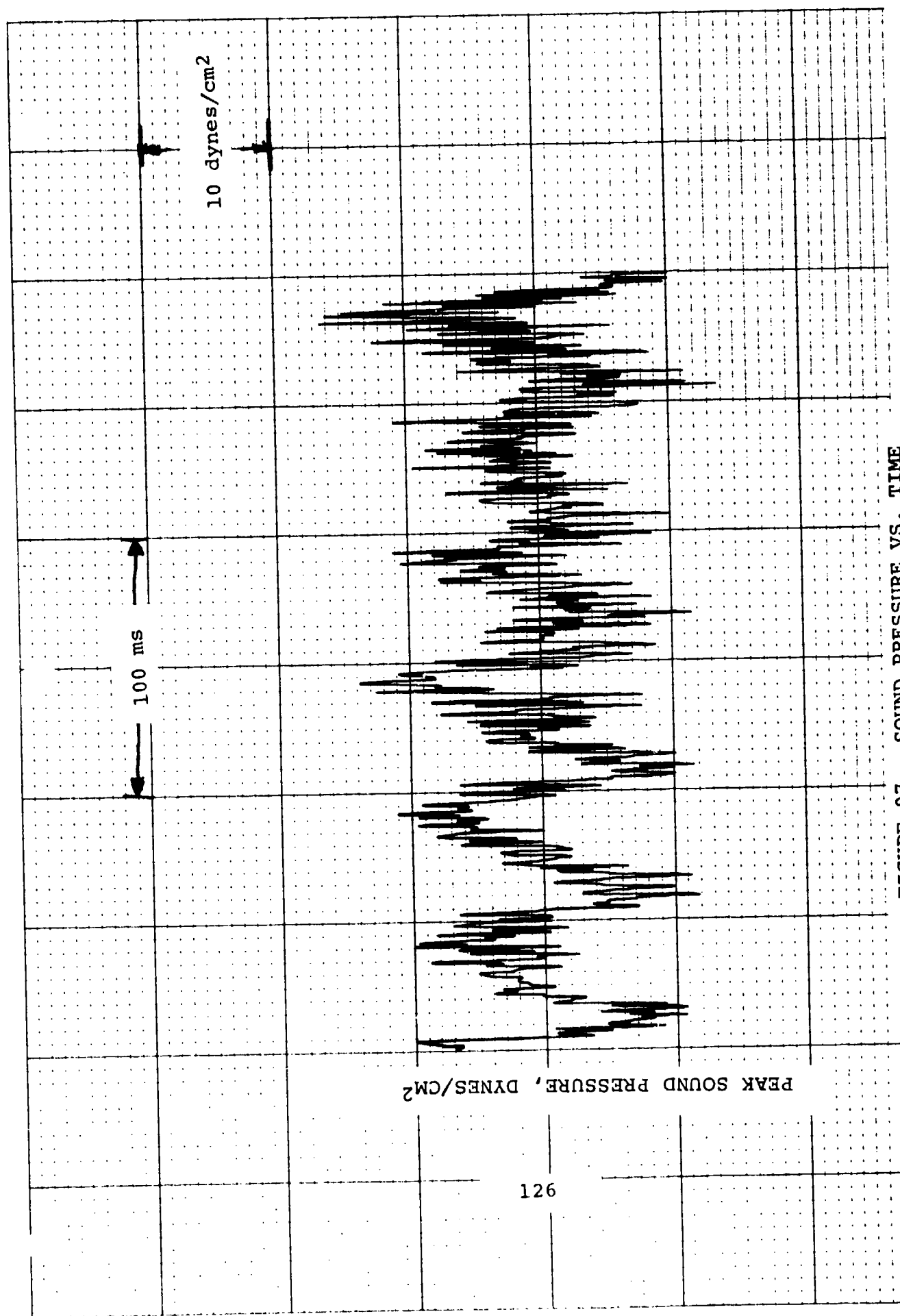
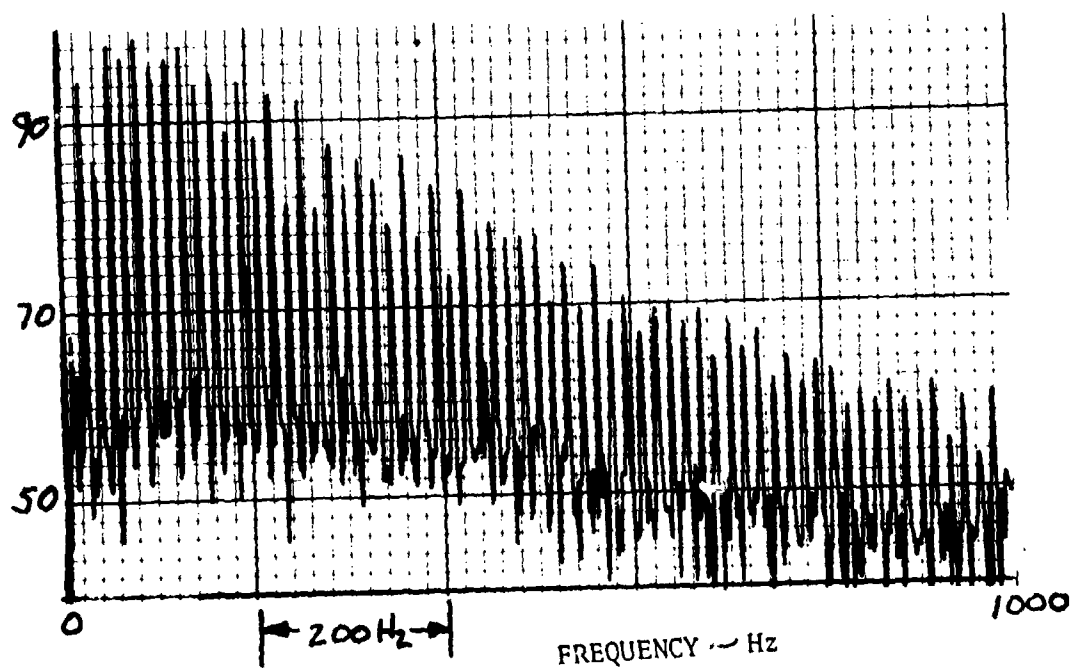


FIGURE 97. SOUND PRESSURE VS. TIME  
 SIKORSKY S-61 (SH-3B), LEVEL FLYOVER  
 AT 100 KNOTS, 500 FOOT ALTITUDE,  
 WAVEFORM AT PNLM, RUN 27.

SOUND PRESSURE LEVEL ~dB



FLYOVER LOCATION = 7 SEC BEFORE OVERHEAD

STATIC BLADE PASSAGE FREQUENCY

ONE ROTOR = 12.5 Hz (3 per rev)

TANDEM ROTORS = 25 Hz

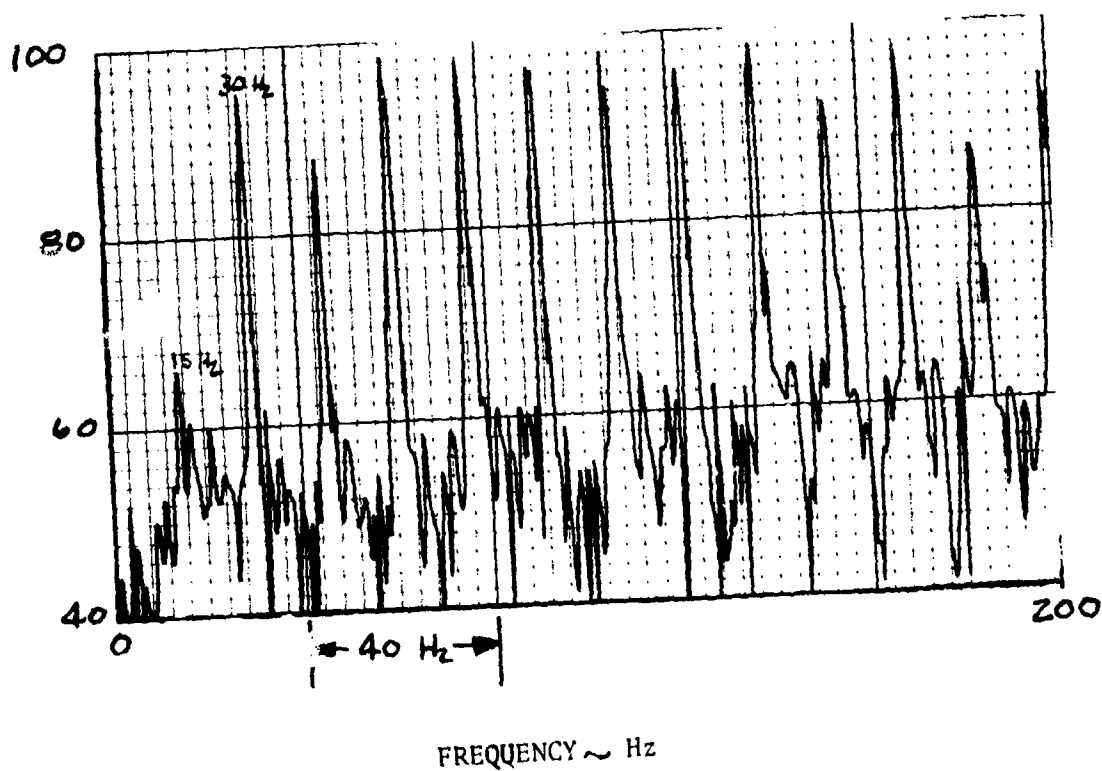
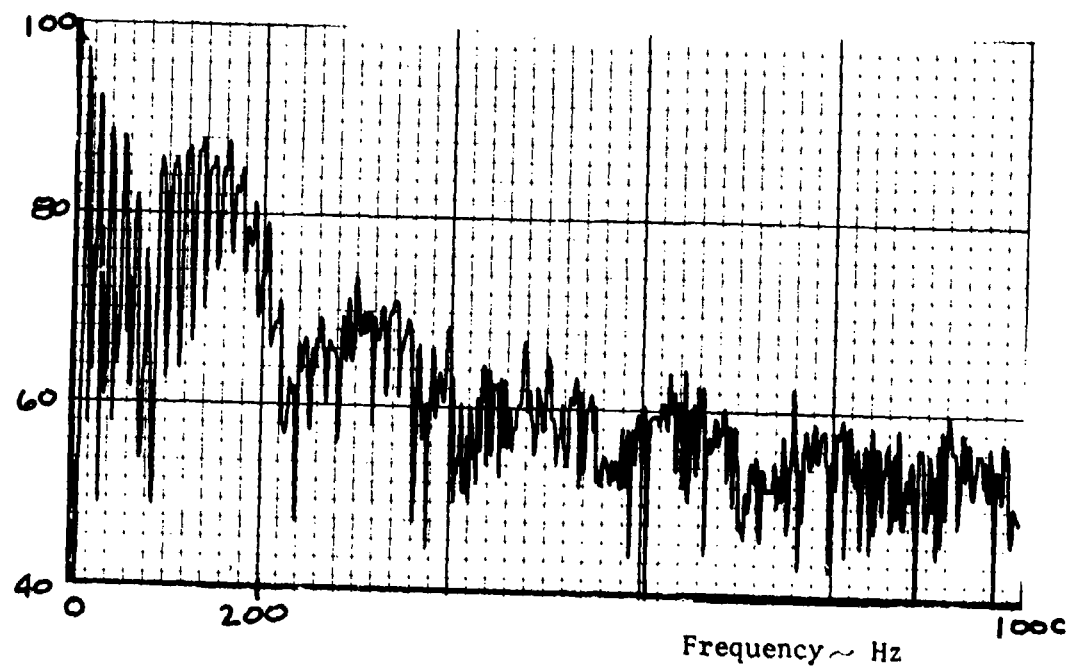


FIGURE 7 CH-47C, RUN 27, CENTERLINE MICROPHONE



SOUND PRESSURE LEVEL ~dB



FLYOVER LOCATION = OVERHEAD

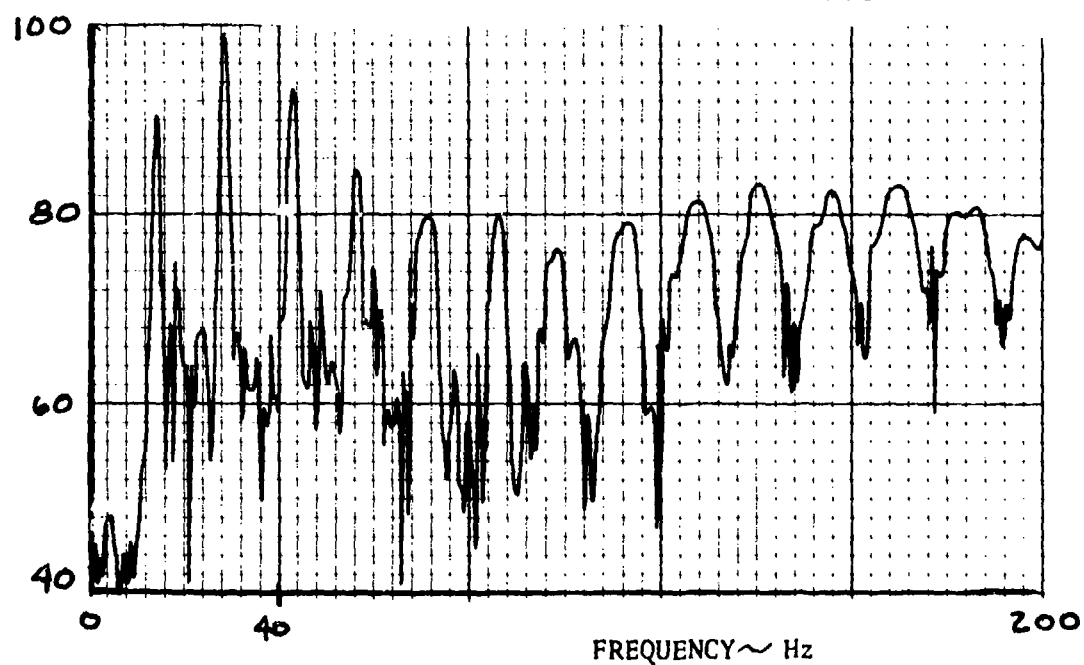
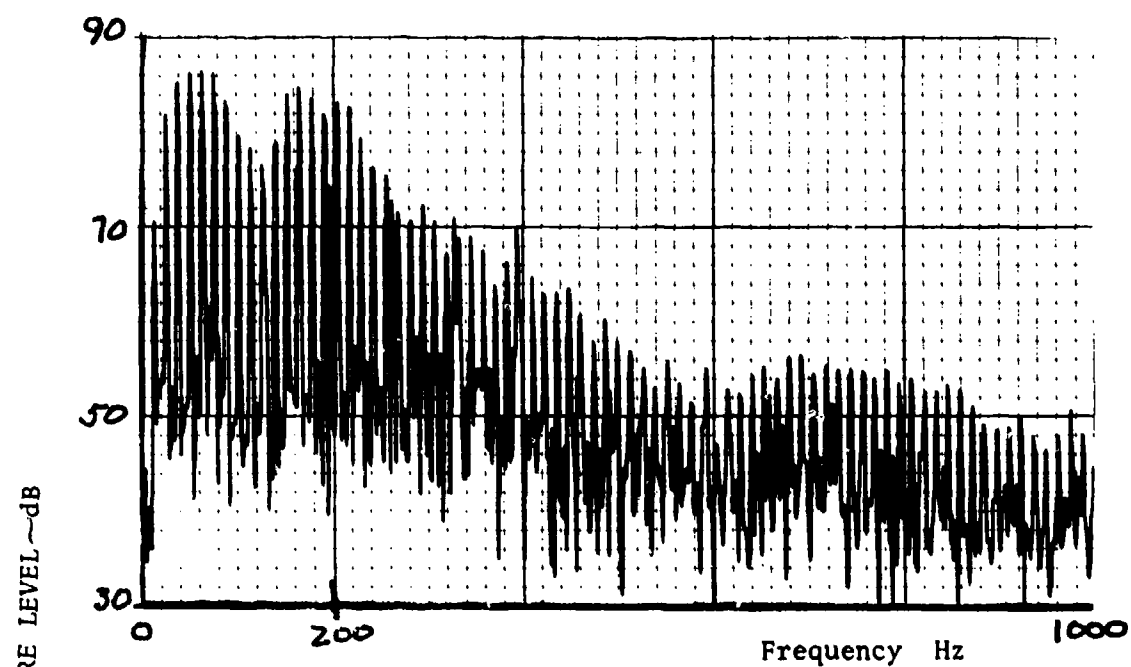


FIGURE 97 CH-47C, RUN 27, CENTERLINE MICROPHONE



STATIC BLADE PASSAGE FREQUENCIES,

MAIN ROTOR = 10.8 Hz

TAIL ROTOR = 55.4 Hz

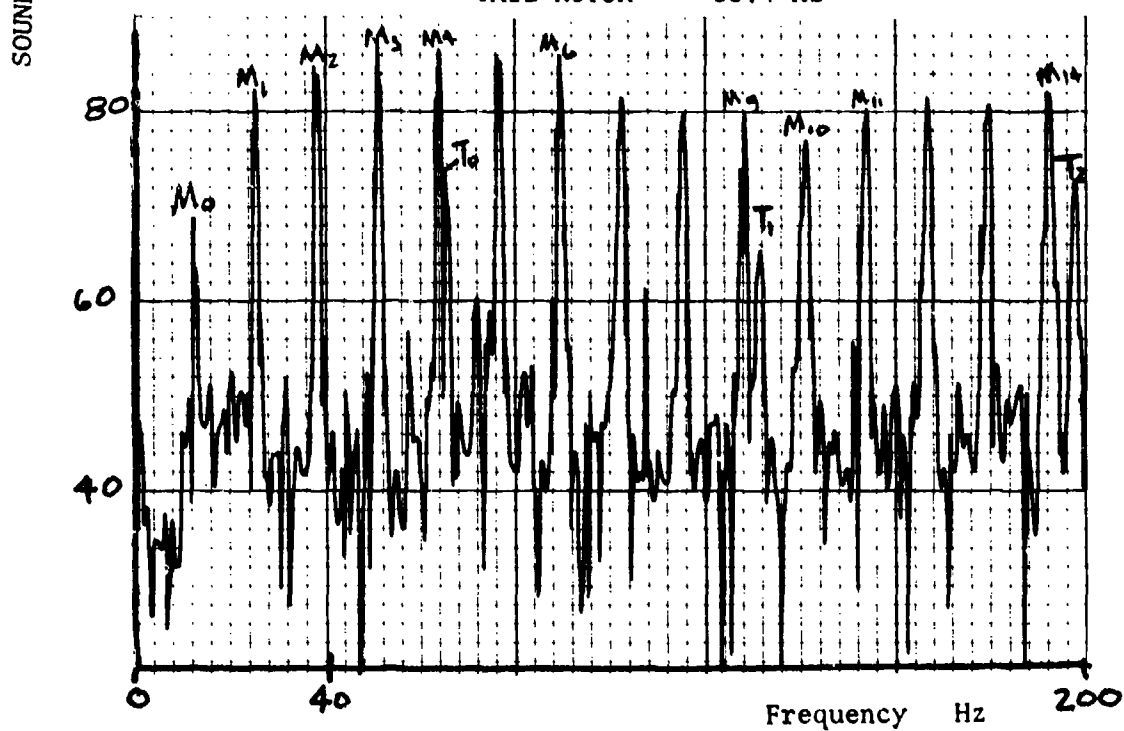
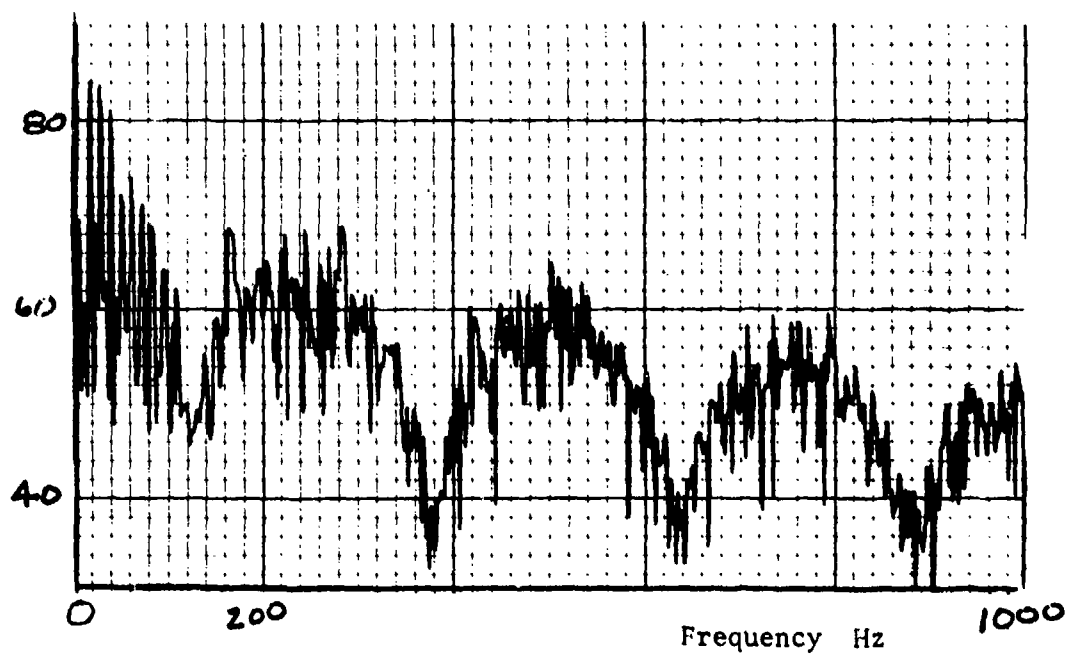


FIGURE 100 UHIN, RUN 37 WEST S.L. MICROPHONE  
FLYOVER LOCATION = 11 SEC BEFORE OVERHEAD

SOUND PRESSURE LEVEL ~dB



STATIC BLADE PASSAGE FREQUENCIES,

MAIN ROTOR = 10.8 Hz  
TAIL ROTOR = 55.4 Hz

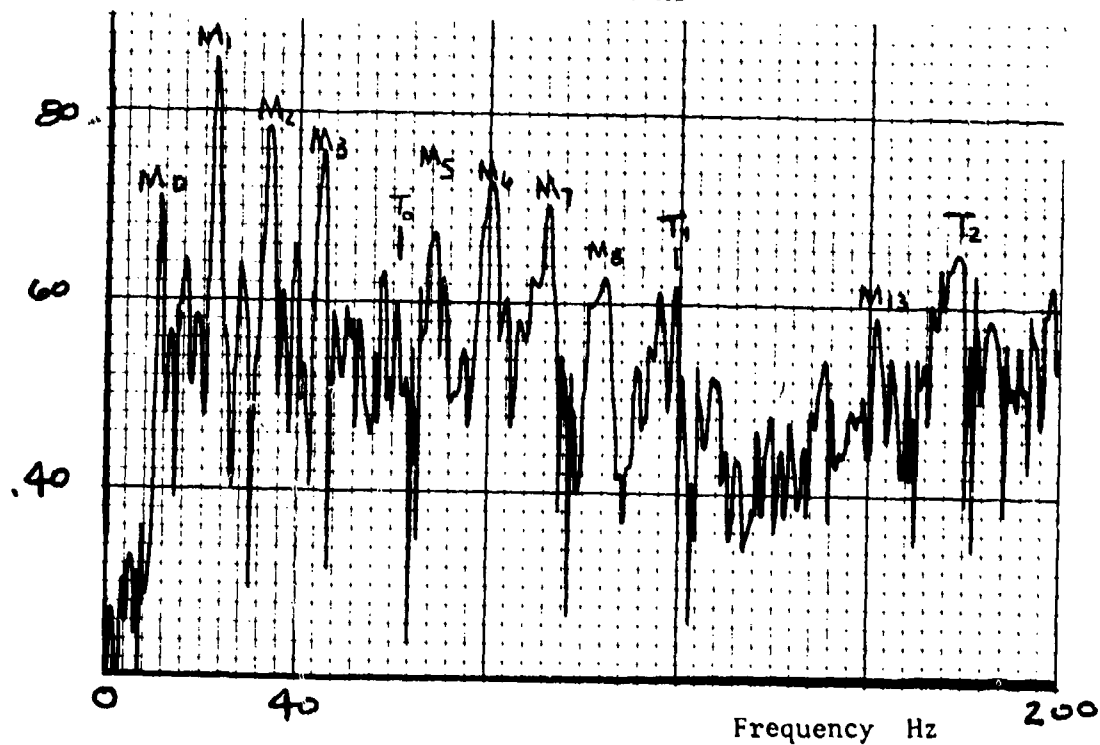
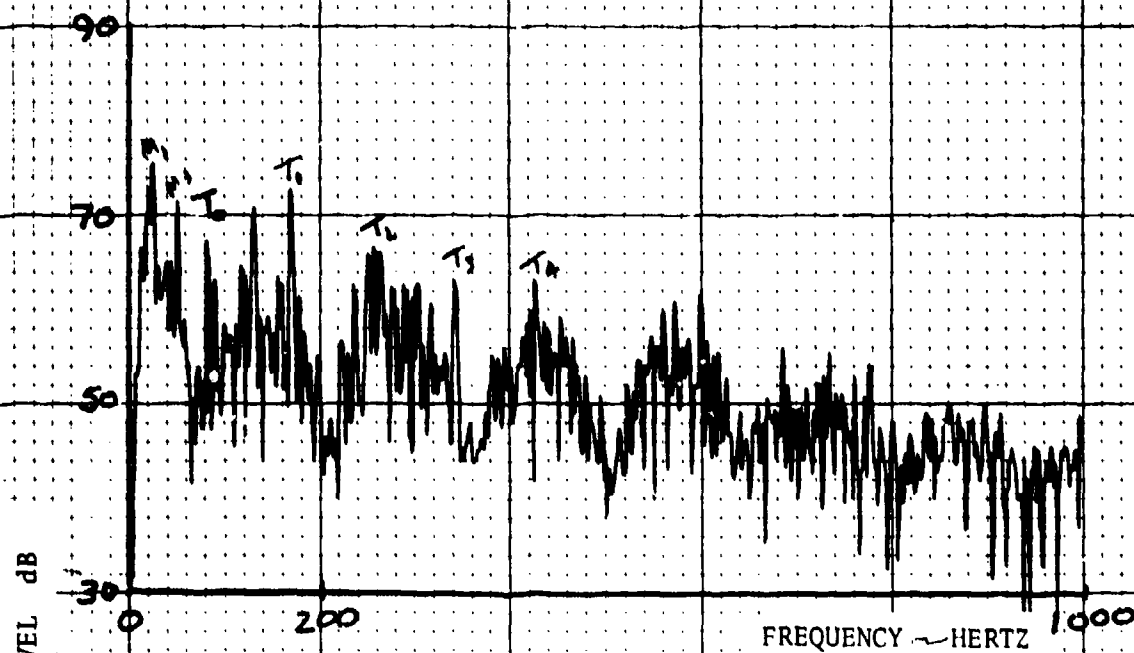


FIGURE 101 UHIN, RUN 37 WEST S.L. MICROPHONE  
FLYOVER LOCATION = OVERHEAD



FLYOVER LOCATION = 1 SEC. BEFORE OVERHEAD

STATIC BLADE PASSAGE FREQUENCY

MAIN ROTOR = 13.1 Hz

TAIL ROTOR = 85.0 Hz

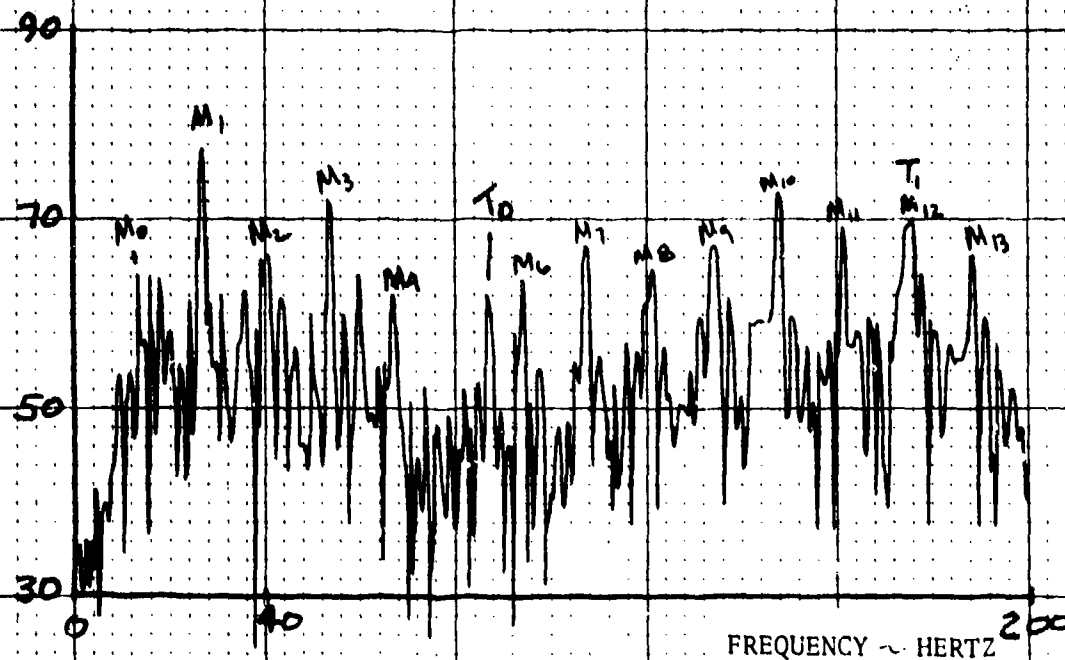
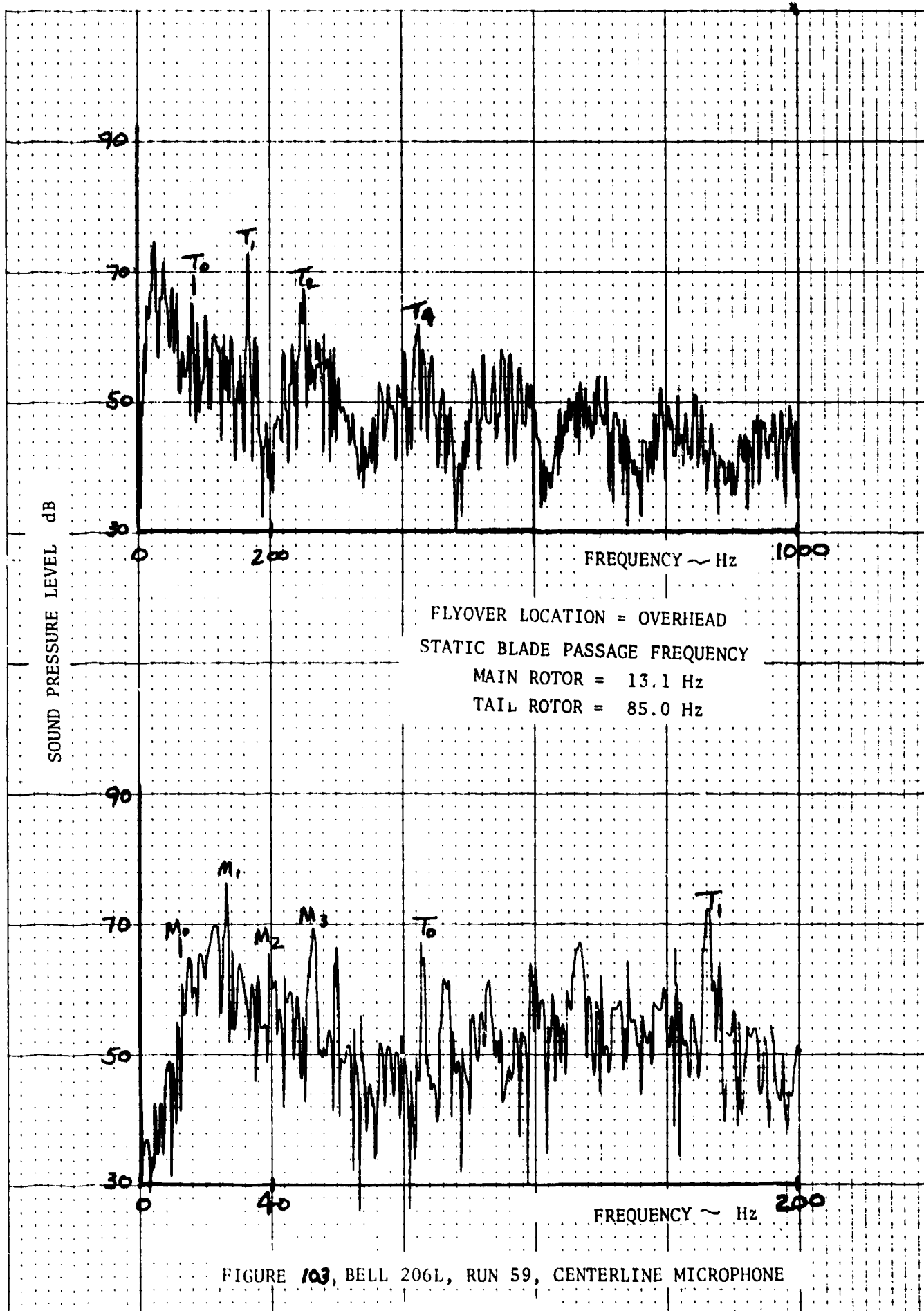
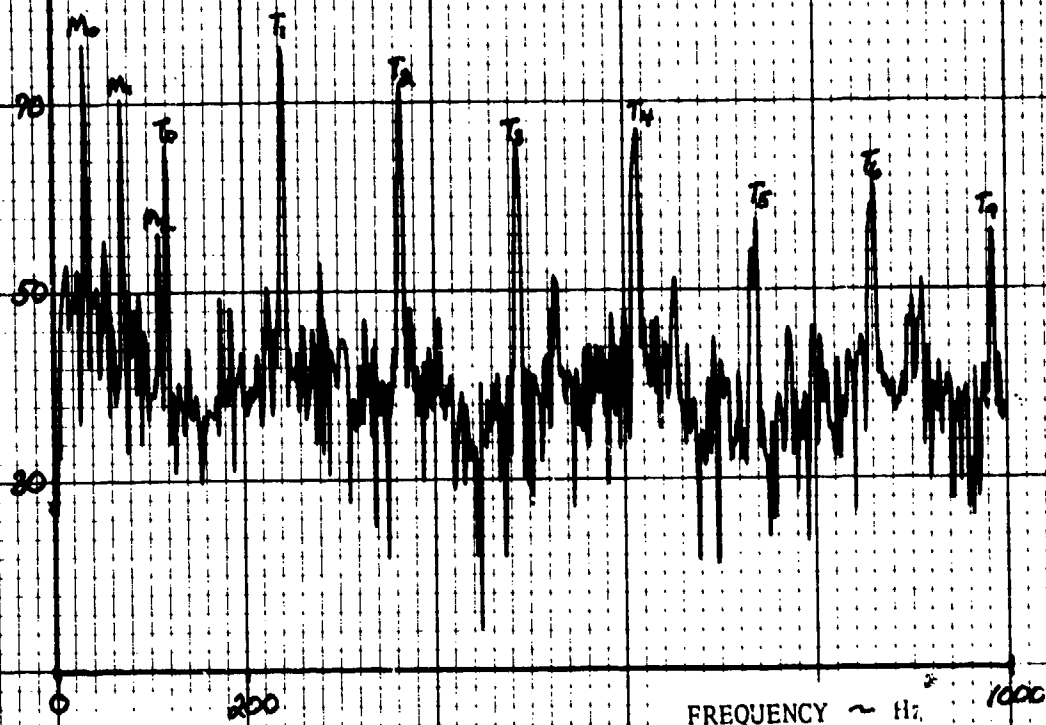


FIGURE 102, BELL 206L, RUN 59, CENTERLINE MICROPHONE



SOUND PRESSURE LEVEL ~ dB



FLYOVER LOCATION = 8 SEC BEFORE OVERHEAD

STATIC BLADE PASSAGE FREQUENCY

MAIN ROTOR = 32.3 Hz

TAIL ROTOR = 103.7 Hz

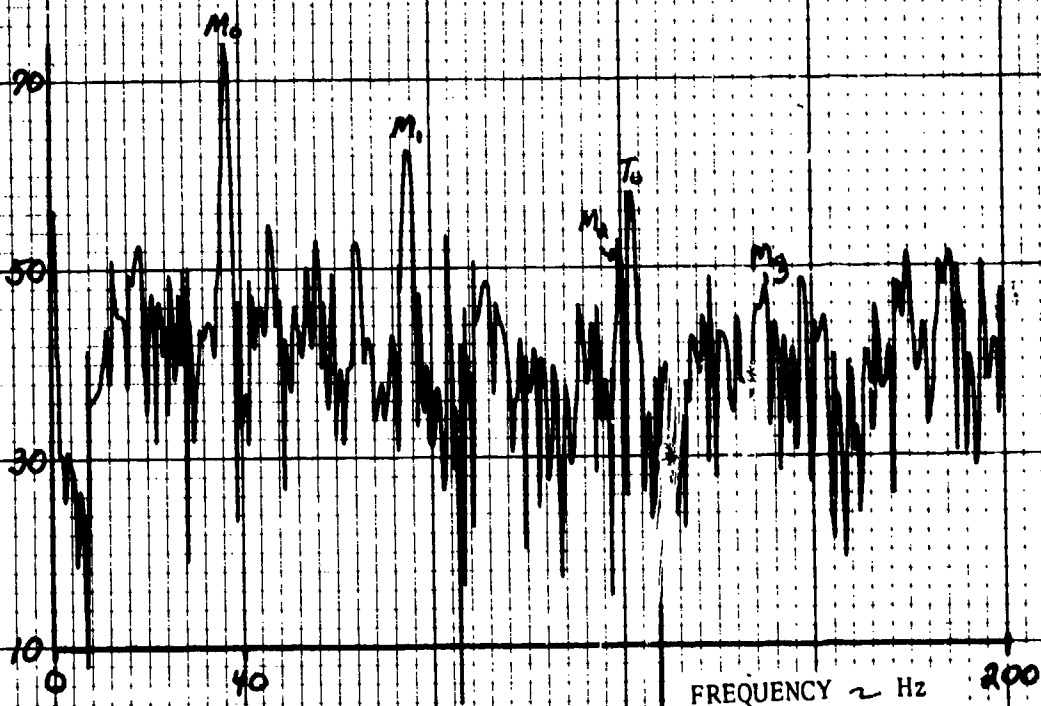
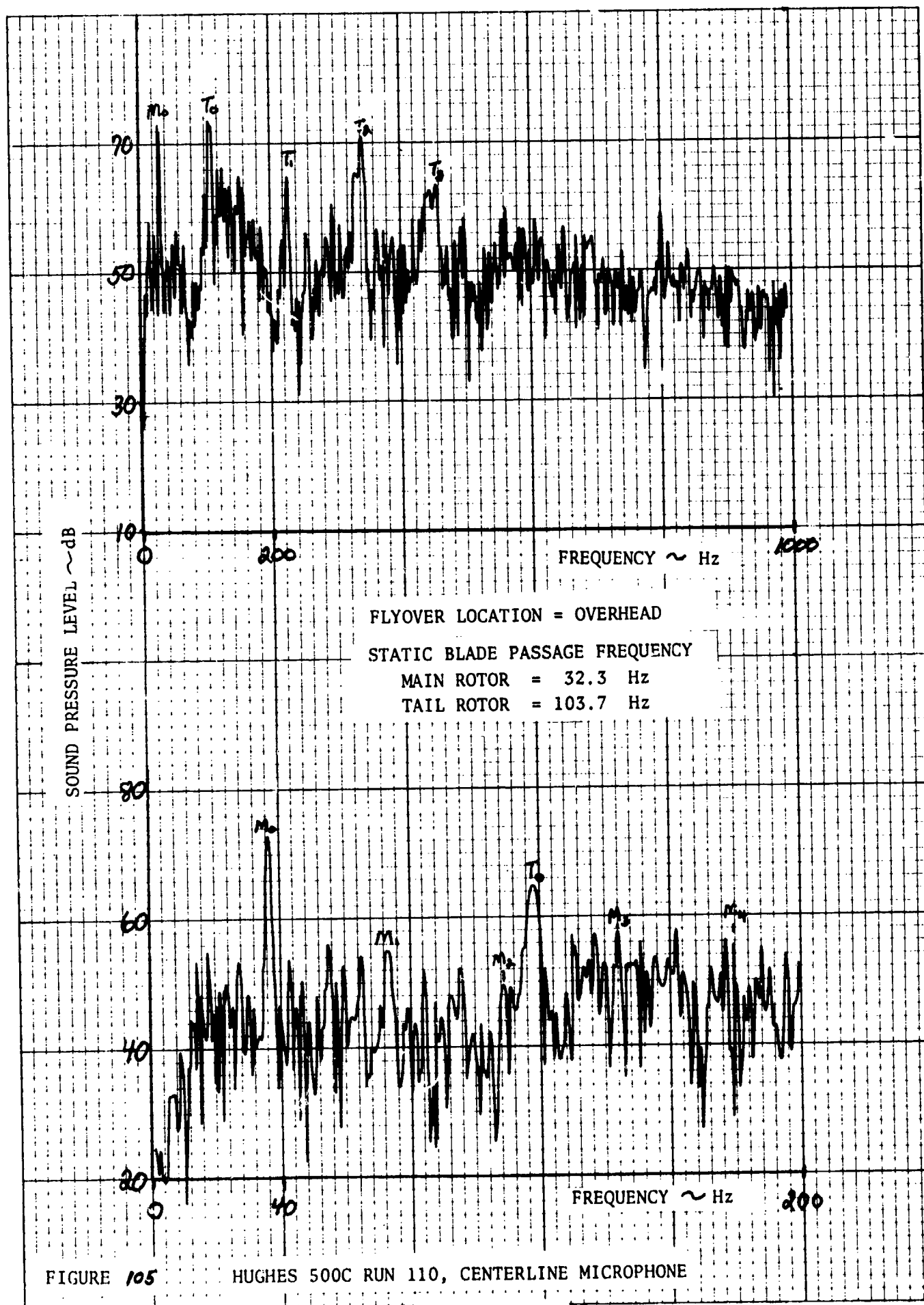
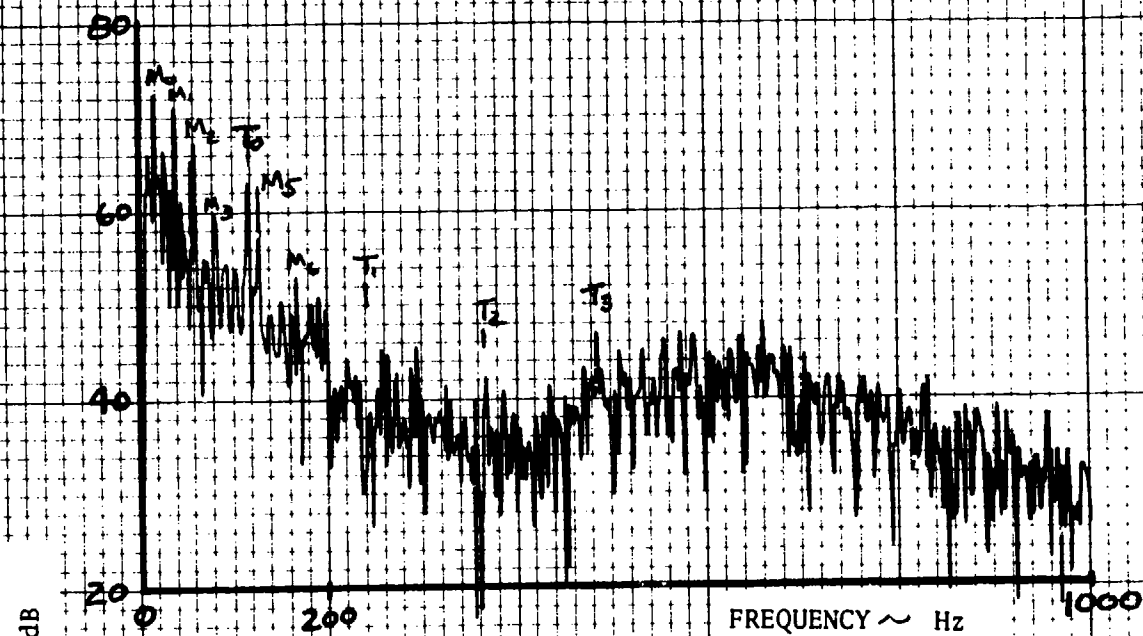


FIGURE 104

HUGHES 500C RUN 110, CENTERLINE MICROPHONE





FLYOVER LOCATION = 6sec. BEFORE OVERHEAD

STATIC BLADE PASSAGE FREQUENCY

MAIN ROTOR = 17. Hz

TAIL ROTOR = 10.4 Hz

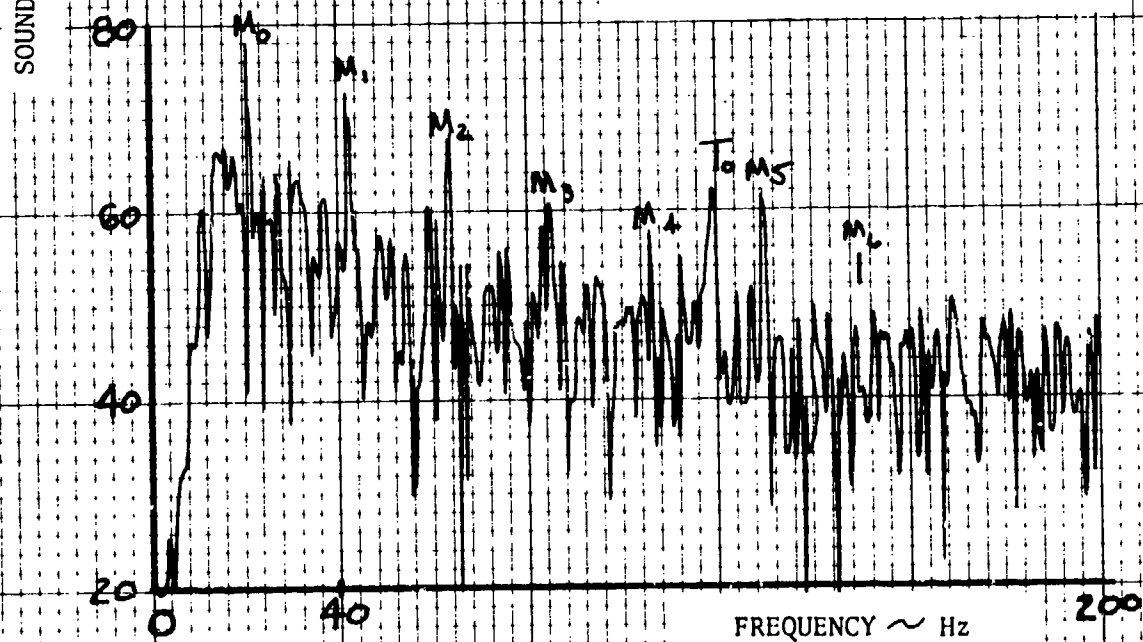
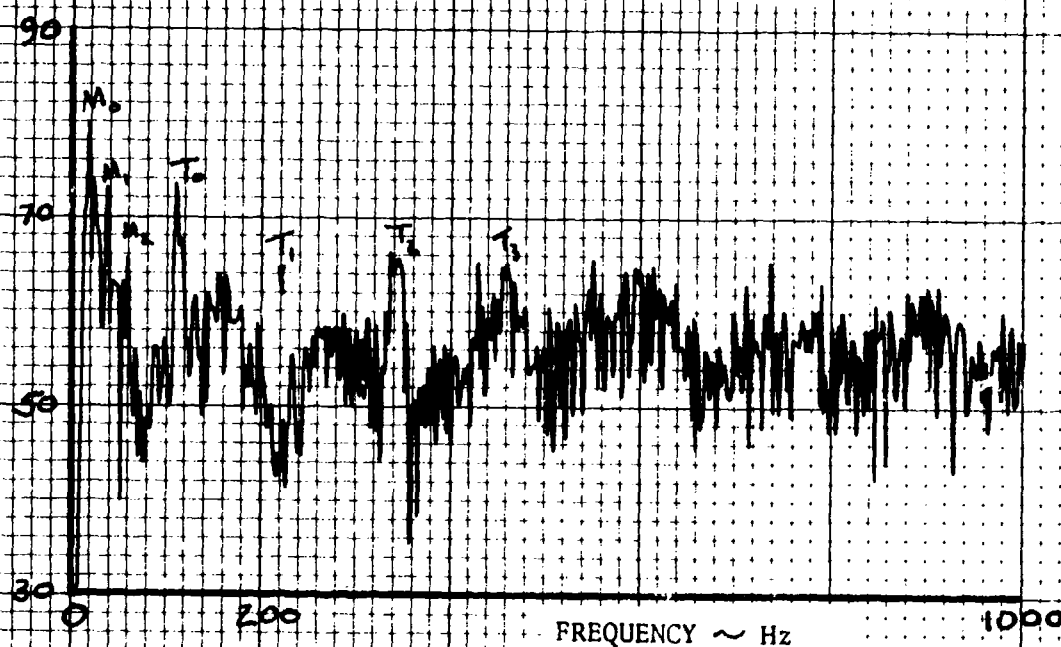


FIGURE 106, S-61 (SH-3), RUN 32, CENTERLINE MICROPHONE



SOUND PRESSURE LEVEL ~ dB



FLYOVER LOCATION = OVERHEAD

STATIC BLADE PASSAGE FREQUENCY

MAIN ROTOR = 17. Hz  
TAIL ROTOR = 10.4 Hz

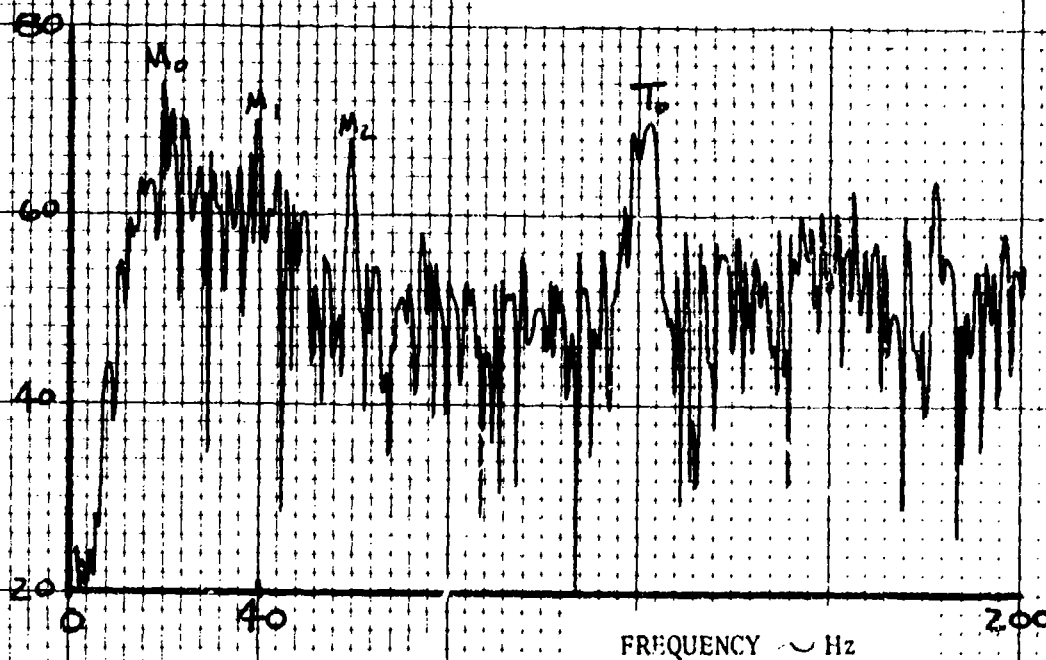


FIGURE 107 S-61 (SH-3), RUN 32, CENTERLINE MICROPHONE

but when alongside and above the microphone the tail rotor begins to dominate at frequencies above 100 Hz.

Figures 102 and 103, Bell 206L, are only one second apart in fly-over position but illustrate the relative level of main and tail rotor noise during a time near the overhead. On Figure 102, with mild subjective slap just before overhead passage, the main rotor harmonics dominate. During overhead passage, Figure 103, the spectra is dominated above 50 Hz by tail rotor harmonics. The 500C, Figures 104 and 105, illustrates a spectra dominated by the tail rotor although the first few harmonics of the main rotor are visible and more noticeable as the helicopter is approaching the microphones. The S-61 Figures 106 and 107, shows the relative importance of main and tail rotor noise. The tail rotor dominates the spectra in the audible range above 50-100 Hz. Although the peak sound pressure levels at the main rotor fundamental and first few harmonics are above the tail rotor fundamental, the subjective response to very low frequencies below about 50-100 Hz is minimal and therefore, in the audible range of interest, the tail rotor controls the subjectively weighted sound level. During main rotor blade slap, such as Figures 98 or 100, the harmonic structure from the main rotor blade passage extends to relative high frequencies well into the audible and subjectively important mid-frequency range.

### 7.3 Impulsive Noise Corrections

The impulsive noise data presented in this section was prepared by Bolt, Beranek and Newman, Inc. (BBN), under FAA Contract W1-77-3683-1. The data was summarized from BBN Report No. 3425, Reference 1, prepared under this contract. Three methods of blade slap correction are presented, a British National Physical Laboratory method, a French method and a peak to rms method. The "blade slap" correction was applied to the flyover time history at half-second intervals for all methods. The British and French methods were proposed before and recommended for evaluation by ISO Working Group ISO/TC43/SC-1/WG2 and ICAO/CAN WG-D. The three methods are described below:

National Physical Laboratory (NPL) -- The noise signal is A-weighted, then digitized at a sampling rate of 5 KHz. Each one-half second time interval is further subdivided into n periods, each of duration  $\tau$ . A quantity  $f(j)$  is computed for each of the n periods.

$$f(j) = \frac{1}{M} \sum_{i=1}^M V_i^2$$

Note:  $f(j)$  = very fast meter response

M is the number of samples in the time  $\tau$ . Since, for the BBN analysis,  $\tau = 10$  milliseconds, there are 50 samples of the sound pressure,  $V_i$ , in each period. The quantity  $f(j)$  then gives a "very fast" meter response. The  $f(j)$ 's in each one-half second time interval were averaged to give a "slow" meter response.

$$s = \frac{1}{n} \sum_{j=1}^n f(j) \quad \text{note: } s = \text{"slow" meter response}$$

Here  $n$  is equal to 50 (.5 sec/.010 sec). An impulsiveness factor,  $I$ , was obtained for the one-half second interval.

$$I = \sum_{j=1}^n \left[ \frac{f(j) - s}{s} \right]^2$$

An impulse correction,  $\Delta I$ , for each one-half second of the flyover time history is obtained by the formula below.

$$\Delta I = K (X - X_0), \text{ where } X = 10 \log I, X_0 \text{ is } 10 \log I \text{ for}$$

A-weighted white noise,  $K$  is approximately 0.6 and  $\Delta I$  is limited to a maximum of 6 dB and is zero for negative values. Important variables in the analysis are the sampling rate  $M$  and the time duration,  $\tau$ , of the "very fast" level.

France -- The noise signal is passed through a 2000 Hz lowpass filter, without a detector, then digitized at a sampling rate of 5000 Hz. A quantity,  $CI$ , is computed from the  $N$  samples of  $V_i$  in 0.5s as;

$$CI = \frac{\frac{1}{N} \sum_{i=1}^N V_i^4}{\left[ \frac{1}{N} \sum_{i=1}^N V_i^2 \right]^2} \quad \text{where } V_i \text{ is the sound pressure level.}$$

This quantity is used to derive a correction factor,  $\Delta F$ , from the relation

$$\Delta F = 1.14 (CI - 3)$$

It is proposed that  $\Delta F$  be added to the PNLT values, in each 0.5s interval, before computing EPNL.

USA (Peak minus rms) -- It has been suggested that, if the purpose in the physical analysis is to determine a quantity related to the crest factor of the signal, a simple direct way of accomplishing this is to measure the peak A-weighted sound pressure level, in each 0.5s interval, as compared to the A-weighted rms level in the same time interval. The difference between the two levels is the A-weighted average crest factor in each 0.5s interval. Recognizing that this value is approximately 12 dB for A-weighted white noise, and typically 12-15 dB (Section 7.1) for conventional aircraft and helicopters without blade slap, values above this indicate the degree of impulsiveness of discrete impulses superposed on general noise backgrounds. The use of this measure should be explored in assessing psychoacoustical results.

The equipment used by BBN to perform the analysis is described below:

NFL -- The tape recorded signal was A-weighted, then digitized with a 12 bit A/D converter at a sampling rate of 5000 Hz. The calculations were performed with a PDP-8 computer and printed out at each 0.5s interval.

France -- The tape recorded signal was passed through a 2000 Hz low pass filter, then digitized as in 2.2.4. The value of CI was computed by the PDP-8 and printed out for each 0.5s interval, along with the value of  $\Delta F$  computed from  $\Delta = 1.14 (CI-3)$ .

Peak-To-rms -- The tape recorded signal was passed to two parallel systems, one being the real time analyzer and the other a 2209 SLM, using the "peak hold" feature of the 2209. The dc output of the 2209 was passed to the A/D converter of the PDP-8. At the termination of each 0.5s interval, the peak A-weighted sound level of the 2209 was sampled by the PDP-8, then reset to zero. The readout and reset took place during the 30 ms interval during which the real time analyzer output was sampled by the PDP-8.

The rms value of A-weighted sound level was computed by the PDP-8, for each 0.5s interval, from the one-third octave band sound pressure levels generated by the real time analyzer with "slow" detection. The difference in peak and rms values of A-weighted sound level in each 0.5s time interval form the crest factor value for use in evaluation of psychoacoustical experiments.

The BBN Report (Reference 1) presented the following discussion of the results by the three methods under discussion. The "Fuller Data" refers to a subjective response experiment performed at the NPL and reported in ISO Working Group Papers ISO/TC43/SC1/WG2, November 1976 and February 1977.

NPL -- The method proposed does identify impulsive signals. Using a "fast" integration time of 10 ms, as proposed by ISO and as used in the BBN analyses, gives quite different results from those reported by NPL using 1 ms integration for "fast". The 10 ms data provide impulsive coefficients,  $I$ , approximately one order of magnitude lower than the 1 ms data, at least for the Fuller/NPL data for which a direct comparison is possible. The 10 ms data are not very sensitive for detecting relatively low peak to rms impulses, although the 1 ms data do seem to do a better job.

Problems of determining threshold values of this impulsiveness coefficient below which no "penalty" is imposed are very dependent on the choice of integration constants. For example, the NPL analysis using 1 ms integration time always yielded a positive value for  $I$  when the Fuller Data were analyzed. The BBN analysis (10 ms) gave a zero value for  $I$  for 10 dB peak-to-rms signals, with positive values only obtained for the 20 and 30 dB peak-to-rms signals.

French -- Most signals, including white noise, produced a value of C.I. around 3 unless distinct impulses were present. For the more impulsive signals higher values of CI were obtained, becoming larger with increase in crest factor. The numerical values of CI obtained in the NPL and BBN analyses of the Fuller data were quite close in all but one case, in which they differed by 30 percent.

Peak-to-rms A-Level -- This method is the easiest to implement and clearly identifies the crest factors (CF) for a signal. In examining this method further, however, some standard must be set for establishing the value below which no impulsiveness "penalty" is to be made. In the case of A-weighted white noise, we found the CF for 0.5s intervals of a 20s sample to be 12.1 decibels with a standard deviation of 0.50 decibels. Random noise with variously shaped spectra will yield different values. For example, the Fuller data for helicopter noise without impulses had a CF of 10.7 decibels, with many of the other real flyover

signals having comparable values. Clearly a better understanding of the effect of the spectral shape of helicopter noise on crest factor must be obtained, since the crest factor theoretically increases with decrease in band width of a gaussian noise signal.

The results of the BBN analysis are presented for each of the eight helicopters tested in Figures 108-115. The flight condition is a level flyover at 500 feet altitude at the velocity for best range. The British method is presented as the "Impulse Coefficient" defined as;

$$\Delta \text{ imp} = K (X - X_0), \text{ dB}$$

$$K \approx 0.6$$

$$X = 10 \log I \text{ (defined previously)}$$

$$X_0 = 10 \log I \text{ for A-weighted white noise}$$

$$\Delta = \text{limited from 0 to 6.0}$$

The French method is presented as:

$$\Delta F = 1.14 (CI-3)$$

The USA Peak-to-rms level is presented as the peak impulsive level minus 12 dB minus the slow A-weighted level. Twelve (12) dB is the approximate value for A-weighted white noise. The A-weighted time history with slow meter response is also shown for reference.

It is apparent from inspection of Figures 108-115 that none of the above three methods appears to be an entirely satisfactory descriptor for helicopter impulsive noise. All methods agree that the CH-47C UHIN, and 206L have impulsive noise characteristics of varying amounts. However, the methods cannot agree on either the magnitude nor time location of the impulses. The USA peak minus rms detector appears the most sensitive although some of the large perturbations at the beginning of the recorded time history appear somewhat suspicious (i.e., inspect the 300C, 500C, UHIN, S-61). Listening to playbacks of the recorded tapes did indeed indicate that "slap" noise did occur sporadically throughout the flyover time history for most helicopters, especially when the helicopter was well before and after the overhead passage. However, this noise was below the peak noise and, being of fairly brief duration, did not appear to appreciably affect the subjective annoyance.

Many of the spurious corrections associated with the peak minus rms method can be alleviated by changing the subtraction factor from the peak A-level of 12 dB associated with white noise to 14-15 dB associated with the noise from conventional jet transports (See Section 7.1). If this was done, impulsive corrections with the peak to rms method would only be applied, within the 10 dB down points, to the CH-47C, UHIN, and 206L. However, it should be emphasized that the 206L was tested on a windy day (15-20 Kt) and its correction could be caused in part by the quartering tailwind and, perhaps, course corrections necessitated by the wind.

The important problem, not addressed here, is the relationship of numerical measures of blade slap to subjective annoyance. Considering the lack of consistency among proposed measures of impulsive noise to define blade slap for real helicopter flyovers this will be a formidable task.

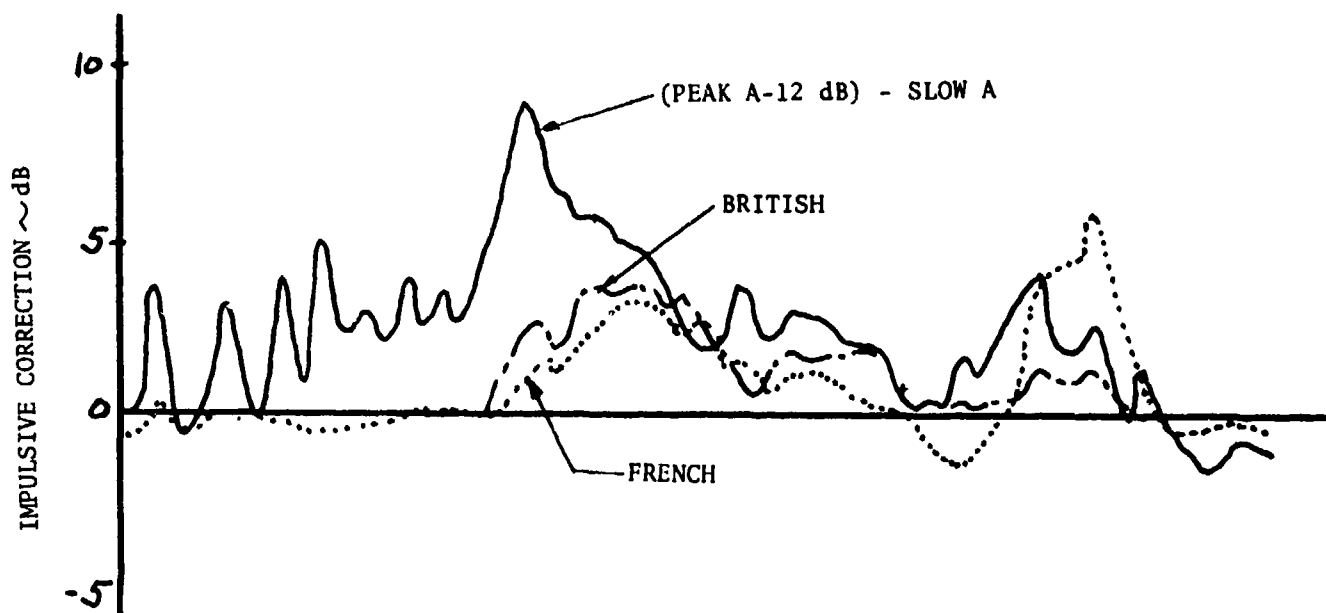
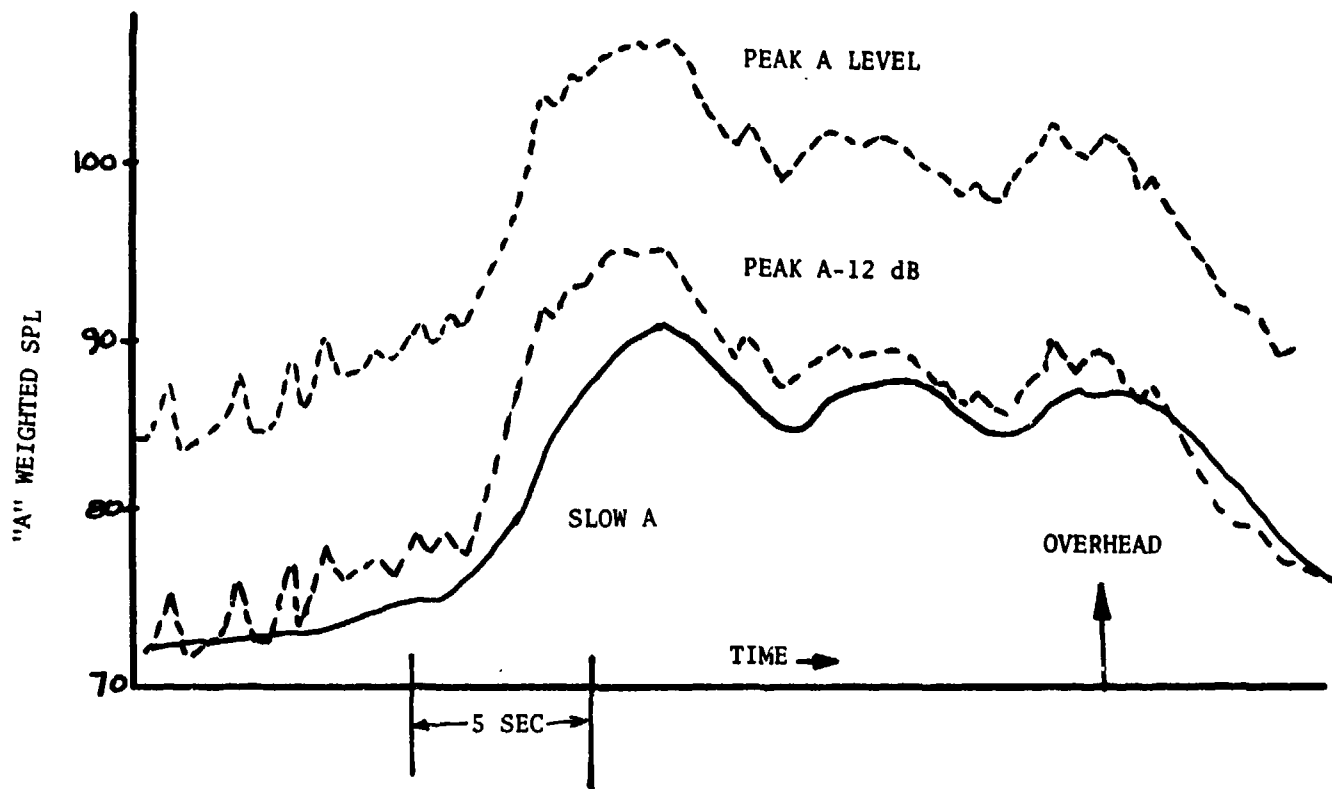


FIGURE 108 IMPULSIVE CORRECTIONS FOR CH-47C, 141KT



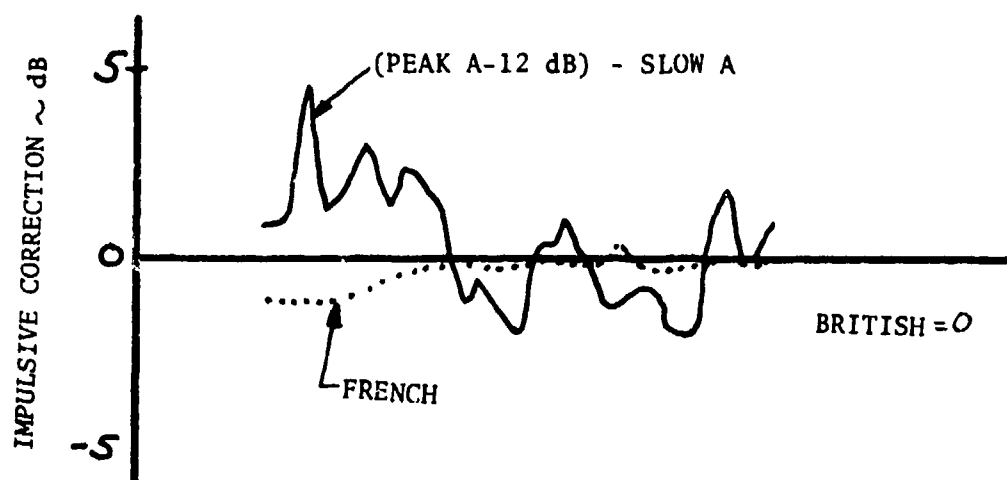
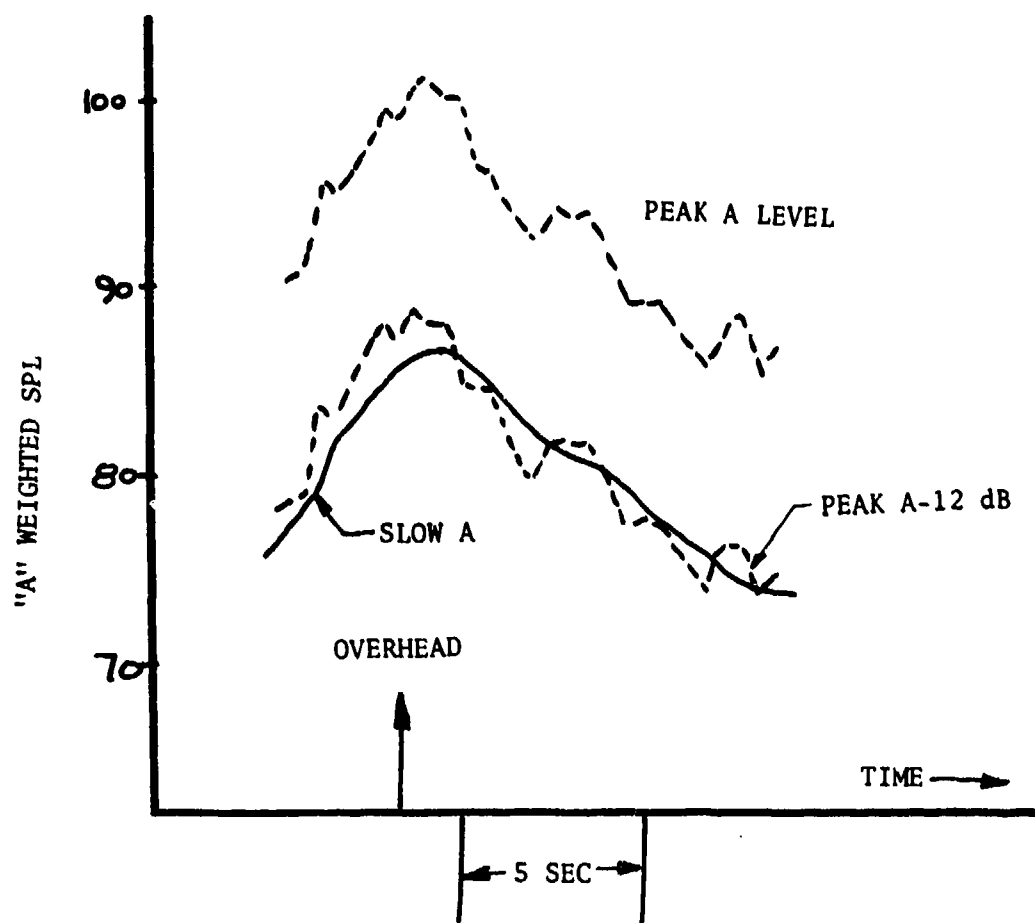


FIGURE 109 IMPULSIVE CORRECTIONS FOR S-64, 95KT

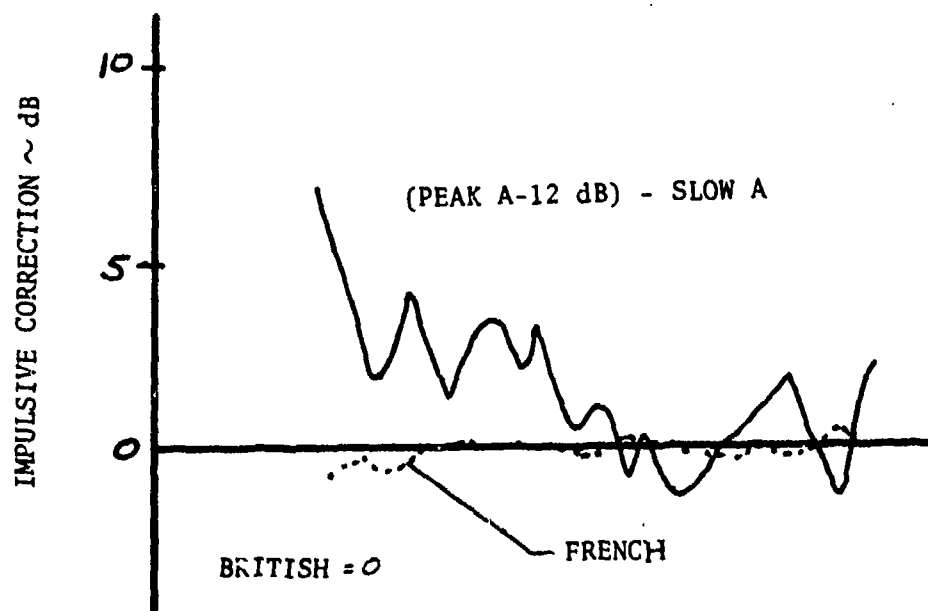
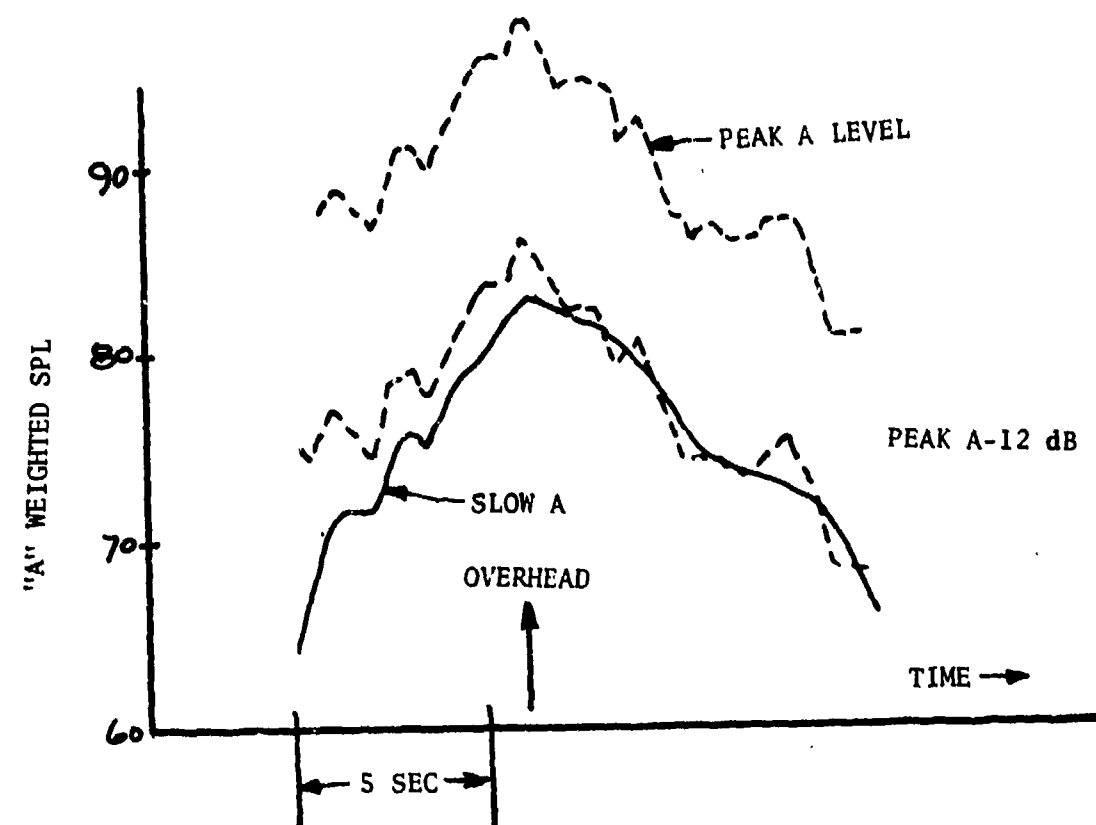


FIGURE 110 IMPULSIVE CORRECTIONS FOR S-61, 115KT

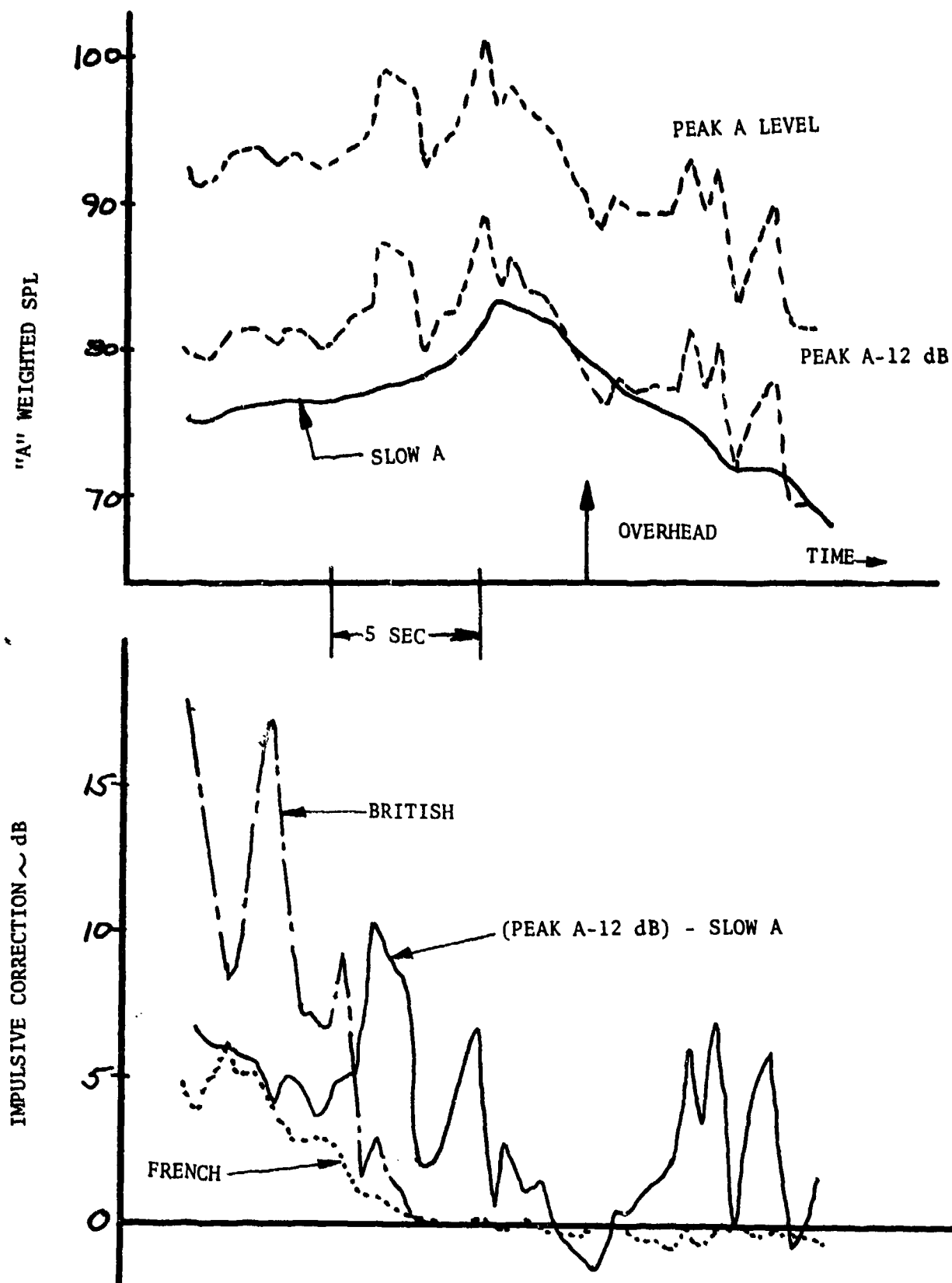


FIGURE 111 IMPULSIVE CORRECTIONS FOR UHIN, 110KT

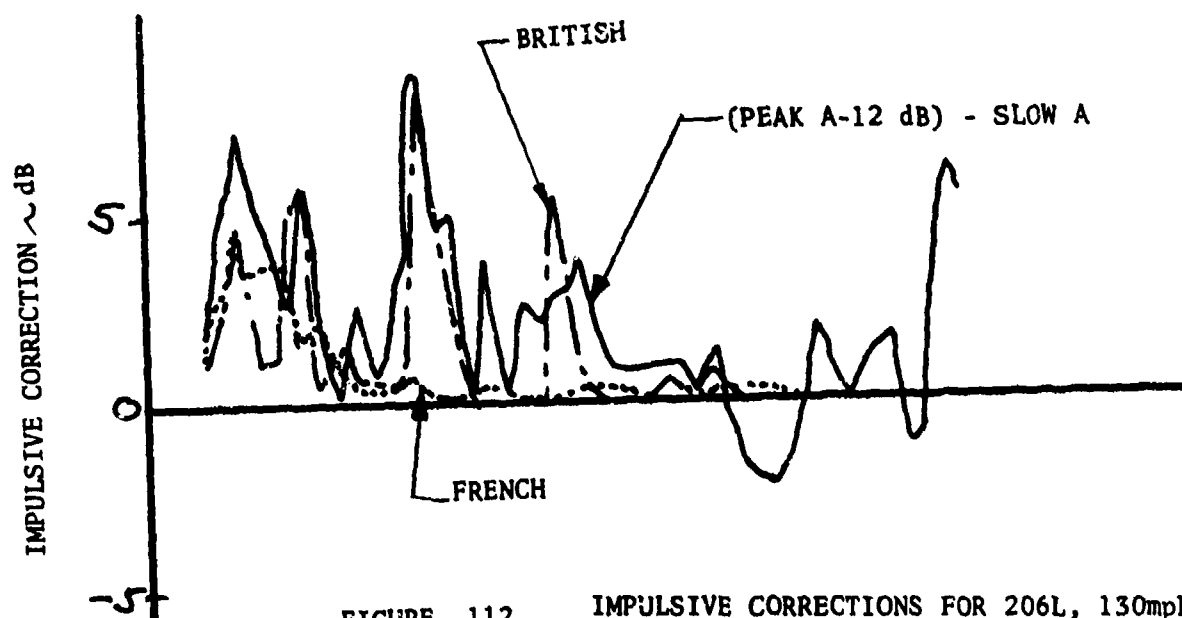
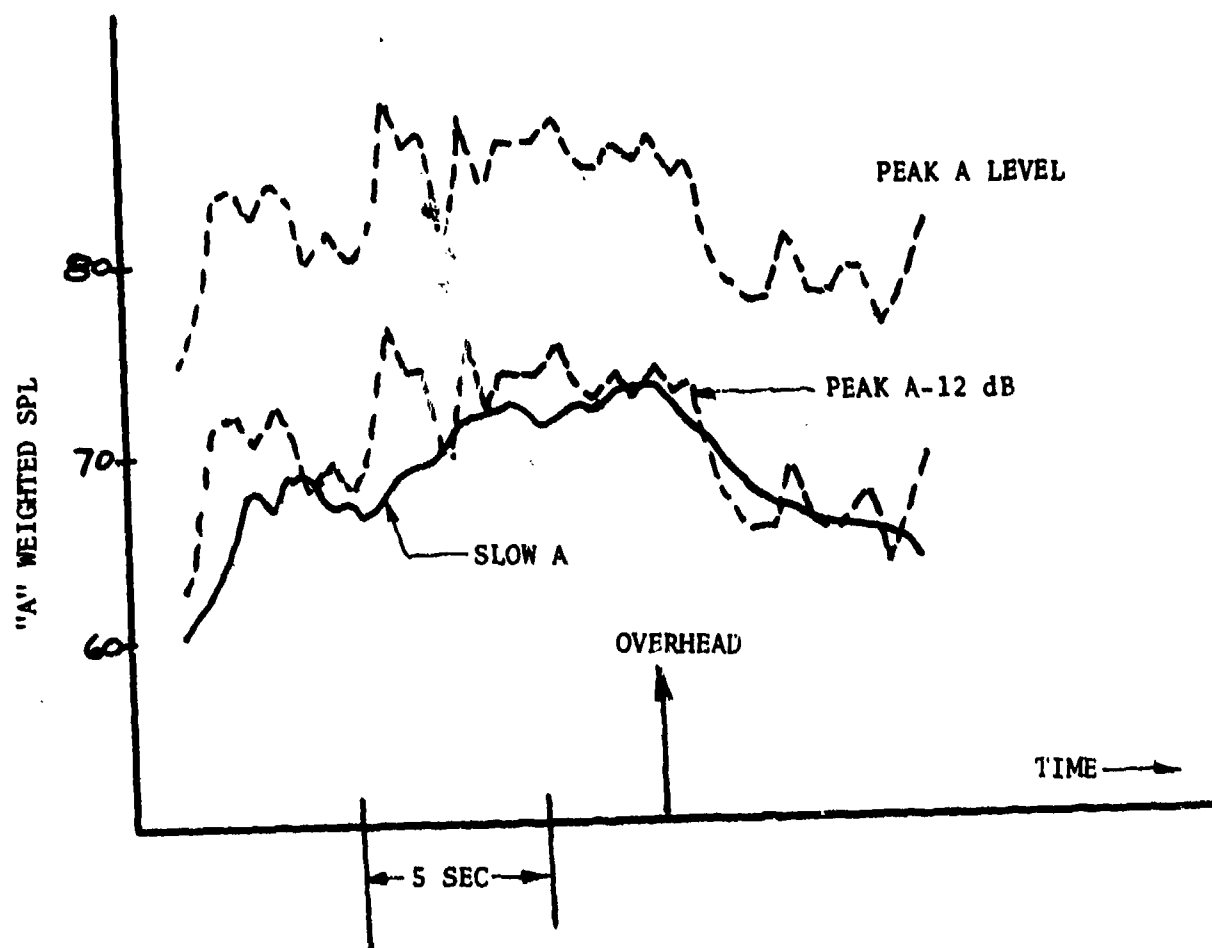


FIGURE 112 IMPULSIVE CORRECTIONS FOR 206L, 130mph

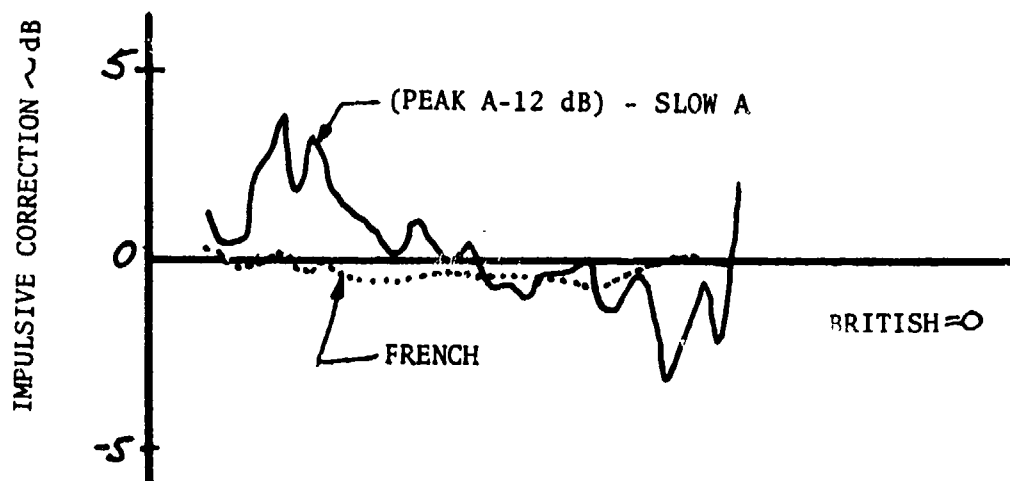
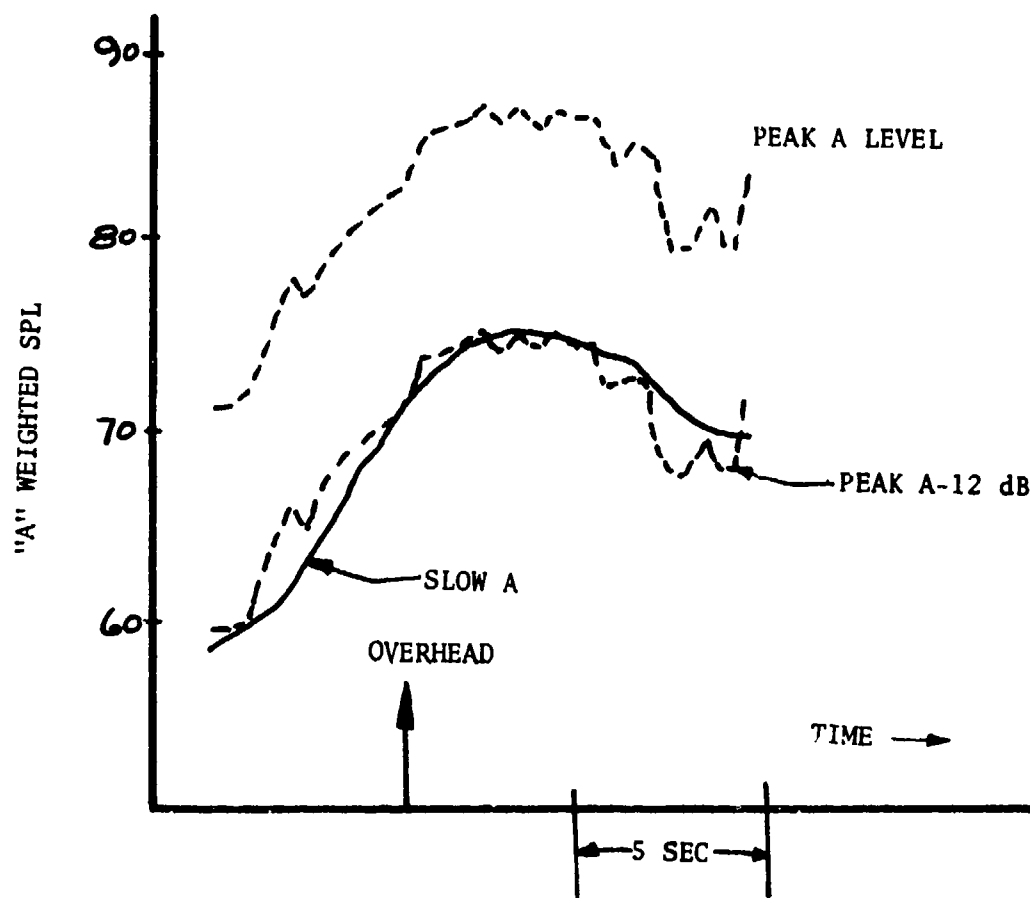


FIGURE 113 IMPULSIVE CORRECTIONS FOR BELL-47G, 75mph

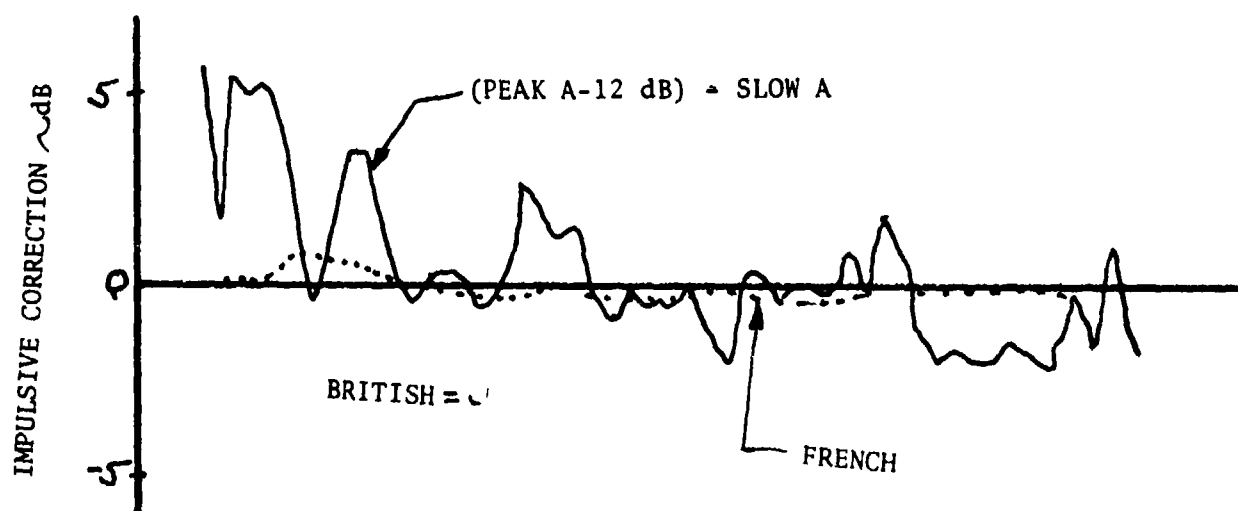
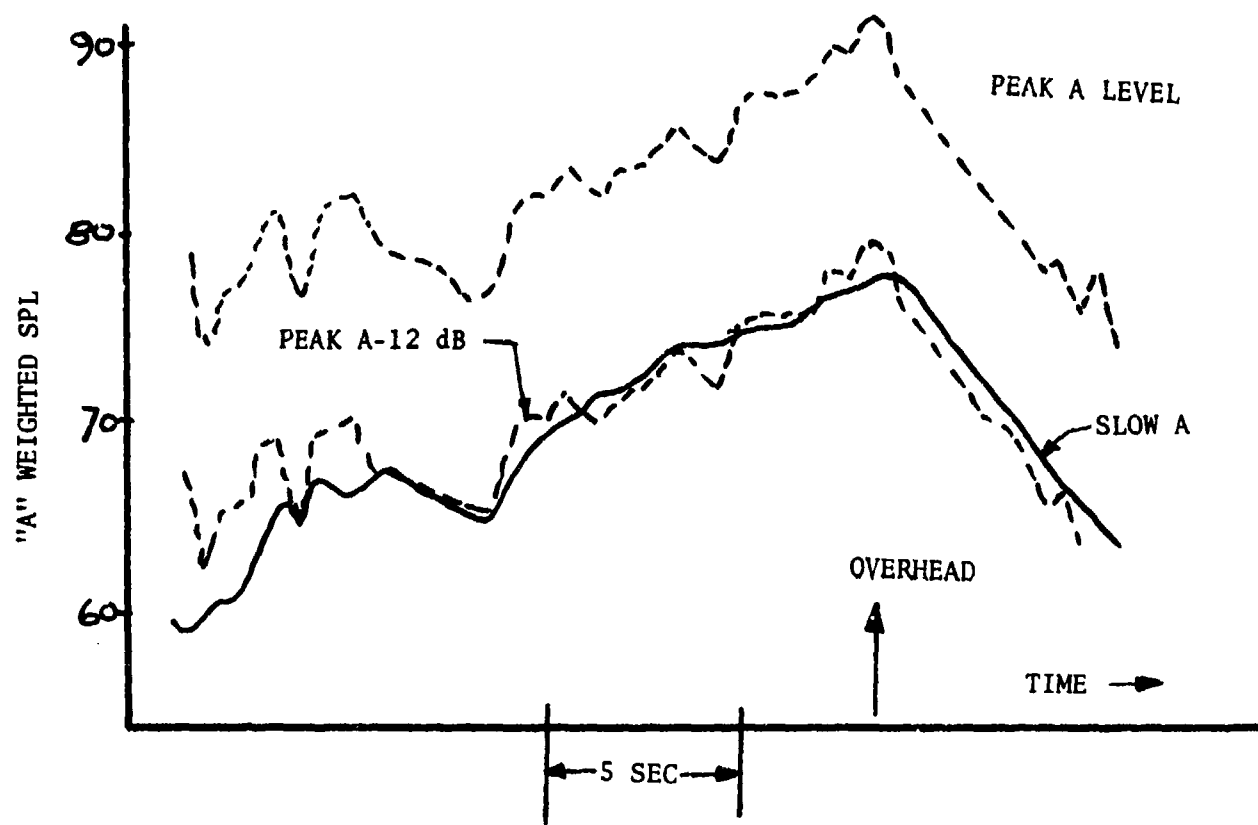


FIGURE 114

IMPULSIVE CORRECTIONS FOR 500C, 130mph

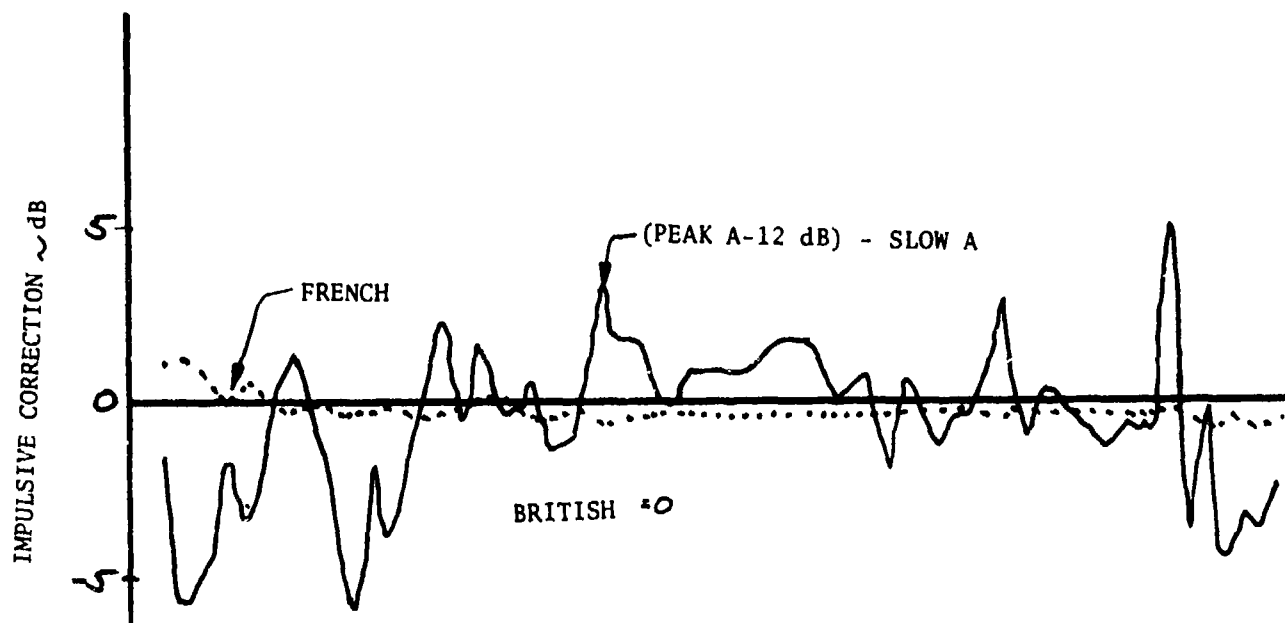
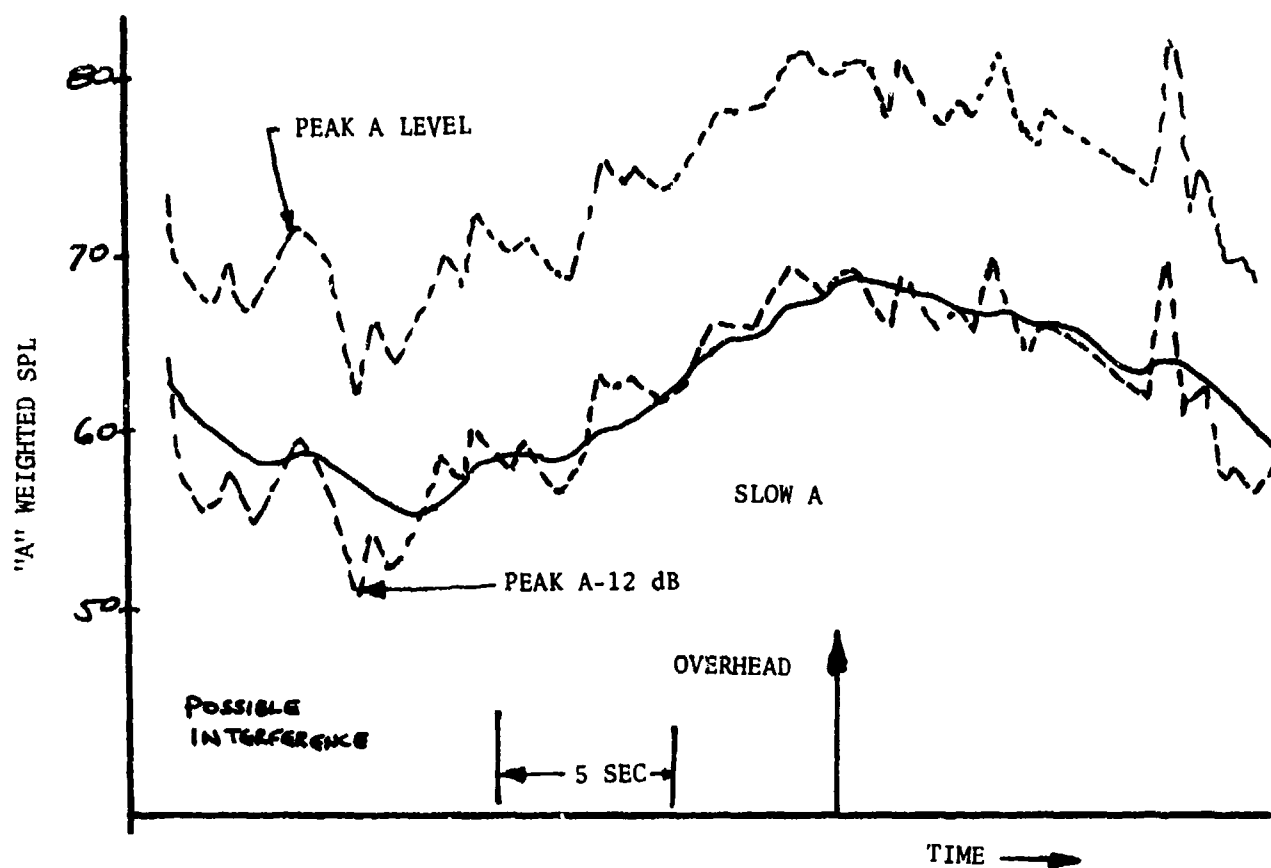


FIGURE 115

IMPULSIVE CORRECTIONS FOR 300C, 75mph

## 8.0 CONCLUSIONS

1. The helicopters tested can be placed into three general noise classes depending upon the shape of their noise time history during a high speed level flyover:
  - (a) Maximum flyover noise levels occur at the overhead position and appear to be controlled by tail rotor noise propagated downwards. The 300C, 500C, S-61, S-64 and 206L fall in this class. Noise levels are nearly independent of airspeed.
  - (b) Maximum flyover noise levels occur ahead of the helicopter and are caused by main rotor compressibility slap. The CH-47C and UHIN are in this category and their flyover noise levels increase with increasing airspeed.
  - (c) Reciprocating engine exhaust noise from the unmuffled 47G caused the noise from this helicopter to occur behind the helicopter. The 300C also had a reciprocating engine but did have a muffler and did not experience this problem.
2. Except for compressibility blade slap, helicopter flyover noise varies directly (10 log) with gross weight. If the CH-47C and UHIN are flown at a slow airspeed to minimize compressibility slap, the noise from the tested helicopters, when correlated against gross weight, falls into a band 7 EPNdB wide with a slope of 10 log of the gross weight. The 47G, UHIN, and CH-47C define the noisy limit of the band. The 300C, S-61, and S-64 were the quietest helicopters and their configurations are characterized by multibladed main and tail rotors with the number of blades proportional to weight and moderate tipspeeds of 660-700 fps.
3. Maximum noise on the helicopters tested occurred below the flight path centerline rather than on the sideline (45° elevation angle). The directivity pattern for compressibility slap maximized this noise directly in front of the helicopter. Tail rotor noise levels were higher in the plane of the tail rotor than 45° away towards the sideline microphones.
4. The noise level during simulated approaches varied with glideslope and no particular glideslope gave the maximum approach noise for all helicopters. Approach noise levels, at the noisiest of the 3, 6, or 9 degree glideslopes tested, were



above the noise level generated during a level of flyover at the same airspeed. This occurred because of the blade slap generated by the main rotor descending through its own wake. The CH-47C and UHIN had the quietest approach noise level relative to a high speed level flyover because the slower approach airspeed reduced the compressibility slap.

5. A duration correction, such as in the EPNL unit, is desirable for the evaluation of helicopter noise and provides an inherent penalty for blade slap because it penalizes the long duration of compressibility slap as the helicopter approaches the observer.
6. Blade slap is characterized by high crest factors defined as the ratio of the peak to rms sound pressure level. "Slow" meter response, per FAR Part 36 does not adequately measure the peak sound pressures associated with blade slap.
7. Narrow band analysis techniques are necessary to determine if the major noise source at a given time is caused by the main or tail rotor. During a flyover, the noise tends to be initially caused by the main rotor, then the tail rotor near overhead, the tail after overhead passage with possibly a contribution from engine noise and finally the main rotor again. It is important to accurately assess the offending component noise source because of the relative ease of suppressing the different noise sources such as engine noise, tail rotor or the main rotor.
8. A comparison of three proposed impulsive noise correction procedures show a high level of inconsistency between them. Further work must be done if a method to penalize for the impulsive noise generated during blade slap is adapted for helicopter noise certification.
9. Hover noise levels were severely affected by winds during the tests. Winds greater than 3-4 Kt caused a "blade slap" on the downwind microphone during hover positions. This phenomenon occurred when the tail rotor was between the wind and the microphone and could be caused by an interaction of the main and tail rotor wakes.

--REFERENCES--

1. W. J. Galloway, "PHYSICAL ANALYSIS OF THE IMPULSIVE ASPECTS OF HELICOPTER NOISE" BBN Report No. 3425 prepared under Contract FAA-WI-77-3683-1, April 1977.
2. True, Rickley and Letty, "HELICOPTER NOISE MEASUREMENTS--DATA REPORT", Report No. FAA-RD-77-57, 2 Volumes, April 1977
3. J. W. Leverton, "HELICOPTER NOISE--BLADE SLAP, PART 1: REVIEW AND THEORETICAL STUDY", NASA CR-1221, October 1968.
4. J. W. Leverton, "HELICOPTER NOISE--BLADE SLAP, PART 2: EXPERIMENTAL RESULTS" NASA CR-1983, March 1972.
5. E. J. Rickley, "HELICOPTER NOISE MEASURING PROGRAM, PRELIMINARY RESULTS", Transportation Systems Center Memorandum, November 16, 1976.
6. E. J. Rickley "HELICOPTER NOISE MEASURING PROGRAM, DATA PACKAGES ON S-64, S-61, 500C, 300C, 206L, CH-47C, BELL-212 AND 47G" Transportation Systems Center Memoranda Dated January 18, 25, 27, February 3, 3, 7, 18, and 22, 1977.
7. ICAO/CAN WGB "HELICOPTER NOISE COMPARISON TEST PROGRAMME" Minutes of Third Meeting of WG "B" May 1976.